AD-A037 155 ARMY ENGINEER WATERWAYS EXPERIMENT STATION VICKSBURG MISS F/G 20/4
LOS ANGELES HARBOR NUMERICAL ANALYSIS OF HARBOR OSCILLATIONS.(U)
FEB 77 J R HOUSTON

UNCLASSIFIED WES-MP-H-77-2 NL

1 OF 3
AD A037155

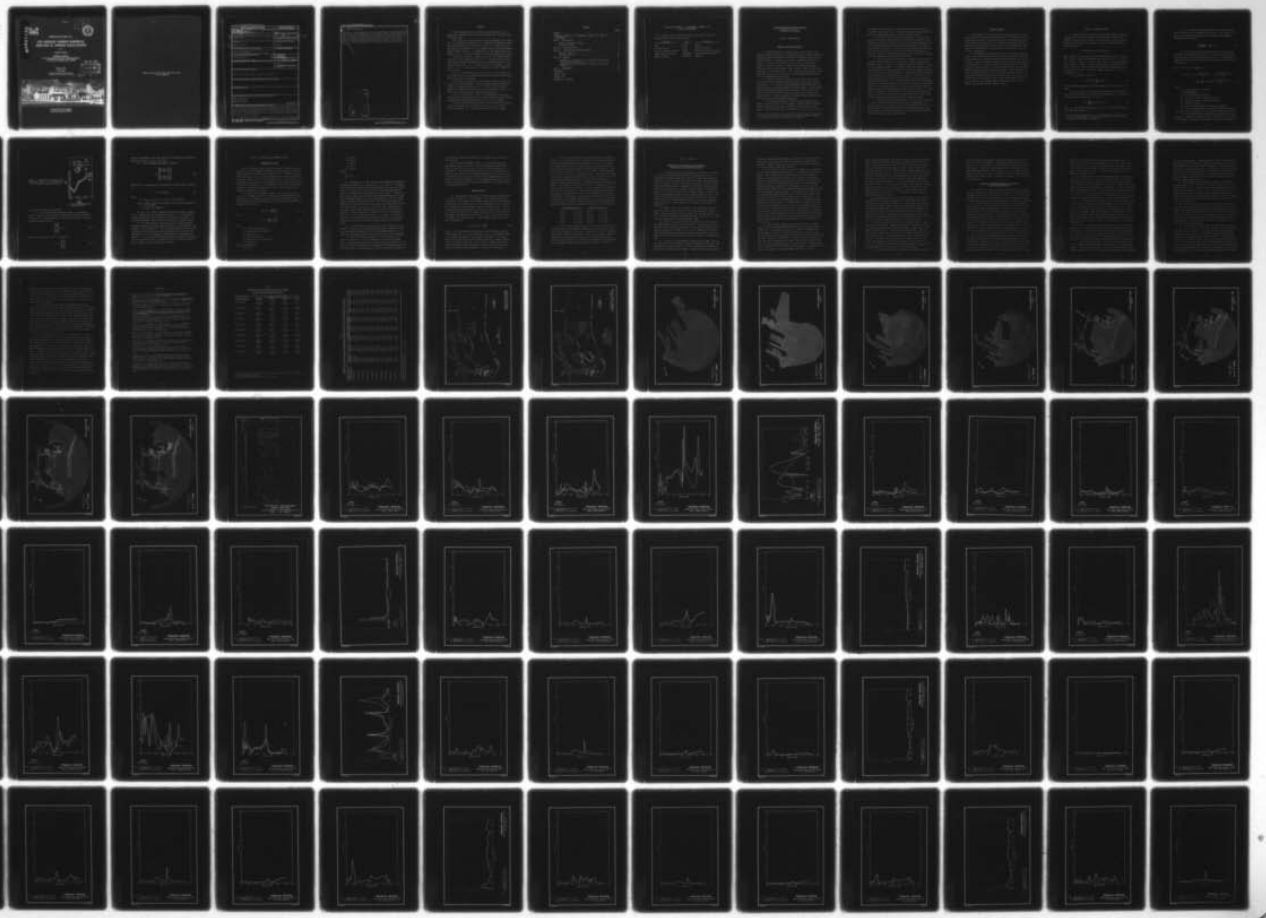

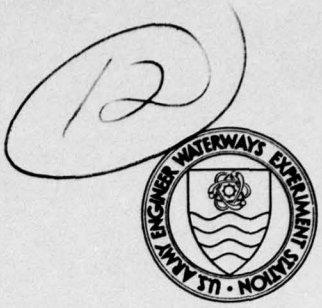

MISCELLANEOUS PAPER H-77-2

LOS ANGELES HARBOR NUMERICAL ANALYSIS OF HARBOR OSCILLATIONS

by

James R. Houston

Hydraulics Laboratory
U. S. Army Engineer Waterways Experiment Station
P. O. Box 631, Vicksburg, Miss. 39180

February 1977
Final Report

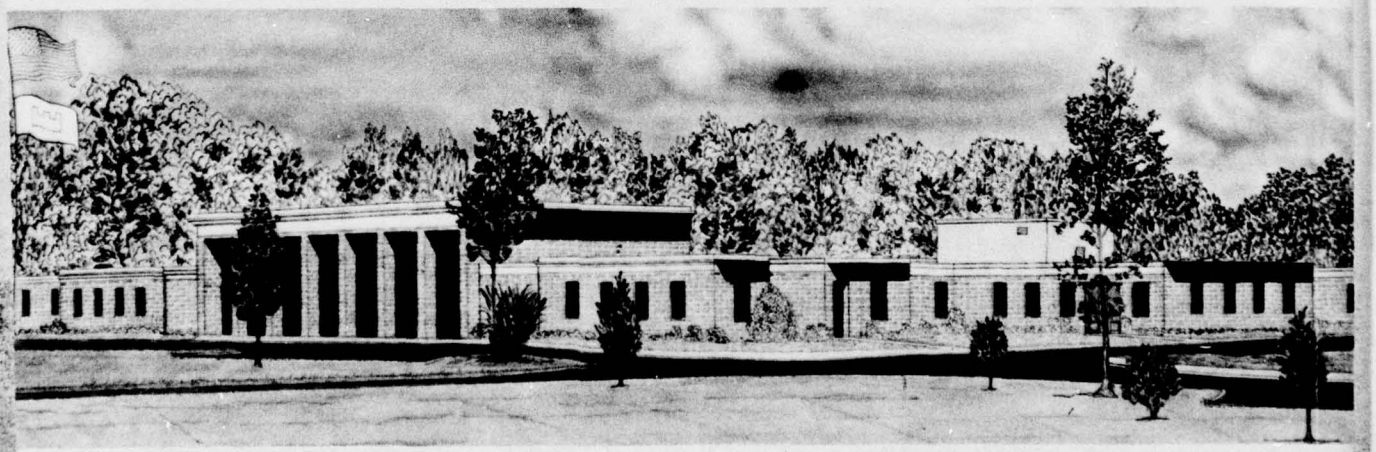

Prepared for Port of Los Angeles
San Pedro, California 90733

Destroy this report when no longer needed. Do not return it to the originator.

Unclassified

SECURITY CLASSIFICATION OF THIS PAGE (When Data Entered)

REPORT DOCUMENTATION PAGE

READ INSTRUCTIONS BEFORE COMPLETING FORM

1. REPORT NUMBER: ~~Miscellaneous Paper~~ H-77-2	2. GOVT ACCESSION NO.
3. RECIPIENT'S CATALOG NUMBER	
4. TITLE (and Subtitle): LOS ANGELES HARBOR NUMERICAL ANALYSIS OF HARBOR OSCILLATIONS	5. TYPE OF REPORT & PERIOD COVERED: Final report
	6. PERFORMING ORG. REPORT NUMBER
7. AUTHOR(s): James R. Houston	8. CONTRACT OR GRANT NUMBER(s): WES 76-5
9. PERFORMING ORGANIZATION NAME AND ADDRESS: U. S. Army Engineer Waterways Experiment Station, Hydraulics Laboratory, P. O. Box 631, Vicksburg, Mississippi 39180	10. PROGRAM ELEMENT, PROJECT, TASK AREA & WORK UNIT NUMBERS
11. CONTROLLING OFFICE NAME AND ADDRESS: Port of Los Angeles, P. O. Box 151, San Pedro, California 90733	12. REPORT DATE: February 1977
	13. NUMBER OF PAGES: 228
14. MONITORING AGENCY NAME & ADDRESS (if different from Controlling Office)	15. SECURITY CLASS. (of this report): Unclassified
	15a. DECLASSIFICATION/DOWNGRADING SCHEDULE

16. DISTRIBUTION STATEMENT (of this Report)

Approved for public release; distribution unlimited.

17. DISTRIBUTION STATEMENT (of the abstract entered in Block 20, if different from Report)

18. SUPPLEMENTARY NOTES

19. KEY WORDS (Continue on reverse side if necessary and identify by block number)

Harbor oscillations
Los Angeles Harbor
Numerical analysis

20. ABSTRACT (Continue on reverse side if necessary and identify by block number)

A hybrid finite element numerical model was used to calculate harbor resonance for existing conditions and proposed improvements of Los Angeles and Long Beach Harbors. The numerical model calculates harbor oscillation for harbors of arbitrary shape and variable depth. Ten finite element numerical grids were used to calculate the response of the harbors complex for incident waves with periods from 1 to 10 min.

Calculations of the model for existing conditions of the harbors were

(Continued)

DD FORM 1 JAN 73 1473 EDITION OF 1 NOV 65 IS OBSOLETE

Unclassified

SECURITY CLASSIFICATION OF THIS PAGE (When Data Entered)

20. ABSTRACT (Continued).

shown to be in good agreement with prototype measurements. The numerical model calculations indicate that resonant oscillations in existing harbor facilities will not be greatly altered by the proposed modifications of the harbors complex. The largest oscillation in the proposed LNG slip and general cargo terminal created by the Terminal Island landfill occurred at a wave period of 258 sec. The seaward side of the Terminal Island landfill did not exhibit significant resonant oscillations for incident waves with periods from 1 to 10 min.

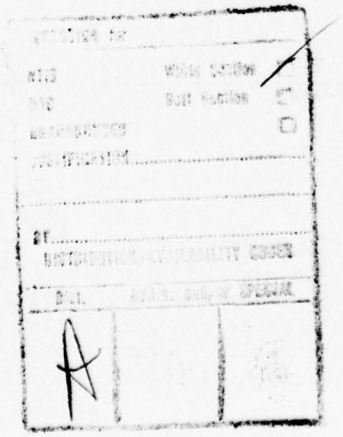

PREFACE

The investigation reported herein was authorized by the Los Angeles Port Authority under a contract, Agreement No. WES 76-5, dated 12 December 1975.

This study was conducted during the period December 1975 to April 1976 in the Hydraulics Laboratory, U. S. Army Engineer Waterways Experiment Station (WES), under the direction of Mr. H. B. Simmons, Chief of the Hydraulics Laboratory, Dr. R. W. Whalin, Chief of the Wave Dynamics Division (WDD), and Mr. C. E. Chatham, Chief of the Harbor Wave Action Branch. Mr. J. R. Houston conducted the study and prepared this report.

Messrs. R. R. Bottin, C. Bryant, and A. W. Garcia (WDD) prepared the finite element numerical grids. Mr. D. G. Outlaw (WDD) developed the computer plotting programs and aided in eliminating errors in the finite element grids. Mr. R. R. Bottin plotted the frequency response curves. Dr. D. C. Raney assisted in running the computer program for several grids.

Mr. H. L. Butler (WDD) rewrote the matrix-solving subroutine of the hybrid finite element computer program, thus reducing significantly the running time of the program.

A significant proportion of the numerical computations were performed on a CDC-7600 computer at the Los Alamos Scientific Laboratory (LASL), Los Alamos, New Mexico. Mr. P. Johnson and Mrs. Margaret McCormick of LASL assisted significantly in coordinating visits to Los Alamos and scheduling computer time on the LASL system.

Drs. H. S. Chen and C. C. Mei of the Massachusetts Institute of Technology provided documentation of the hybrid finite element computer program they developed and materials to aid in its utilization.

Directors of WES during the conduct of the study and the preparation and publication of this report were COL G. H. Hilt, CE, and COL John L. Cannon, CE. Technical Director was Mr. F. R. Brown.

CONTENTS

	Page
PREFACE	1
CONVERSION FACTORS, U. S. CUSTOMARY TO METRIC (SI) UNITS OF MEASUREMENT	3
PART I: INTRODUCTION	4
Harbor Oscillation Problem	4
Purpose of Study	6
PART II: NUMERICAL MODEL	7
PART III: APPLICATION OF NUMERICAL MODEL	13
Boundary Conditions	13
Numerical Grids	15
PART IV: RESULTS	17
Comparison of Prototype Data and Numerical Calculations for Existing Conditions	17
Comparison of Harbor Response for Existing and Revised Conditions	20
PART V: CONCLUSIONS	24
REFERENCES	26
TABLES 1 and 2	
PLATES 1-198	
APPENDIX A: NOTATION	

CONVERSION FACTORS, U. S. CUSTOMARY TO METRIC (SI) UNITS OF MEASUREMENT

U. S. customary units of measurement used in this report can be converted to metric (SI) units as follows:

Multiply	By	To Obtain
feet	0.3048	metres
feet per second	0.3048	metres per second
feet per second per second	0.3048	metres per second per second
square feet per second	0.09290304	square metres per second
degrees (angle)	0.01745329	radians

LOS ANGELES HARBOR NUMERICAL ANALYSIS OF HARBOR OSCILLATIONS

PART I: INTRODUCTION

Harbor Oscillation Problem

1. A harbor excited by long waves with a period close to the natural oscillation period of the harbor experiences a resonant reaction that may produce wave heights in the harbor far greater than the incident wave heights. Generally, the vertical movement of water in the harbor is still only a few tenths of a foot due to the very small heights of incident long waves. However, the horizontal movement of water may cover a distance greater than 10 ft* as a result of the long wavelength of the incident waves. Such horizontal water movements cause surge and sway motion of moored ships that may hamper unloading operations and damage mooring facilities.

2. A number of harbors on the west coast of the United States have histories of ship motion problems resulting from harbor resonant oscillations. It is likely that the long-period waves responsible for exciting harbor oscillations permeate the Pacific Basin. Lack of modern harbor development may prevent the occurrence of any problem for most coastal areas of the Pacific. Many places that have a problem may merely tolerate it through ignorance of possible remedial measures with the result that the problem goes unreported.

3. The generating mechanism of the very small amplitude long waves that excite harbors is still unknown. However, Munk's surf-beat theory[1] suggested an attractive explanation of the origin of these waves. Surf beats result from the superposition of two trains of waves

---

* A table of factors for converting U. S. customary units of measurement to metric (SI) units is presented on page 3.

of slightly different period. The beats are an amplitude modulation of a shorter period wave train. Swell, for example, almost always exhibits an irregular beating up to several minutes in period.

4. Carr[2] argued that local surf beat could not cause the long-period waves known to excite harbors. Although the surf-beat process produces a long-period vertical water motion, the really important factor of long-period horizontal water motion is lacking in surf beats. Severe harbor surging also is known to occur during otherwise calm seas with identical long-period wave activity reported along hundreds of miles of a coastline. Carr maintained that such activity is not compatible with long-wave generation by local surf beat.

5. True long-period wave trains may be generated from surf beats through nonlinear processes in the surf zone. Munk[1] estimated that beaches reflected 1 percent of the energy incident upon them in the form of these long-period waves. It is perhaps these waves reflected from distant shores of the Pacific that cause oscillation problems in harbors on the west coast of the United States. Long-period wave activity would then increase after distant storms of the south or west Pacific Ocean created large swell conditions and the resulting surf beat generated long-period wave trains in the surf zone which reflected off shorelines. Wilson[3] has noted that harbor oscillation in Los Angeles and Long Beach Harbors has a seasonal fluctuation of frequency and intensity which is greatest during the summer months and least during the winter. He noted that such a pattern is almost identical with that found for Table Bay Harbour, Cape Town, South Africa, and suggests that the storms in the Southern Hemisphere are responsible for the long-period waves.

6. Further evidence that long-period wave trains exist from time to time as a general ocean condition and are not generated by local surf beats comes from a harbor study for San Nicholas Bay, Peru.[4] It was concluded from horizontal water velocity measurements that long-period waves affecting San Nicholas Harbor were progressive waves unassociated with the concurrent swell waves.

Purpose of Study

7. The purpose of this study was to investigate harbor oscillations excited by long waves with periods from 1 to 10 min using a finite element numerical model. Existing conditions of Los Angeles and Long Beach Harbors and conditions of a proposed harbor expansion were considered to ensure that the expansion would not cause undesirable oscillations in existing basins or characteristic oscillations of its own that were undesirable.

8. The amplification peaks predicted by the numerical model may be much larger than the peaks which actually occur in nature, since the model neglects all dissipative processes except radiation of energy by a harbor. However, the model adequately predicts the relative severity of various modes of oscillation, and the results can be used to compare oscillation characteristics of the existing Los Angeles and Long Beach Harbors complex and proposed harbor expansions. Information about periods of resonant peaks and the spatial patterns of wave heights and currents when areas of the harbor are excited also will be used to determine both the incident wave period ranges which need to be tested and the optimum gage placement during future wave tests in the Los Angeles and Long Beach Harbors hydraulic model.

PART II: NUMERICAL MODEL

9. Response of the Los Angeles and Long Beach Harbors complex to long wave excitation was determined by using a hybrid finite element numerical model developed recently by Chen and Mei at the Massachusetts Institute of Technology.[5] The model solves the following generalized Helmholtz equation:

$$\nabla \cdot [h(x,y)\nabla\phi(x,y)] + \frac{w^2}{g}\phi(x,y) = 0 \qquad (1)$$

where $\phi(x,y)$* is the velocity potential defined by $U(x,y) = -\nabla\phi(x,y)$, with $U(x,y)$ being a two-dimensional velocity vector and w an angular frequency, $h(x,y)$ is the water depth, and g is the acceleration due to gravity. Equation 1 governs small amplitude undamped oscillations of water in a basin of arbitrary shape and variable depth forced by periodic long waves. It has been further assumed that the flow is irrotational.

10. The Helmholtz equation:

$$\nabla^2\phi(x,y) + \frac{w^2}{gh}\phi(x,y) = 0 \qquad (2)$$

is the governing equation for a constant-depth ocean region outside the basin.

11. For a harbor in a semi-infinite ocean with a straight coastline there is an incident, reflected, and scattered wave. The scattered wave has a velocity potential ϕ_s given by

$$\phi_s = \sum_{n=0}^{\infty} \alpha_n H_n(kr) \cos n\theta \qquad (3)$$

where α_n are unknown coefficients and $H_n(kr)$ are Hankel functions of the first kind of order n.

---

* For convenience, symbols and unusual abbreviations are listed and defined in the Notation: Appendix A.

12. ϕ_s satisfies the radiation condition that the scattered wave must behave as an outgoing wave at infinity. This condition is known as the Sommerfeld radiation condition and may be expressed mathematically as follows:

$$\lim_{r\to\infty} \sqrt{r}\left(\frac{\partial}{\partial r} - ik\right) \phi_s = 0 \tag{4}$$

13. Chen and Mei used a calculus of variations approach and obtained a Euler-Lagrange formulation of the boundary value problem. The following functional with the property that it is stationary with respect to arbitrary first variations of $\phi(x,y)$ was constructed by Chen and Mei:

$$F(\phi) = \iint 1/2 \{h(\nabla\phi)^2 - \frac{w^2}{g}\phi^2\}\, dA$$

$$+ 1/2 \int\{h(\phi_R - \phi_I) \frac{\partial(\phi_R - \phi_I)\}}{\partial n_a} da - \int\{h\phi_a \frac{\partial(\phi_R - \phi_I)\}}{\partial n_a} da$$

$$- \int\{h\phi_a \frac{\partial\phi_I}{\partial n_a}\} da + \int\{h\phi_I \frac{\partial(\phi_R - \phi_I)}{\partial n_a}\} da \tag{5}$$

where

A = the region inside the harbor

$\int$ = line integral

ϕ_R = far field velocity potential

ϕ_I = velocity potential of the incident wave

n_a = unit normal vector outward from region A

a = boundary of region A

ϕ_a = total velocity potential evaluated on boundary a

14. Proof was given by Chen and Mei that the stationarity of this functional is equivalent to the original boundary value problem.

15. The integral equation obtained from extremizing the functional is solved by utilizing the finite element method. This method is a technique of numerical approximation that involves dividing a

domain into a number of nonoverlapping subdomains which are called elements.

16. The solution of the problem is approximated within each element by suitable interpolation functions in terms of a finite number of unknown parameters. These unknown parameters are the values of the field variable $\phi(x,y)$ at a finite number of points which are called nodes. The relations for individual elements are combined into a system of equations for all unknown parameters.

17. In the region outside the basin, the velocity potentials are solved analytically in terms of unknown coefficients. The region is considered a single element with an "interpolation function" given by Equation 3. The infinite series is terminated at some finite value such that the addition of further terms does not significantly influence the calculated values of $\phi(x,y)$. The resulting equation is combined with the system of equations for unknown parameters at nodal points within the basin and this complete system is solved using Gaussian elimination matrix methods.

18. $\eta(x,y)$ is related to $\phi(x,y)$ through the linearized dynamic free surface boundary condition

$$\eta(x,y) = -\frac{1}{g}\frac{\partial\phi(x,y)}{\partial t} \tag{6}$$

19. The horizontal velocity components have the following form:

$$u(x,y) = -\frac{g}{w}\frac{\partial\eta(x,y)}{\partial x} \; ; \; v(x,y) = \frac{-g}{w}\frac{\partial\eta(x,y)}{\partial y} \tag{7}$$

20. The hybrid finite element method (so named by Chen and Mei because the method involves the combination of analytical and finite element numerical solutions) is a steady-state solution of the boundary value problem. The response of a harbor to an arbitrary forcing function can be easily determined within the framework of a linearized theory. For example, an arbitrary incident wave amplitude at the harbor mouth in the absence of the harbor can be Fourier decomposed as follows:

$$b_o(t) = \int_{-\infty}^{\infty} b(w)e^{-iwt}\, dw$$

If $\eta(x,y,w)$ is the response amplitude at any point (x,y) inside the harbor due to an incident plane wave of unit amplitude and frequency w, then the response of the harbor to the arbitrary incident wave amplitude $b_o(t)$ is given by

$$\xi(x,y,t) = R_e\left[\int_{-\infty}^{\infty} b(w)\eta(x,y,w)e^{-iwt}\, dw\right] \tag{9}$$

where the operation $R_e[\ ]$ takes the real part of the bracketed quantity.

21. Therefore, as soon as $\eta(x,y,w)$ is known for all w, the harbor response to an arbitrary incident wave can be calculated.

22. Chen and Mei[5] verified their finite element numerical model by comparing the model's calculations with analytical and experimental results for simple wave problems. Figure 1 is a comparison of analytical and numerical results of wave diffraction by a vertical circular cylinder. Similar excellent agreement was obtained by comparing numerical calculations with an analytical solution for a semicircular harbor with two openings. Experimental data for the oscillation of a rectangular harbor also were compared with the finite element numerical calculations. Calculated periods of the resonant peaks agreed with experimental data; however, calculated amplitudes of the resonant peaks were larger since the numerical model did not consider frictional effects.

23. Several modifications were made to the numerical computer program of Reference 5 before calculations were made for Los Angeles and Long Beach Harbors. Slight modifications were made to allow the model to handle harbors with variable depths. Chen and Mei[5] applied their numerical model only to constant-depth problems. The subroutine which solves the large system of algebraic equations arising from finite elements was modified to be more efficient. This modification resulted in a decrease in the computational time of the numerical model

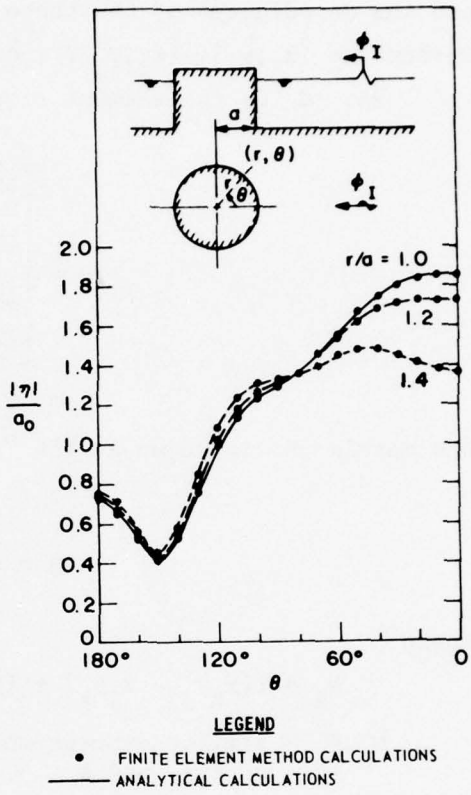

Figure 1. Comparison of numerical and analytical results for wave scattering off a vertical circular cylinder[5]

by a factor of between two and three.

24. Velocity calculations also were added to the numerical model.[6] Velocities are calculated using the expressions in Equation 7. The slope of η may be obtained at any point (x,y) within an element through the matrix equation

$$\begin{bmatrix} \frac{\partial \eta}{\partial x} \\ \\ \frac{\partial \eta}{\partial y} \end{bmatrix} = G\{\eta\}^e \tag{10}$$

where the matrix vector $\{\eta\}^e$ is defined as

$$\{\eta\}^e = \begin{bmatrix} \eta_i \\ \eta_j \\ \eta_k \end{bmatrix} \tag{11}$$

and the coordinates of the three nodes (i,j,k) forming the elements are defined as (x_i,y_i), (x_j,y_j), and $(x_k y_k)$.

25. G is the element slope matrix defined as

$$G = \begin{bmatrix} \frac{\partial N_i}{\partial x} & \frac{\partial N_j}{\partial x} & \frac{\partial N_k}{\partial x} \\ \\ \frac{\partial N_i}{\partial y} & \frac{\partial N_j}{\partial y} & \frac{\partial N_k}{\partial y} \end{bmatrix} \tag{12}$$

and matrix N is known as the "interpolation" function and is defined as

$$N = \{N_i, N_j, N_k\} \tag{13}$$

where

$N_i = \{(x_k y_j - x_j y_k) + (y_k - y_j)x + (x_j - x_k)y\}/2\Delta$

N_j, N_k = similar expressions obtained by the cyclical permutation of i,j, and k

Δ = area of the element A^e

26. The $\{\eta\}^e$ matrix is known from the finite element computations. Together with the interpolation function N , the horizontal velocity at any point (x,y) within an element can be determined. Velocities presented in this report were calculated at element centers.

27. The finite element numerical model has several important advantages compared with other numerical harbor oscillation models such as that of Lee and Raichlen.[7] First, the model allows a variable depth. Furthermore, the computational time requirement for the model is substantially less than computational times required by other numerical models.[8] It is the only present numerical model for harbor oscillations which can feasibly calculate resonance effects in a harbor as large as the Los Angeles and Long Beach Harbors complex.

PART III: APPLICATION OF NUMERICAL MODEL

Boundary Conditions

28. The boundary condition used in the numerical model along the shoreline of the Los Angeles and Long Beach Harbors complex is that the normal component of the velocity be equal to zero. The same boundary condition was used for the detached breakwater surrounding the proposed oil tanker terminal at Pier J in Long Beach Harbor. The breakwater core extends above still water and is impermeable to incident wave energy and is therefore represented as a solid barrier in this study. The eastern entrance to the tanker terminal basin is 600 ft wide and the basin is dredged to a depth of 62 ft mllw.

29. The San Pedro breakwater (Plate 1) does not have a solid core. It is composed of class B rock having an average diameter of approximately 1.8 ft and has a crown at mllw of fitted concrete blocks. Keulegan[9] gives the following formula for calculating wave transmission through rock structures:

$$\frac{a_i}{a_t} = 1 + \gamma \left(\frac{a_i}{h}\right) \frac{L}{\lambda} \tag{14}$$

where

$$\gamma = 2.11 \frac{\lambda}{d} \left(gh \frac{T^2}{\lambda^2}\right)^{4/3} \tag{15}$$

and

a_i = incident wave amplitude

a_t = transmitted wave amplitude

h = water depth

L = width of breakwater

λ = wavelength of incident waves

T = wave period

Using these parameters

h = 50 ft

$L = 125$ ft

$T = 180$ sec

$\lambda = 7222$ ft

$d = 1.8$ ft

$a_i = 0.05$ ft

yields

$$\frac{a_t}{a_i} = 0.87$$

30. This figure is a lower bound for the transmission through the San Pedro breakwater for a 3-min wave since $a_i = 0.05$ ft is probably the upper bound wave amplitude for a 3-min wave at the San Pedro breakwater. This upper bound can be deduced from prototype measurements taken in Los Angeles and Long Beach Harbors by the WES.[10] Long-period wave activity cannot be discerned in wave gage measurements at the San Pedro breakwater because of the large wave heights in the swell regime. However, a gage off Reservation Point in the Los Angeles Harbor was sufficiently protected from swell that visual inspections could be made of long-period wave activity. A total of 107 visual inspections of 4-hr analog charts taken during ship motion occurrences from a year's prototype recording reveal only a single instance of a wave height as great as 0.1 ft for waves with periods of 1 to 10 min. The single recording was of a 6-min wave and probably results from the large 6-min resonant oscillation that occurs in the East Channel of Los Angeles Harbor.

31. A 3-min wave was considered in the above calculations since longer period waves of the same amplitude would more readily be transmitted through the breakwater and the finite element grids for 1- to 3-min waves (paragraphs 34-36) do not extend as far as this breakwater.

32. Since the San Pedro breakwater is very pervious to 3- to 10-min incident waves, it is not represented in the finite element grids. Although the breakwater looks impervious from the water as a result of the fitted concrete blocks extending up from the waterline, Wilson[3] noted that this breakwater has long been considered an ineffective

filter against long waves because of its 43 percent voids; this is indeed the case.

33. The Middle breakwater (Plate 1) of Los Angeles and Long Beach Harbors has a solid core to -26 ft mllw which is covered with a layer of class B rock and a layer of class A rock (approximately 3 ft in diameter). The rock covering of the solid core is at least as permeable to long waves as the San Pedro breakwater, since it consists of rock the same size or larger. Therefore, the Middle breakwater is represented by a depth change with the core impermeable, and small finite element triangles are placed along the breakwater in the numerical grid to properly represent it.

Numerical Grids

34. The numerical grids used in the numerical model computations are shown in Plates 3-12. The elements are all triangular and often equilateral. The lengths of the triangle sides were in general selected so that they were one eighth of the local wavelength or less. Chen and Mei[5] compared the finite element solution of diffraction by a vertical cylinder with an exact analytical solution and found a global error of 0.7 percent when they used an element length of one tenth the incident wavelength. They defined a global error as $\frac{1}{n}\sum_{n}$ (local error), where the summation is performed over n finite element nodes. The local error is defined as

$$\text{Local error} = \frac{\eta - \eta_t}{\eta_t} \tag{16}$$

where η is the magnitude calculated by the finite element method at a nodal point and η_t is the theoretical value. In the present study, it was judged that element lengths equal to one eighth of the local wavelength or less would provide sufficient accuracy. Element lengths vary in the grids in relation to local depths. Element lengths near harbor entrances are made much smaller than may be strictly necessary in order to ensure proper propagation of waves into inner basins.

35. Five grids were used for each case tested and are tabulated below. It is not feasible to use a single grid to calculate harbor response for incident waves with periods from 1 to 10 min. For example, 1- to 3-min grids could not be constructed to cover the entire harbor complex because of computer memory and running time limitations. Separate grids were used for 3- to 4-, 4- to 6-, and 6- to 10-min calculations to reduce the cost of operating the model. The computational time of the model is approximately proportional to the number of nodes in the grid times the bandwidth squared. The bandwidth is the greater of either the maximum difference for all elements between two adjacent node numbers in an element of the grid or the sum of the number of nodes on the grid semicircle plus the number of terms retained in truncating the infinite series of Equation 3. In general, the bandwidth increases approximately linearly with a decrease in the lengths of the triangular element sides. The number of nodes increases approximately as the inverse square of the triangle side lengths. Thus a grid for 3-min waves (eight nodes per wavelength) requires approximately 16 times more computational time than one for 6-min waves (eight nodes per wavelength).

Existing Conditions		Revised Conditions	
Grid 1	1 to 2 min	Grid 1A	1 to 2 min
Grid 2	2 to 3 min	Grid 2A	2 to 3 min
Grid 3	3 to 4 min	Grid 3A	3 to 4 min
Grid 4	4 to 6 min	Grid 4A	4 to 6 min
Grid 5	6 to 10 min	Grid 5A	6 to 10 min

36. Many of the numerical grids for existing conditions were designed so that they could be more readily modified to construct grids for the harbor expansion conditions. However, the design of the harbor was modified several times during the course of this study. Therefore, some element patterns in the grids may have no particular purpose. Grids also were constructed to minimize the bandwidth, and this requirement occasionally governed triangle shapes for areas of the grids.

PART IV: RESULTS

Comparison of Prototype Data and Numerical Calculations for Existing Conditions

37. Prototype wave gage recordings were collected at Los Angeles and Long Beach Harbors from 26 May 1971 to 29 June 1972 by the U. S. Army Engineer Waterways Experiment Station.[10] Energy spectra were determined for 10 time periods of the year during which ship motion problems were reported. Spectral analyses were performed via Fast Fourier Transform (FFT) techniques. Variability of spectral estimates was decreased by smoothing over 10 adjacent frequency bands. Ten bands were chosen so that there would still be sufficient frequency resolution to define the long-period energy for wave periods as great as 10 min. The data record length analyzed for each spectral analysis was 24,576 sec (6.83 hr) and the lag time between successive record start times was chosen to be 3 hr. Further details of the analyses can be found in Reference 10.

38. Tables 1 and 2 give estimates of wave periods and spectral energy densities of peak energies for prototype wave gages 1 and 5; Plate 1 shows the locations of these gages. The starting times in Tables 1 and 2 give the year, Julian day, and hour on a 24-hr clock. Each of the 10 time periods lasts approximately 2 days.

39. Tables 1 and 2 give the wave period with the greatest spectral energy density within a range of periods. The range of periods is such that the spectral lines within the range cannot be resolved by the spectral analysis; for example, in the range of 480-360 sec the adjacent frequency lines corresponding to periods of 459.36 and 387.02 sec cannot be resolved by the spectral analysis and should be considered the same.

40. Plate 13 is a time-dependent spectral plot of gage 1 data for the time period of 1500 November 27 through 0300 November 29, 1971. The variability of energy levels in this plate illustrates the nonstationarity of the variance in energy bands. Long-period waves are in general

transient (time-dependent) phenomena, and some caution must be observed in the application of spectral analysis techniques to nonstationary processes. However, Tables 1 and 2 do give an indication of characteristic energy bands for each gage location.

41. It should be noted that the finite element model calculations provide only the response characteristics of Los Angeles and Long Beach Harbors. This response must be multiplied by the input spectrum of waves for a comparison with prototype data. However, the input wave spectrum is not known since long waves arriving from the deep ocean had heights too small to be measured by gages near the outer breakwaters during the prototype collection (see paragraph 30). Still, a correspondence exists between resonant peaks calculated by the numerical model and those measured in the prototype. Plates 14-18 and 24-28 are plots of the wave-height amplification factor calculated by the finite element numerical model for prototype gages 1 and 5, respectively. The frequency response for the existing conditions of Los Angeles and Long Beach Harbors shown in Plate 1 is compared with the frequency response for the revised conditions shown in Plate 2. The wave-height amplification factor is defined at each point as the wave height at the point divided by twice the incident wave height. This definition of amplification factor is traditional and is a result of the fact that the standing wave height for a straight coast with no harbor would be twice the incident wave height due to the superposition of the incident and reflected waves.

42. Table 1 shows a large resonant peak at 387 sec for gage 1. Plate 18 shows large wave-height amplification for the period range of 360-480 sec. As was mentioned earlier, the adjacent frequency lines corresponding to periods of 459.36 and 387.02 sec in the range 360-480 sec cannot be resolved by spectral analysis and should be considered the same. Appendix C of Reference 1 presents a spectral analysis of data taken over a 2-day period for gage 1 which has not been smoothed over 10 adjacent frequency bands to reduce variability. Resonant peaks occur at 482, 410, 372, and 346 sec in this analysis. The period location of these peaks is in good agreement with Plates 17 and 18.

Plate 16 shows a moderately large resonant peak at 233 sec and spectral plots in Reference 10 show a small but well-defined peak at 263 sec. Table 1 shows a resonant peak from 115 to 142 sec and Plate 15 shows a similar peak predicted by the numerical model. Table 1 also shows a small peak from 66 to 78 sec. Plate 14 shows a similar peak, but it is no larger than peaks from 85 to 95 sec and 105 to 115 sec also shown in Plate 14. The water depths in the dredge spoil area just outside the East Channel which were used on the numerical model were taken from National Ocean Survey (formerly U. S. Coast and Geodetic Survey) maps published in 1973. It is possible that depths in this area have changed enough since the prototype measurement to influence some of the oscillation characteristics of the East Channel. The resonant peaks displayed in Table 1 are generally in fair agreement with the numerical results shown in Plates 14-18.

43. A comparison of predictions of the numerical model and spectral analysis of the prototype data for five gages, prototype gages 5, 6, 7, 8, and 14, was made in Reference 11. These gages were located in the Long Beach Harbor complex. Excellent agreement was found between the numerical results and the prototype data for all five gages. Table 2 shows estimates of wave periods and spectral energy density of peak energies for gage 5 and Plates 24-28 show numerical model calculations of the wave-height amplification factor at this gage. The solid line in these plots shows calculations for existing conditions.

44. Table 2 indicates that there is no resonant peak for gage 5 data between 8 and 10 min. Numerical calculations presented in Plate 28 also show no resonant peak for this period range. Table 2 shows large peaks at 387 and 237 sec. Plates 26-28 show large peaks at 396 and 222 sec and no peaks from 240 to 360 sec. Neither the numerical computations in Plate 25 nor the prototype data of Table 2 indicate peaks from 120 to 210 sec. The prototype data have peaks at 100, 93, and 64 sec. The numerical model calculates peaks at 92, 89, and 63 sec (Plate 24). Excellent agreement on the resonant peaks is apparent between prototype data and the numerical model calculations.

45. A detailed analysis of the prototype data for gages 2 and 11

was not performed in Reference 10 because no significant oscillations from 1 to 10 min were apparent. Time-dependent spectral plots for gages 2 and 11 in Reference 10 indeed show no significant long-period oscillations. Plates 18-23 show numerical model calculations of the wave-height amplification factor at gage 2. No significant resonant peaks occur from 1 to 10 min. Similarly, the numerical model does not predict large resonant peaks at the gage 11 location. Plots for gage 11 have been omitted.

Comparison of Harbor Response for Existing and Revised Conditions

46. Plates 14-23 show a comparison of plots of the wave-height amplification factor as a function of wave period at gages 1 and 2 for existing and revised harbor conditions. Plates 1 and 2 show the existing harbor and the proposed modifications. The modifications include landfills and dredge cuts. Wave periods from 1 to 10 min are considered.

47. Plates 29-33 are frequency response plots of wave-height amplification for the proposed Liquified Natural Gas (LNG) slip (sta 1) of Los Angeles Harbor. The largest resonant peaks occur at 110, 216, 238, and 258 sec. The 258-sec peak is fairly large and the mode of oscillation rather complicated. Plate 187 shows contours of the wave-height amplification factor for this resonant peak. The oscillation of the LNG slip is in phase with an oscillation of the end basin of Fish Harbor and 180 degrees out of phase with the proposed general cargo terminal to be created by the Terminal Island landfill and the center basin of Fish Harbor. These harbor areas are undergoing coupled oscillations with water flowing back and forth between different areas.

48. Plates 34-42 are frequency response plots of wave-height amplification for sites around the Los Angeles Harbor complex at which prototype gages were not located but which may experience resonant problems (LA-1 through LA-5). Plate 2 shows locations of these gages. Plots of the frequency response for gage LA-2 at the northern tip of the Watchorn Basin are not included in this report because areas of this basin were too shallow to allow adequate resolution of the waves.

This basin is a small-boat harbor and waves with periods from 1 to 10 min do not cause ship motion problems for such small craft. Frequency response plots of wave-height amplification for gages LA-3 and LA-4 are not shown since they are similar to the plots for prototype gage 1 but have smaller peaks. Current velocity plots for these two gages are presented later.

49. Resonant peaks of the wave-height amplification factor for gages LA-1 and LA-5 occur at about the same wave periods for existing and modified conditions. Sometimes the resonant peaks are larger for one of these conditions and sometimes for the other. Many of these differences are probably attributable to difficulties in locating the peaks and not differences in response. Response calculations were initially made every 2, 3, and 5 sec for incident waves with periods from 1 to 3, 3 to 7, and 7 to 10 min, respectively. Resonant peaks were then further defined by calculation intervals of 0.5 to 2 sec and sometimes 0.1 to 0.25 sec. If a resonant peak appeared for one harbor configuration and not another or was larger for one configuration, an effort was usually made to locate the peak and resolve it. Occasionally, it was difficult to locate a very sharp peak or it was not considered crucial to resolve peaks for some gages. Ship motion problems, for example, are of more concern in the East Channel than at gage locations LA-1 and LA-5. Very sharp resonant peaks also are probably not important in the prototype since only a small amount of energy in the incoming wave spectrum would be amplified.

50. Plates 43-89 show frequency response plots of wave-height amplification for 10 gages located along the landfill areas of the modified harbor. Plots for gages LA-6 through LA-10 display peaks at 90, 157, and 258 sec. LA-11 has an additional peak at 116 sec, and LA-12 has a broad peak at 186 sec and no noticeable peak at 258 sec. Plots for gages LA-13, LA-14, and LA-15 display no significant resonant peaks.

51. Ship motion problems due to very long wave excitation are due, of course, to horizontal water movement and not to vertical water movement. Waves with periods from 1 to 10 min have amplitudes of only several tenths of a foot at most; therefore, the heave of a ship induced

by waves is insignificant. Horizontal motions of sway and surge may be large, however. Plates 90-170 are frequency response plots of normalized maximum current velocity (NMCV). The NMCV is a maximum horizontal velocity over one wave period, and it is normalized so that multiplication by the incident wave amplitude in feet yields velocity in units of feet per second. Incident waves in the prototype may have amplitude orders of magnitude less than 1 ft, and the water velocities they produce are correspondingly smaller.

52. Plates 90-99 show the NMCV as a function of wave period for prototype gages 1 and 2. Velocities are small at gage 1, of course, since it is at the end of the East Channel where antinodes usually develop when the channel is excited. Plots of the NMCV at gage 2 show several resonant peaks for both existing and modified conditions. Gage 2 was located at an oil terminal, and reports of heavy ship motion were received from tankers several times during the prototype data collection of Reference 10.

53. The NMCV plotted as a function of wave period is shown in Plates 100-104 for the sta 2 LNG slip; this gage location is near the mouth of the LNG slip as shown in Plate 2. A NMCV plot is not shown for the sta 1 LNG slip because the velocity plot is very similar to the plot for the sta 2 LNG slip, but the velocities are lower. Plates 100, 102, and 103 show resonant peaks at 110, 216, and 258 sec. Spatial velocity plots of the NMCV are shown for the 110- and 258-sec plot in Plates 174 and 188, respectively.

54. Plates 105-123 show the NMCV as a function of wave period for gage locations sta LA-1, LA-3, LA-4, and LA-5. LA-1 was located at the end of the West Channel in Los Angeles Harbor and consequently there are no large peaks in the NMCV plots shown in Plates 105-109. Gages LA-3 and LA-4 were both in the East Channel. Plates 110-119 show plots of the NMCV for these gages. Velocities are quite large for the 4- to 8-min period range. The two major resonant peaks from 4 to 6 min are larger for the modified harbor conditions than for the existing conditions; however, these peaks are fairly sharp. The response of the East Channel to a spectrum of incident wave periods may be larger

for existing conditions as a result of the larger current velocities for wave periods in a range between the two peaks. Velocities are larger for existing conditions for the 6- to 8-min period range. Plates 120-123 indicate that the NMCV values at gage LA-5 are quite similar for existing and modified conditions.

55. Gages LA-6 through LA-11 are within the proposed general cargo terminal to be created by the Terminal Island landfill shown in Plate 2. The NMCV plots shown in Plates 124-153 for these gages all display resonant peaks at 90, 157, 216, 238, 258, and 370 sec and a broad peak from 305 to 350 sec. The magnitudes of these peaks change from gage to gage. Whether or not these resonant peaks would induce ship motion problems depends upon response characteristics of the type of ship moored at these locations in the terminal area.

56. No large resonant peaks are seen in the NMCV plots for gages LA-12 through LA-15 shown in Plates 154-170. Plate 2 shows the locations of these gages.

57. Plates 171-198 are plots of contours of wave-height amplification and plots of normalized maximum current velocity for many of the resonant peaks shown in Plates 14-170. The velocities are represented by arrows whose centers lie at element centroids. Water particles move horizontally back and forth in a direction parallel to the arrows. The amplitude of the incident waves is assumed to equal 1 ft. The velocities are in units of feet per second for this amplitude incident wave. Incident waves in the prototype may have amplitude orders of magnitude less than 1 ft. Plates 171-198 basically illustrate patterns of wave-height amplification and current velocity, that is, they show how the harbor area is oscillating.

PART V: CONCLUSIONS

58. The good agreement between prototype measurements in the Los Angeles and Long Beach Harbors complex and calculations of the hybrid finite element numerical model confirms the reliability of this numerical model as a viable engineering tool for studying resonant oscillations of complex harbors. Amplitudes of resonant peaks predicted by the numerical model will always be too large since the model does not include any dissipative effects other than radiation dissipation. However, the model can predict relative severities (except that friction is likely to increase with increasing amplitude) and is, therefore, extremely useful in comparing the oscillation characteristics for existing conditions with those for proposed modifications. The rapid calculation time of the numerical model makes it feasible to apply the model to large harbors and broad incident wave period bands. This numerical model can be used as an aid to hydraulic model tests since it pinpoints the periods of resonant peaks and shows oscillation patterns which are useful in optimizing wave gage placement to measure extreme conditions.

59. The numerical model calculations indicate that resonant oscillations in existing harbor facilities in the Los Angeles and Long Beach Harbors complex will not be substantially altered by the proposed modifications of the harbors complex. Resonant oscillations in Long Beach Harbor are, in general, somewhat smaller for the modified conditions of the harbor complex than for existing conditions (Reference 11). Several peaks are larger for the modified conditions; however, they are not significantly larger. Some resonant peaks in existing harbor facilities of Los Angeles Harbor are increased and others decreased by the proposed modifications of the harbors complex. However, most of the peaks which are increased are sharp peaks. Sharp resonant peaks probably are not important in the prototype since only a small amount of energy in the incoming wave spectrum would be contained in the narrow period range of the sharp peak. The broad peaks displayed in the frequency response plots presented in this report for gages in existing facilities are usually similar for existing and

modified harbor conditions. The greatest difference in broad peaks of the wave amplification factor and the NMCV for existing and modified harbor conditions occurs over the period range from 400-500 sec in the East Channel. The broad peaks for the modified harbor conditions are substantially less than those for existing conditions over this period range in the East Channel.

60. The largest resonant peaks of the NMCV in the LNG slip occurred at incident wave periods of 110, 157, and 258 sec. The largest peaks of the NMCV in the general cargo terminal created by the Terminal Island landfill occurred at wave periods of 90, 157, and 258 sec. Spatial plots of the NMCV and contour plots of the wave-height amplification factor for the incident wave periods of 90, 110, 157, and 258 sec are shown in the text in order to completely define the resonant modes. This information would be required as input to a numerical model which calculated ship response. The seaward side of the Terminal Island landfill did not exhibit significant resonant oscillations for incident waves with periods from 1 to 10 min.

61. Detailed information on moored ship response as a function of incident wave amplitude and period, the incident wave spectrum, and the resonant response of the harbors complex to incident wave excitation must be known before definite conclusions can be made on the precise degrees of ship motion in Los Angeles and Long Beach Harbors. Numerical model calculations presented in this report indicate that the reso[illegible] responses of existing harbor facilities in the Los Angeles and Long Beach Harbors complex would probably not be changed enough to cause an increase in the severity of resonant oscillations. Whether or not ships using facilities in the proposed harbor expansion of the Los Angeles Harbor would experience resonant oscillation difficulties depends upon the characteristics of the ships themselves. Problems would develop only if the natural free oscillations of the ship were close in period to resonant oscillations predicted by the numerical model for basin areas.

REFERENCES

1. Munk, W. H., "Surf Beats," Transactions, American Geophysical Union, Vol 30, No. 6, Dec 1949, pp 849-854.

2. Carr, J. H., "Long Period Waves or Surges in Harbors," Transactions, American Society of Civil Engineers, Vol 118, 1953, pp 588-603.

3. Wilson, B. W. et al., "Wave and Surge-Action Study for Los Angeles-Long Beach Harbors," Vol II, Jul 1968, Science Engineering Associates, San Marino, Calif.

4. Keith, J. M. and Murphy, E. J., "Harbor Study for San Nicolas Bay, Peru," Journal, Waterways and Harbors Division, American Society of Civil Engineers, Vol 96, No. WW2, May 1970, pp 251-273.

5. Chen, H. S. and Mei, C. C., "Oscillations and Wave Forces in an Off-shore Harbor (Applications of the Hybrid Finite Element Method to Water-Wave Scattering)," Report No. 190, 1974, Massachusetts Institute of Technology, Cambridge, Mass.

6. Crosby, L. G., Durham, D. L., and Chatham, C. E., Jr., "Expansion of Port Hueneme, California; Hydraulic Model Investigation," Technical Report H-75-8, Apr 1975, U. S. Army Engineer Waterways Experiment Station, CE, Vicksburg, Miss.

7. Lee, J.-J. and Raichlen, F., "Wave Induced Oscillations in Harbors with Connected Basins," Report No. KH-R-20, Dec 1969, W. M. Keck Laboratory of Hydraulics and Water Resources, California Institute of Technology, Pasadena, Calif.

8. Houston, J. R., "Comparison of Numerical Models for Harbor Resonant Oscillations" (In preparation), U. S. Army Engineer Waterways Experiment Station, CE, Vicksburg, Miss.

9. Keulegan, G. H., "Wave Transmission Through Rock Structures; Hydraulic Model Investigation," Research Report H-73-1, Feb 1973, U. S. Army Engineer Waterways Experiment Station, CE, Vicksburg, Miss.

10. Durham, D. L. et al., "Los Angeles and Long Beach Harbors Model Study; Analyses of Wave and Ship Motion Data," Technical Report H-75-4, Report 3, Jul 1976, U. S. Army Engineer Waterways Experiment Station, CE, Vicksburg, Miss.

11. Houston, J. R., "Long Beach Harbor Numerical Analysis of Harbor Oscillations; Alternate Plans for Pier J Completion and Tanker Terminal Project," Miscellaneous Paper H-76-20, Report 2, Sep 1976, U. S. Army Engineer Waterways Experiment Station, CE, Vicksburg, Miss.

Table 1

Estimates of Wave Periods and Spectral Energy Density of Peak Energies for Gage 1

Starting Time of Time History	Ranges of Wave Periods			
	480-360	170-95	80-60	35-25
71-166-1800	387.02*	133.93	69.52	30.21
	739.7**	231.6	88.09	23.84
71-168-0300	387.02	133.93	71.55	33.51
	386.4	174.4	64.98	9.666
71-289-1600	387.02	120.77	67.61	29.85
	279.9	180.4	78.82	10.70
71-304-1200	387.02	141.65	78.39	29.84
	451.5	39.53	13.44	8.717
71-314-1500	387.02	120.77	69.52	29.84
	533.9	182.9	86.19	10.52
71-316-0900	387.02	115.11	67.61	30.21
	408.5	82.45	46.07	6.463
71-324-0000	387.02	133.93	69.52	29.84
	483.4	68.19	28.66	5.244
71-329-0300	387.02	133.93	73.69	29.84
	660.9	282.5	48.70	13.27
71-331-1500	387.02	115.11	65.80	29.14
	428.1	39.72	14.81	8.086
72-155-0600	387.02	133.93	67.61	29.48
	311.4	97.05	66.26	11.01

* Wave periods in seconds.

** Spectral energy densities in 10^{-2} ft^2-sec.

Table 2

Estimates of Wave Periods and Spectral Energy Densities of Peak Energies for Gage 5

Starting Time of Time History	Ranges of Wave Periods							
	1800-480	480-360	270-210	110-100	95-85	70-60	55-45	45-35
71-166-1800	733.61*	459.36	262.85	109.97	93.27	69.52	54.19	44.40
	189.6**	210.1	1415.0	144.2	11.80	35.41	33.58	18.91
71-168-0300	733.61	459.36	262.85	109.97	93.27	67.61	55.41	42.85
	153.6	167.1	560.9	100.9	10.74	35.61	25.84	13.55
71-289-1600	733.61	387.02	237.45	105.25	93.27	62.45	50.83	38.79
	204.9	118.8	383.1	38.20	58.08	30.48	8.900	8.456
71-304-1200	733.61	387.02	237.45	100.93	93.28	62.45	51.90	38.79
	197.8	40.54	151.85	9.332	11.84	19.20	4.345	3.723
71-314-1500	733.61	387.02	237.45	105.25	93.27	64.08	50.83	39.42
	675.2	56.74	342.7	70.77	70.35	56.34	9.781	11.36
71-316-0900	733.61	387.02	237.45	105.25	93.27	64.08	50.83	41.41
	238.7	74.96	118.3	19.80	26.91	22.06	5.045	5.696
71-324-0000	733.61	387.02	237.45	100.93	93.27	64.08	50.83	41.41
	211.7	440.2	175.6	19.01	19.85	28.77	6.284	5.110
71-329-0300	733.61	387.02	237.45	105.25	93.27	64.08	51.90	41.41
	370.7	105.1	558.9	56.95	55.97	40.26	10.15	9.978
71-331-1500	733.61	387.02	237.45	100.93	93.27	64.08	50.83	41.41
	555.1	76.85	136.8	16.04	7.381	15.74	4.401	4.157
72-155-0600	733.61	387.02	237.45	100.93	93.27	64.08	50.83	41.41
	248.3	36.55	158.8	20.97	45.39	45.55	13.34	8.966

* Wave periods in seconds.

** Spectral energy densities in 10^{-2} ft^2-sec.

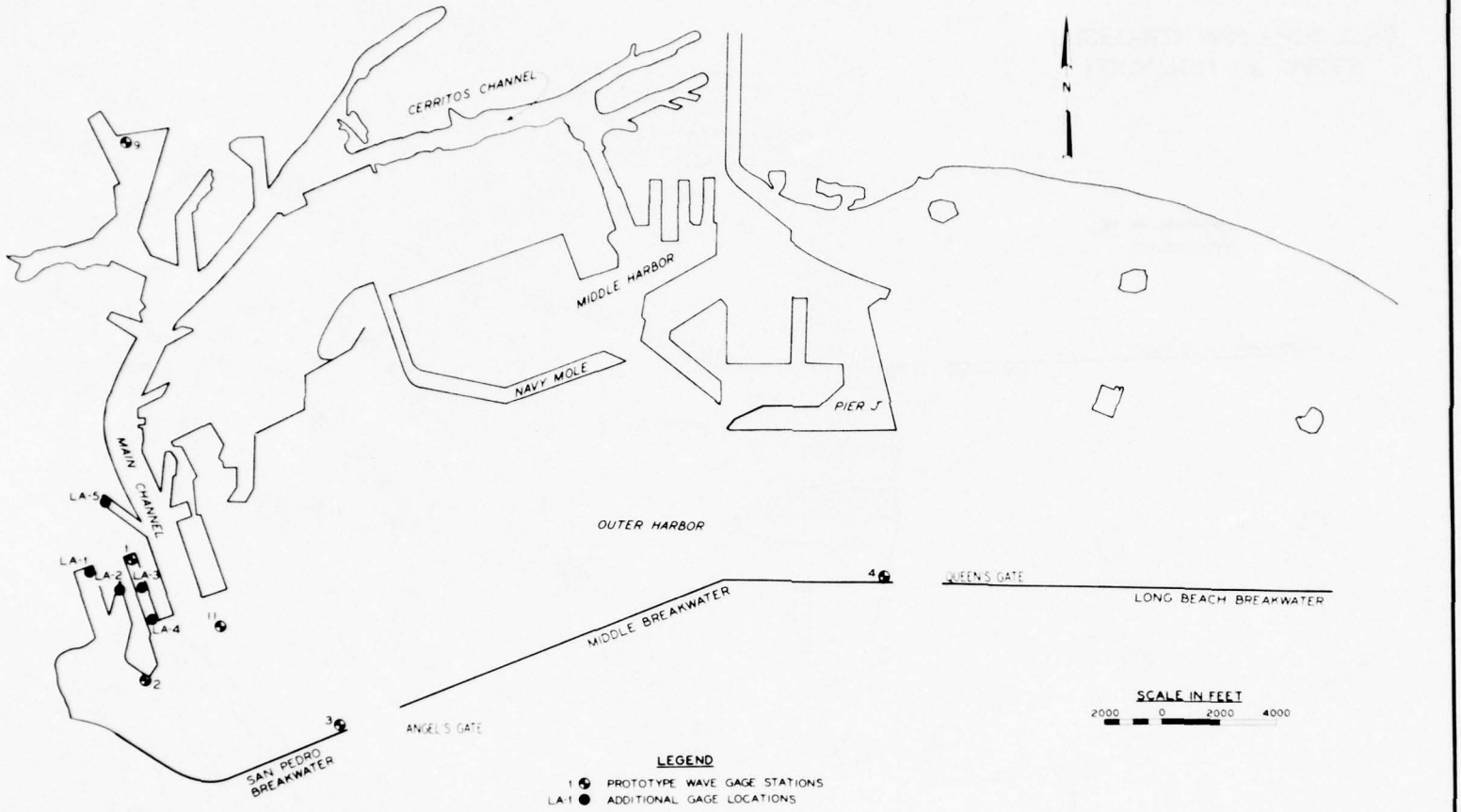

LOCATION OF GAGES
EXISTING CONDITIONS

PLATE 1

PLATE 2

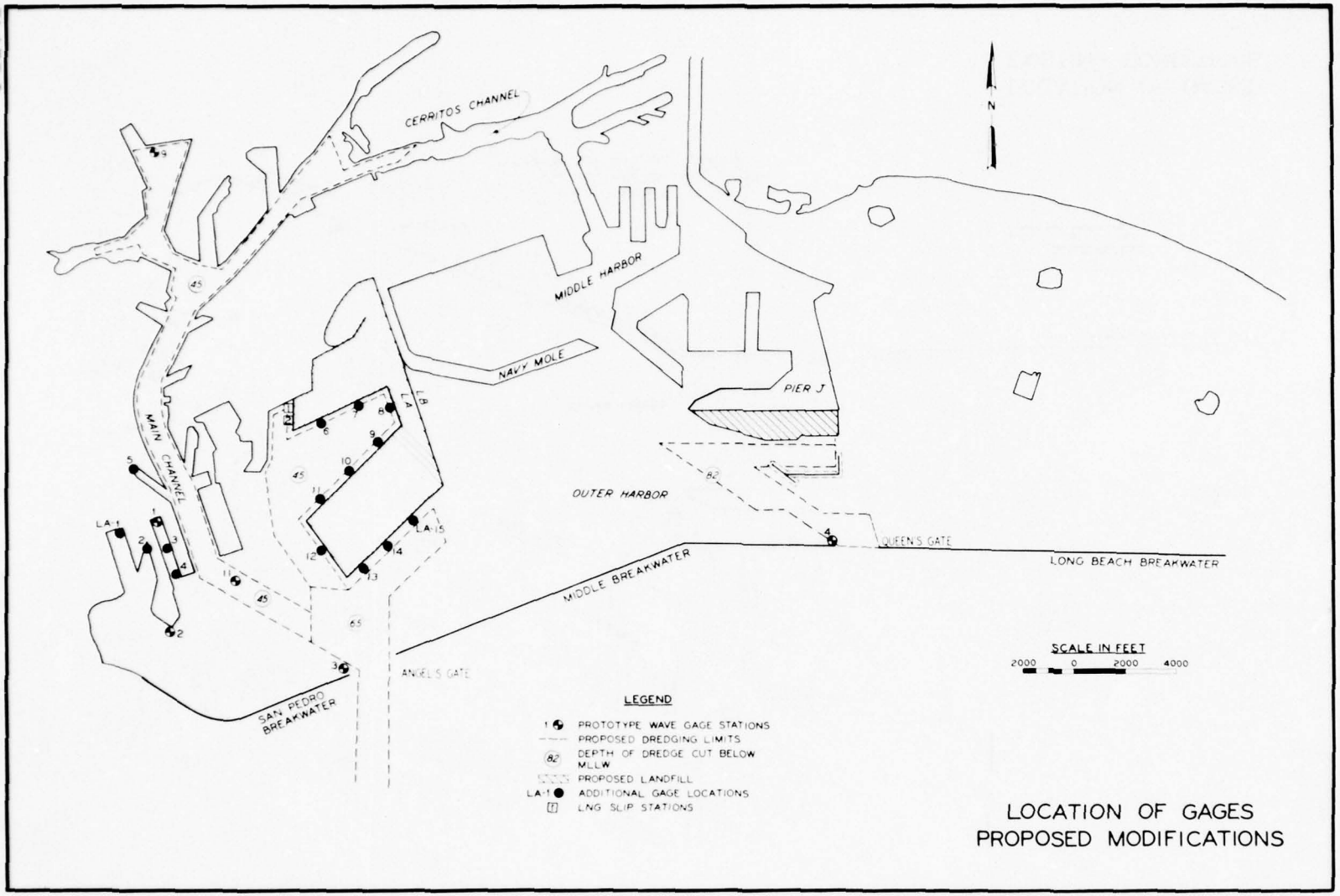

LOCATION OF GAGES
PROPOSED MODIFICATIONS

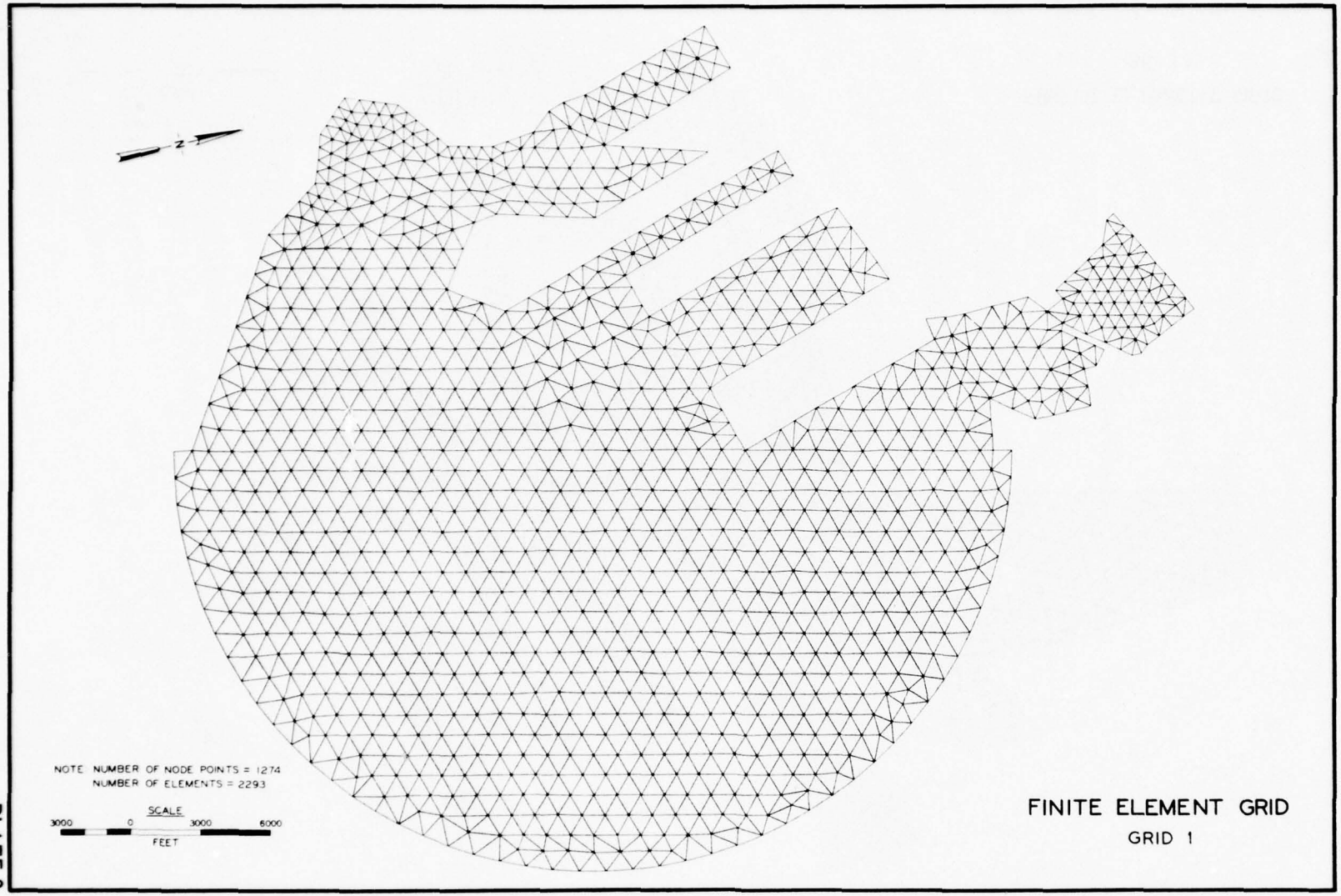

FINITE ELEMENT GRID

GRID 1

PLATE 3

PLATE 4

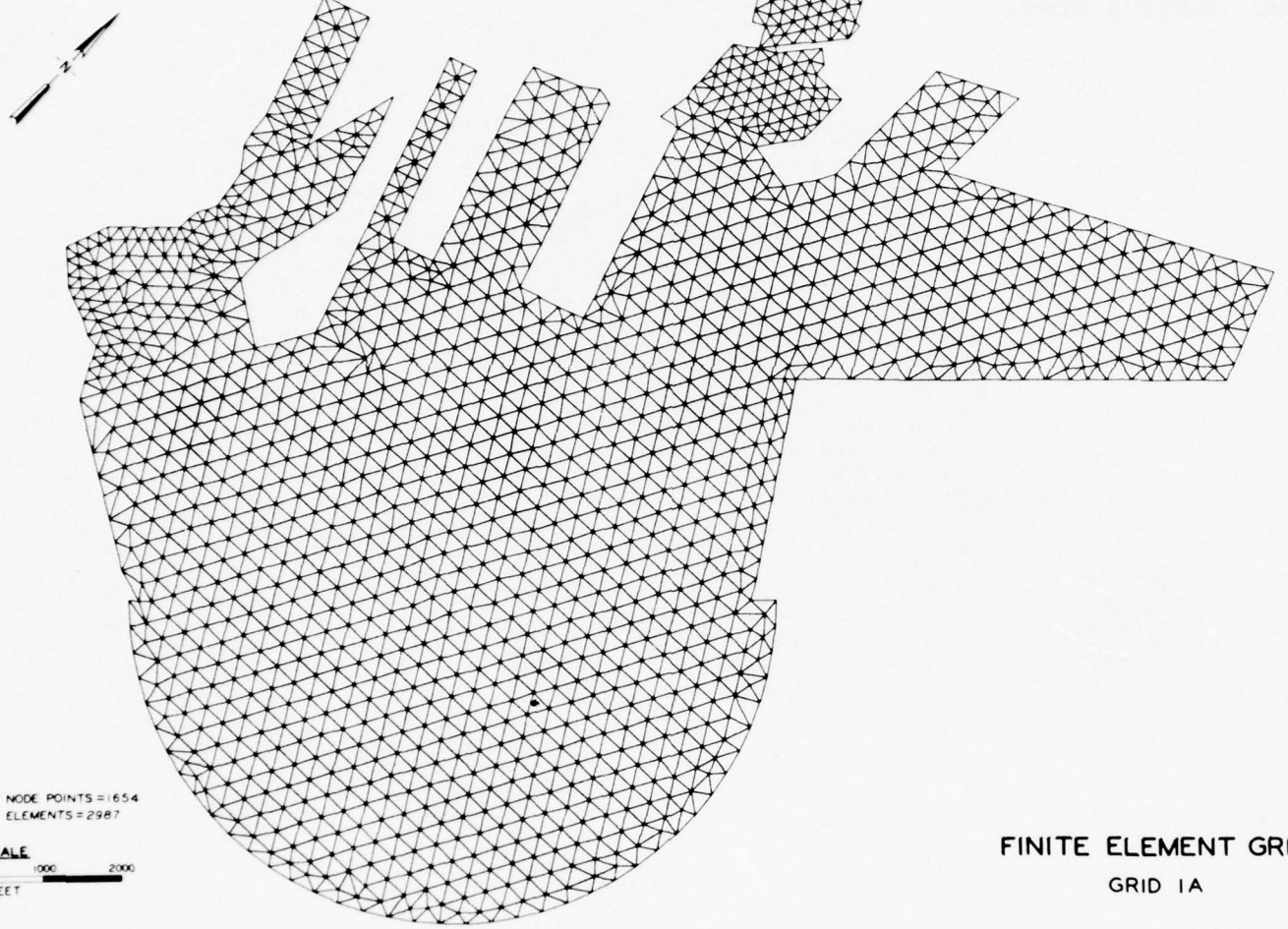

NOTE: NUMBER OF NODE POINTS = 1654
NUMBER OF ELEMENTS = 2987

SCALE

1000 0 1000 2000

FEET

FINITE ELEMENT GRID

GRID 1A

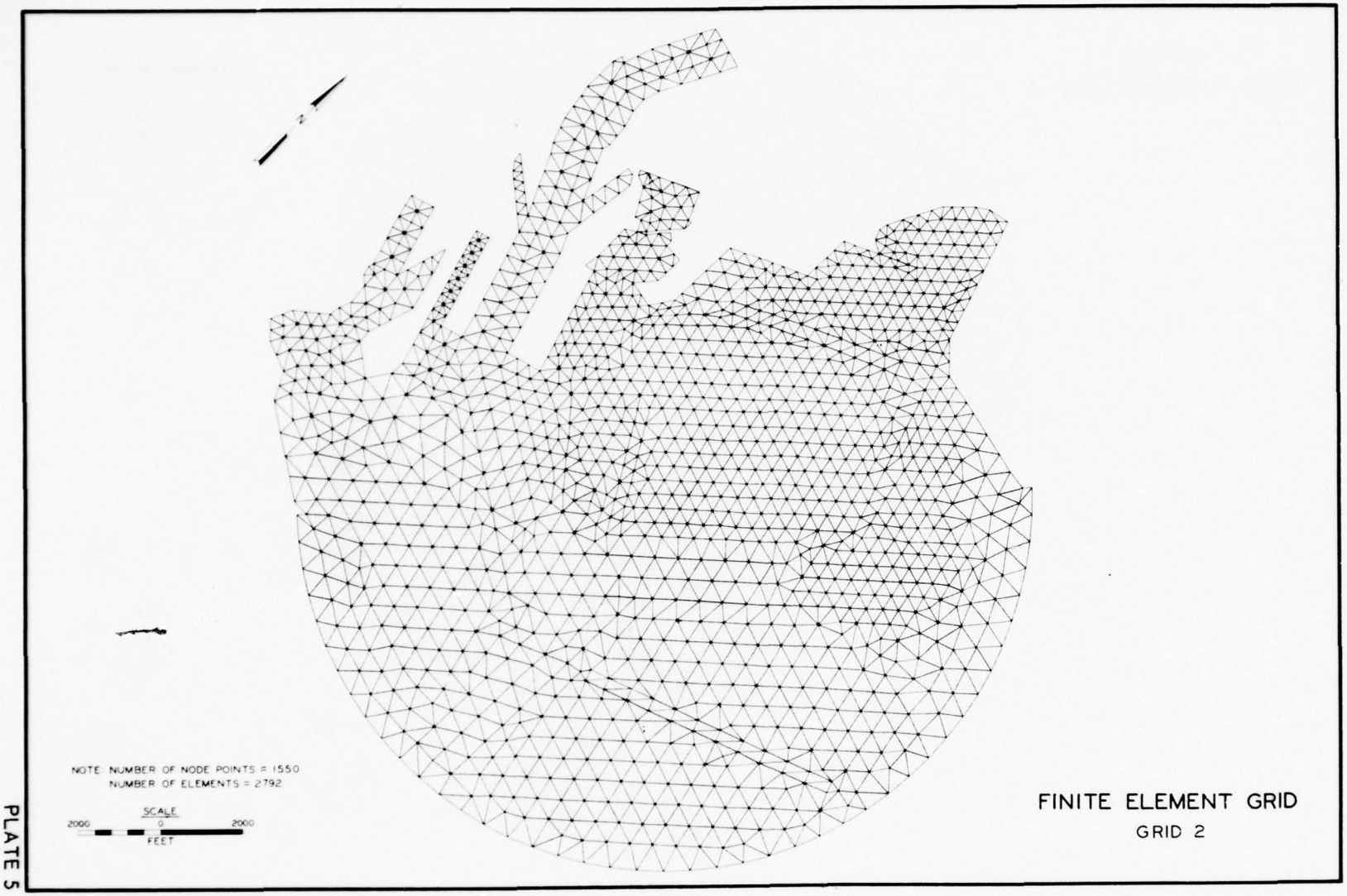
N
NOTE NUMBER OF NODE POINTS = 1550
NUMBER OF ELEMENTS = 2792
SCALE
2000
0
2000
FEET
FINITE ELEMENT GRID
GRID 2

PLATE 5

PLATE 6

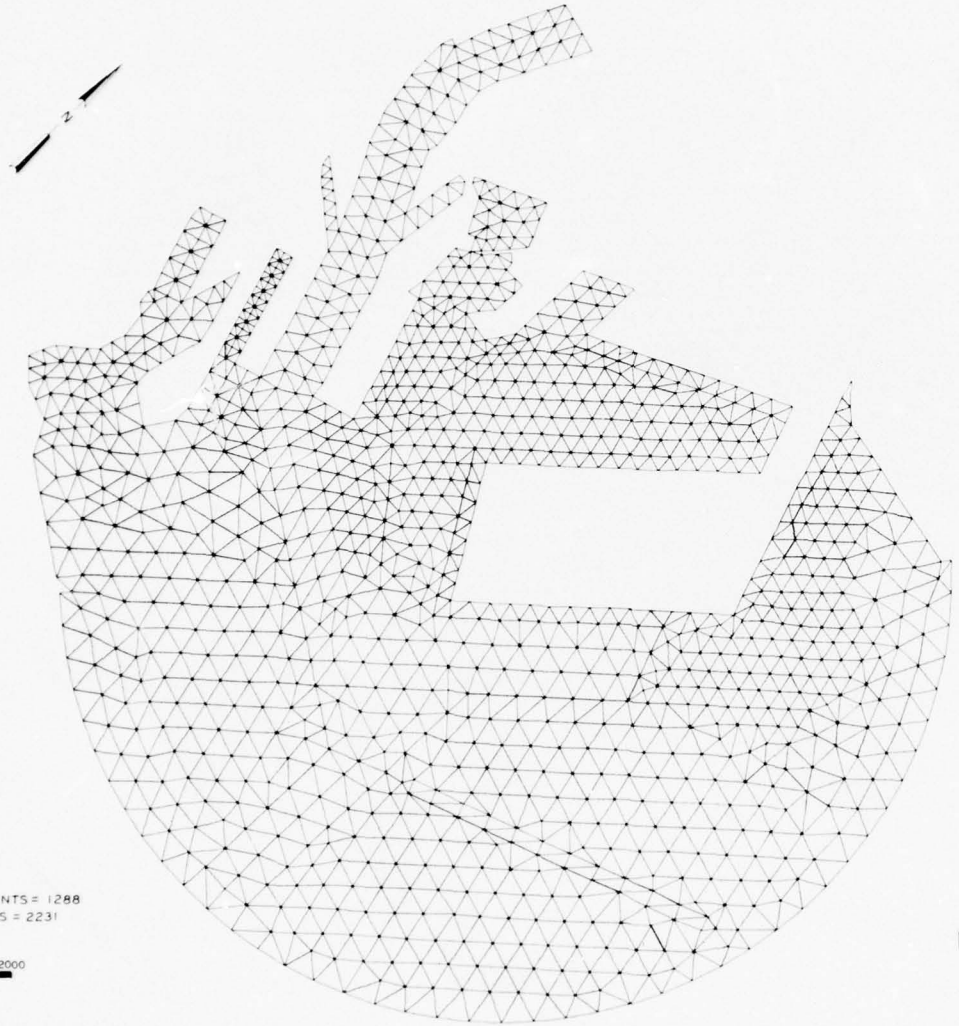

NOTE: NUMBER OF NODE POINTS = 1288
NUMBER OF ELEMENTS = 2231

SCALE
2000 0 2000
FEET

FINITE ELEMENT GRID
GRID 2A

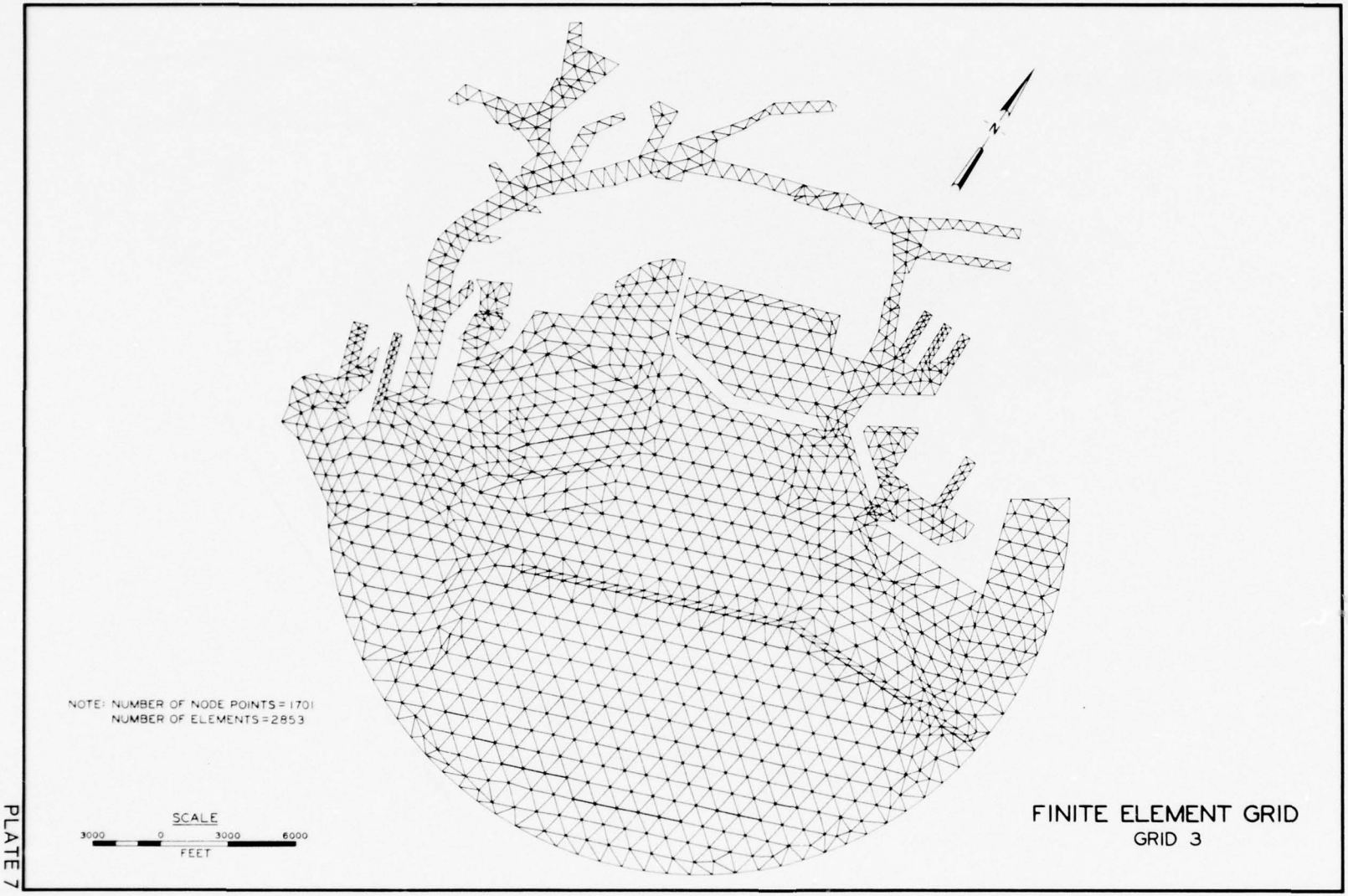
N
NOTE: NUMBER OF NODE POINTS = 1701
NUMBER OF ELEMENTS = 2853
SCALE
3000 0 3000 6000
FEET
FINITE ELEMENT GRID
GRID 3

PLATE 7

PLATE 8

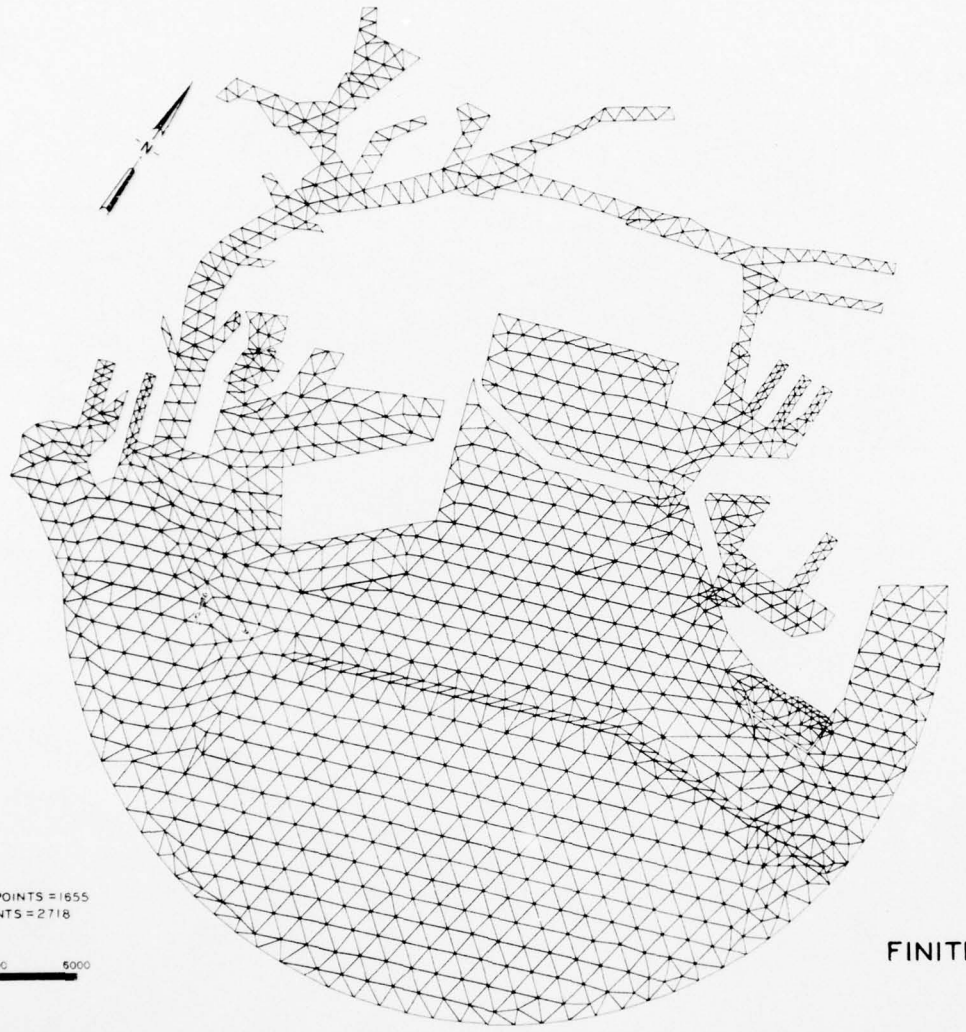

NOTE: NUMBER OF NODE POINTS = 1655
NUMBER OF ELEMENTS = 2718

SCALE

3000 0 3000 5000

FEET

FINITE ELEMENT GRID

GRID 3A

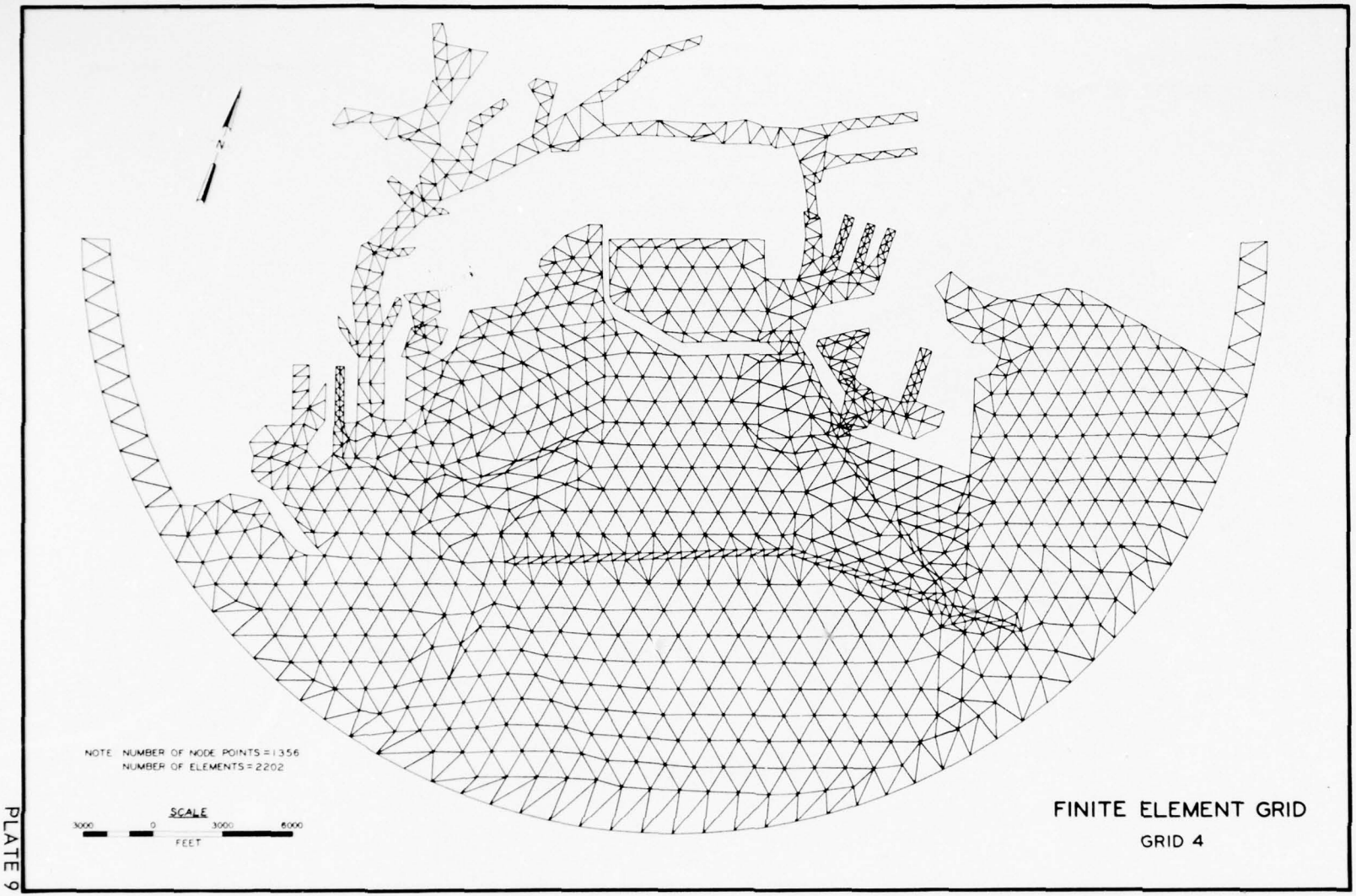

FINITE ELEMENT GRID

GRID 4

PLATE 9

PLATE 10

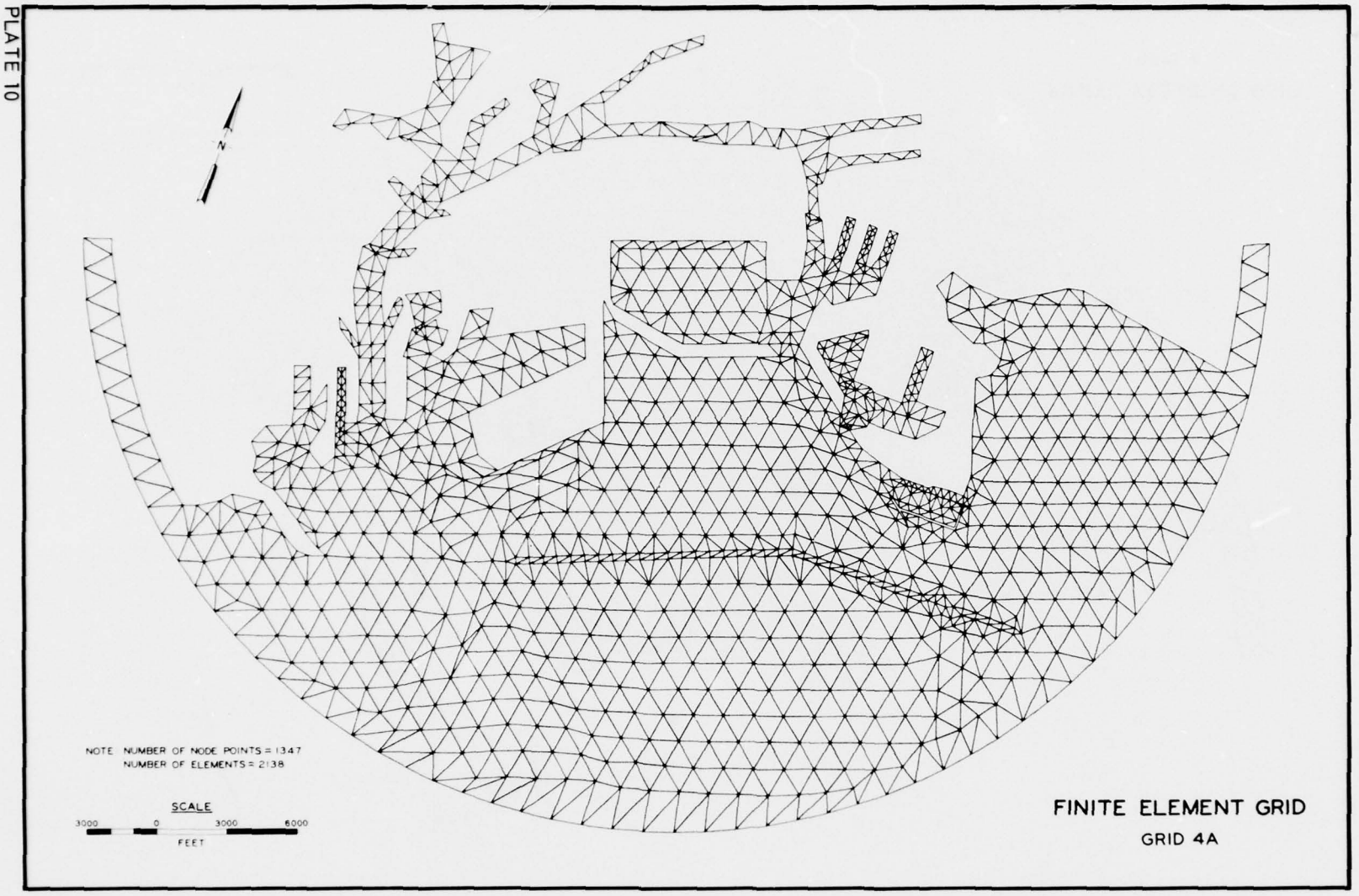

FINITE ELEMENT GRID

GRID 4A

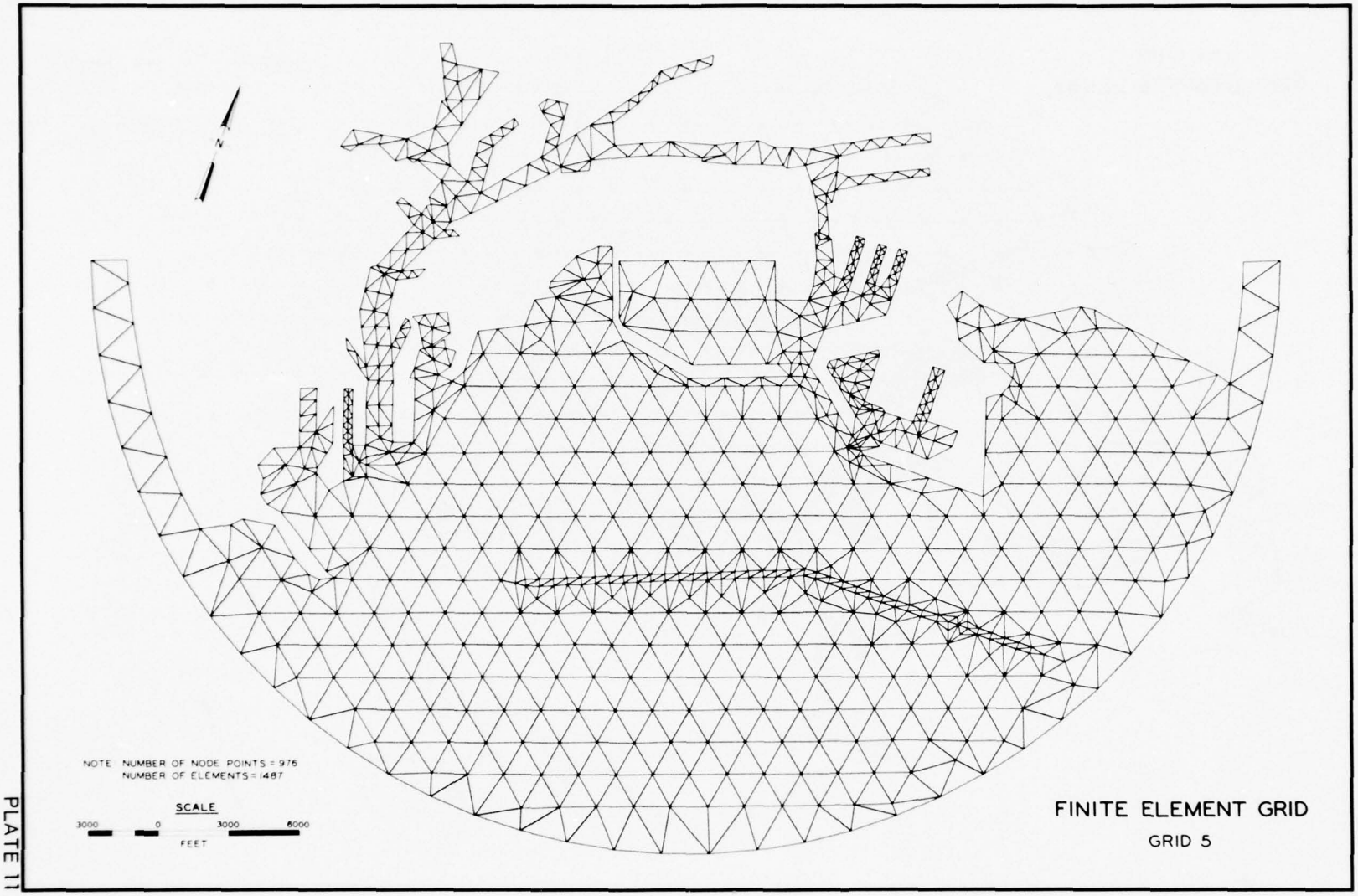

FINITE ELEMENT GRID

GRID 5

PLATE 11

PLATE 12

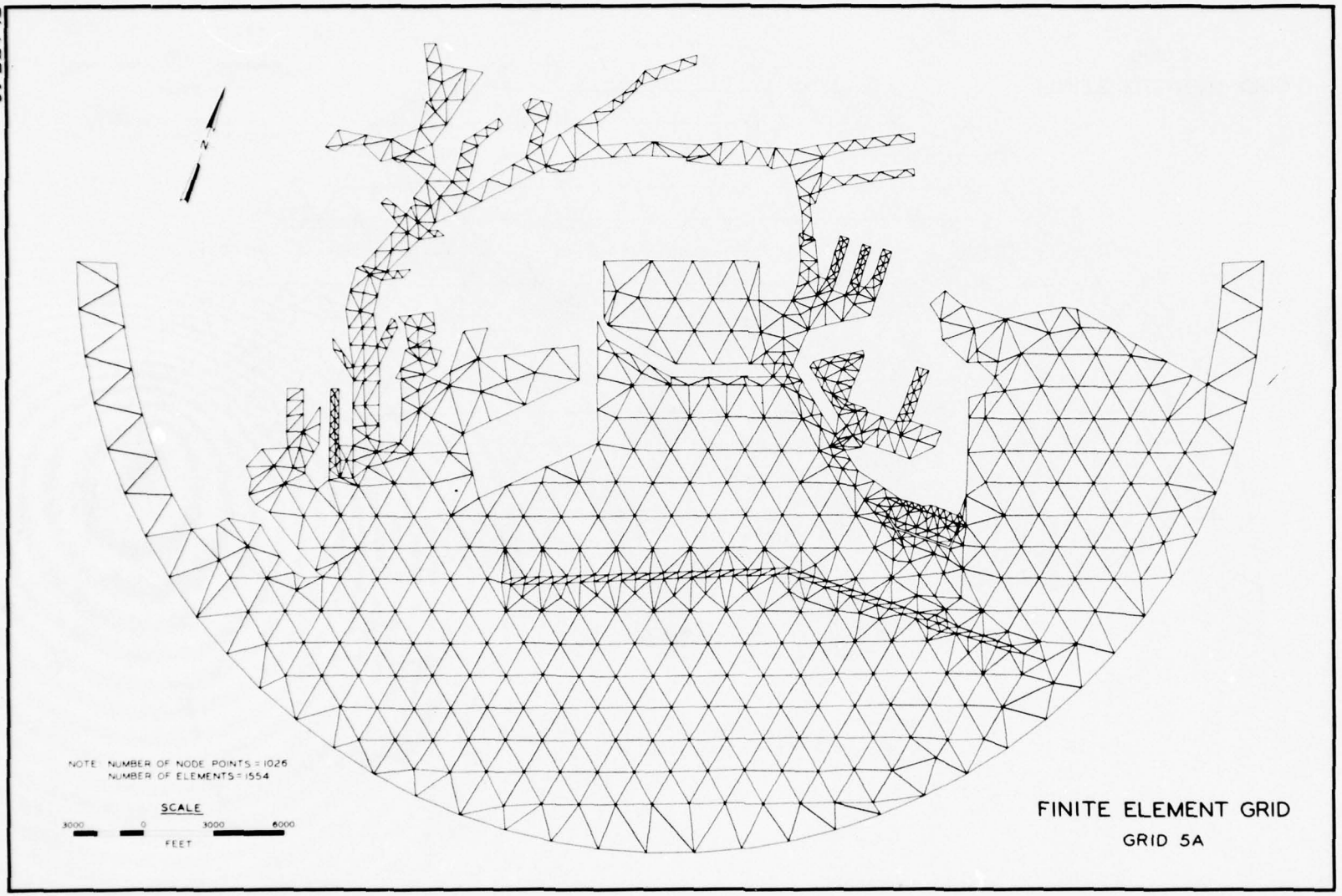

FINITE ELEMENT GRID

GRID 5A

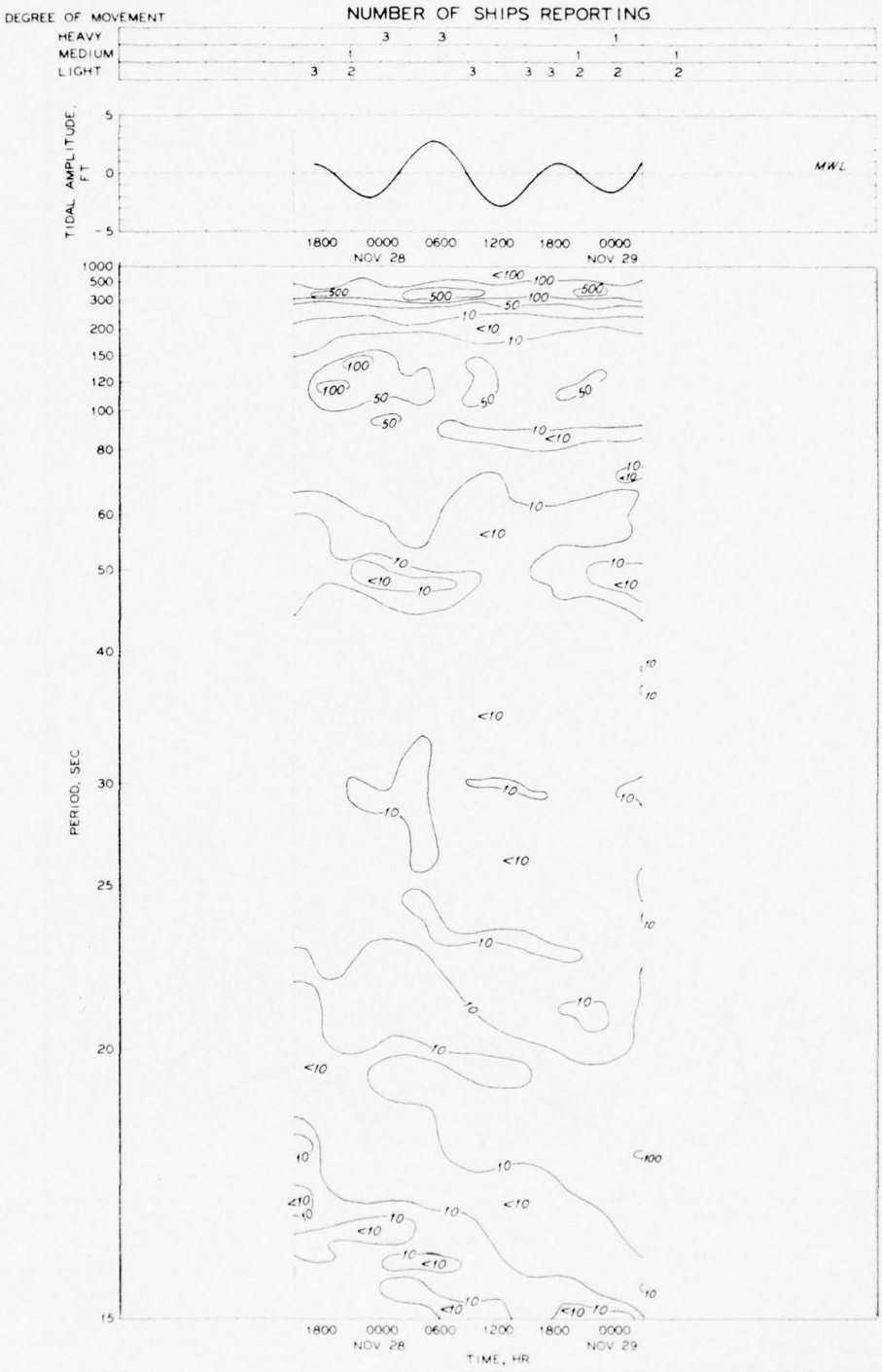

NOTE ENERGY UNITS = 10^{-2} FT^2-SEC
MLW = MEAN WATER LEVEL

CONTOURS OF TIME-DEPENDENT ENERGY SPECTRUM

1500 NOVEMBER 27 - 0300 NOVEMBER 29, 1971
GAGE 1 EAST CHANNEL

PLATE 13

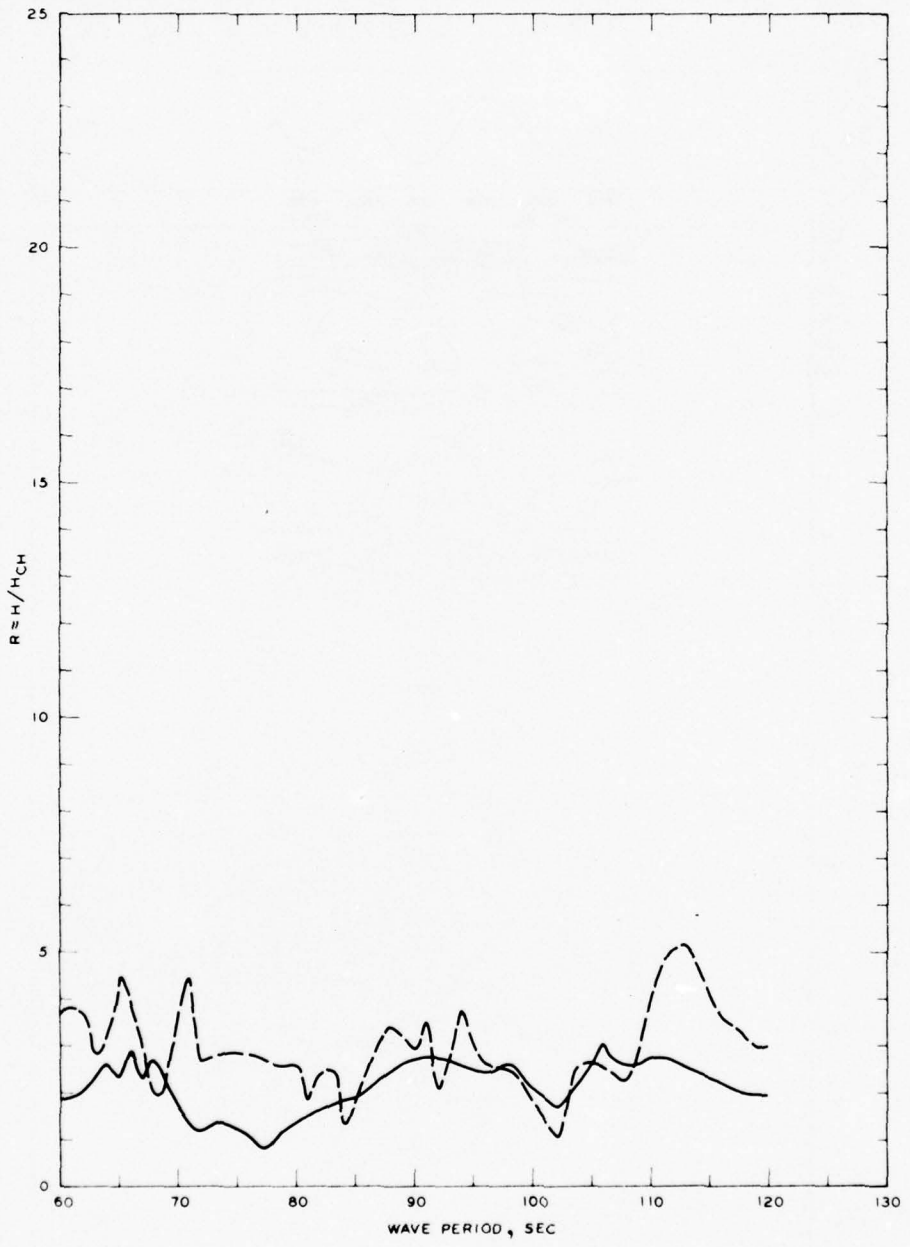

LEGEND

——— GRID I

— — — GRID IA

NOTE R = WAVE-HEIGHT AMPLIFICATION FACTOR
H = WAVE HEIGHT, FT
H_{CH} = WAVE HEIGHT FOR CLOSED HARBOR, FT

FREQUENCY RESPONSE

WAVE-HEIGHT AMPLIFICATION FACTOR
GAGE 1, GRIDS I AND IA

PLATE 14

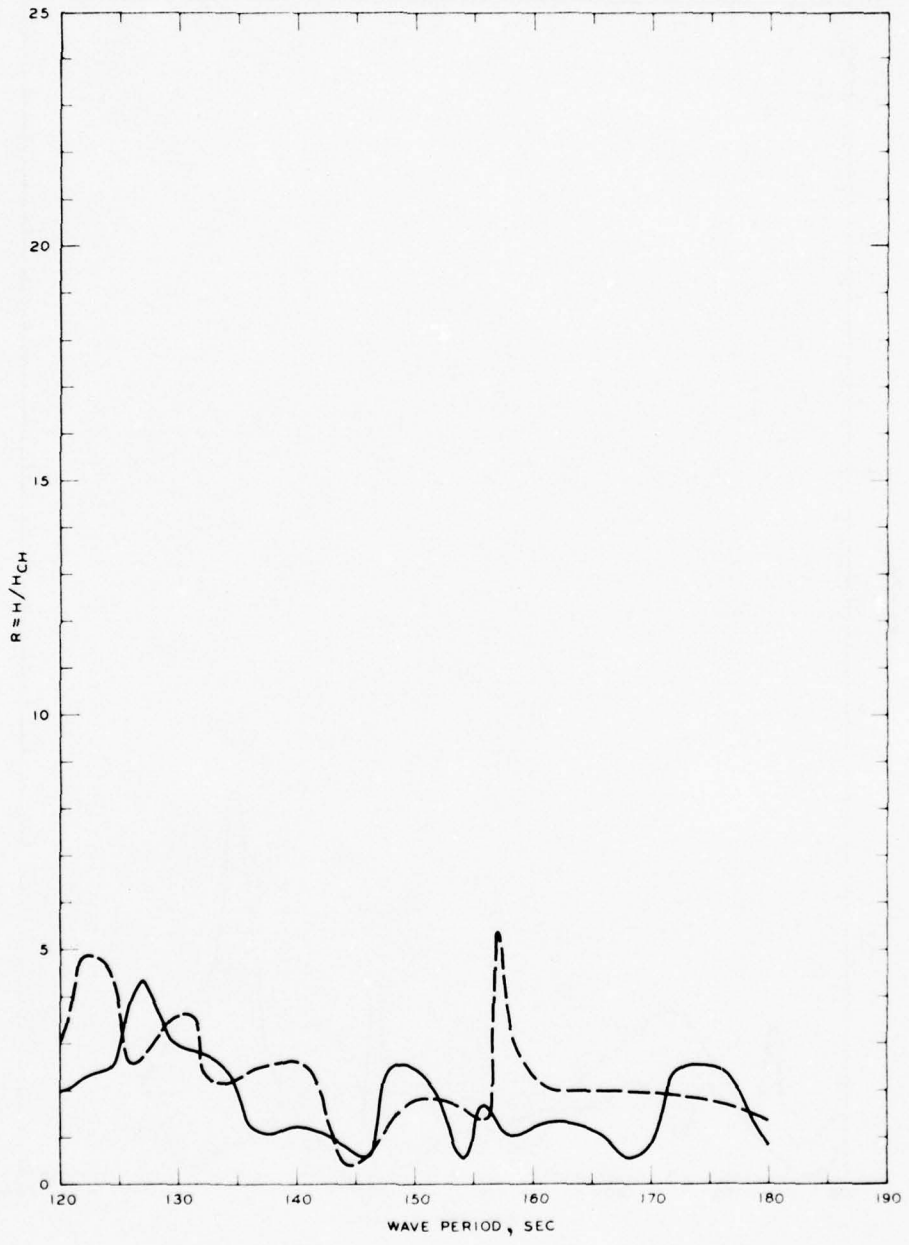

LEGEND

——— GRID 2

— — — GRID 2A

NOTE R = WAVE-HEIGHT AMPLIFICATION FACTOR
H = WAVE HEIGHT, FT
H_{CH} = WAVE HEIGHT FOR CLOSED HARBOR, FT

FREQUENCY RESPONSE

WAVE-HEIGHT AMPLIFICATION FACTOR
GAGE 1, GRIDS 2 AND 2A

PLATE 15

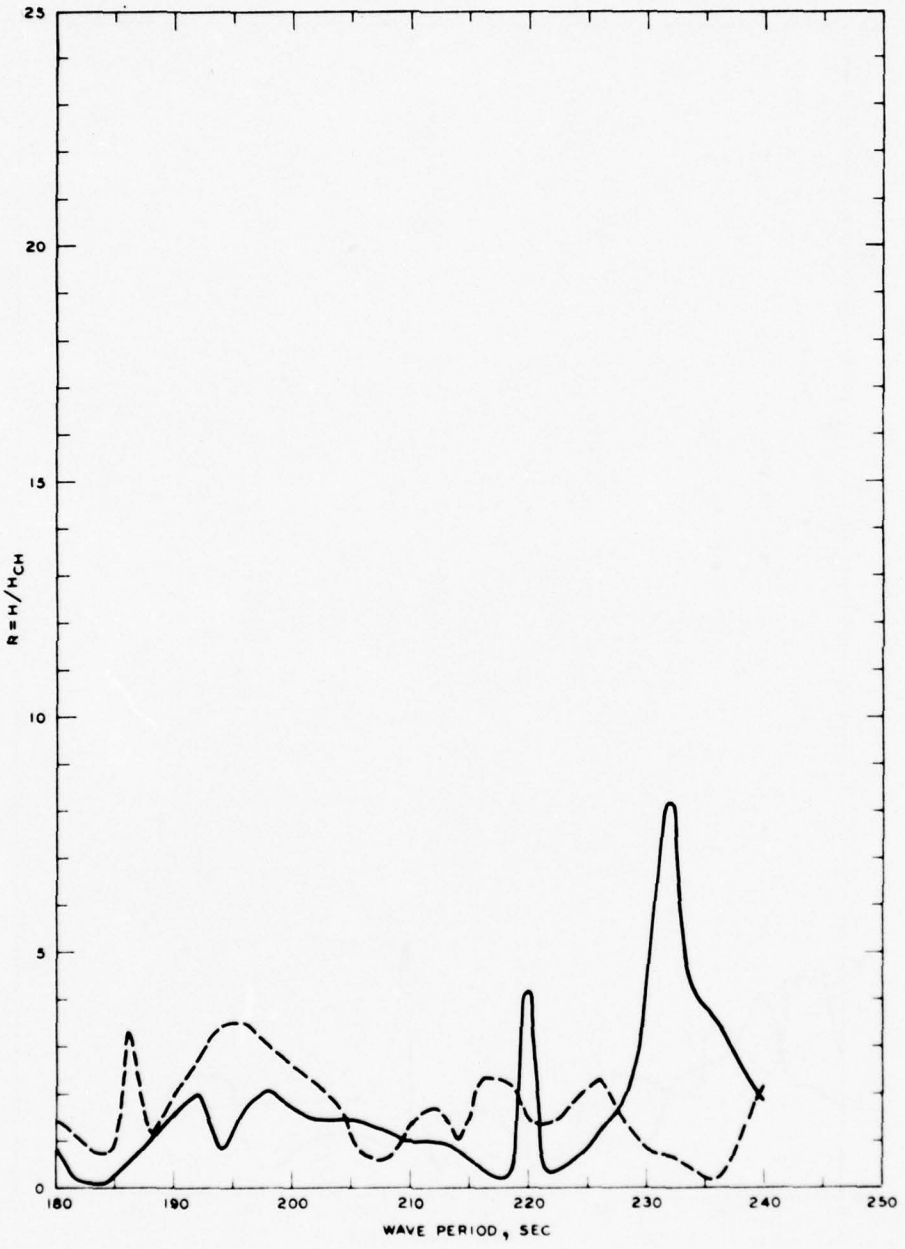

LEGEND

——— GRID 3

— — — GRID 3A

NOTE R = WAVE-HEIGHT AMPLIFICATION FACTOR
H = WAVE HEIGHT, FT
H_{CH} = WAVE HEIGHT FOR CLOSED HARBOR, FT

FREQUENCY RESPONSE

WAVE-HEIGHT AMPLIFICATION FACTOR
GAGE 1, GRIDS 3 AND 3A

PLATE 16

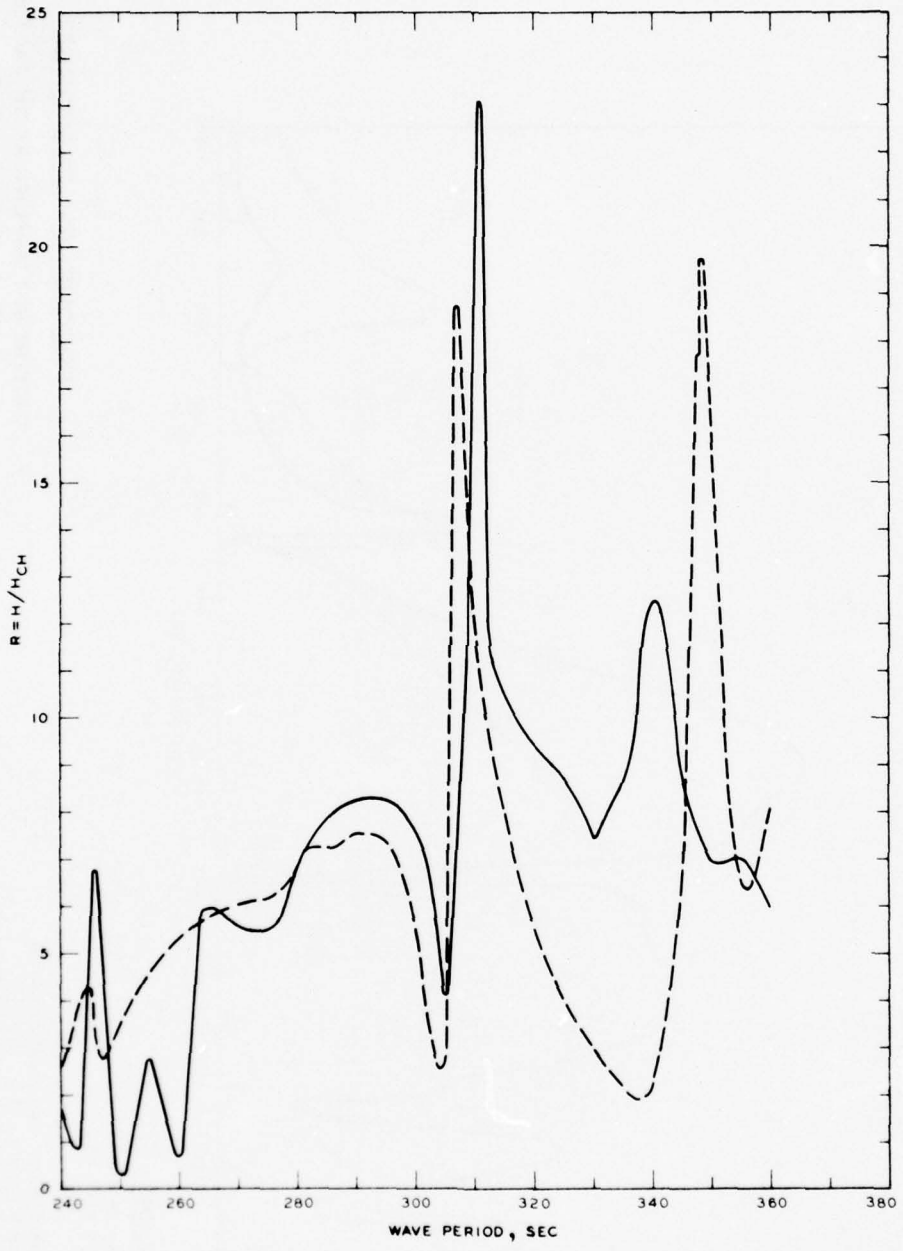

LEGEND

——— GRID 4

— — — GRID 4A

NOTE R = WAVE-HEIGHT AMPLIFICATION FACTOR
H = WAVE HEIGHT, FT
H_{CH} = WAVE HEIGHT FOR CLOSED HARBOR, FT

FREQUENCY RESPONSE

WAVE-HEIGHT AMPLIFICATION FACTOR
GAGE 1, GRIDS 4 AND 4A

PLATE 17

PLATE 18

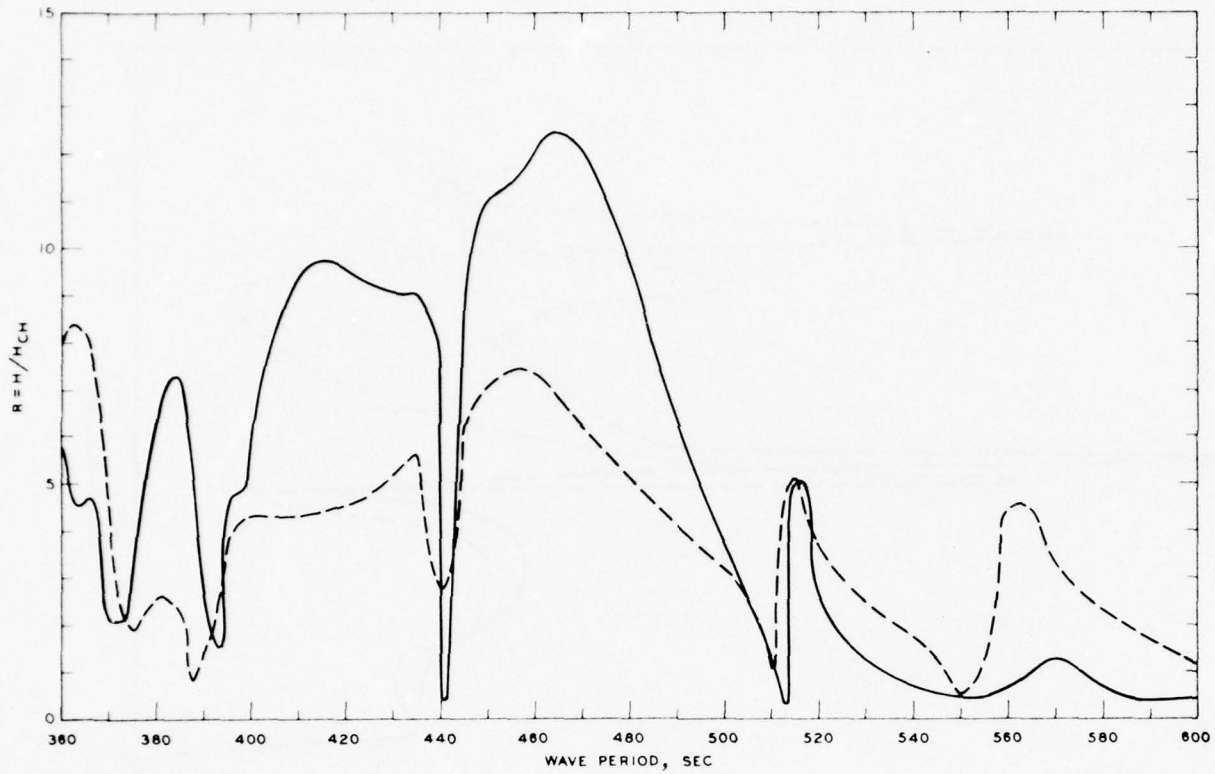

LEGEND

——— GRID 5

— — — GRID 5A

NOTE: R = WAVE-HEIGHT AMPLIFICATION FACTOR
H = WAVE HEIGHT, FT
H_{CH} = WAVE HEIGHT FOR CLOSED HARBOR, FT

FREQUENCY RESPONSE

WAVE-HEIGHT AMPLIFICATION FACTOR
GAGE 1, GRIDS 5 AND 5A

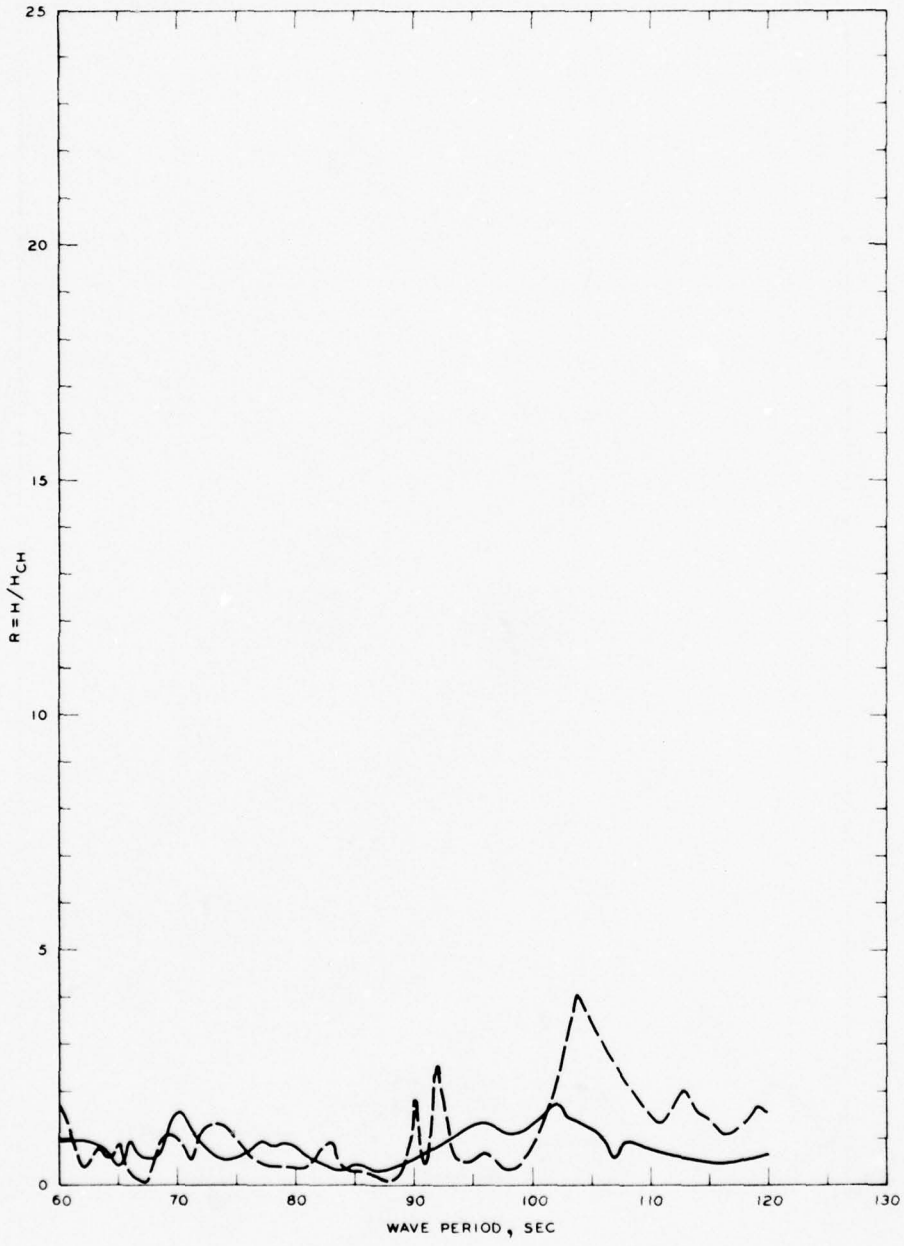

LEGEND

——— GRID 1

— — — GRID 1A

NOTE R = WAVE-HEIGHT AMPLIFICATION FACTOR
H = WAVE HEIGHT, FT
H_{CH} = WAVE HEIGHT FOR CLOSED HARBOR, FT

FREQUENCY RESPONSE

WAVE-HEIGHT AMPLIFICATION FACTOR
GAGE 2, GRIDS 1 AND 1A

PLATE 19

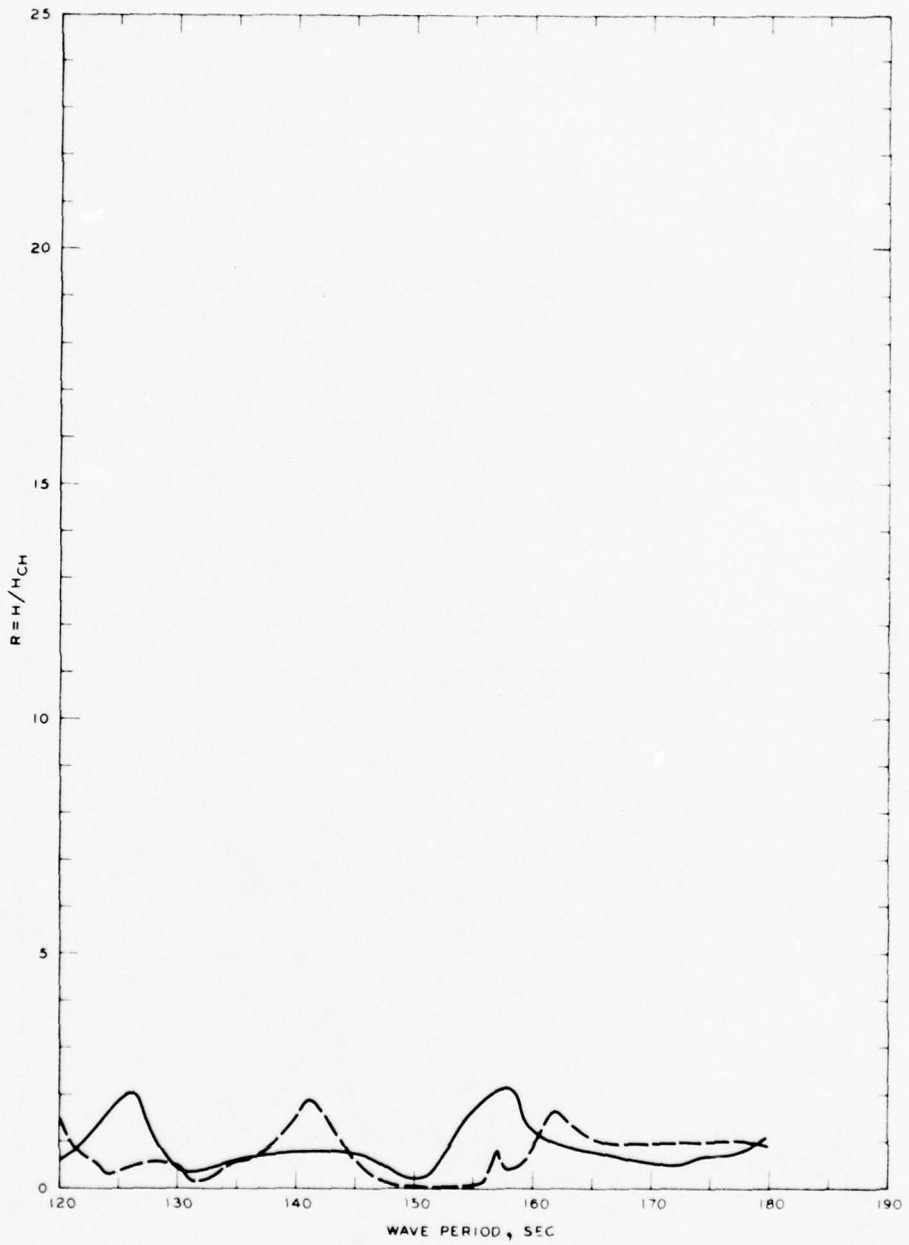

LEGEND

——— GRID 2

– – – GRID 2A

NOTE R = WAVE-HEIGHT AMPLIFICATION FACTOR
H = WAVE HEIGHT, FT
H_{CH} = WAVE HEIGHT FOR CLOSED HARBOR, FT

FREQUENCY RESPONSE

WAVE-HEIGHT AMPLIFICATION FACTOR
GAGE 2, GRIDS 2 AND 2A

PLATE 20

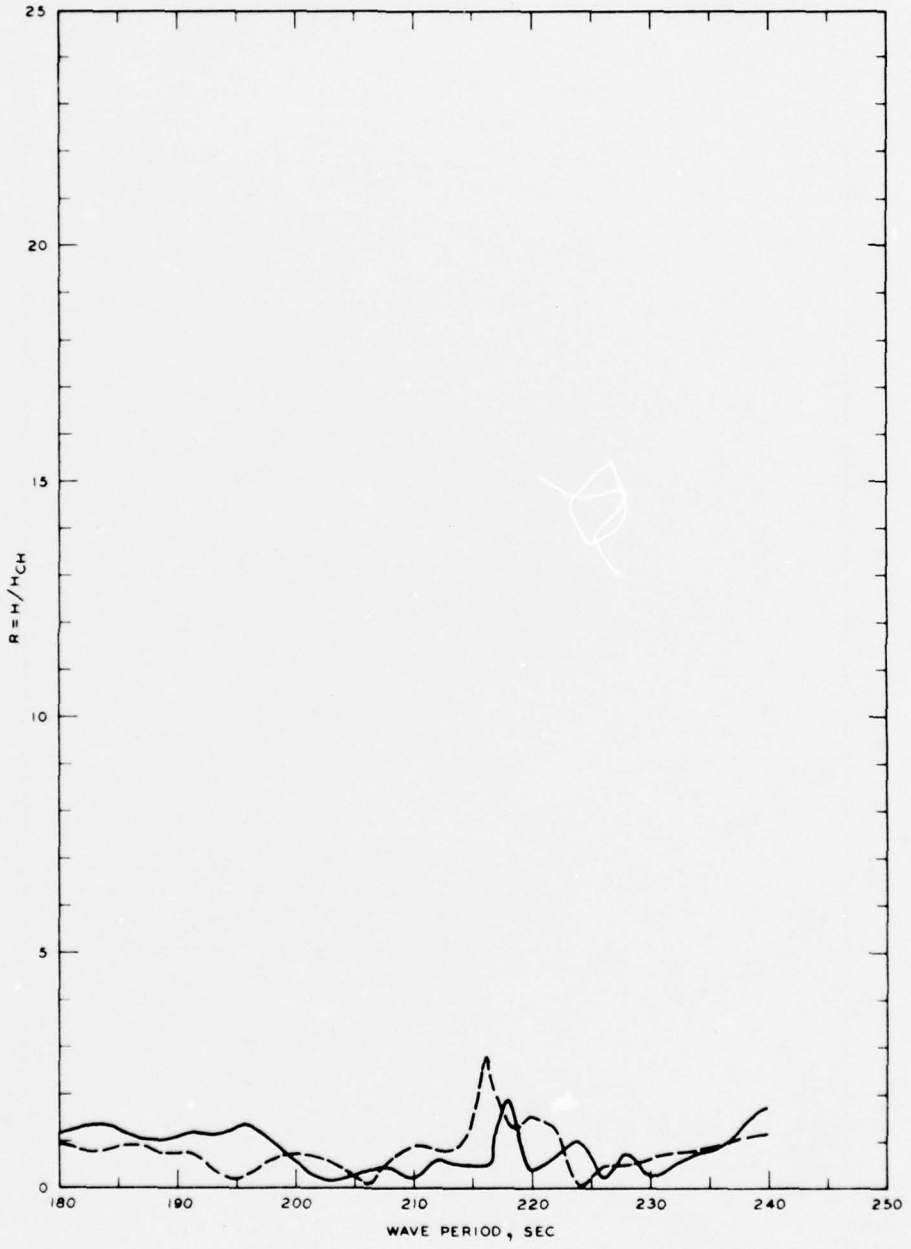

LEGEND

——— GRID 3

– – – GRID 3A

NOTE R = WAVE-HEIGHT AMPLIFICATION FACTOR
H = WAVE HEIGHT, FT
H_{CH} = WAVE HEIGHT FOR CLOSED HARBOR, FT

FREQUENCY RESPONSE

WAVE-HEIGHT AMPLIFICATION FACTOR
GAGE 2, GRIDS 3 AND 3A

PLATE 21

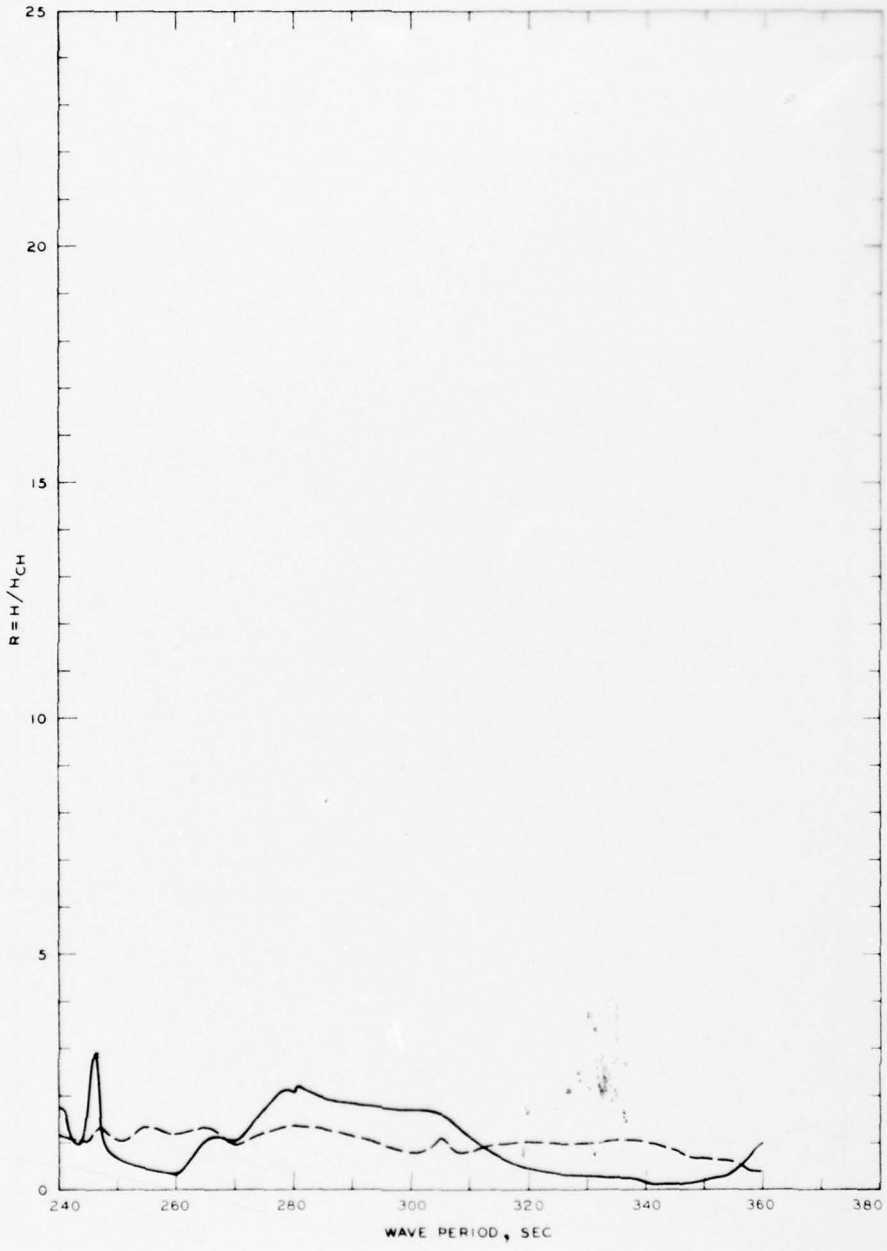

LEGEND

——— GRID 4

— — — GRID 4A

NOTE R = WAVE-HEIGHT AMPLIFICATION FACTOR
H = WAVE HEIGHT, FT
H_{CH} = WAVE HEIGHT FOR CLOSED HARBOR, FT

FREQUENCY RESPONSE

WAVE-HEIGHT AMPLIFICATION FACTOR
GAGE 2, GRIDS 4 AND 4A

PLATE 22

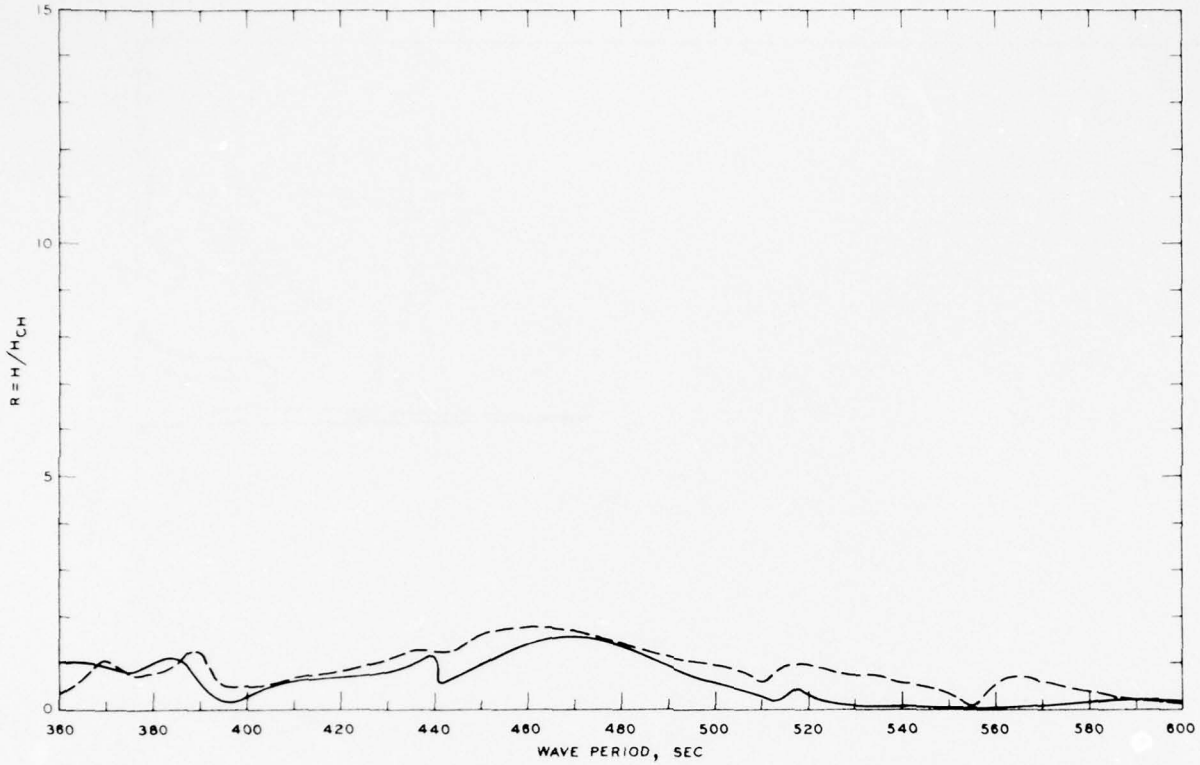

LEGEND

——— GRID 5

— — — GRID 5A

NOTE: R = WAVE-HEIGHT AMPLIFICATION FACTOR
H = WAVE HEIGHT, FT
H_{CH} = WAVE HEIGHT FOR CLOSED HARBOR, FT

FREQUENCY RESPONSE

WAVE-HEIGHT AMPLIFICATION FACTOR
GAGE 2, GRIDS 5 AND 5A

PLATE 23

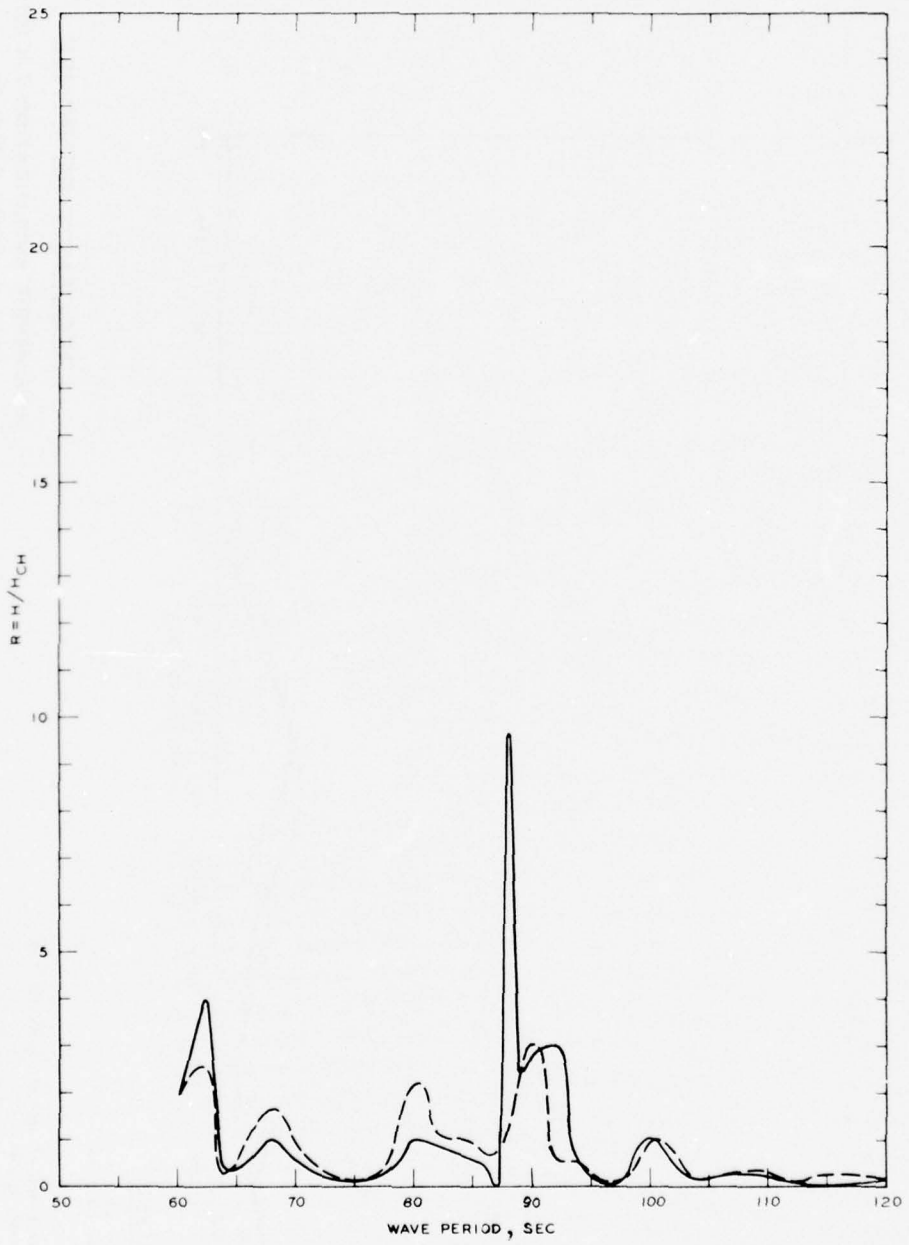

LEGEND

——— GRID 1

— — — GRID 1A

NOTE R = WAVE-HEIGHT AMPLIFICATION FACTOR
H = WAVE HEIGHT, FT
H_{CH} = WAVE HEIGHT FOR CLOSED HARBOR, FT

FREQUENCY RESPONSE

WAVE-HEIGHT AMPLIFICATION FACTOR
GAGE 5, GRIDS 1 AND 1A

PLATE 24

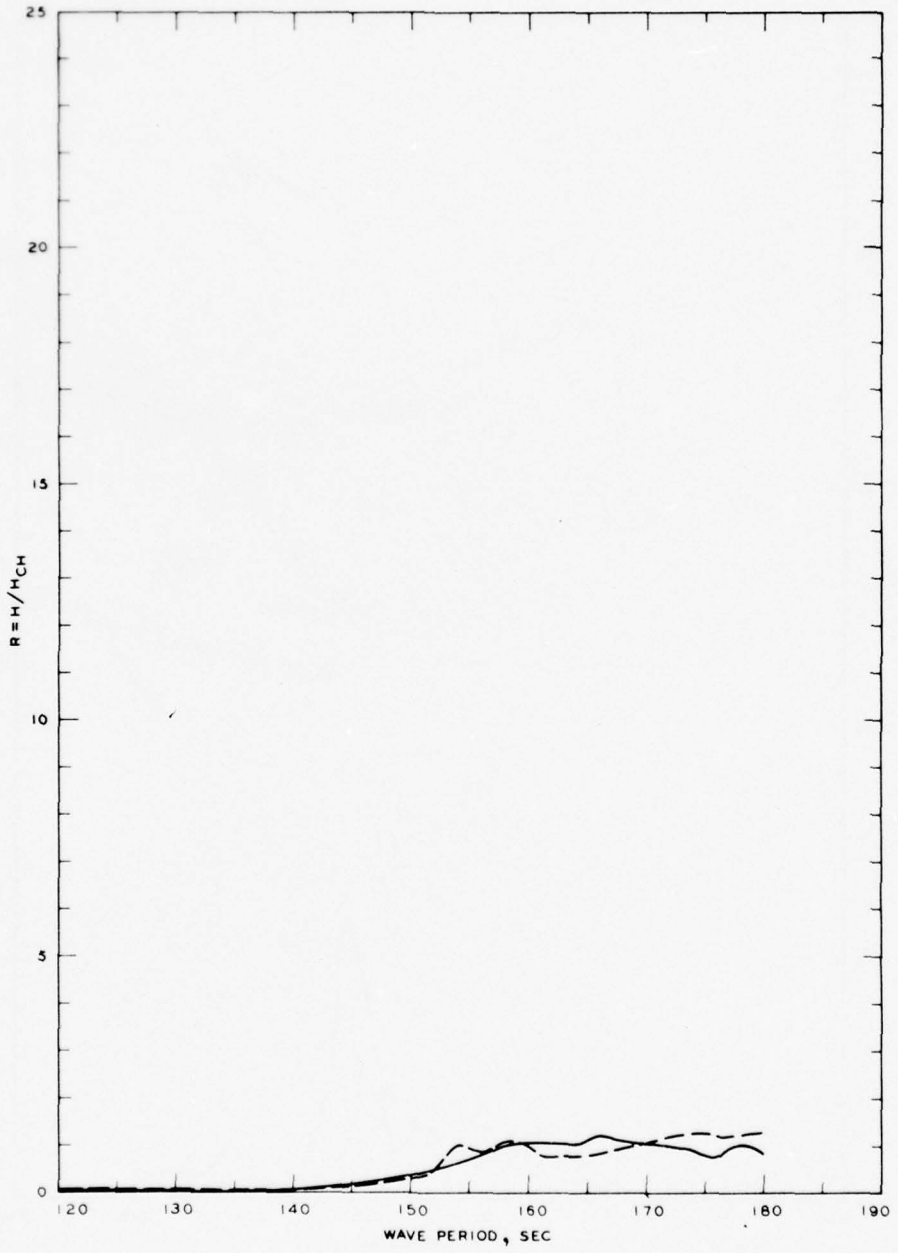

LEGEND

——— GRID 2

— — — GRID 2A

NOTE R = WAVE-HEIGHT AMPLIFICATION FACTOR
H = WAVE HEIGHT, FT
H_{CH} = WAVE HEIGHT FOR CLOSED HARBOR, FT

FREQUENCY RESPONSE

WAVE-HEIGHT AMPLIFICATION FACTOR
GAGE 5, GRIDS 2 AND 2A

PLATE 25

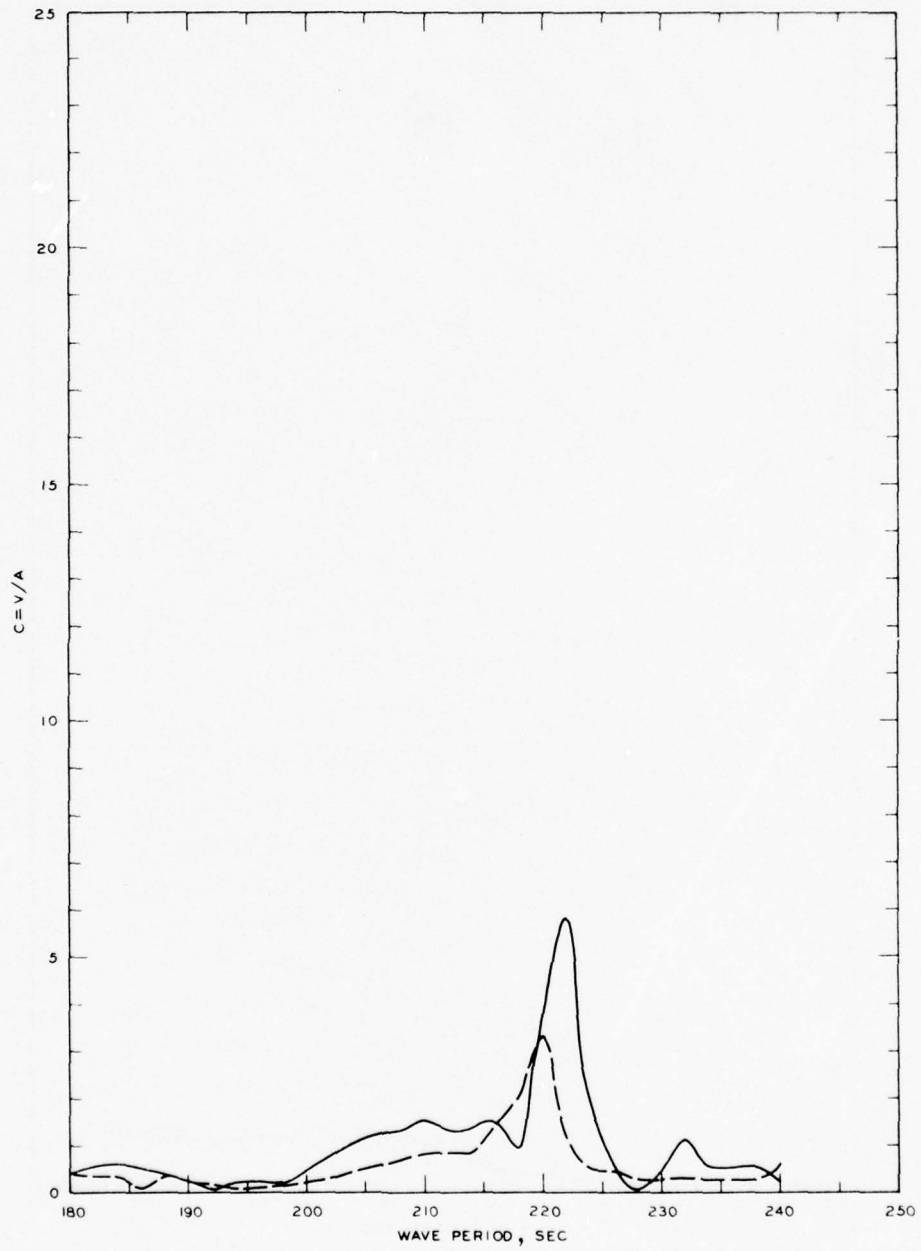

NOTE: C = NORMALIZED MAXIMUM CURRENT VELOCITY
V = CURRENT VELOCITY, FT/SEC
A = INCIDENT WAVE AMPLITUDE

FREQUENCY RESPONSE

NORMALIZED MAXIMUM CURRENT VELOCITY
GAGE 5, GRIDS 3 AND 3A

PLATE 26

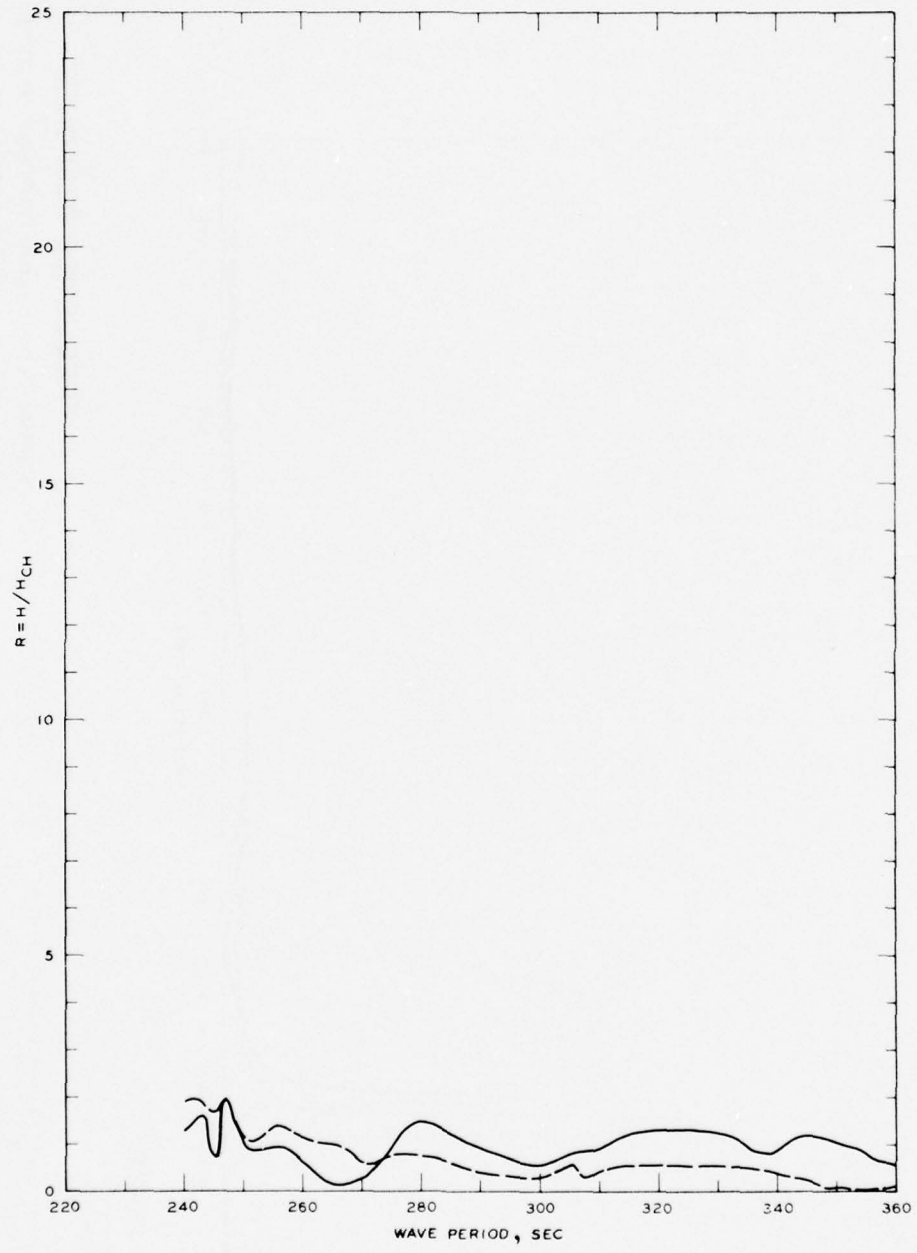

LEGEND

——— GRID 4

– – – GRID 4A

NOTE R = WAVE-HEIGHT AMPLIFICATION FACTOR
H = WAVE HEIGHT, FT
H_{CH} = WAVE HEIGHT FOR CLOSED HARBOR, FT

FREQUENCY RESPONSE

WAVE-HEIGHT AMPLIFICATION FACTOR
GAGE 5, GRIDS 4 AND 4A

PLATE 27

PLATE 28

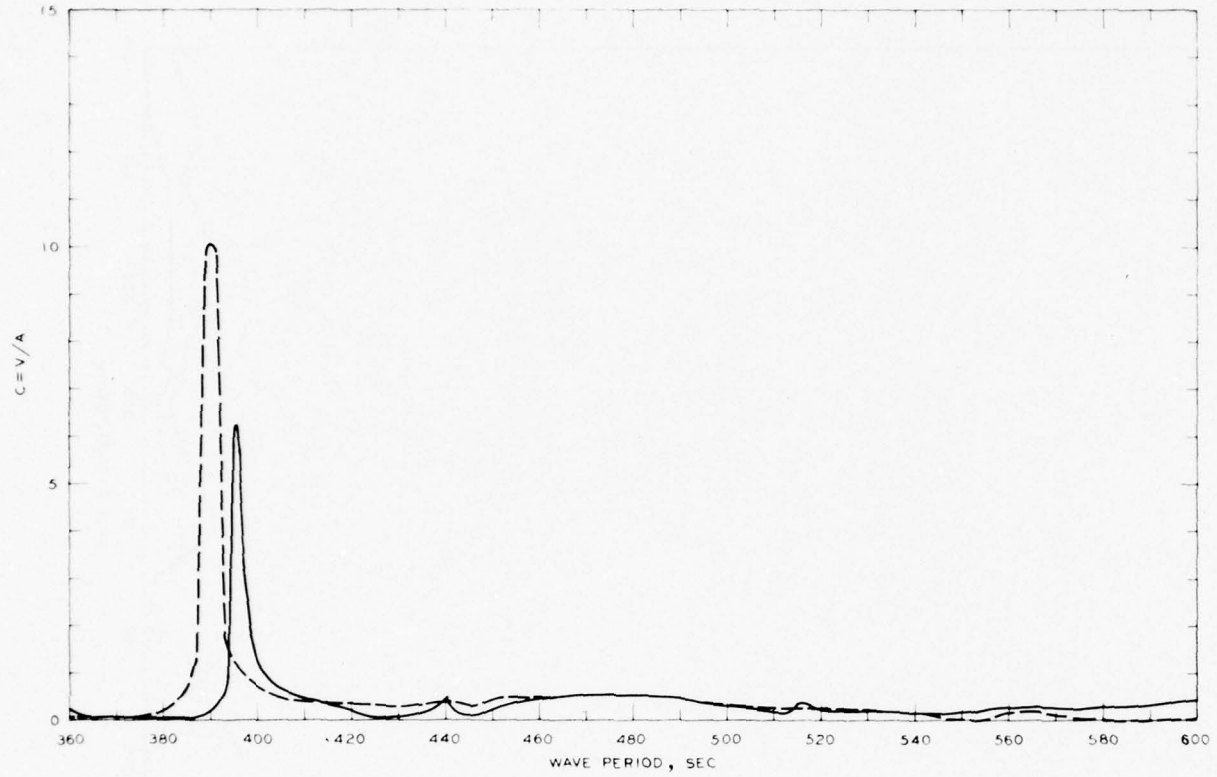

LEGEND

——— GRID 5

— — — GRID 5A

NOTE: C = NORMALIZED MAXIMUM CURRENT VELOCITY
V = CURRENT VELOCITY, FT/SEC
A = INCIDENT WAVE AMPLITUDE

FREQUENCY RESPONSE

NORMALIZED MAXIMUM CURRENT VELOCITY
GAGE 5, GRIDS 5 AND 5A

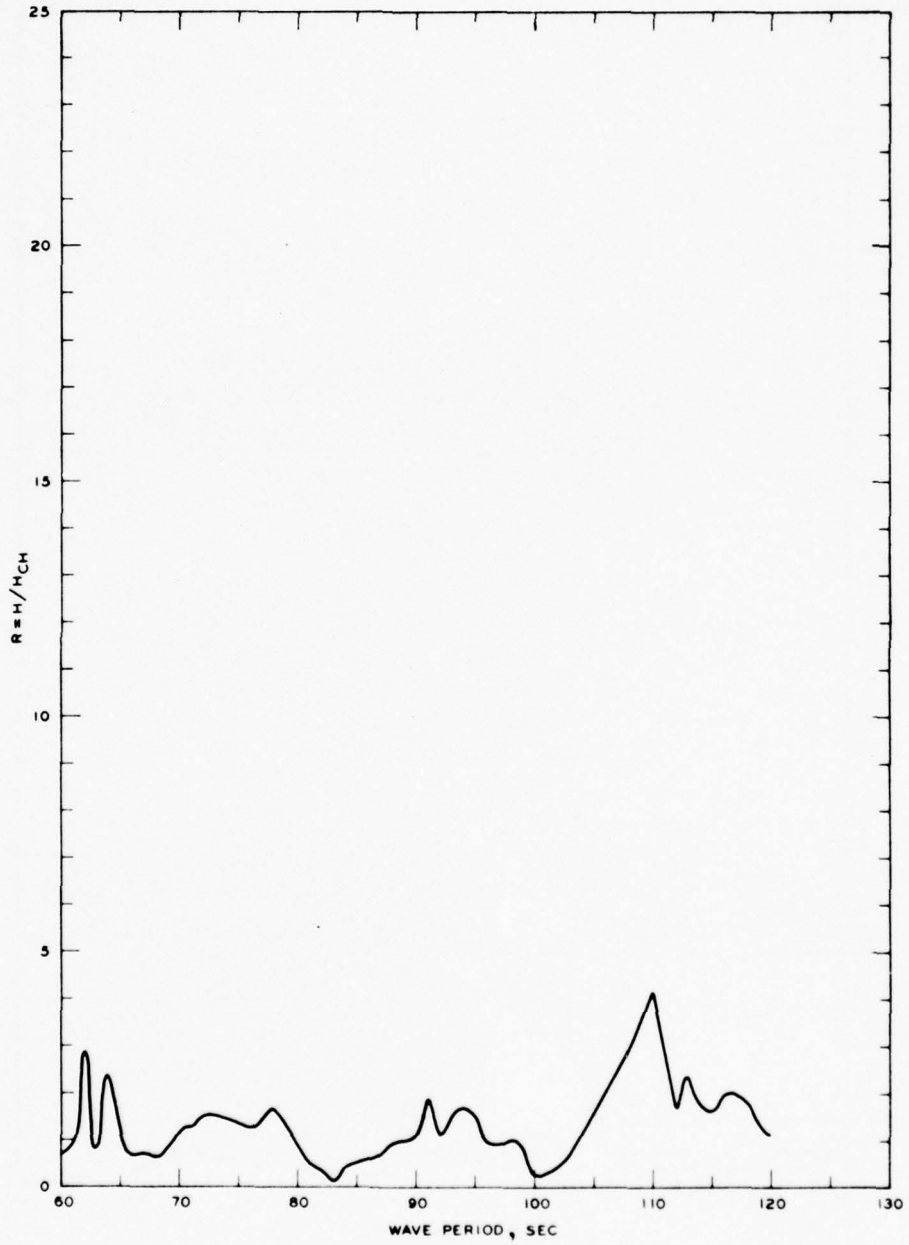

NOTE R = WAVE-HEIGHT AMPLIFICATION FACTOR
H = WAVE HEIGHT, FT
H_{CH} = WAVE HEIGHT FOR CLOSED HARBOR, FT

FREQUENCY RESPONSE

WAVE-HEIGHT AMPLIFICATION FACTOR
STA 1, LNG SLIP, GRID 1A

PLATE 29

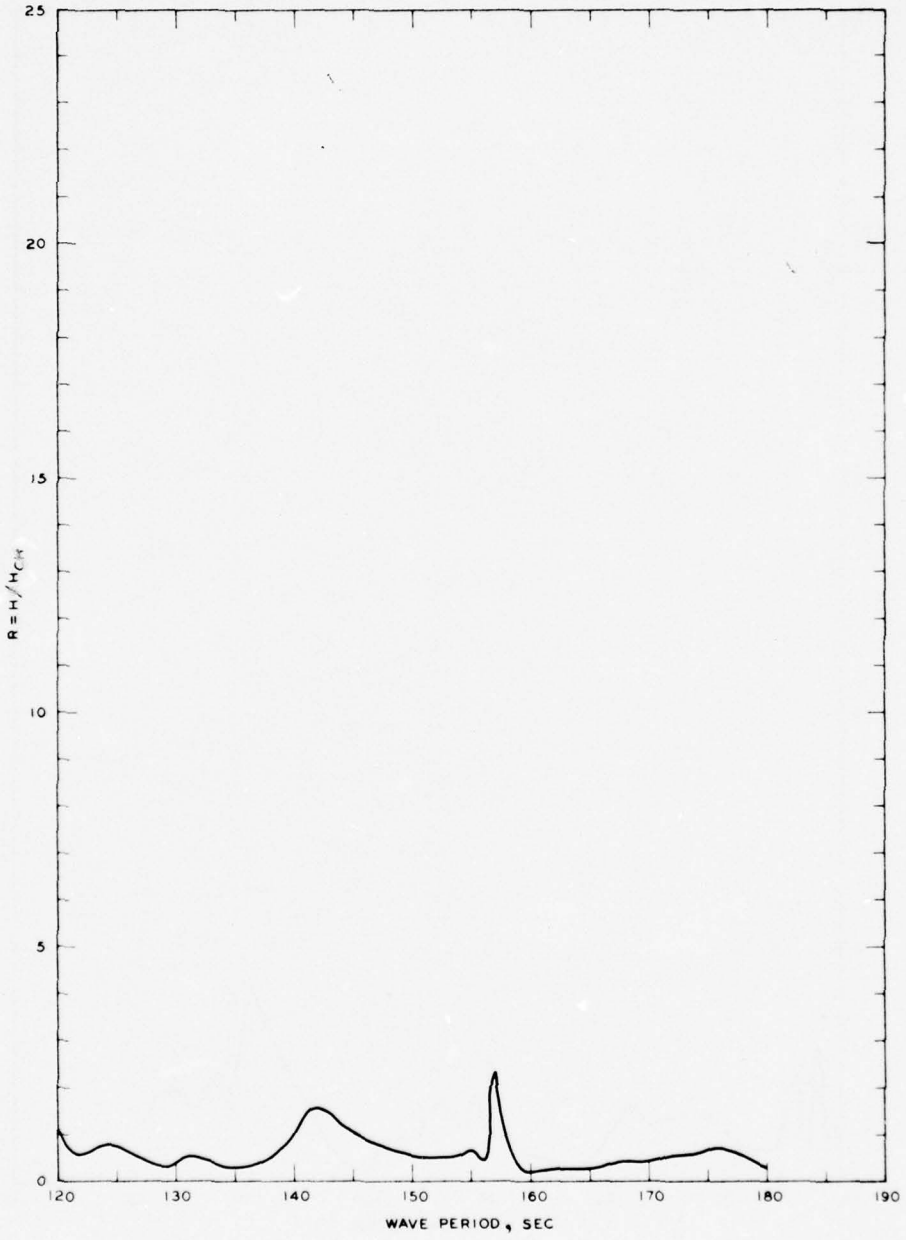

NOTE R = WAVE-HEIGHT AMPLIFICATION FACTOR
H = WAVE HEIGHT, FT
H_{CH} = WAVE HEIGHT FOR CLOSED HARBOR, FT

FREQUENCY RESPONSE

WAVE-HEIGHT AMPLIFICATION FACTOR
STA 1, LNG SLIP, GRID 2A

PLATE 30

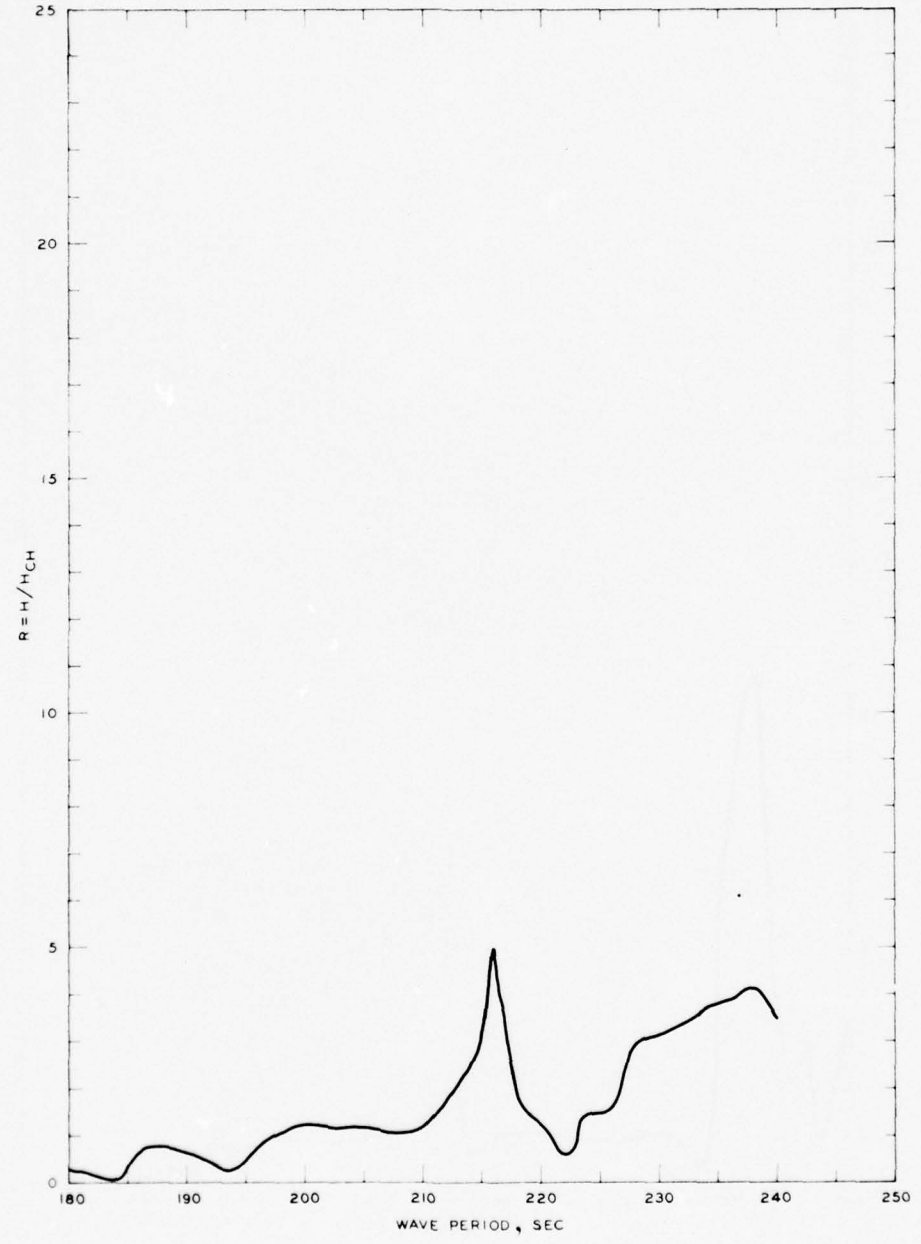

NOTE R = WAVE-HEIGHT AMPLIFICATION FACTOR
H = WAVE HEIGHT, FT
H_{CH} = WAVE HEIGHT FOR CLOSED HARBOR, FT

FREQUENCY RESPONSE

WAVE-HEIGHT AMPLIFICATION FACTOR
STA 1, LNG SLIP, GRID 3A

PLATE 31

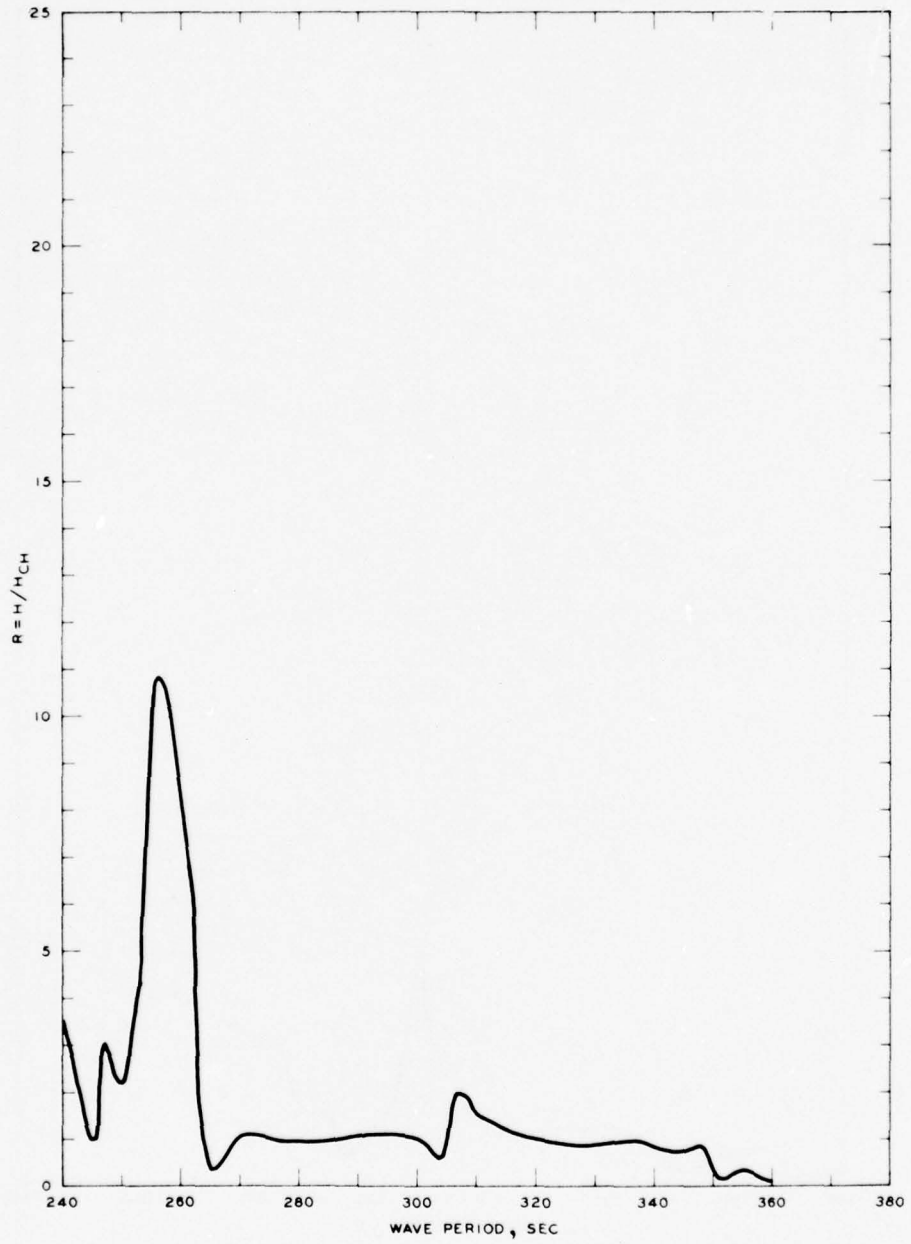

NOTE R = WAVE-HEIGHT AMPLIFICATION FACTOR
H = WAVE HEIGHT, FT
H_{CH} = WAVE HEIGHT FOR CLOSED HARBOR, FT

FREQUENCY RESPONSE

WAVE-HEIGHT AMPLIFICATION FACTOR
STA 1, LNG SLIP, GRID 4A

PLATE 32

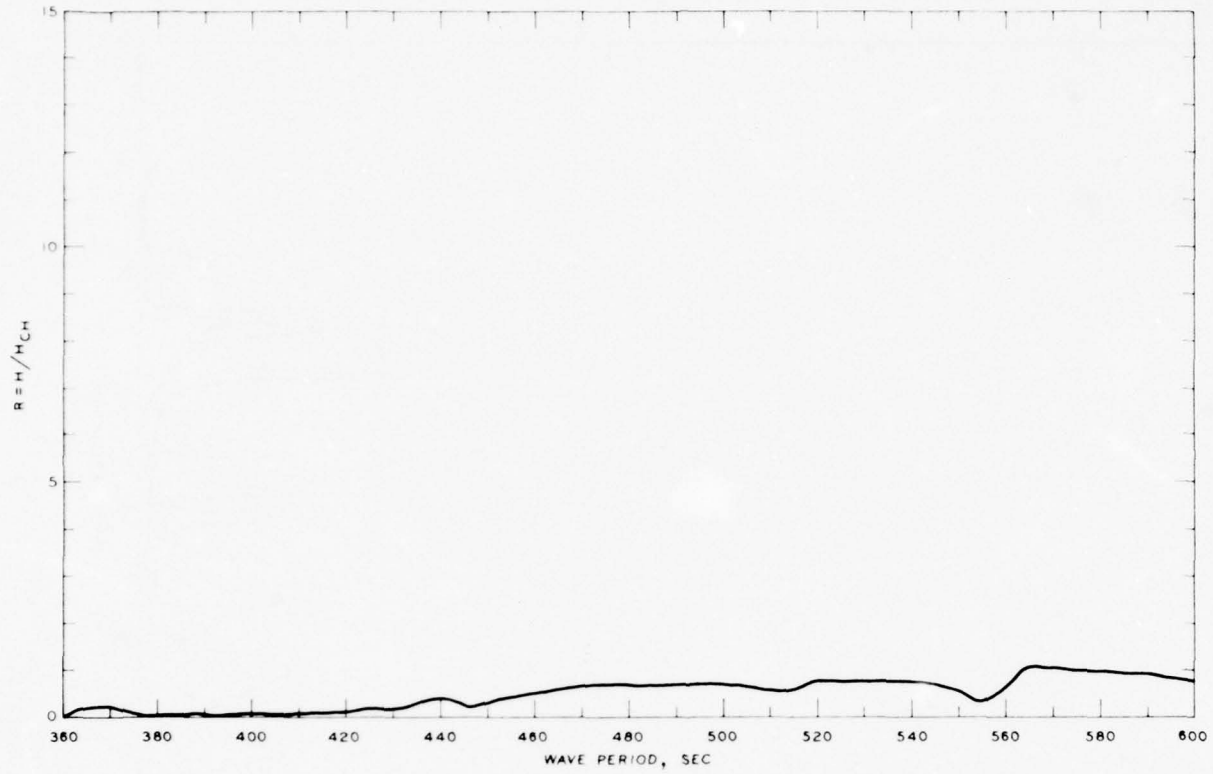

NOTE: R = WAVE-HEIGHT AMPLIFICATION FACTOR
H = WAVE HEIGHT, FT
H_{CH} = WAVE HEIGHT FOR CLOSED HARBOR, FT

FREQUENCY RESPONSE

WAVE-HEIGHT AMPLIFICATION FACTOR

STA 1, LNG SLIP, GRID 5A

PLATE 33

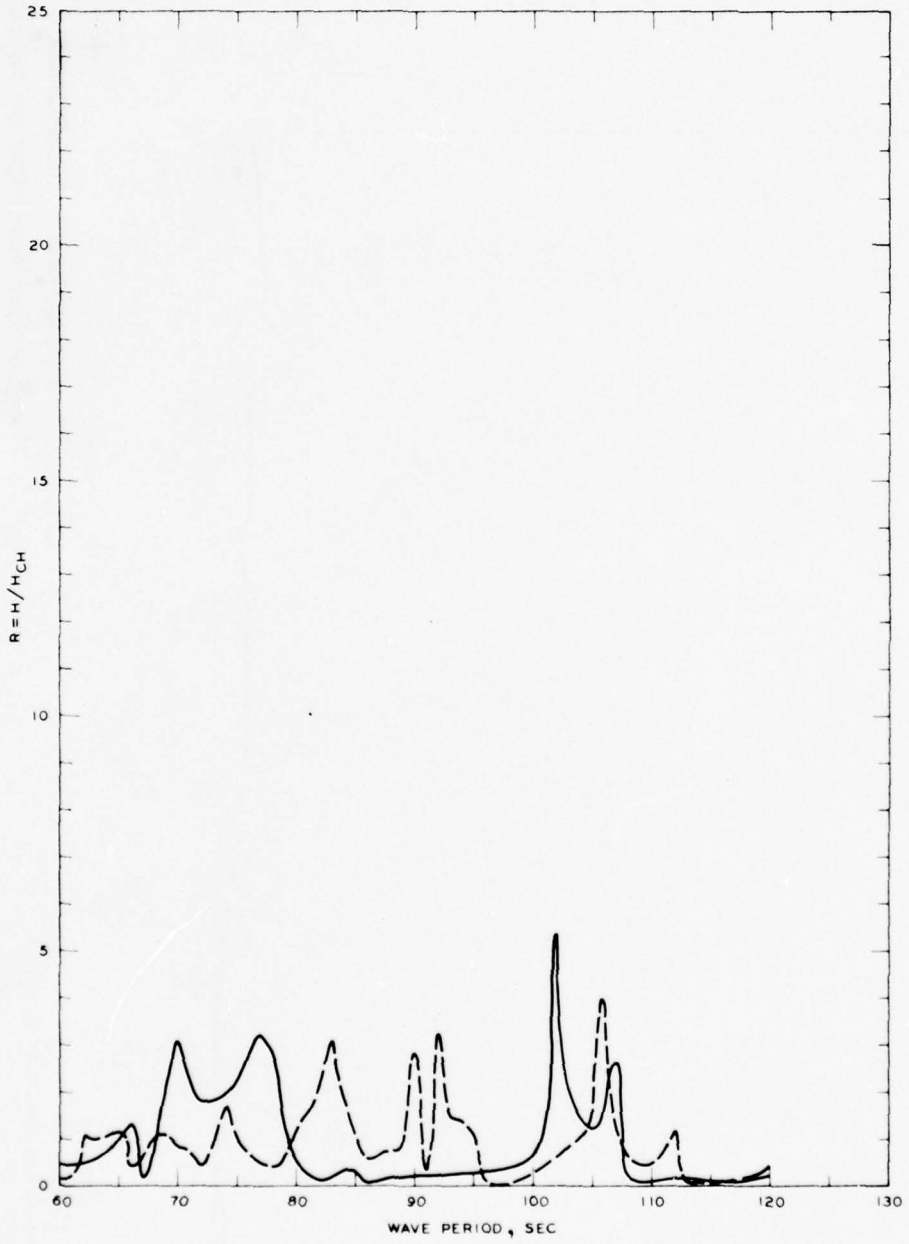

LEGEND

——— GRID I

— — — GRID IA

NOTE R = WAVE-HEIGHT AMPLIFICATION FACTOR
H = WAVE HEIGHT, FT
H_{CH} = WAVE HEIGHT FOR CLOSED HARBOR, FT

FREQUENCY RESPONSE

WAVE-HEIGHT AMPLIFICATION FACTOR
STA LA-1, GRIDS I AND IA

PLATE 34

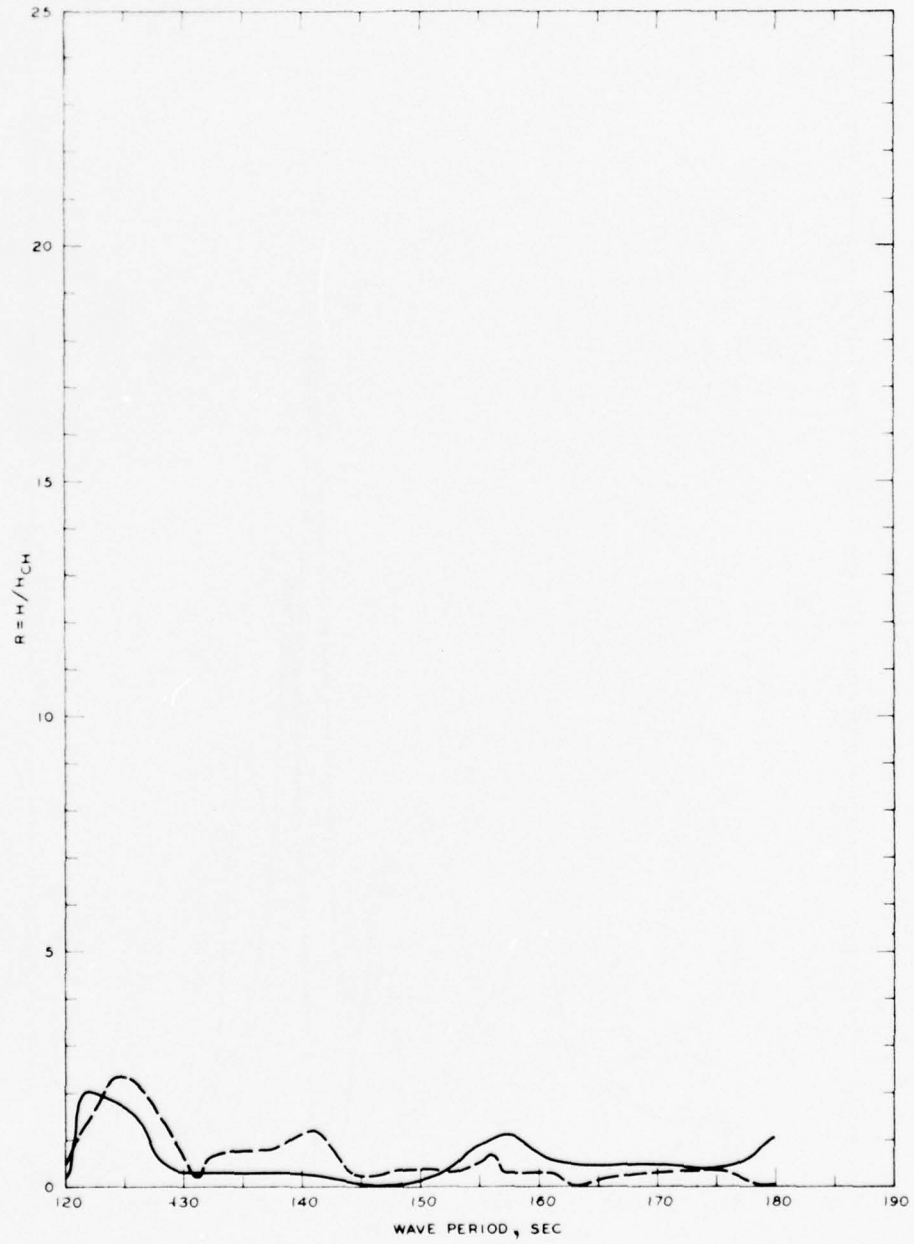

LEGEND

——— GRID 2

— — — GRID 2A

NOTE R = WAVE-HEIGHT AMPLIFICATION FACTOR
H = WAVE HEIGHT, FT
H_{CH} = WAVE HEIGHT FOR CLOSED HARBOR, FT

FREQUENCY RESPONSE

WAVE-HEIGHT AMPLIFICATION FACTOR
STA LA-1, GRIDS 2 AND 2A

PLATE 35

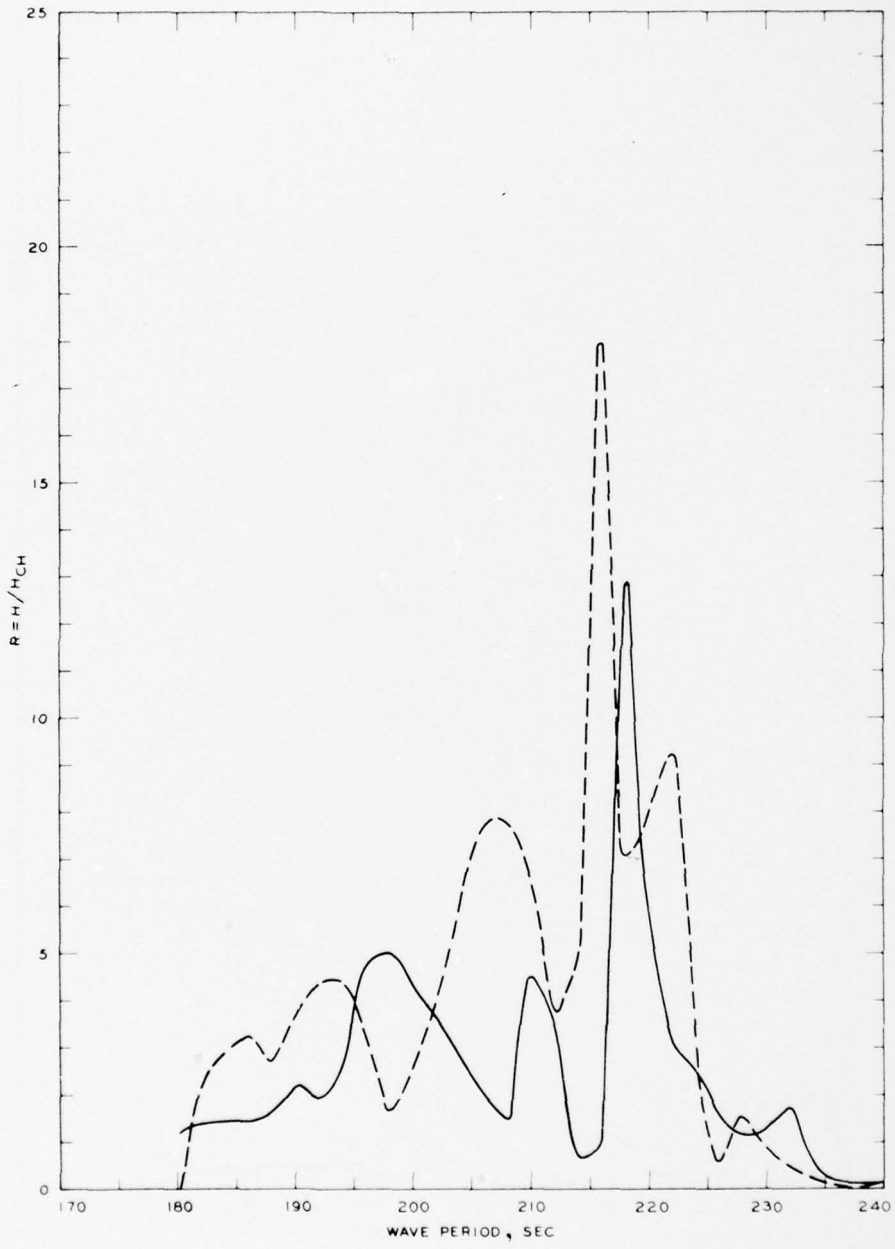

LEGEND

——— GRID 3

— — — GRID 3A

NOTE R = WAVE-HEIGHT AMPLIFICATION FACTOR
H = WAVE HEIGHT, FT
H_{CH} = WAVE HEIGHT FOR CLOSED HARBOR, FT

FREQUENCY RESPONSE

WAVE-HEIGHT AMPLIFICATION FACTOR
STA LA-1, GRIDS 3 AND 3A

PLATE 36

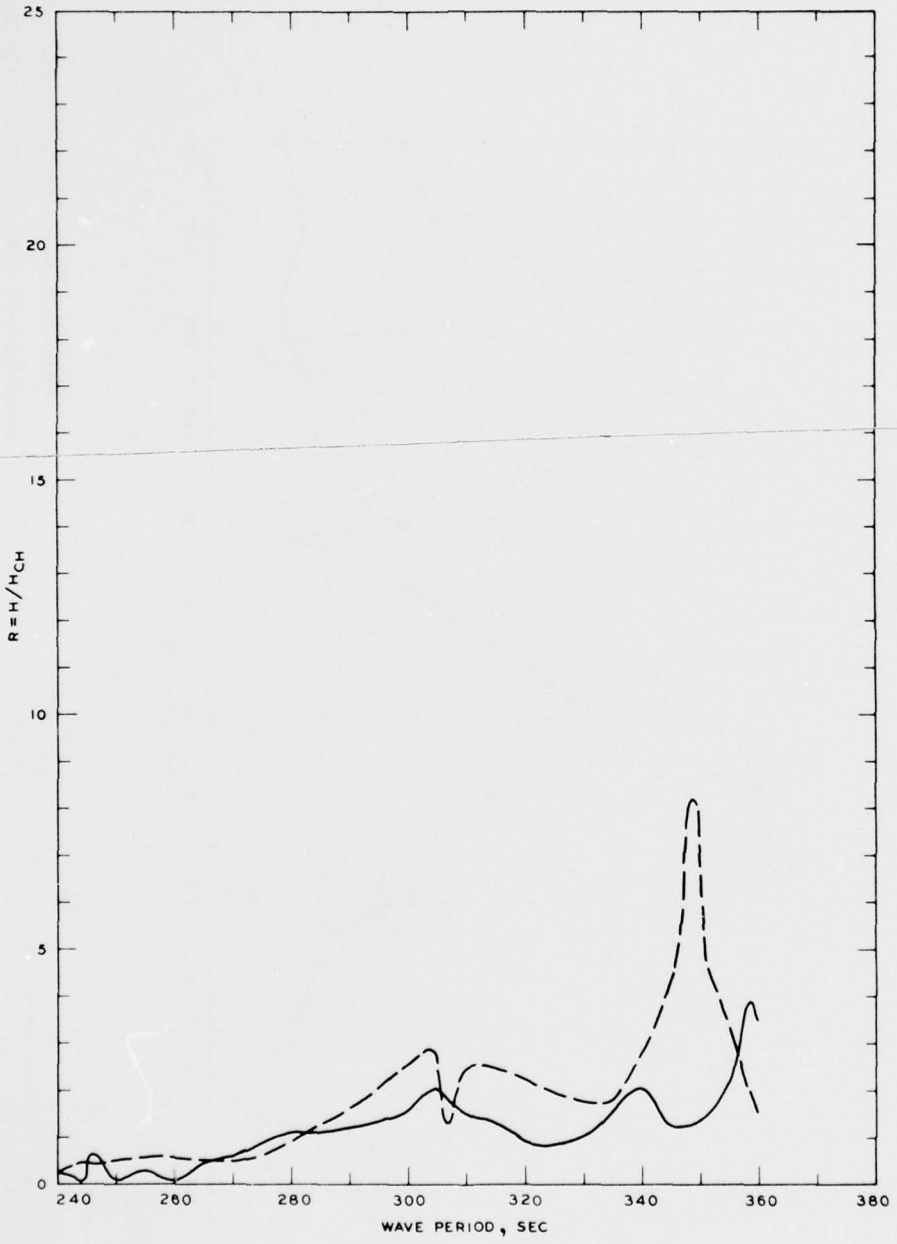

LEGEND

——— GRID 4

— — — GRID 4A

NOTE R = WAVE-HEIGHT AMPLIFICATION FACTOR
H = WAVE HEIGHT, FT
H_{CH} = WAVE HEIGHT FOR CLOSED HARBOR, FT

FREQUENCY RESPONSE

WAVE-HEIGHT AMPLIFICATION FACTOR
STA LA - 1, GRIDS 4 AND 4A

PLATE 37

PLATE 38

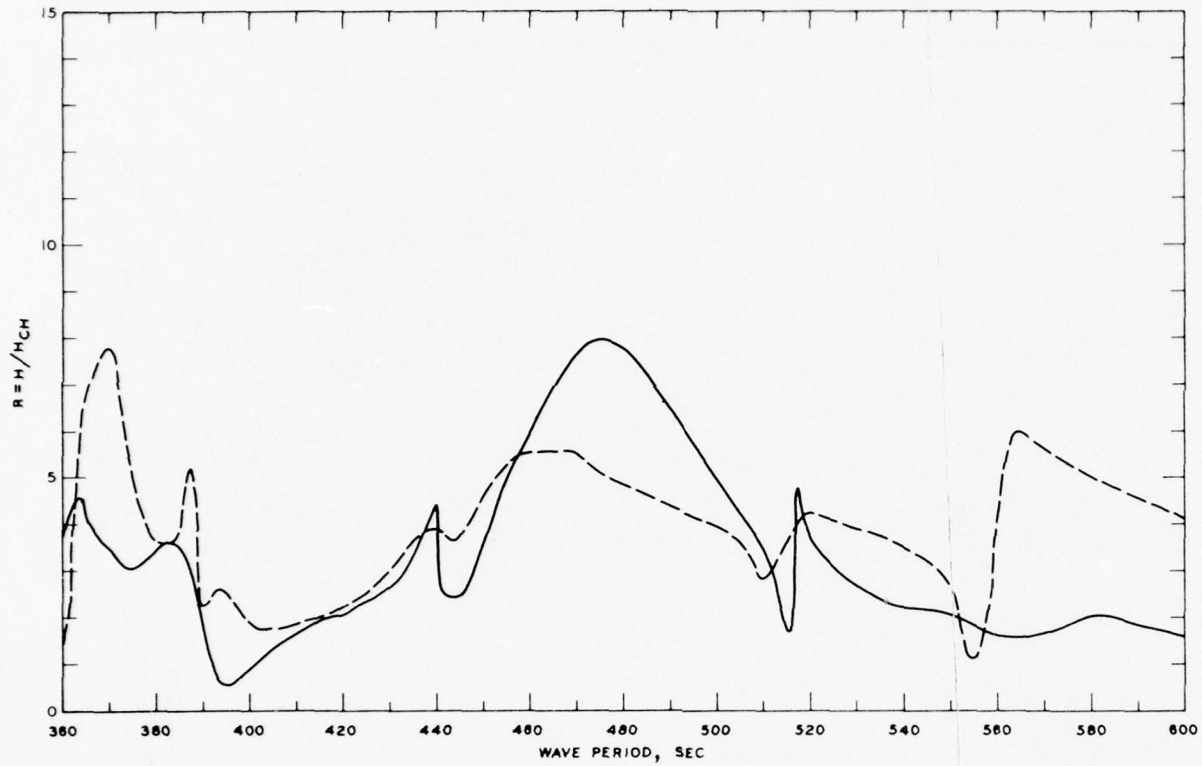

LEGEND

——— GRID 5

— — — GRID 5A

NOTE: R = WAVE-HEIGHT AMPLIFICATION FACTOR
H = WAVE HEIGHT, FT
H_{CH} = WAVE HEIGHT FOR CLOSED HARBOR, FT

FREQUENCY RESPONSE

WAVE-HEIGHT AMPLIFICATION FACTOR
STA LA-1 , GRIDS 5 AND 5A

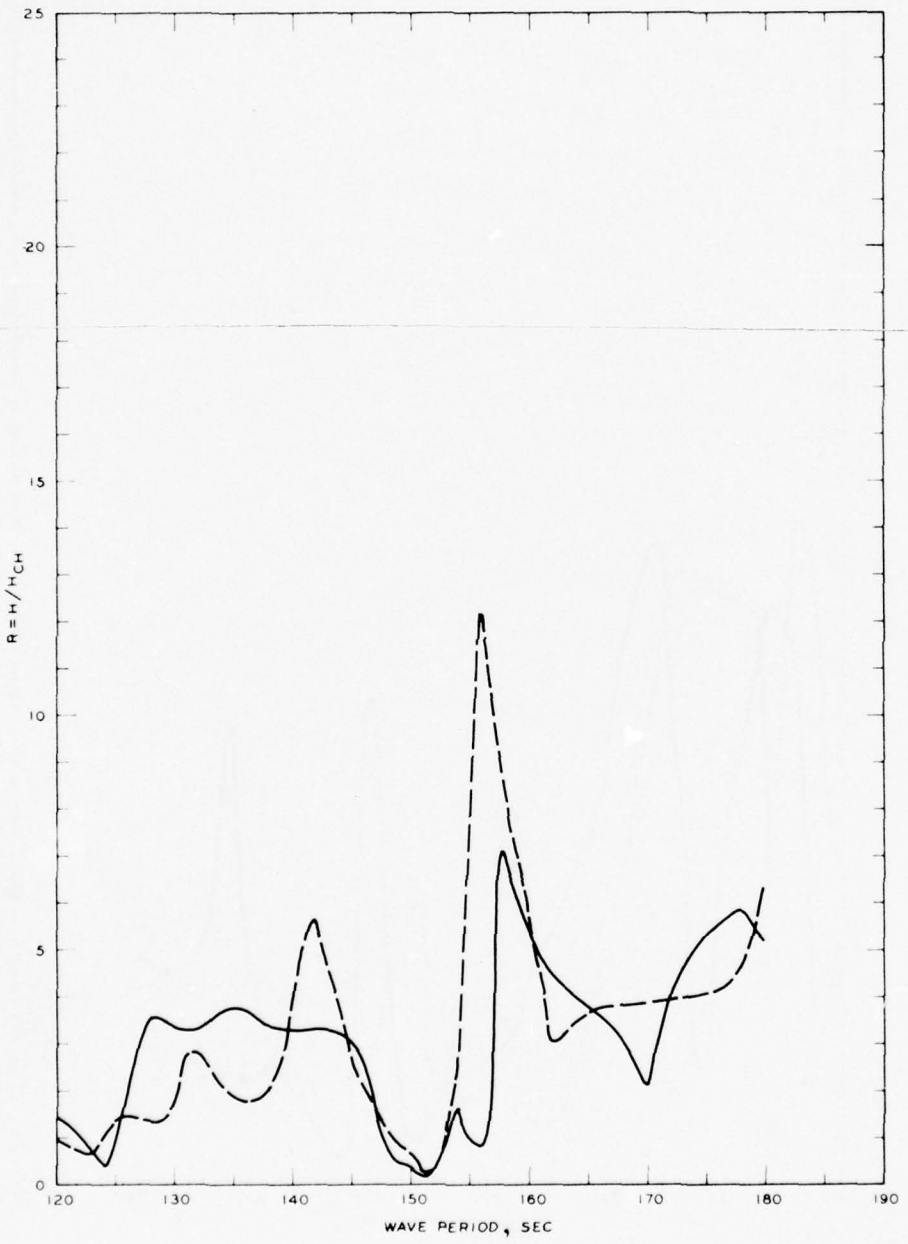

LEGEND

——— GRID 2

— — — GRID 2A

NOTE R = WAVE-HEIGHT AMPLIFICATION FACTOR
H = WAVE HEIGHT, FT
H_{CH} = WAVE HEIGHT FOR CLOSED HARBOR, FT

FREQUENCY RESPONSE

WAVE-HEIGHT AMPLIFICATION FACTOR
STA LA-5, GRIDS 2 AND 2A

PLATE 39

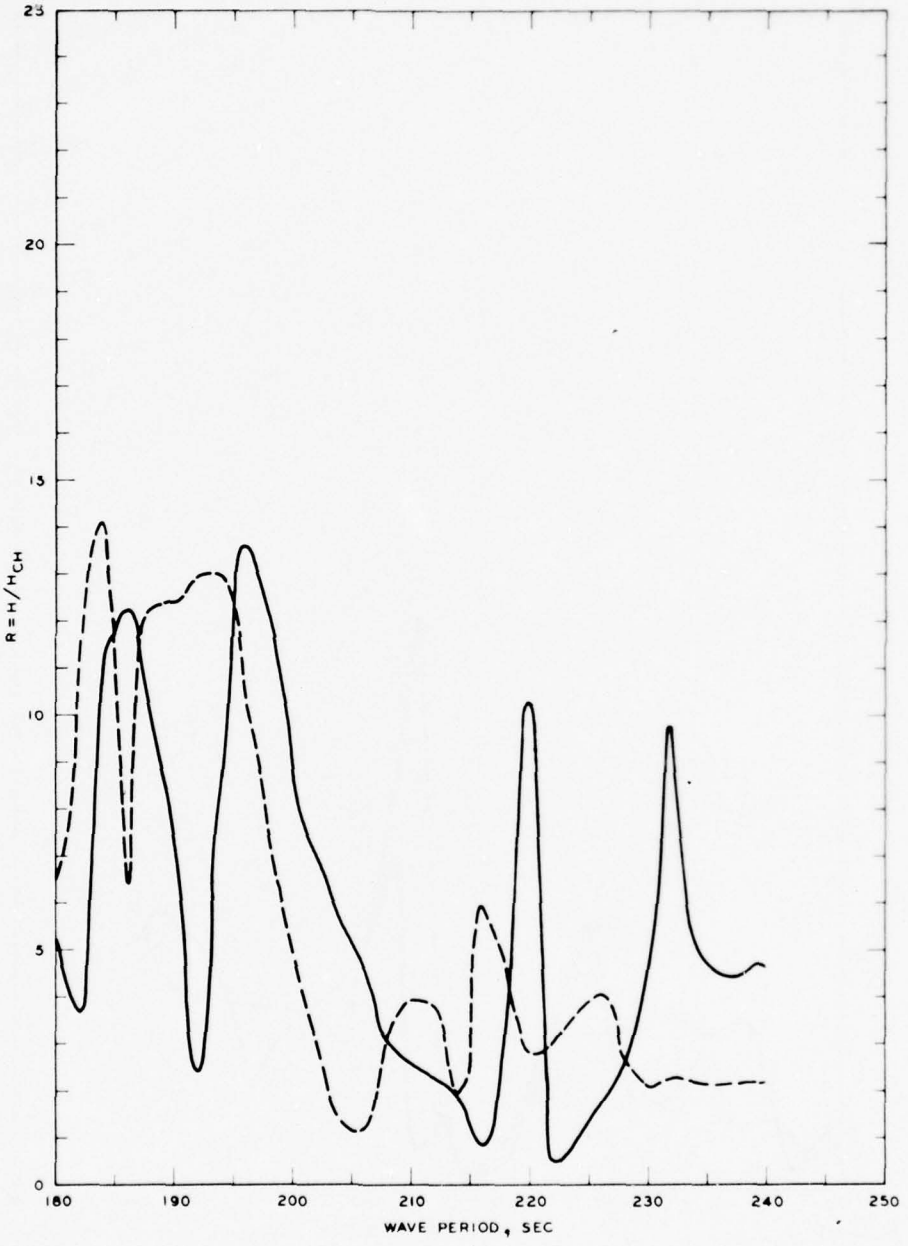

LEGEND

——— GRID 3

— — — GRID 3A

NOTE R = WAVE-HEIGHT AMPLIFICATION FACTOR
H = WAVE HEIGHT, FT
H_{CH} = WAVE HEIGHT FOR CLOSED HARBOR, FT

FREQUENCY RESPONSE

WAVE-HEIGHT AMPLIFICATION FACTOR
STA LA-5, GRIDS 3 AND 3A

PLATE 40

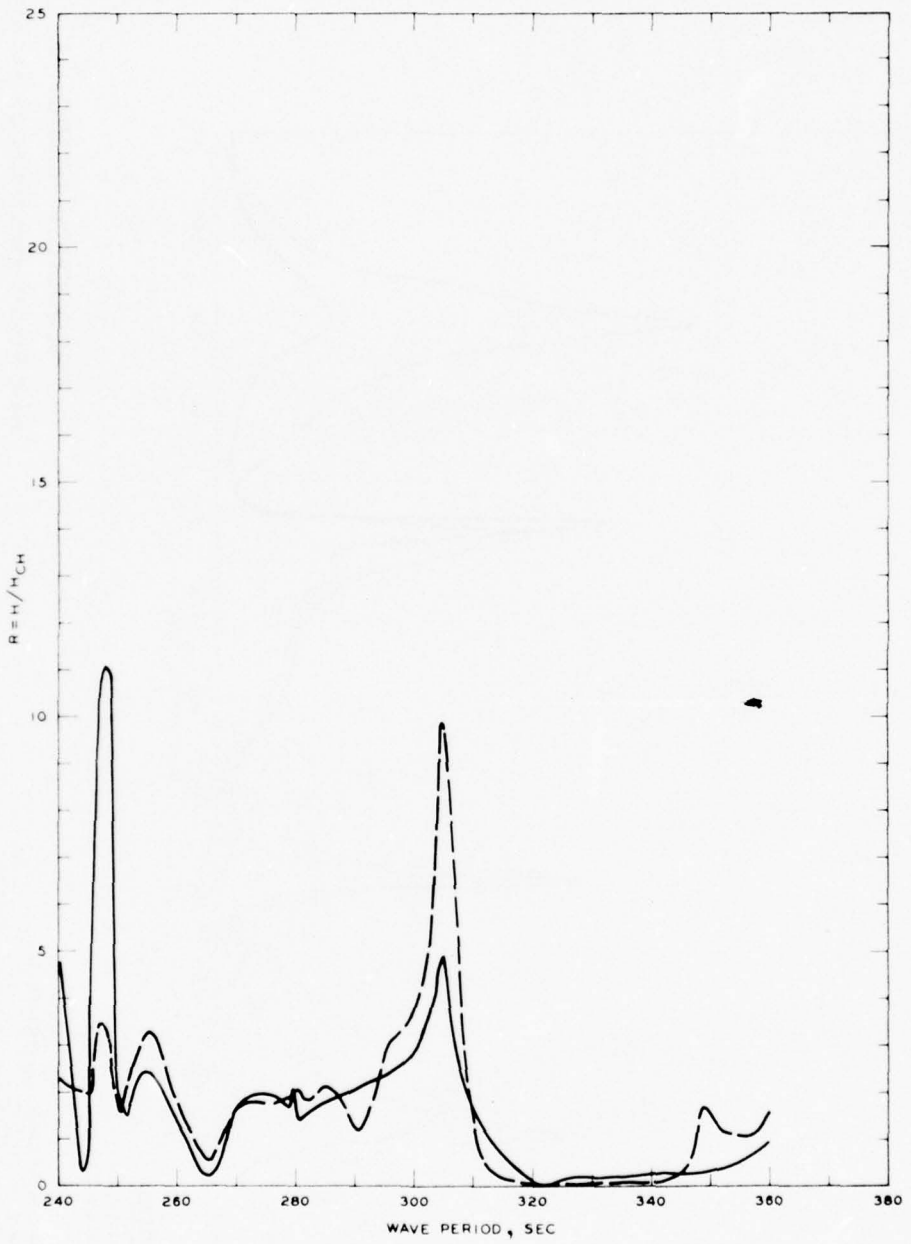

LEGEND

——— GRID 4

— — — GRID 4A

NOTE R = WAVE-HEIGHT AMPLIFICATION FACTOR
H = WAVE HEIGHT, FT
H_{CH} = WAVE HEIGHT FOR CLOSED HARBOR, FT

FREQUENCY RESPONSE

WAVE-HEIGHT AMPLIFICATION FACTOR
STA LA-5, GRIDS 4 AND 4A

PLATE 41

PLATE 42

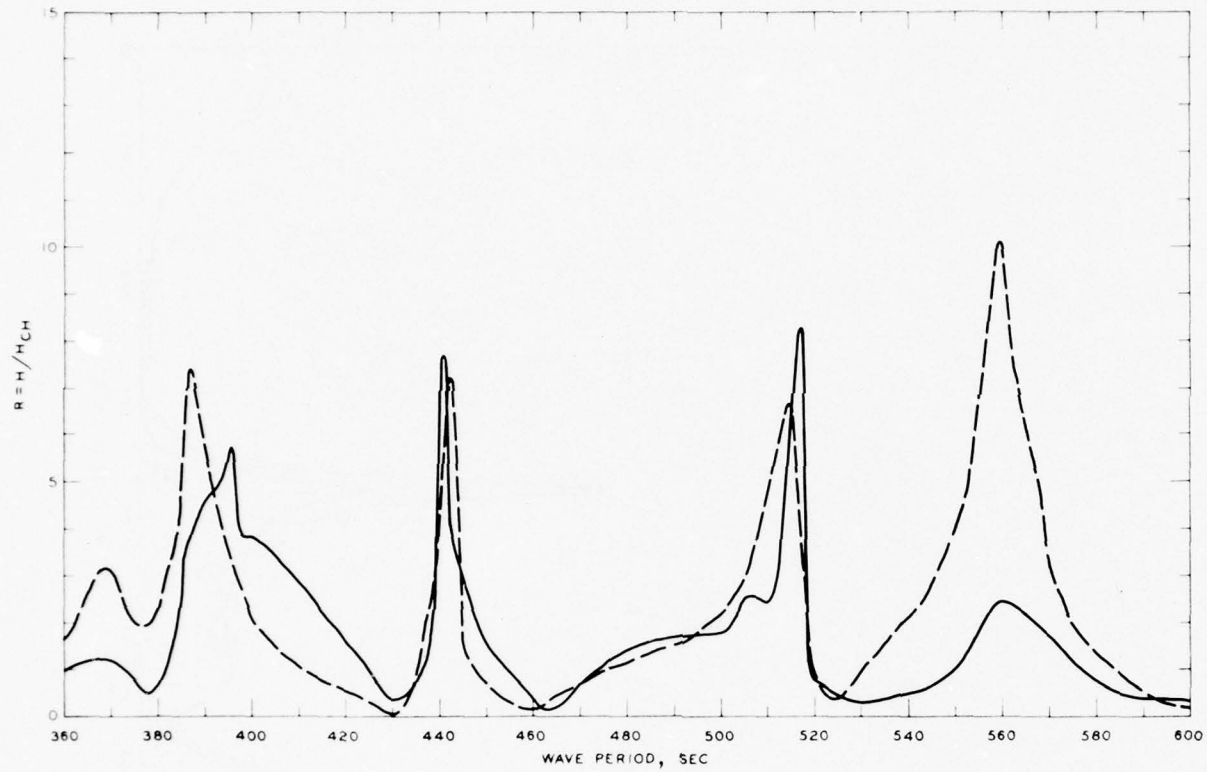

LEGEND

——— GRID 5

— — — GRID 5A

NOTE: R = WAVE-HEIGHT AMPLIFICATION FACTOR
H = WAVE HEIGHT, FT
H_{CH} = WAVE HEIGHT FOR CLOSED HARBOR, FT

FREQUENCY RESPONSE

WAVE-HEIGHT AMPLIFICATION FACTOR
STA LA - 5, GRIDS 5 AND 5A

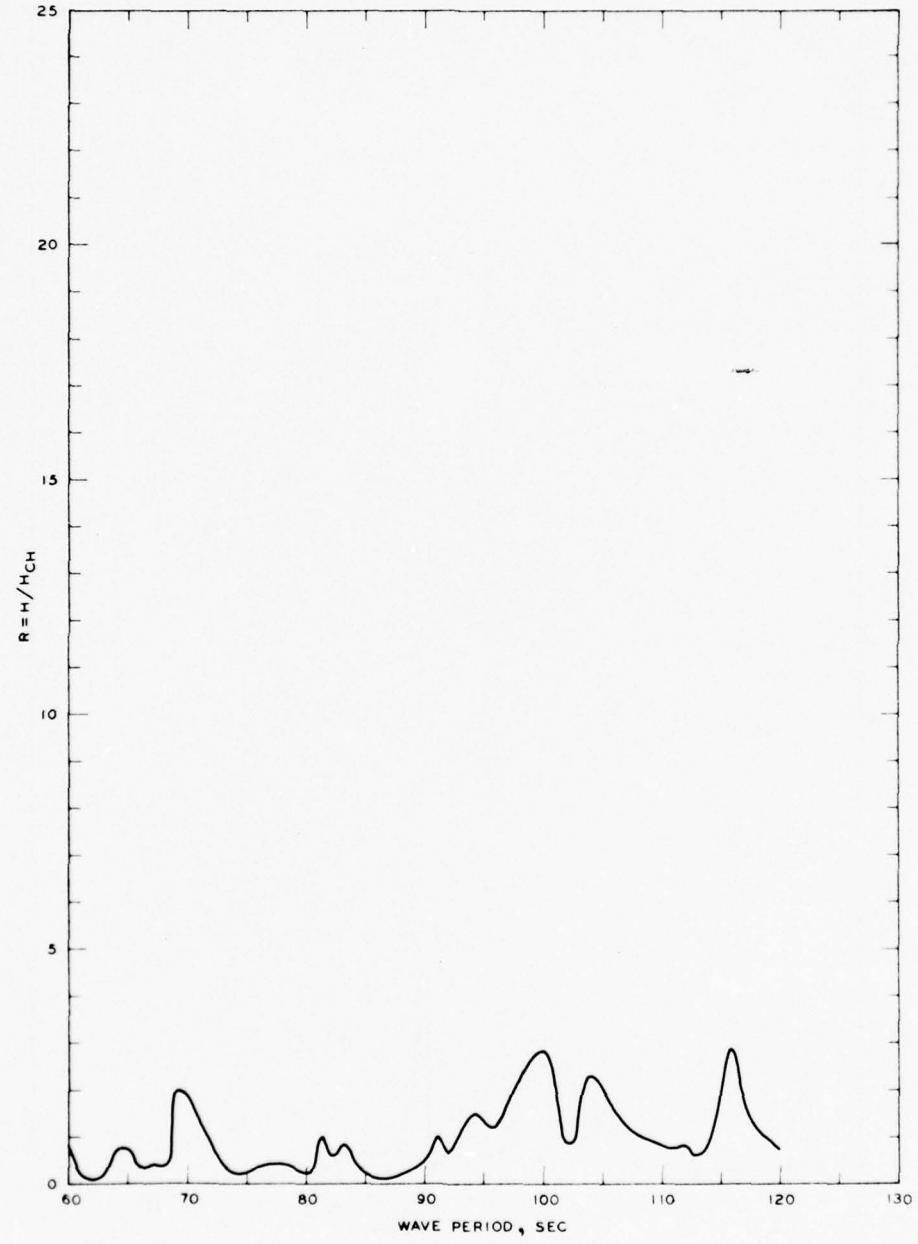

NOTE R = WAVE-HEIGHT AMPLIFICATION FACTOR
H = WAVE HEIGHT, FT
H_{CH} = WAVE HEIGHT FOR CLOSED HARBOR, FT

FREQUENCY RESPONSE

WAVE-HEIGHT AMPLIFICATION FACTOR
STA LA-6, GRID 1A

PLATE 43

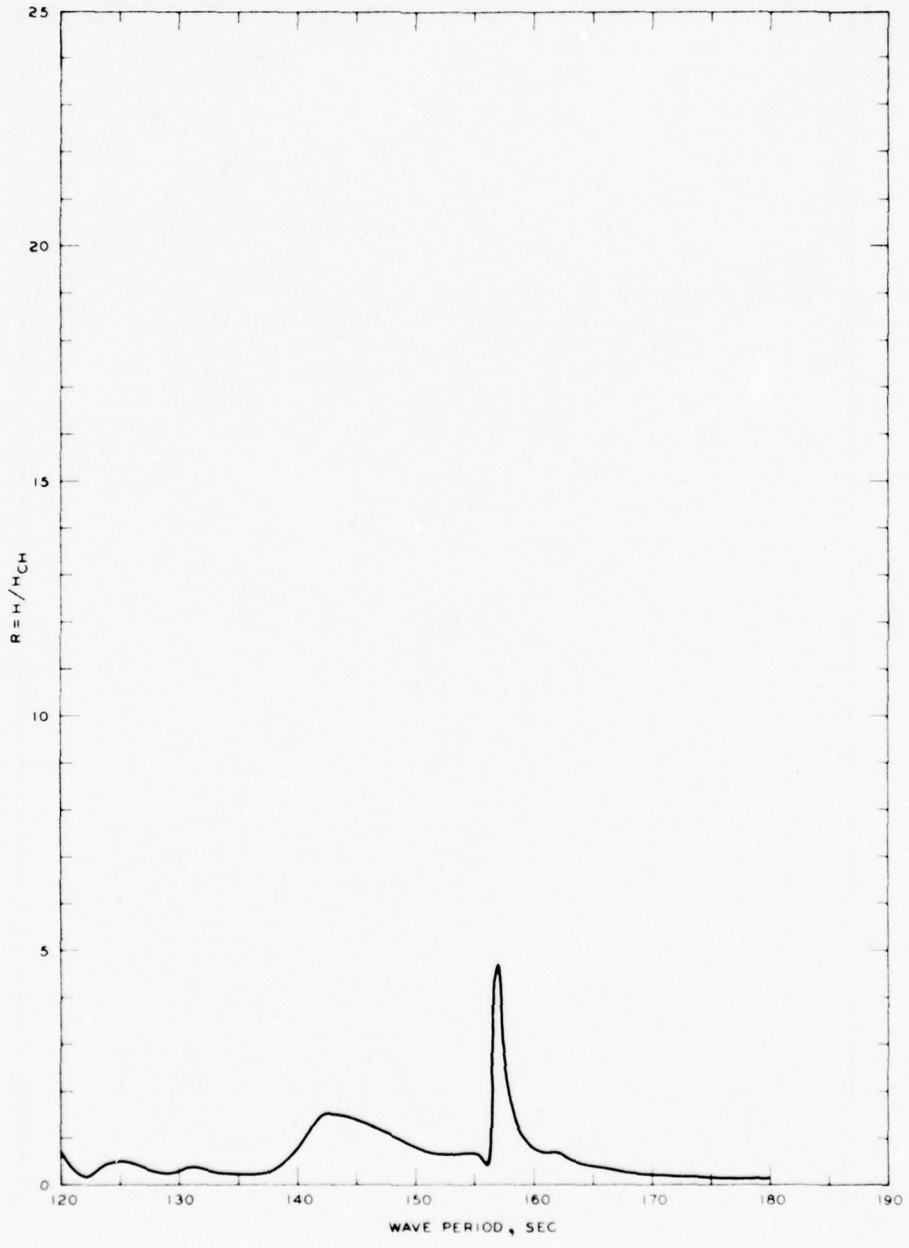

NOTE R = WAVE-HEIGHT AMPLIFICATION FACTOR
H = WAVE HEIGHT, FT
H_{CH} = WAVE HEIGHT FOR CLOSED HARBOR, FT

FREQUENCY RESPONSE

WAVE-HEIGHT AMPLIFICATION FACTOR
STA LA-6, GRID 2A

PLATE 44

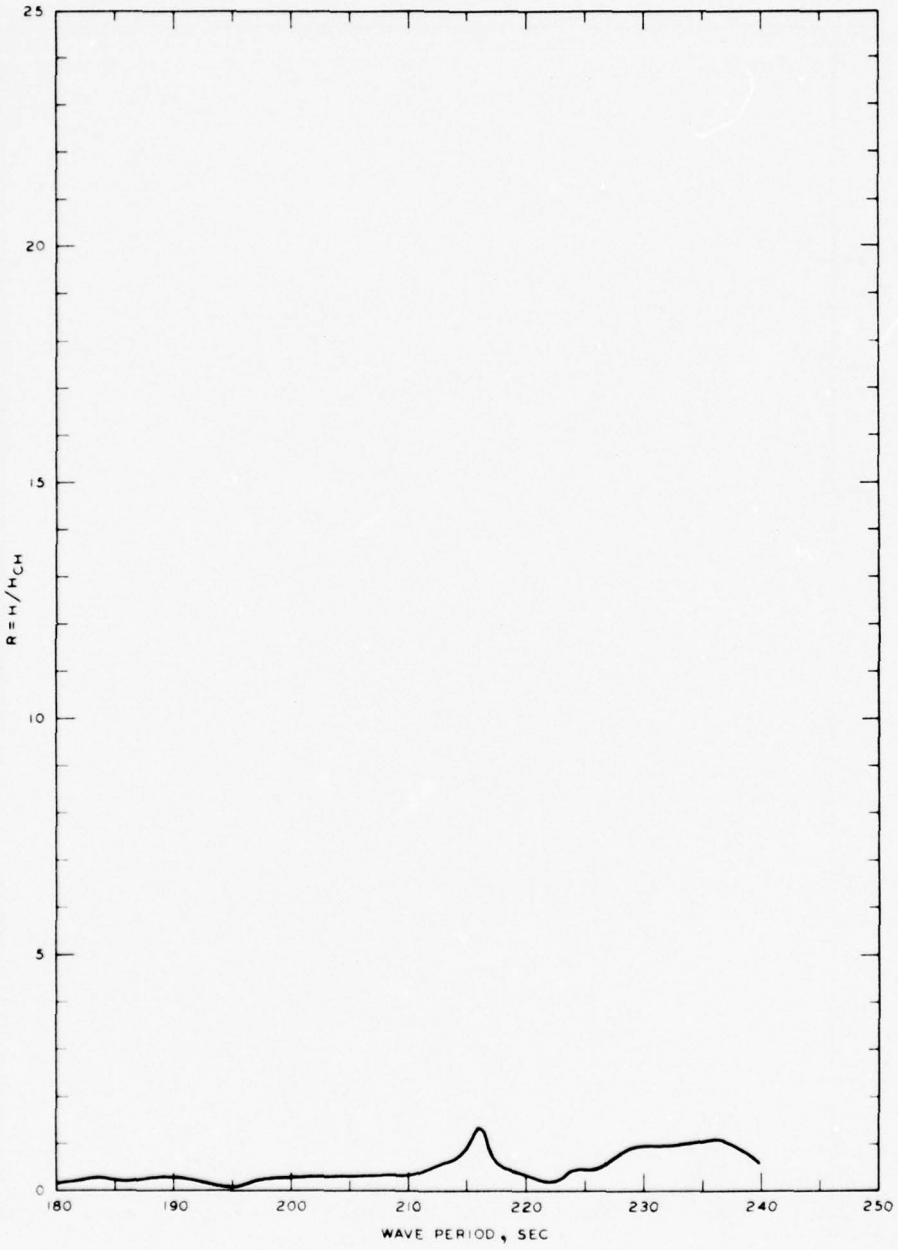

NOTE R = WAVE-HEIGHT AMPLIFICATION FACTOR
H = WAVE HEIGHT, FT
H_{CH} = WAVE HEIGHT FOR CLOSED HARBOR, FT

FREQUENCY RESPONSE

WAVE-HEIGHT AMPLIFICATION FACTOR
STA LA-6, GRID 3A

PLATE 45

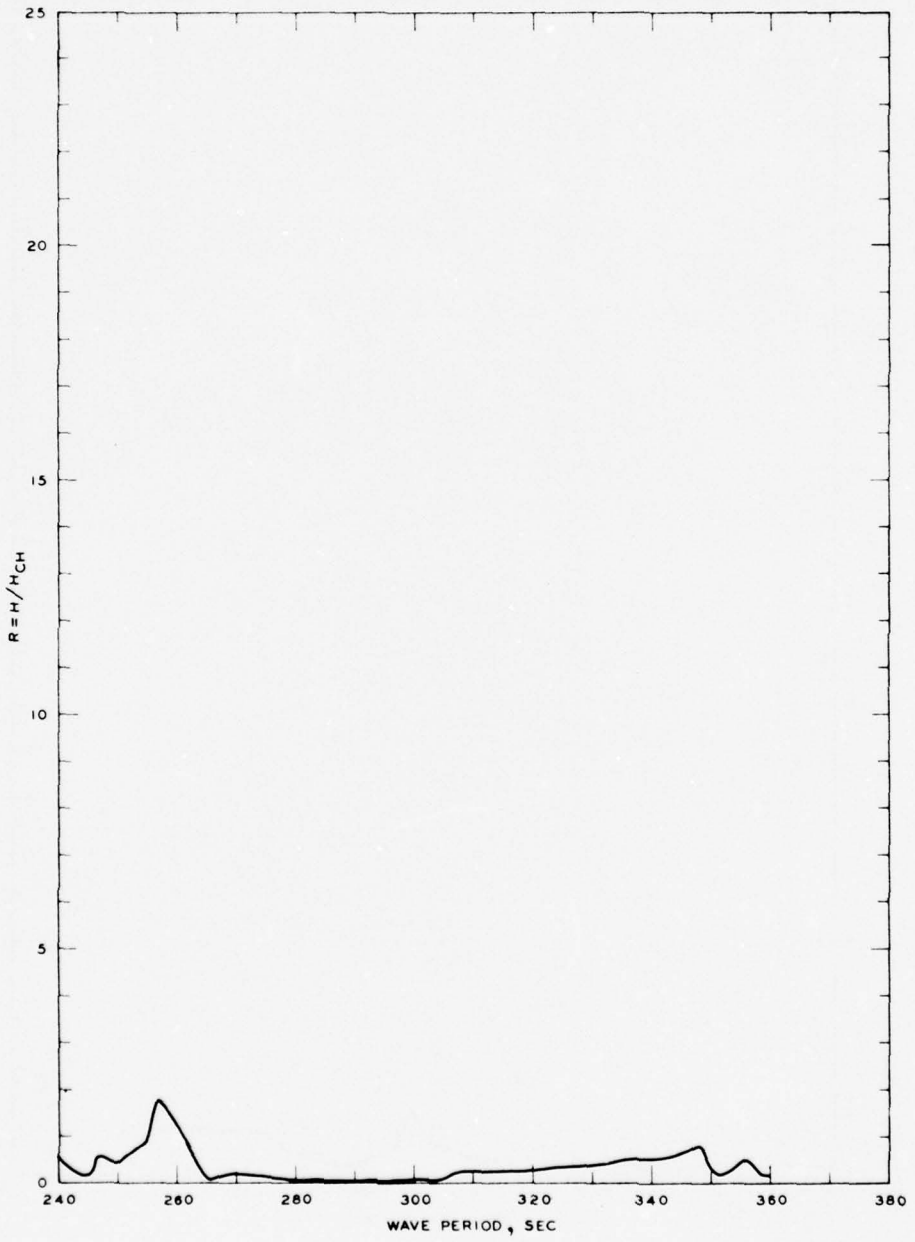

NOTE R = WAVE-HEIGHT AMPLIFICATION FACTOR
H = WAVE HEIGHT, FT
H_{CH} = WAVE HEIGHT FOR CLOSED HARBOR, FT

FREQUENCY RESPONSE

WAVE-HEIGHT AMPLIFICATION FACTOR
STA LA-6, GRID 4A

PLATE 46

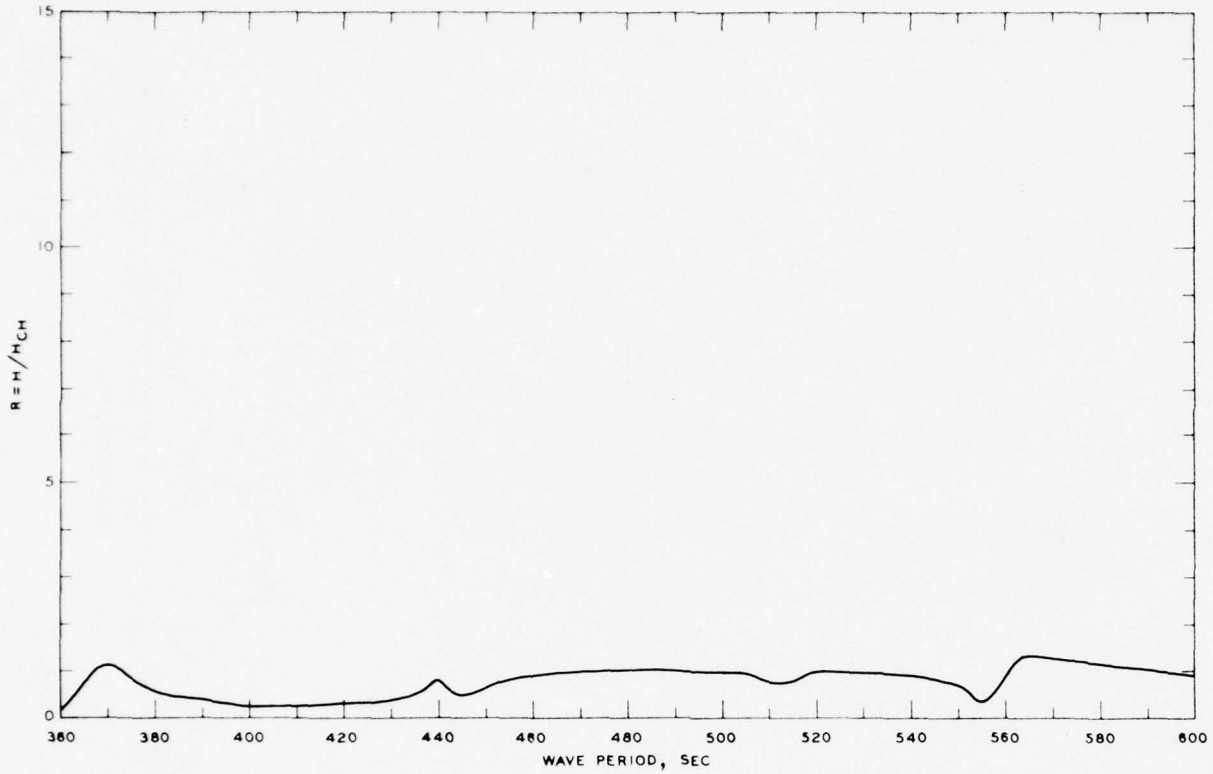

NOTE: R = WAVE-HEIGHT AMPLIFICATION FACTOR
H = WAVE HEIGHT, FT
H_{CH} = WAVE HEIGHT FOR CLOSED HARBOR, FT

FREQUENCY RESPONSE

WAVE-HEIGHT AMPLIFICATION FACTOR
STA LA-6, GRID 5A

PLATE 47

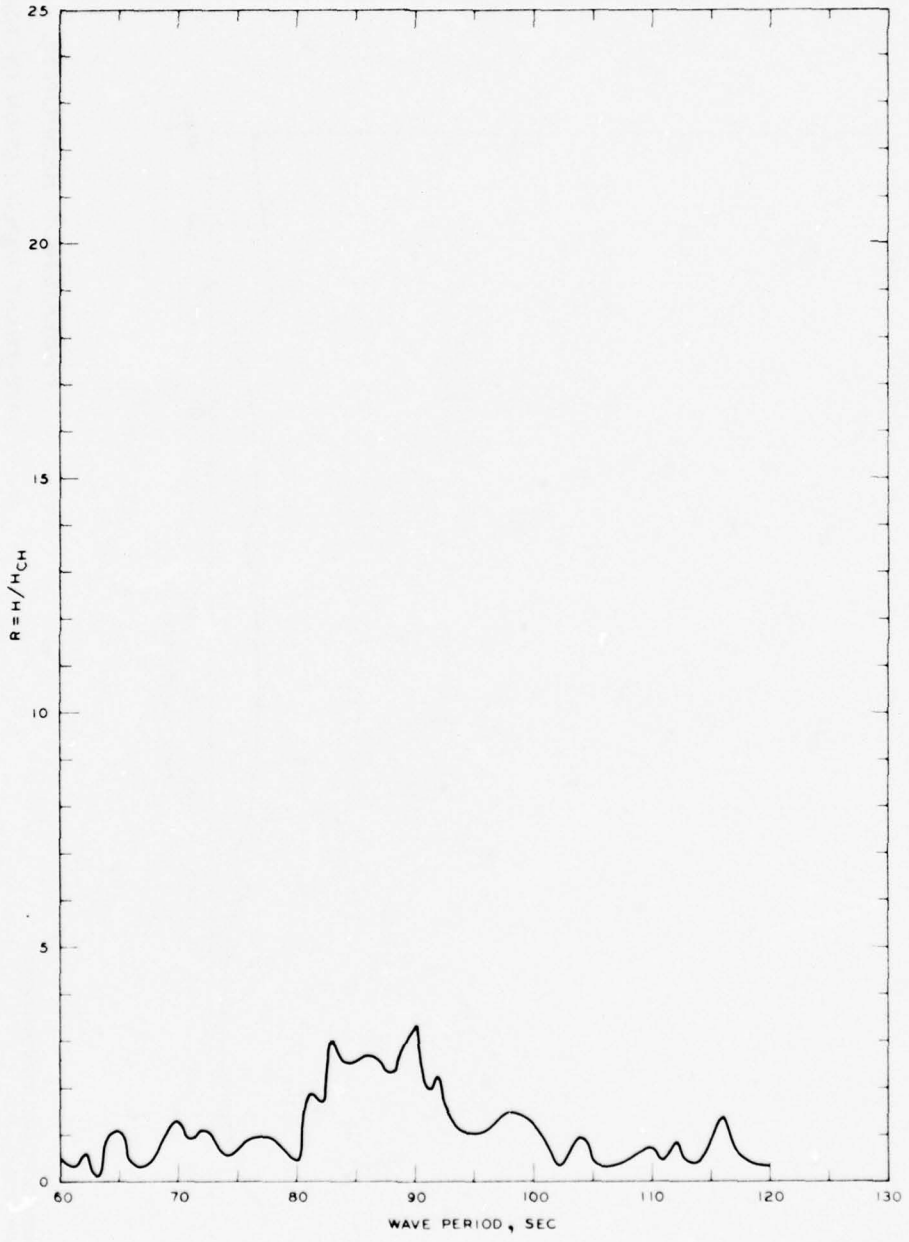

NOTE R = WAVE-HEIGHT AMPLIFICATION FACTOR
H = WAVE HEIGHT, FT
H_{CH} = WAVE HEIGHT FOR CLOSED HARBOR, FT

FREQUENCY RESPONSE

WAVE-HEIGHT AMPLIFICATION FACTOR
STA LA-7, GRID 1A

PLATE 48

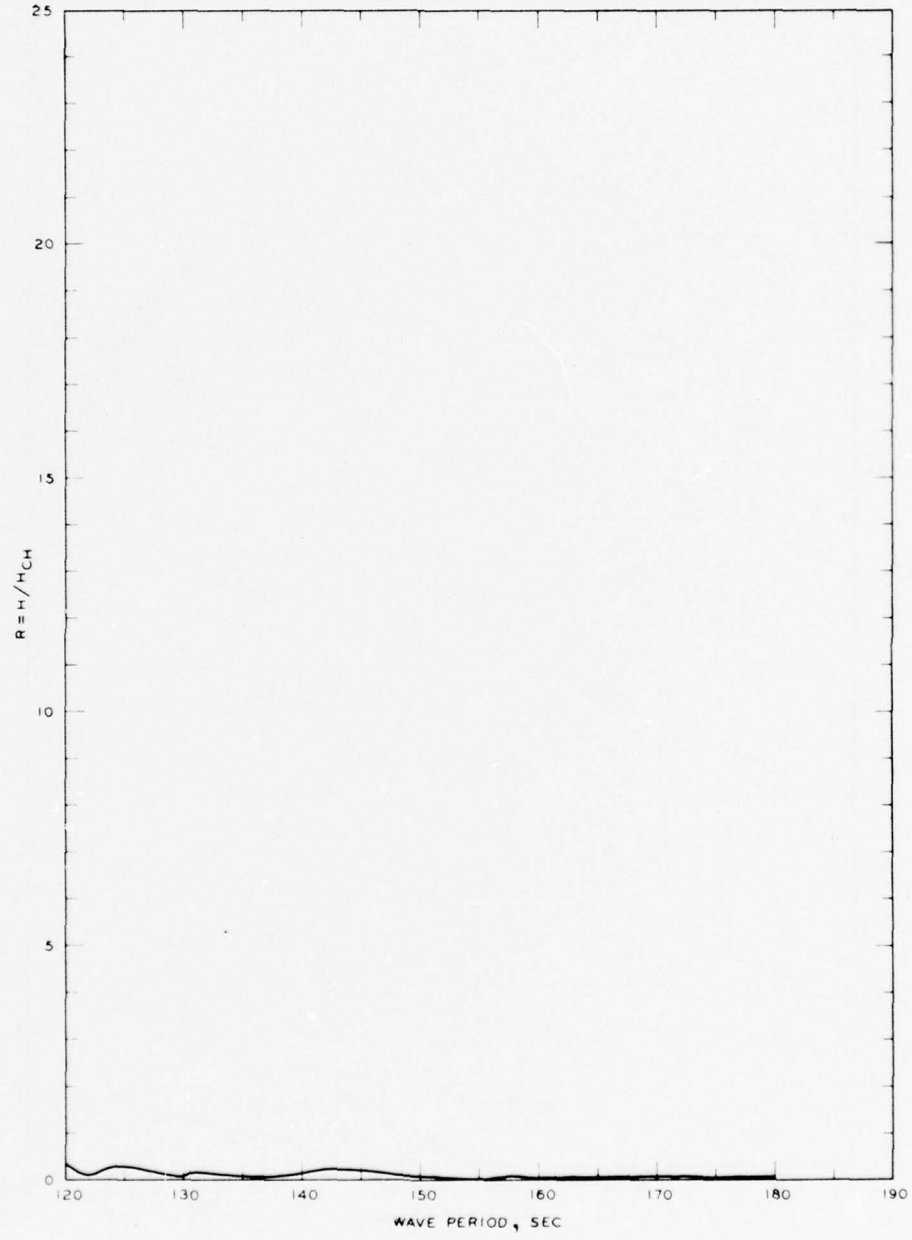

NOTE R = WAVE-HEIGHT AMPLIFICATION FACTOR
H = WAVE HEIGHT, FT
H_{CH} = WAVE HEIGHT FOR CLOSED HARBOR, FT

FREQUENCY RESPONSE

WAVE-HEIGHT AMPLIFICATION FACTOR
STA LA-7, GRID 2A

PLATE 49

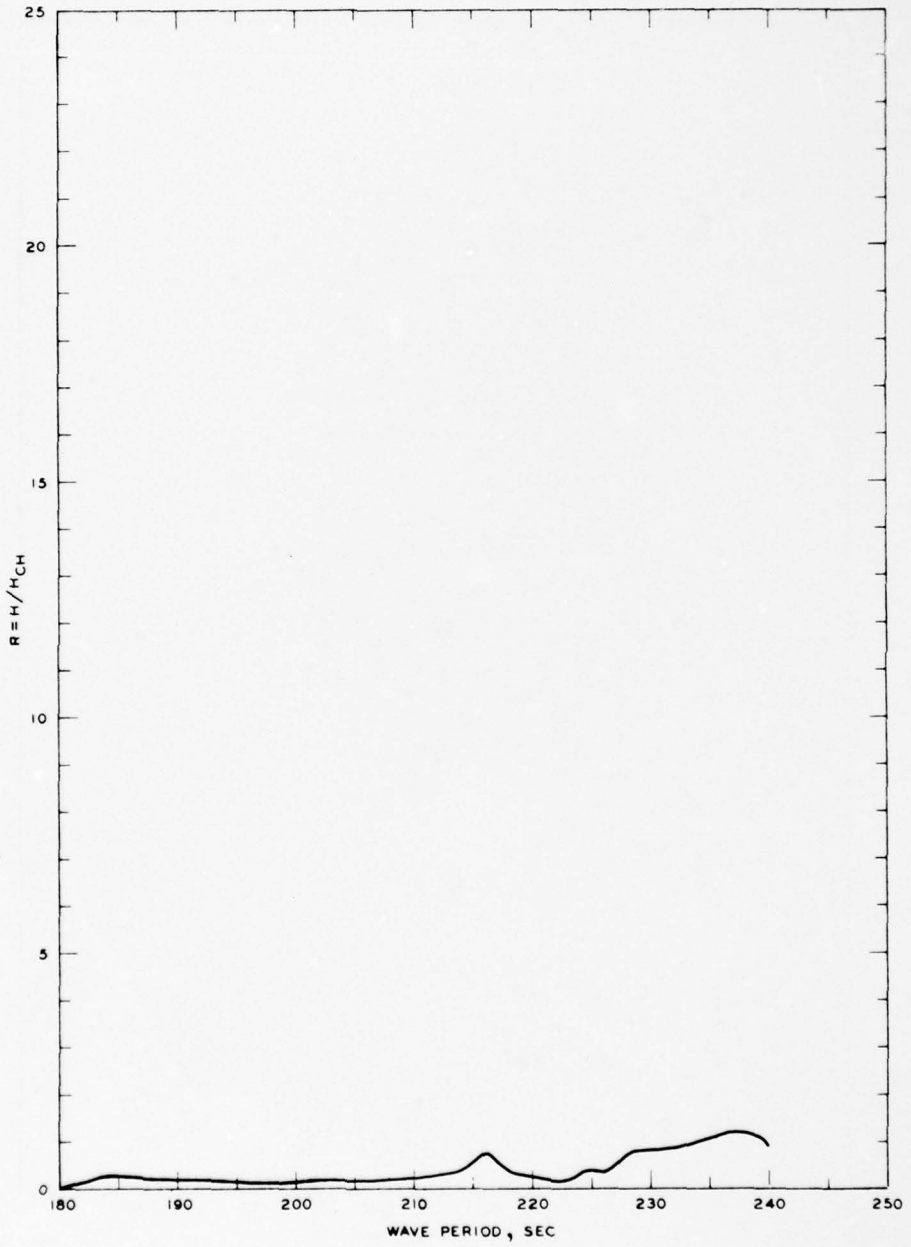

NOTE R = WAVE-HEIGHT AMPLIFICATION FACTOR
H = WAVE HEIGHT, FT
H_{CH} = WAVE HEIGHT FOR CLOSED HARBOR, FT

FREQUENCY RESPONSE

WAVE-HEIGHT AMPLIFICATION FACTOR
STA LA-7, GRID 3A

PLATE 50

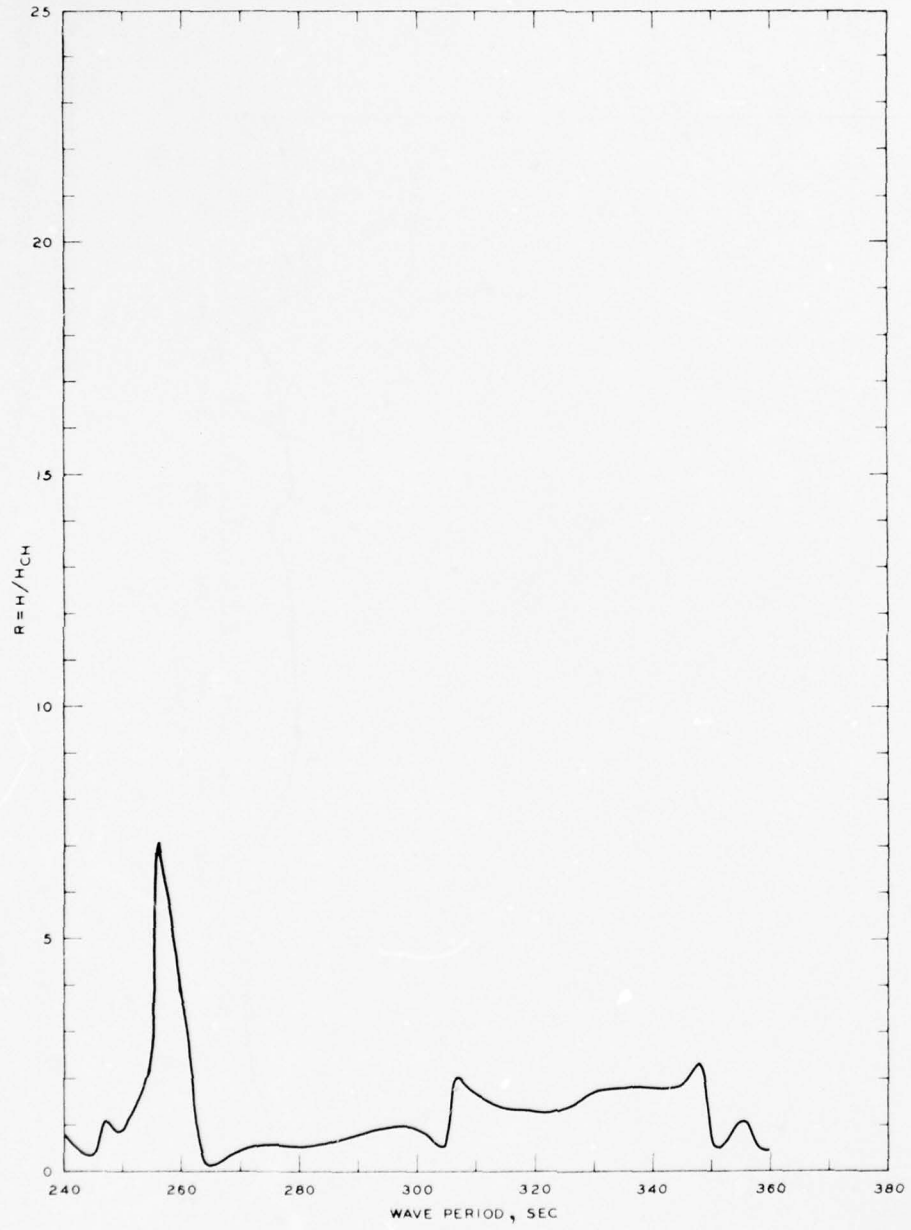

NOTE R = WAVE-HEIGHT AMPLIFICATION FACTOR
H = WAVE HEIGHT, FT
H_{CH} = WAVE HEIGHT FOR CLOSED HARBOR, FT

FREQUENCY RESPONSE

WAVE-HEIGHT AMPLIFICATION FACTOR
STA LA-7, GRID 4A

PLATE 51

PLATE 52

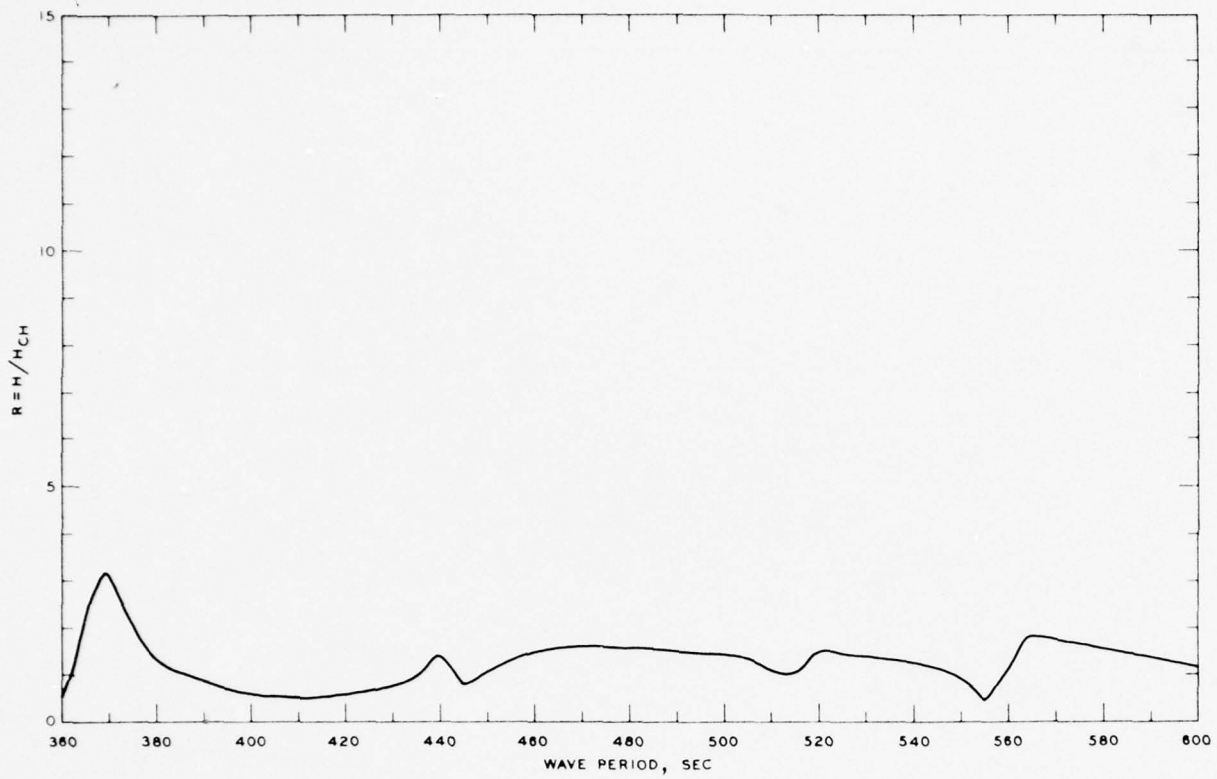

NOTE: R = WAVE-HEIGHT AMPLIFICATION FACTOR
H = WAVE HEIGHT, FT
H_{CH} = WAVE HEIGHT FOR CLOSED HARBOR, FT

FREQUENCY RESPONSE

WAVE-HEIGHT AMPLIFICATION FACTOR
STA LA-7, GRID 5A

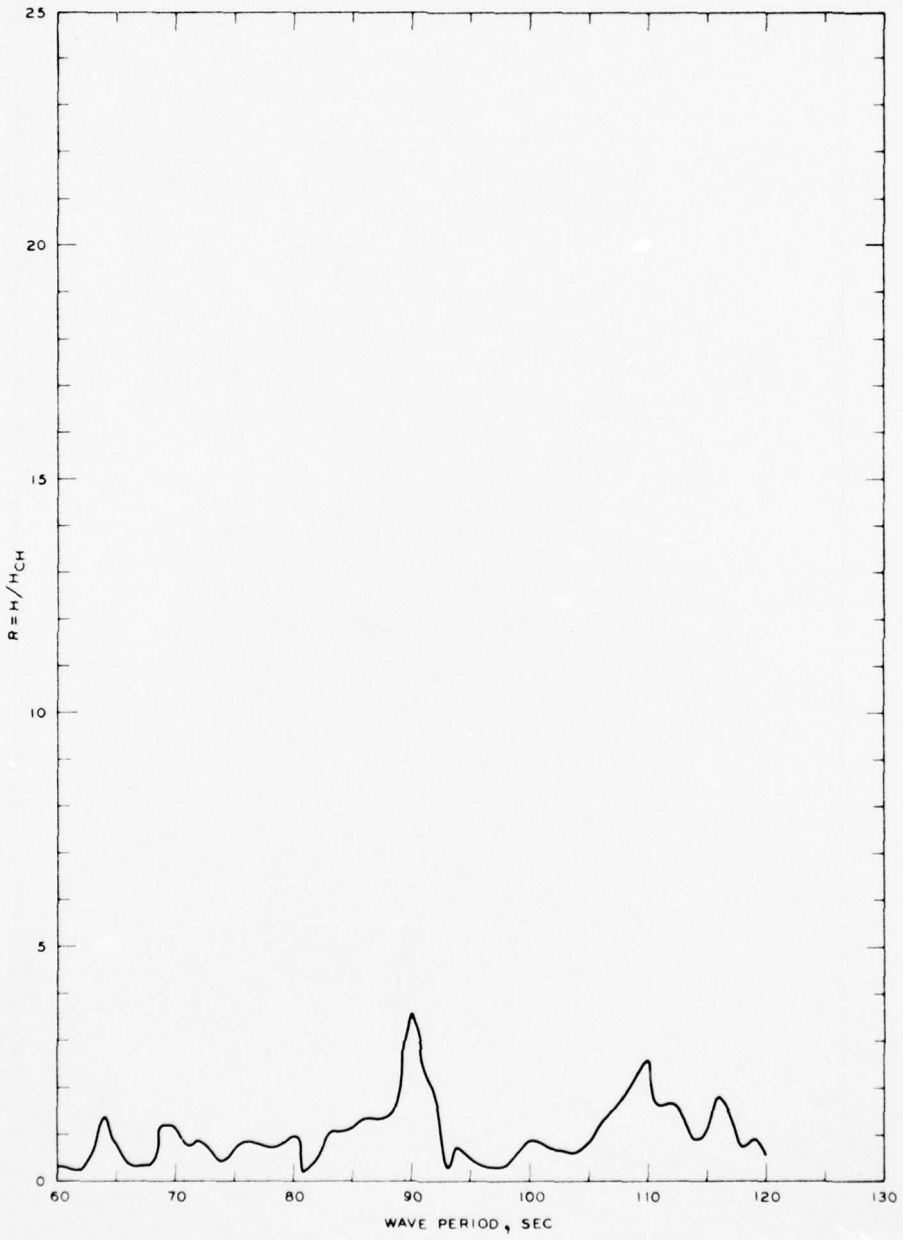

NOTE R = WAVE-HEIGHT AMPLIFICATION FACTOR
H = WAVE HEIGHT, FT
H_{CH} = WAVE HEIGHT FOR CLOSED HARBOR, FT

FREQUENCY RESPONSE

WAVE-HEIGHT AMPLIFICATION FACTOR
STA LA-8, GRID 1A

PLATE 53

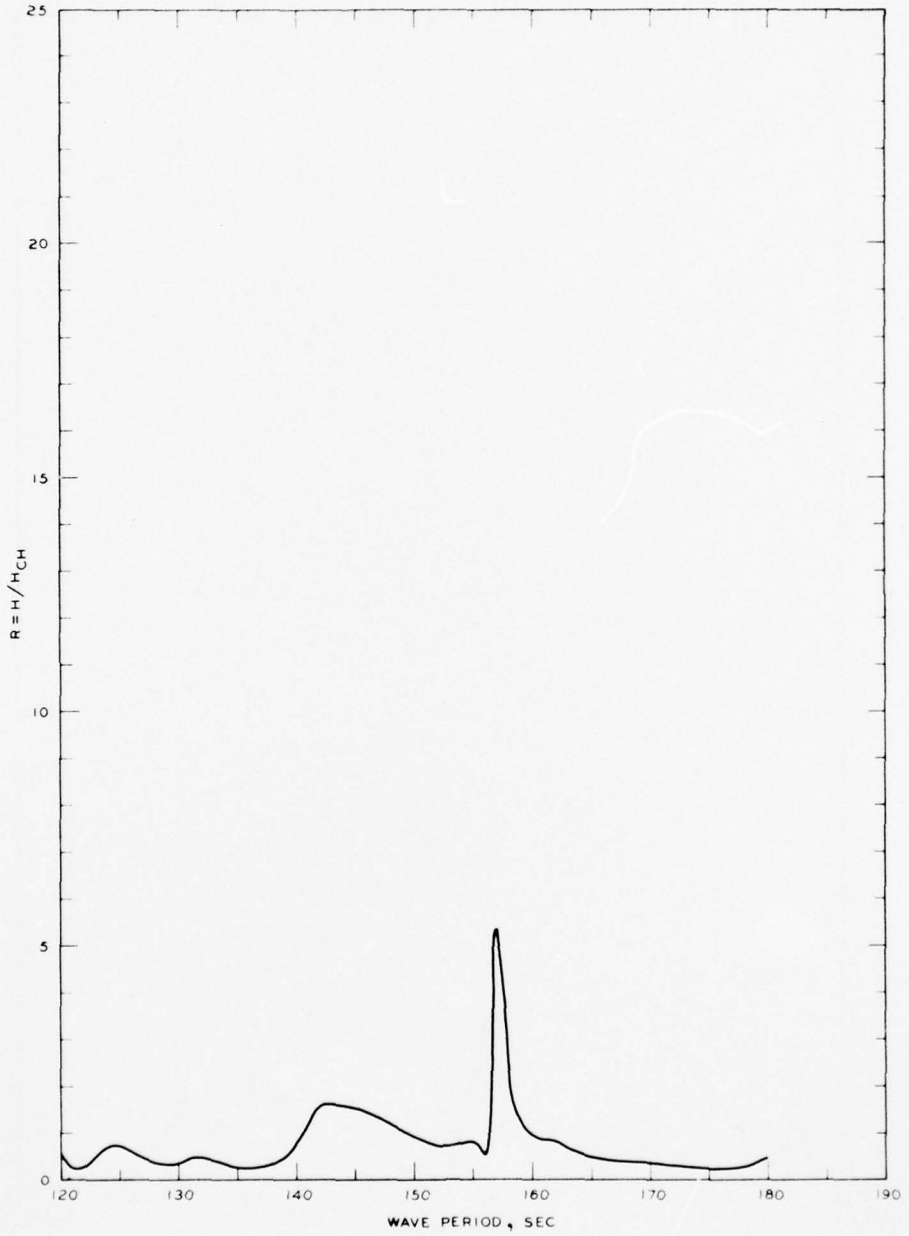

NOTE R = WAVE-HEIGHT AMPLIFICATION FACTOR
H = WAVE HEIGHT, FT
H_{CH} = WAVE HEIGHT FOR CLOSED HARBOR, FT

FREQUENCY RESPONSE

WAVE-HEIGHT AMPLIFICATION FACTOR
STA LA-8, GRID 2A

PLATE 54

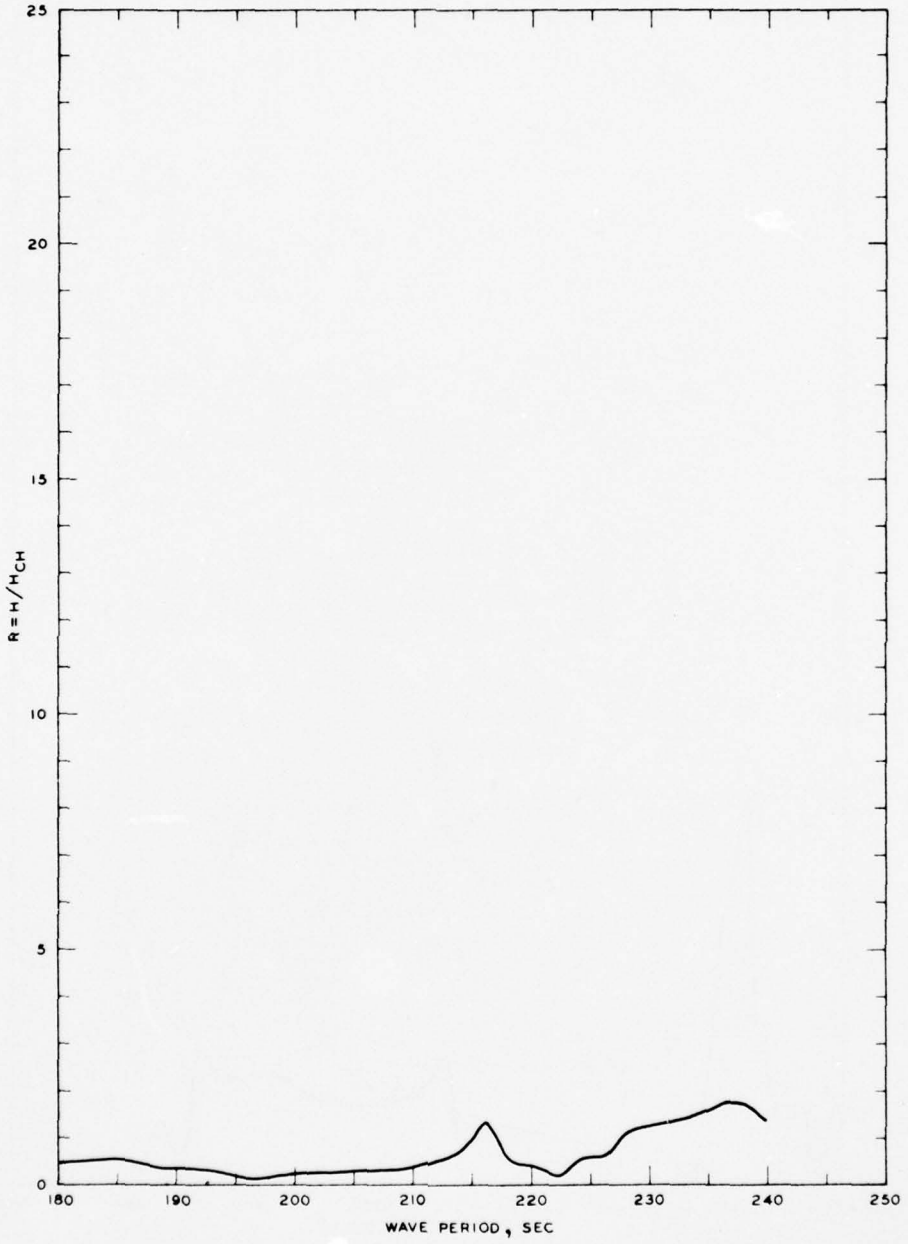

NOTE R = WAVE-HEIGHT AMPLIFICATION FACTOR
H = WAVE HEIGHT, FT
H_{CH} = WAVE HEIGHT FOR CLOSED HARBOR, FT

FREQUENCY RESPONSE

WAVE-HEIGHT AMPLIFICATION FACTOR
STA LA-8 , GRID 3A

PLATE 55

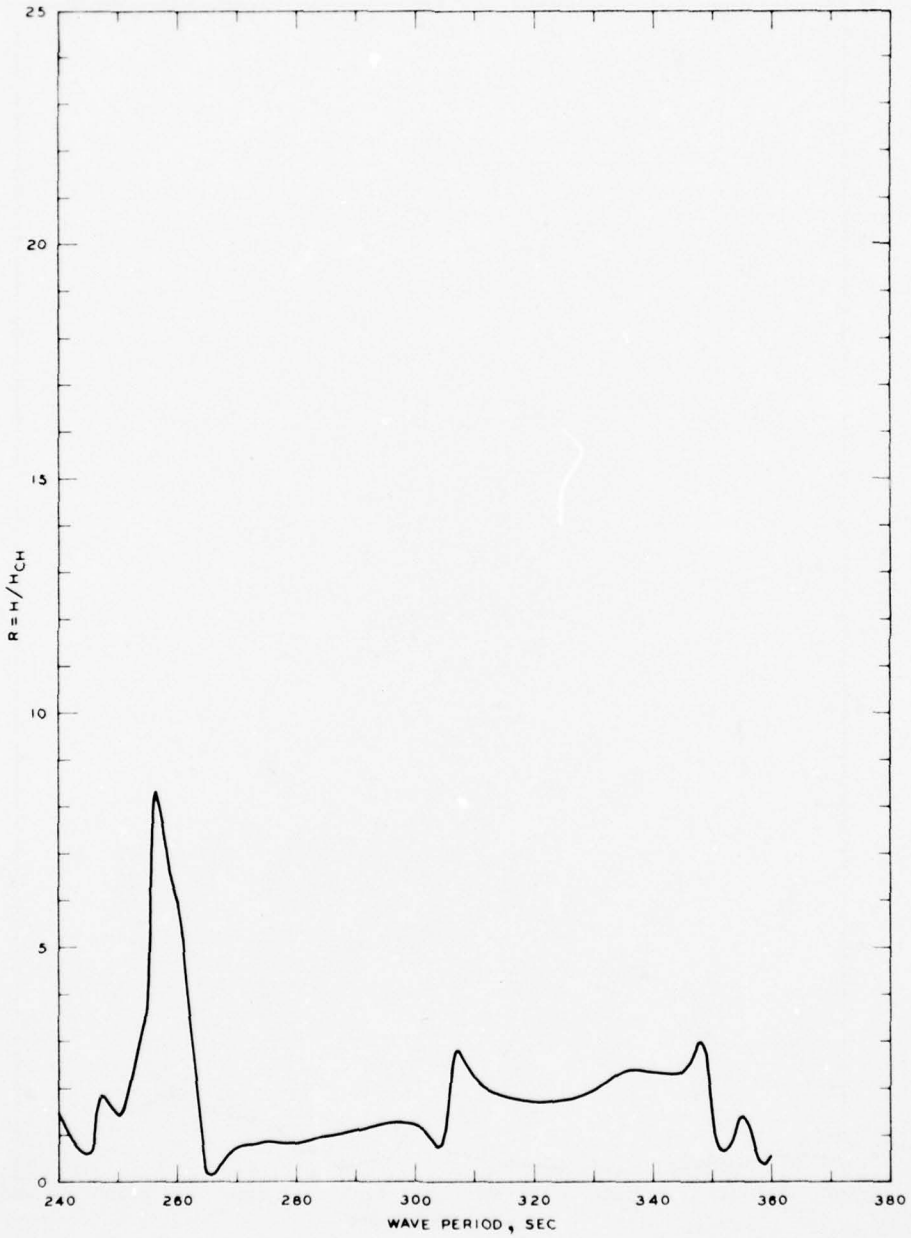

NOTE R = WAVE-HEIGHT AMPLIFICATION FACTOR
H = WAVE HEIGHT, FT
H_{CH} = WAVE HEIGHT FOR CLOSED HARBOR, FT

FREQUENCY RESPONSE

WAVE-HEIGHT AMPLIFICATION FACTOR
STA LA-8, GRID 4A

PLATE 56

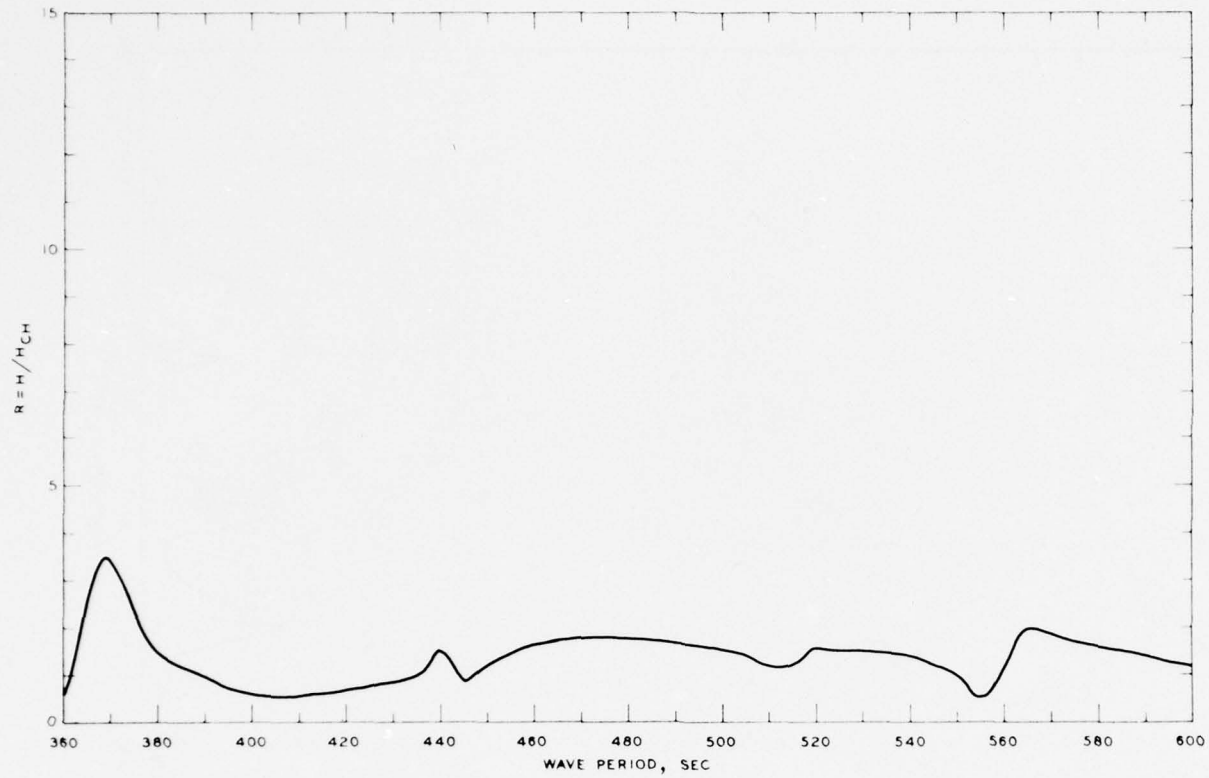

NOTE: R = WAVE-HEIGHT AMPLIFICATION FACTOR
H = WAVE HEIGHT, FT
H_{CH} = WAVE HEIGHT FOR CLOSED HARBOR, FT

FREQUENCY RESPONSE

WAVE-HEIGHT AMPLIFICATION FACTOR
STA LA-8 , GRID 5A

PLATE 57

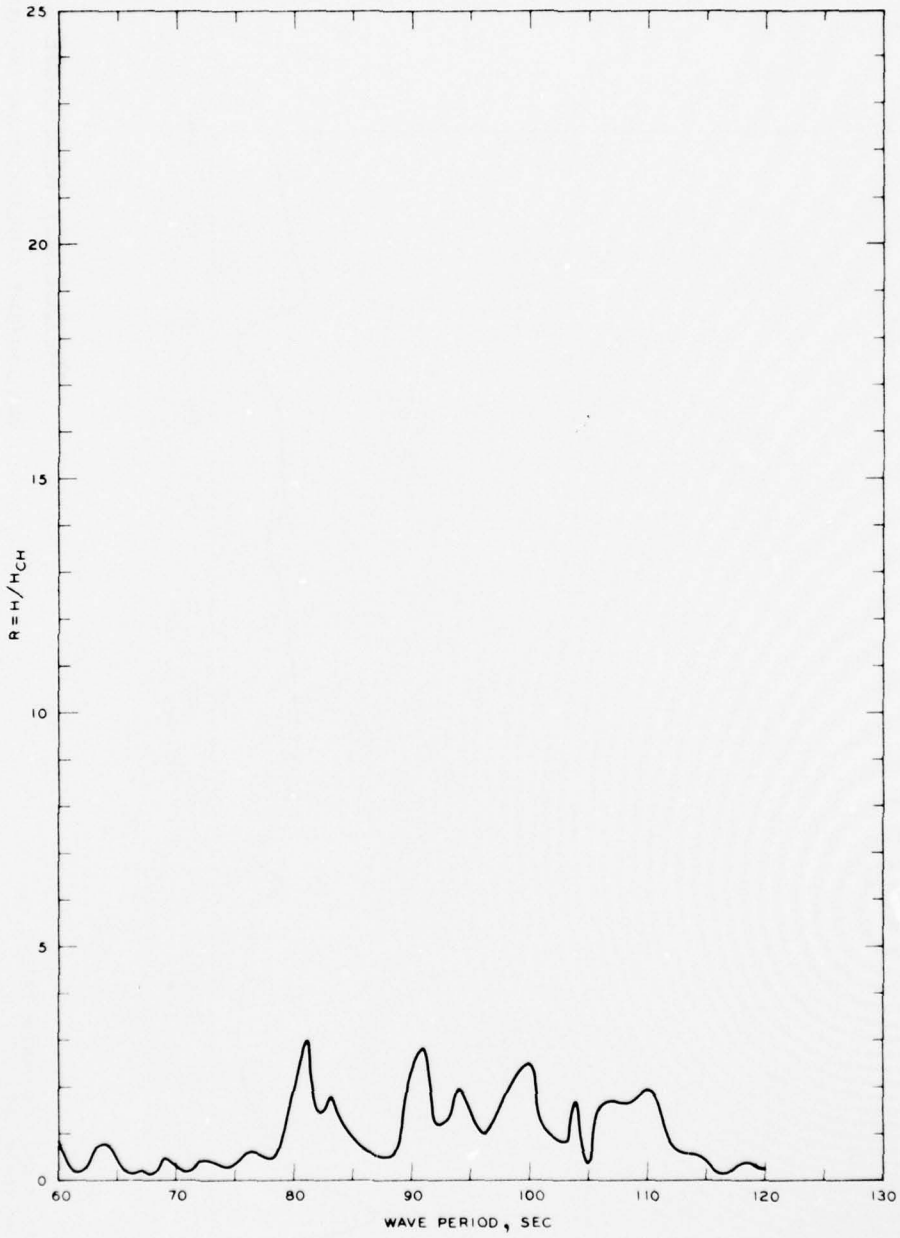

NOTE R = WAVE-HEIGHT AMPLIFICATION FACTOR
H = WAVE HEIGHT, FT
H_{CH} = WAVE HEIGHT FOR CLOSED HARBOR, FT

FREQUENCY RESPONSE

WAVE-HEIGHT AMPLIFICATION FACTOR
STA LA-9, GRID 1A

PLATE 58

NOTE R = WAVE-HEIGHT AMPLIFICATION FACTOR
H = WAVE HEIGHT, FT
H_{CH} = WAVE HEIGHT FOR CLOSED HARBOR, FT

FREQUENCY RESPONSE

WAVE-HEIGHT AMPLIFICATION FACTOR
STA LA-9, GRID 2A

PLATE 59

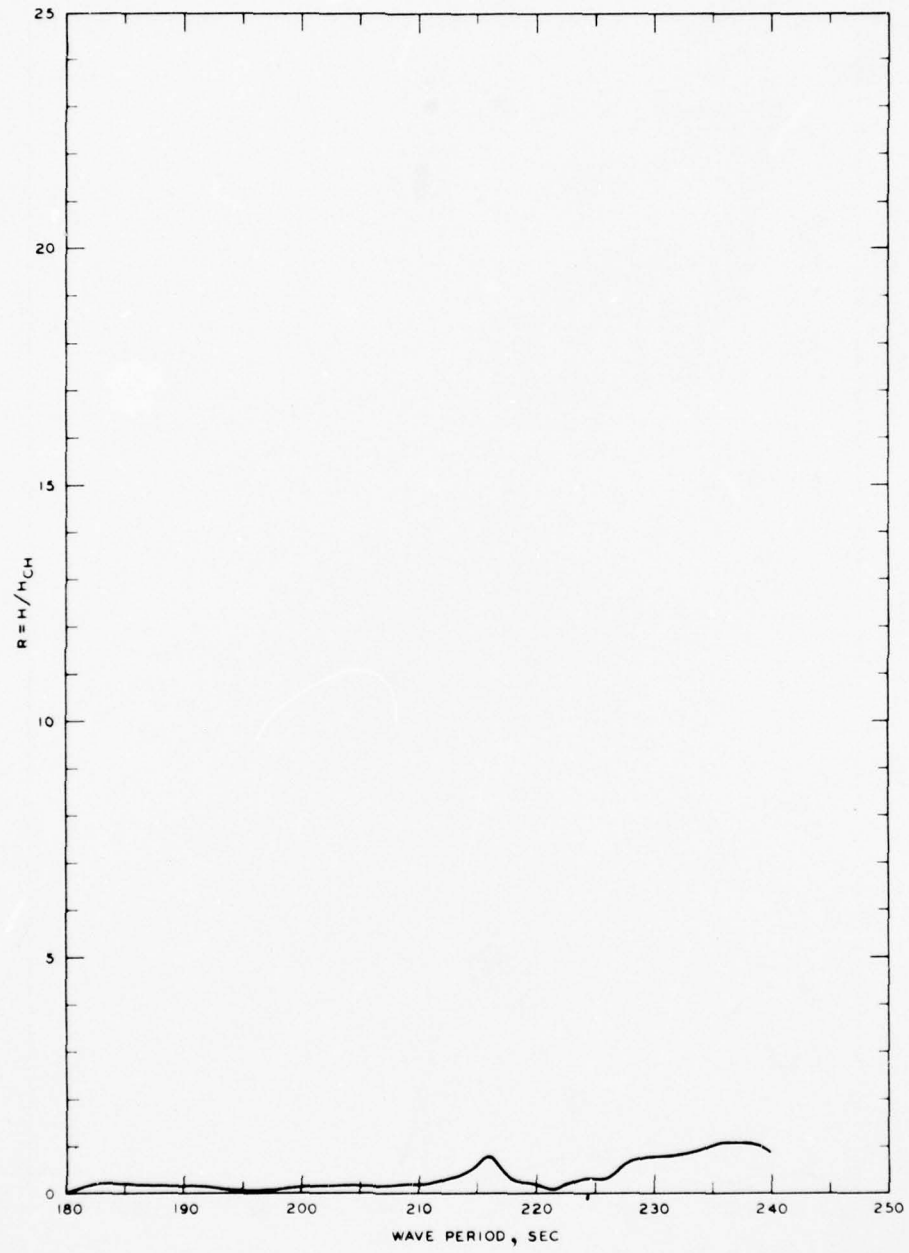

NOTE R = WAVE-HEIGHT AMPLIFICATION FACTOR
H = WAVE HEIGHT, FT
H_{CH} = WAVE HEIGHT FOR CLOSED HARBOR, FT

FREQUENCY RESPONSE

WAVE-HEIGHT AMPLIFICATION FACTOR
STA LA-9, GRID 3A

PLATE 60

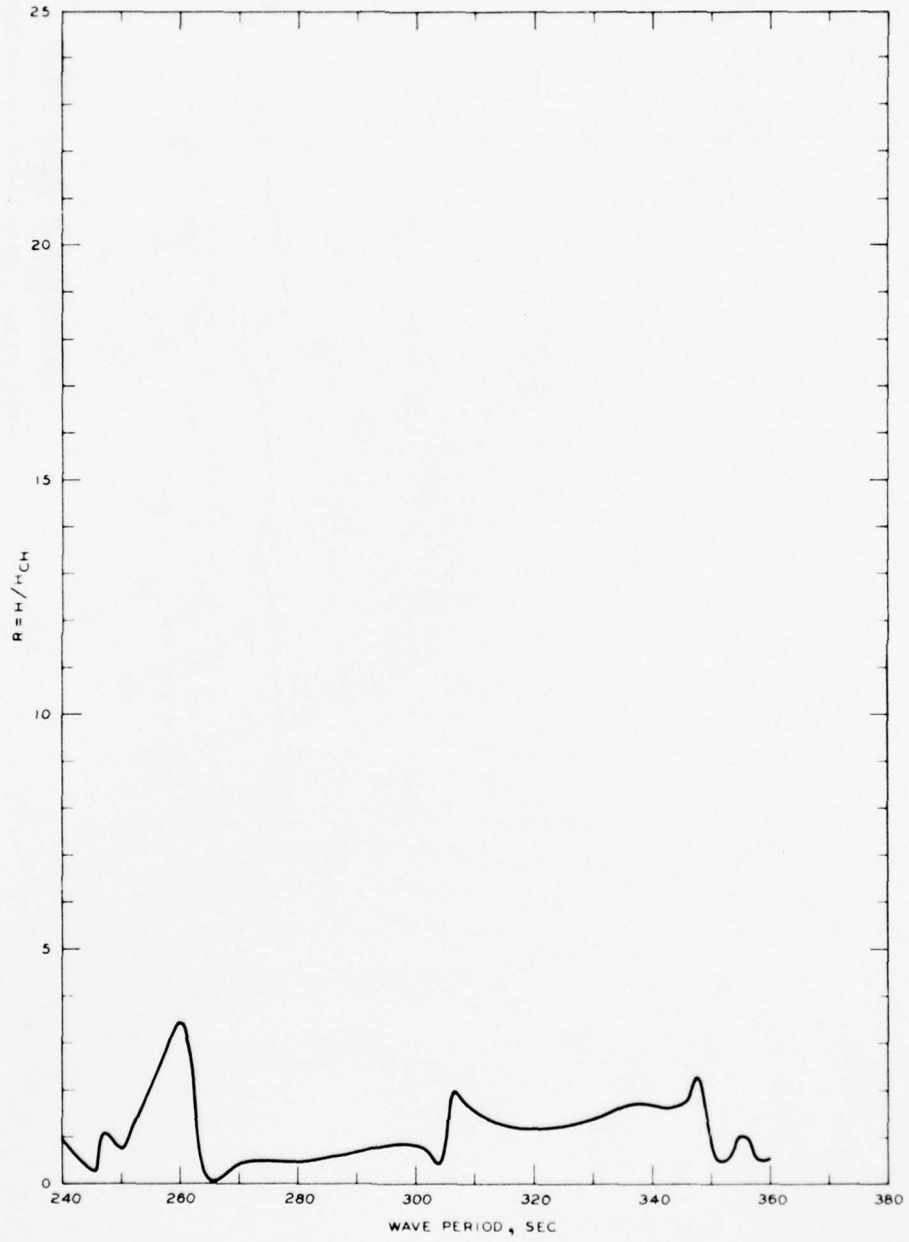

NOTE R = WAVE-HEIGHT AMPLIFICATION FACTOR
H = WAVE HEIGHT, FT
H_{CH} = WAVE HEIGHT FOR CLOSED HARBOR, FT

FREQUENCY RESPONSE

WAVE-HEIGHT AMPLIFICATION FACTOR
STA LA-9, GRID 4A

PLATE 61

PLATE 62

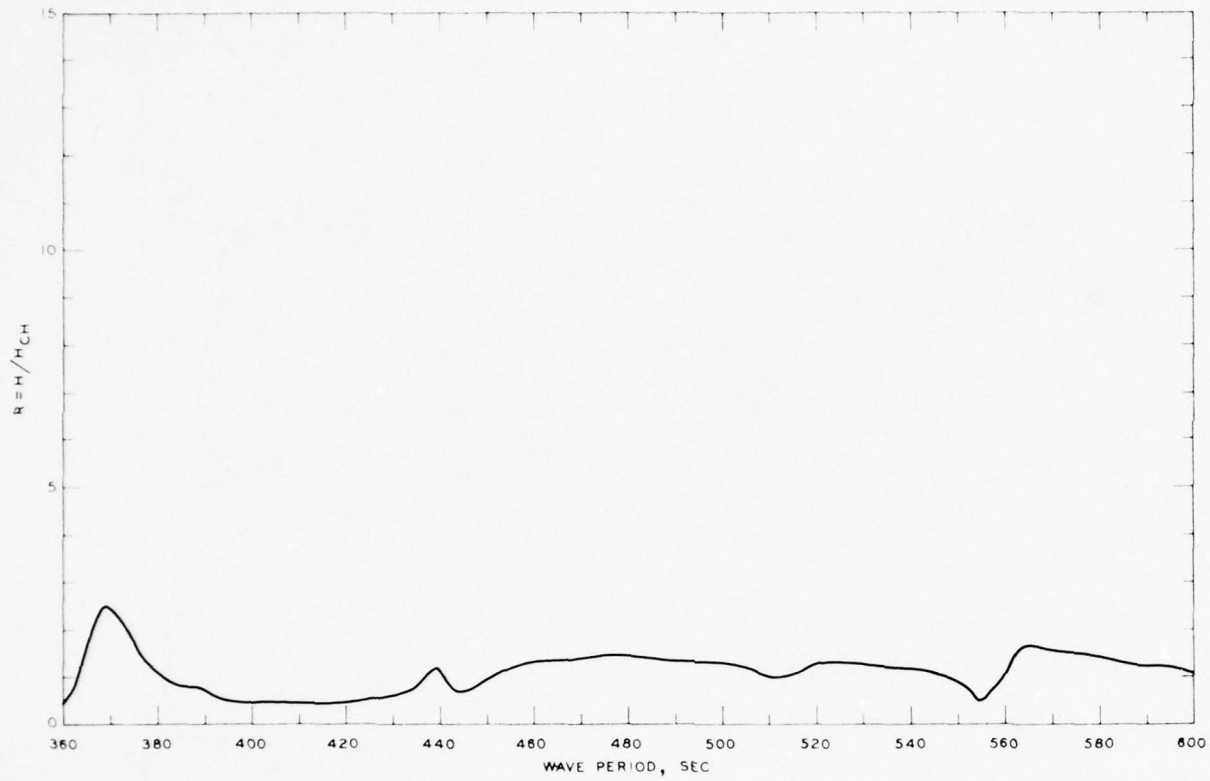

NOTE: R = WAVE-HEIGHT AMPLIFICATION FACTOR
H = WAVE HEIGHT, FT
H_{CH} = WAVE HEIGHT FOR CLOSED HARBOR, FT

FREQUENCY RESPONSE

WAVE-HEIGHT AMPLIFICATION FACTOR
STA LA-9, GRID 5A

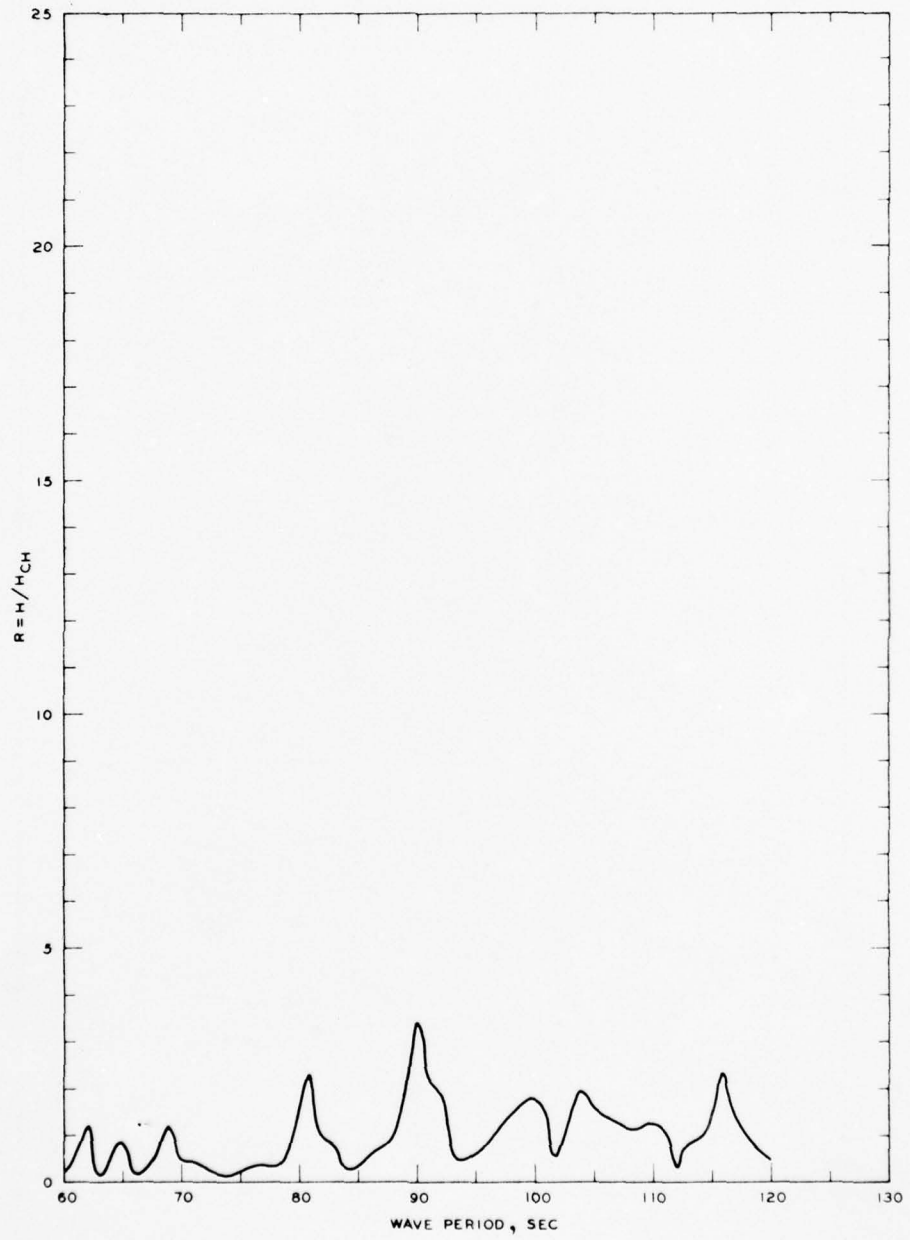

NOTE R = WAVE-HEIGHT AMPLIFICATION FACTOR
H = WAVE HEIGHT, FT
H_{CH} = WAVE HEIGHT FOR CLOSED HARBOR, FT

FREQUENCY RESPONSE

WAVE-HEIGHT AMPLIFICATION FACTOR
STA LA-10, GRID 1A

PLATE 63

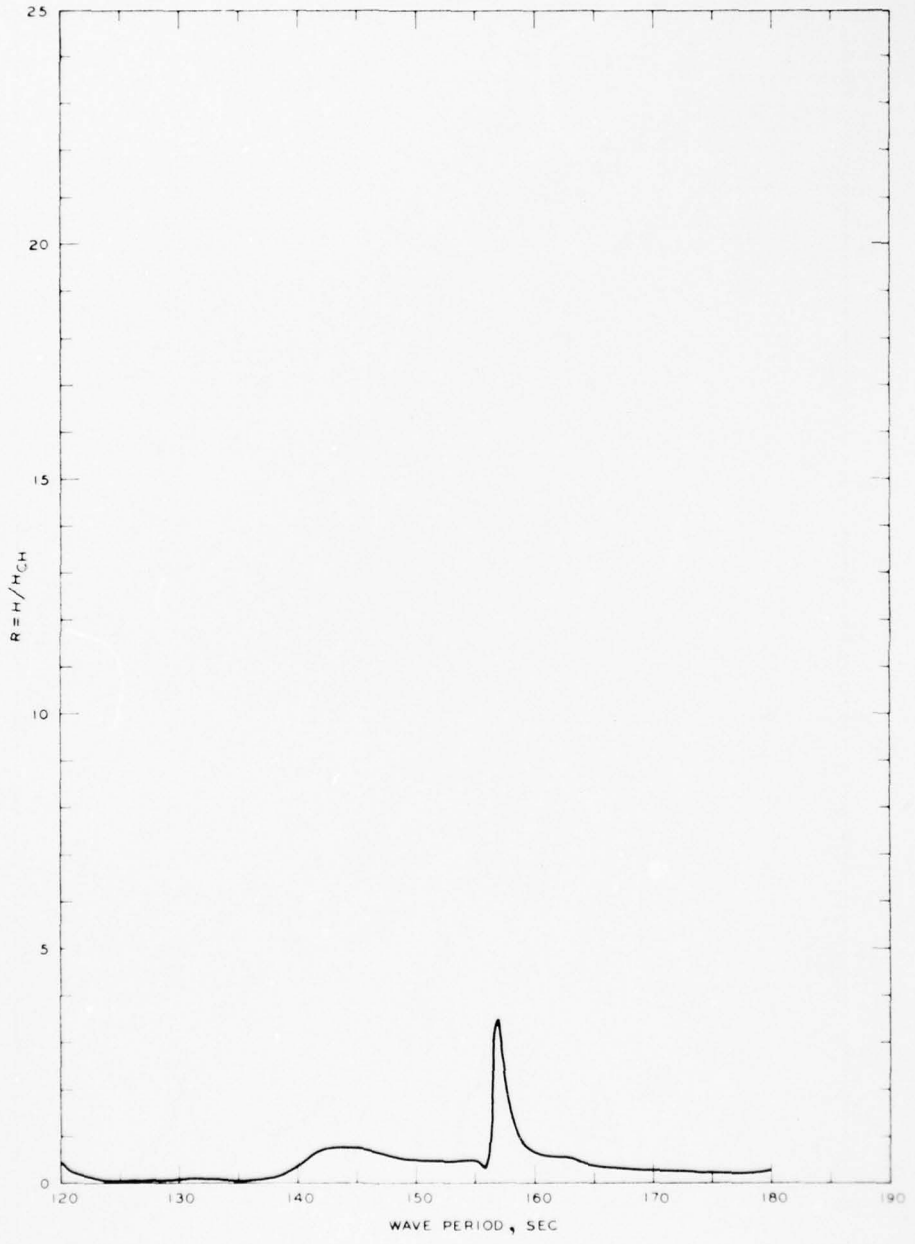

NOTE R = WAVE-HEIGHT AMPLIFICATION FACTOR
H = WAVE HEIGHT, FT
H_{CH} = WAVE HEIGHT FOR CLOSED HARBOR, FT

FREQUENCY RESPONSE

WAVE-HEIGHT AMPLIFICATION FACTOR
STA LA-10, GRID 2A

PLATE 64

AD-A037 155 ARMY ENGINEER WATERWAYS EXPERIMENT STATION VICKSBURG MISS F/G 20/4
LOS ANGELES HARBOR NUMERICAL ANALYSIS OF HARBOR OSCILLATIONS.(U)
FEB 77 J R HOUSTON
UNCLASSIFIED WES-MP-H-77-2 NL

2 OF 3
AD A037155

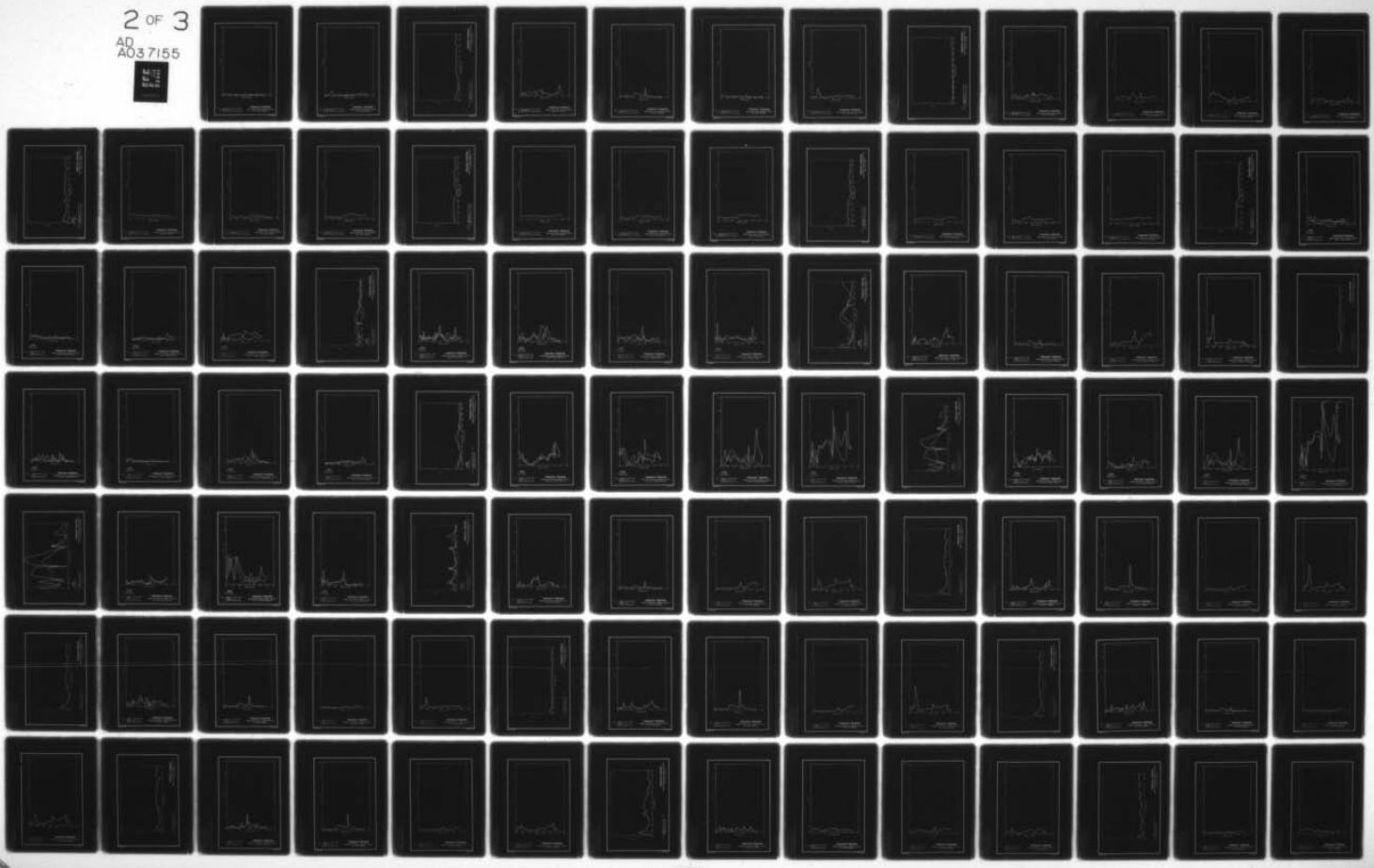

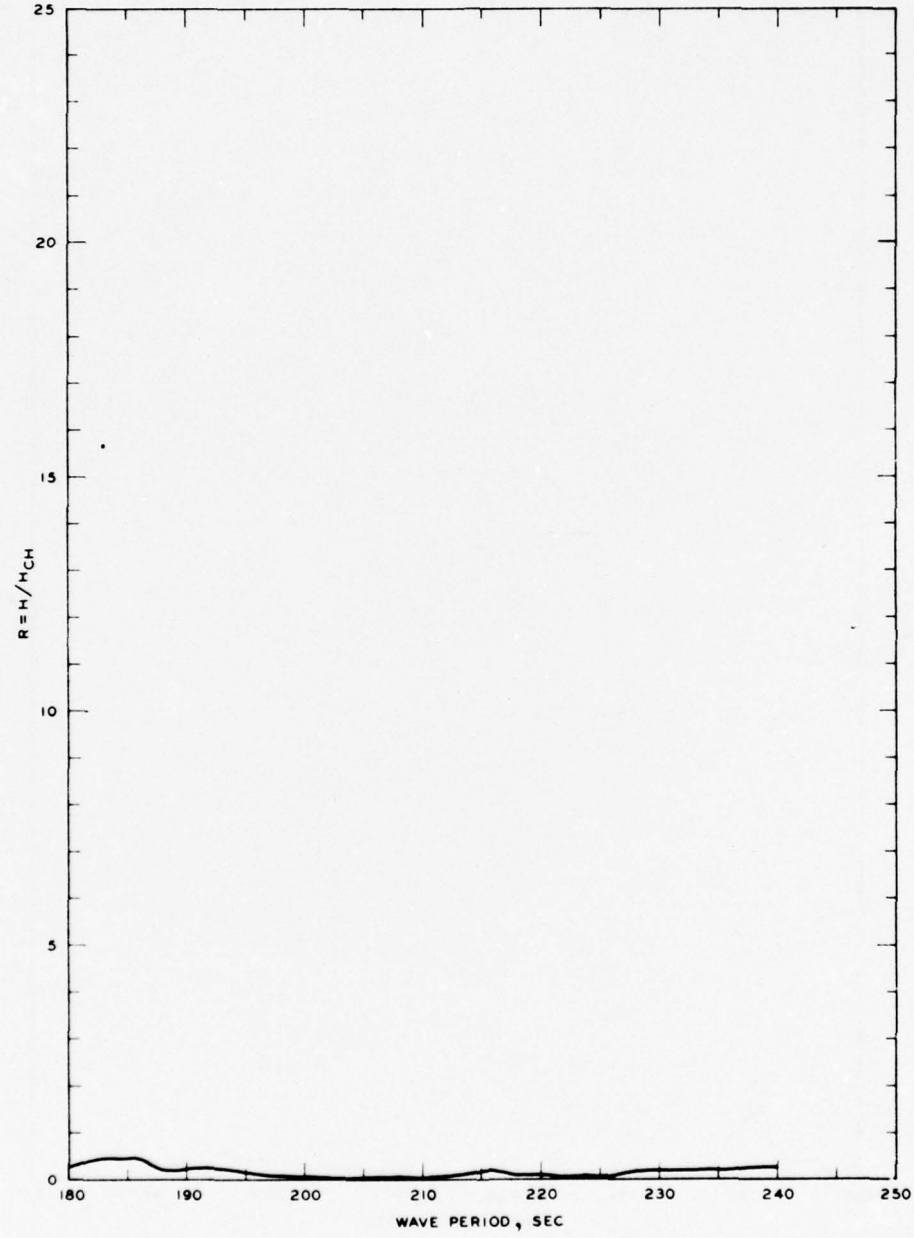

NOTE R = WAVE-HEIGHT AMPLIFICATION FACTOR
H = WAVE HEIGHT, FT
H_{CH} = WAVE HEIGHT FOR CLOSED HARBOR, FT

FREQUENCY RESPONSE

WAVE-HEIGHT AMPLIFICATION FACTOR
STA LA-10, GRID 3A

PLATE 65

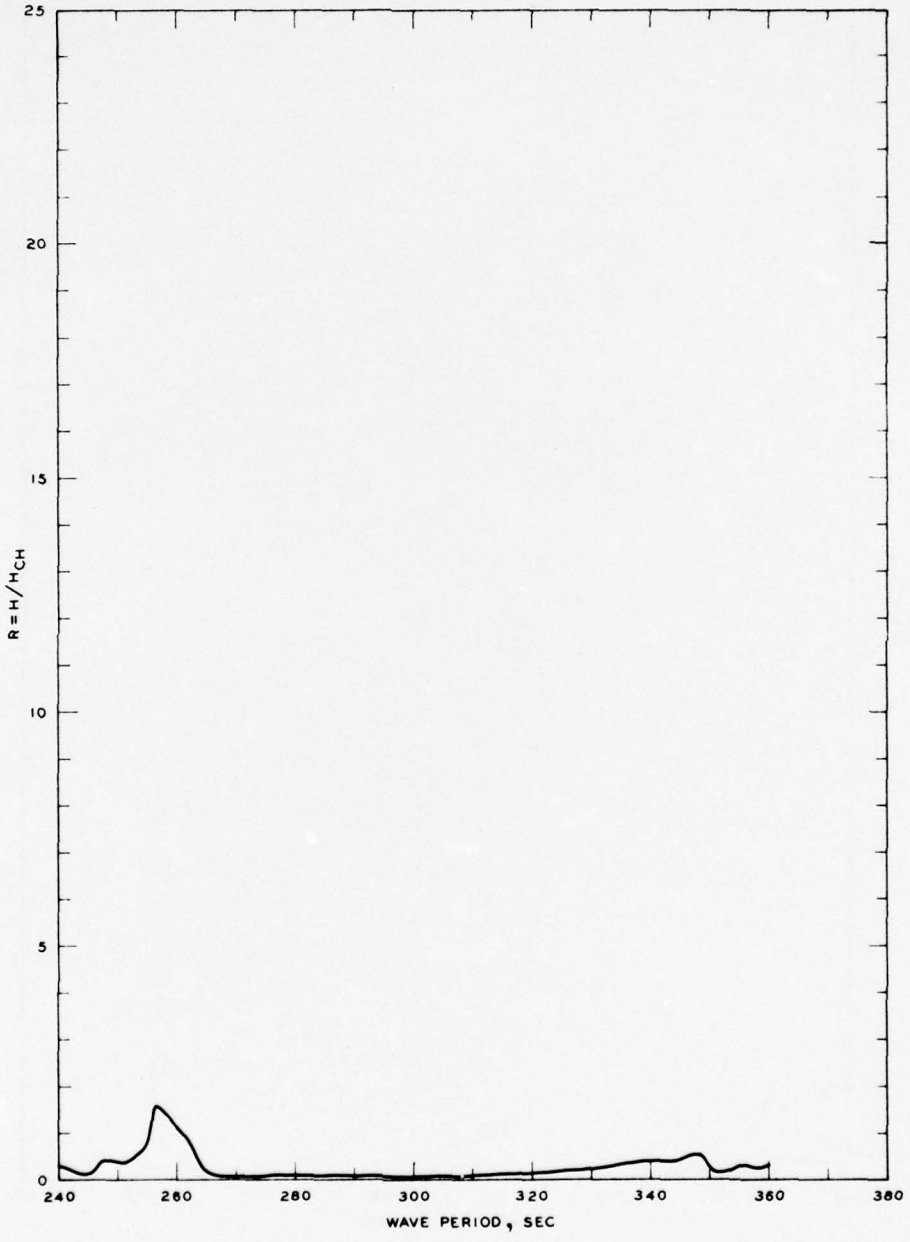

NOTE R = WAVE-HEIGHT AMPLIFICATION FACTOR
H = WAVE HEIGHT, FT
H_{CH} = WAVE HEIGHT FOR CLOSED HARBOR, FT

FREQUENCY RESPONSE

WAVE-HEIGHT AMPLIFICATION FACTOR
STA LA-10, GRID 4A

PLATE 66

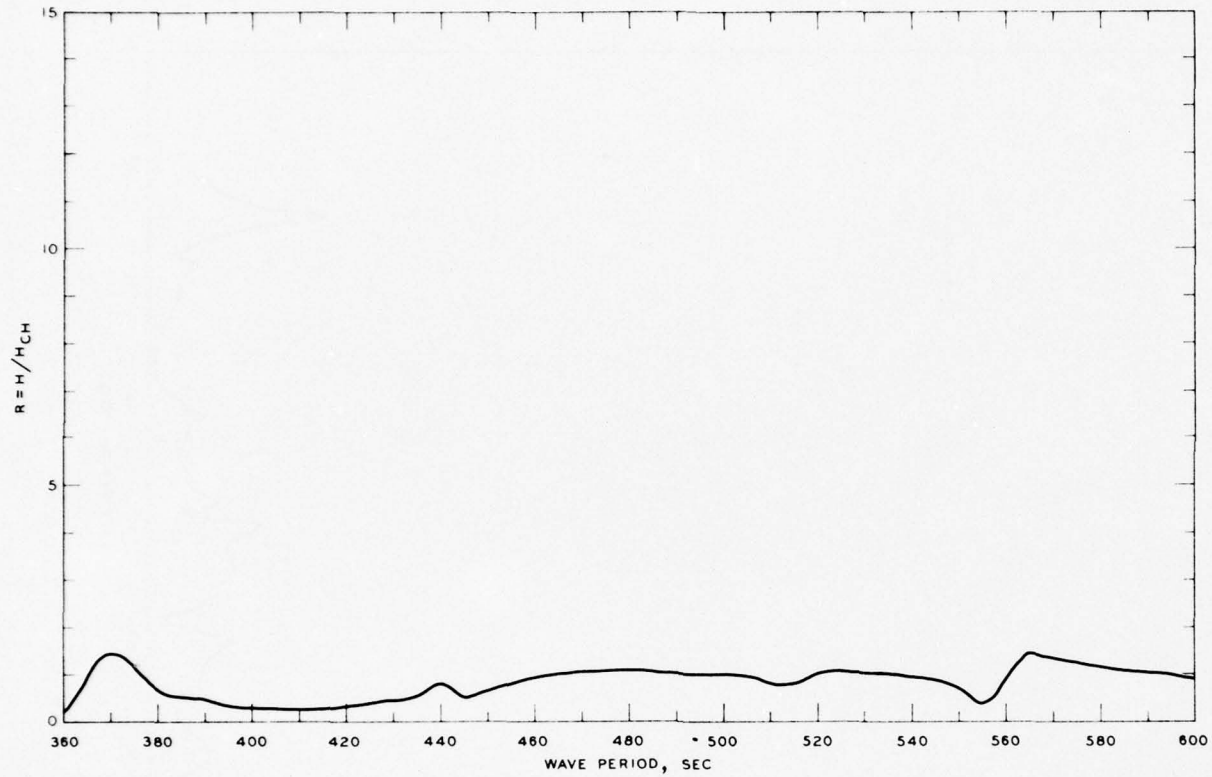

NOTE: R = WAVE-HEIGHT AMPLIFICATION FACTOR
H = WAVE HEIGHT, FT
H_{CH} = WAVE HEIGHT FOR CLOSED HARBOR, FT

FREQUENCY RESPONSE

WAVE-HEIGHT AMPLIFICATION FACTOR
STA LA-10, GRID 5A

PLATE 67

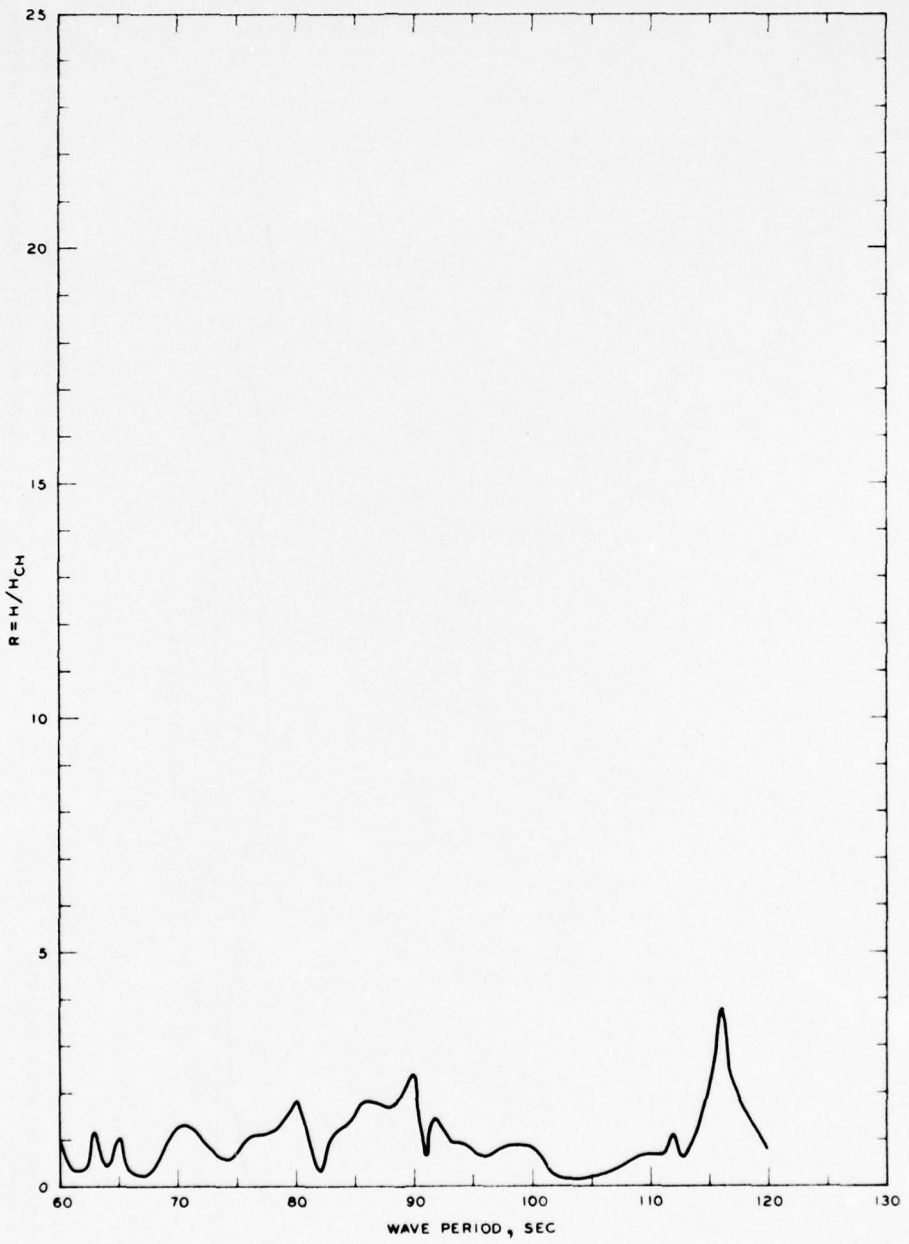

NOTE R = WAVE-HEIGHT AMPLIFICATION FACTOR
H = WAVE HEIGHT, FT
H_{CH} = WAVE HEIGHT FOR CLOSED HARBOR, FT

FREQUENCY RESPONSE

WAVE-HEIGHT AMPLIFICATION FACTOR
STA LA-11, GRID 1A

PLATE 68

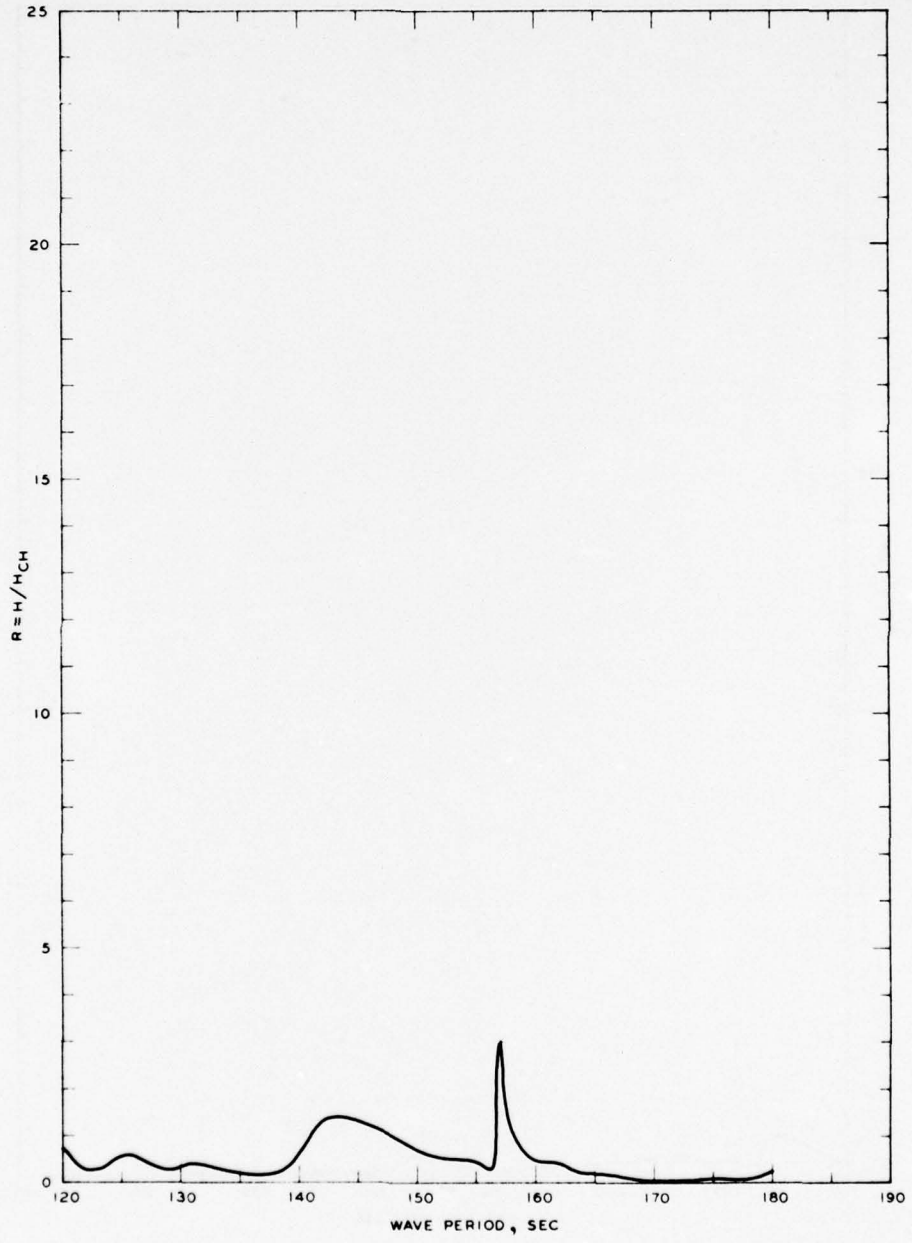

NOTE R = WAVE-HEIGHT AMPLIFICATION FACTOR
H = WAVE HEIGHT, FT
H_{CH} = WAVE HEIGHT FOR CLOSED HARBOR, FT

FREQUENCY RESPONSE

WAVE-HEIGHT AMPLIFICATION FACTOR
STA LA-11, GRID 2A

PLATE 69

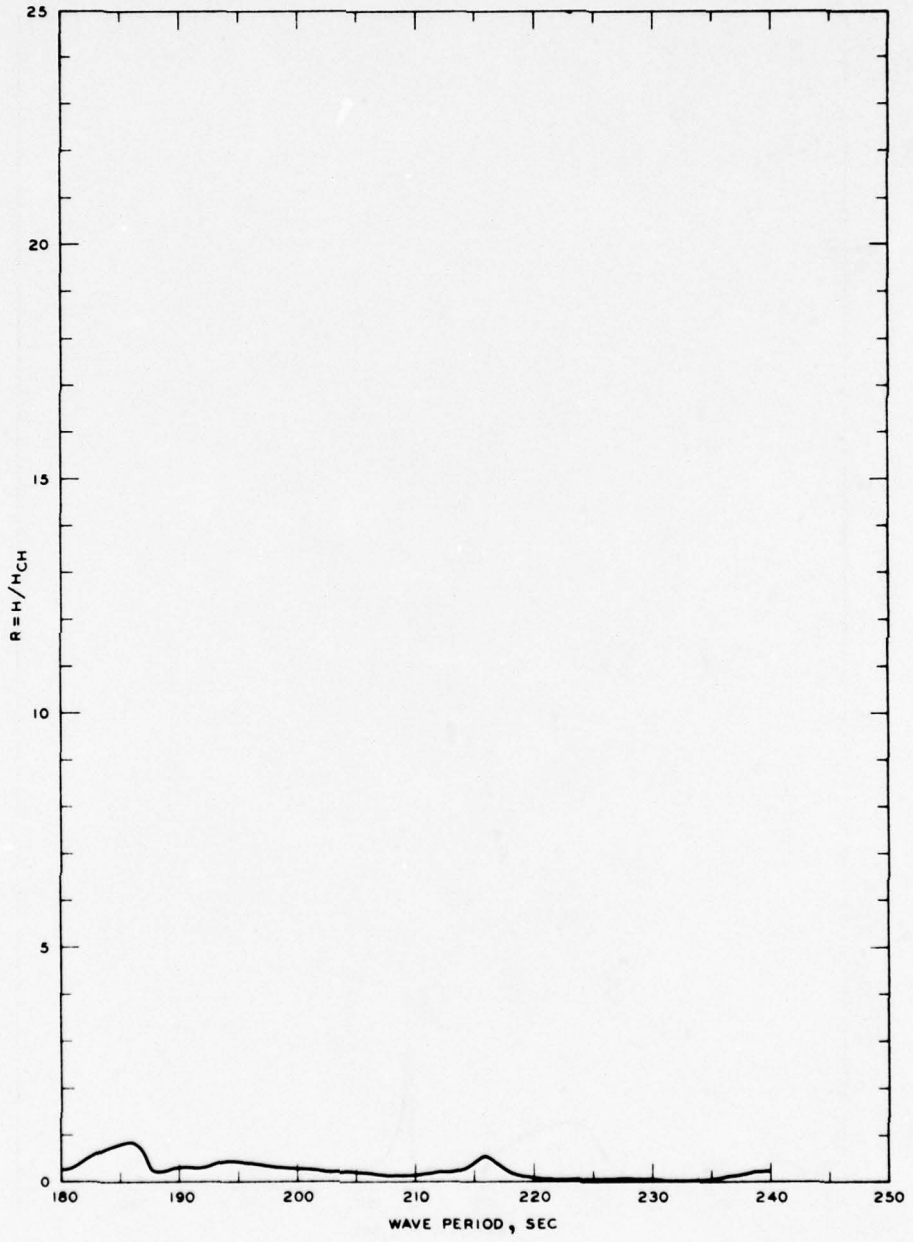

NOTE R = WAVE-HEIGHT AMPLIFICATION FACTOR
H = WAVE HEIGHT, FT
H_{CH} = WAVE HEIGHT FOR CLOSED HARBOR, FT

FREQUENCY RESPONSE

WAVE-HEIGHT AMPLIFICATION FACTOR
STA LA-11, GRID 3A

PLATE 70

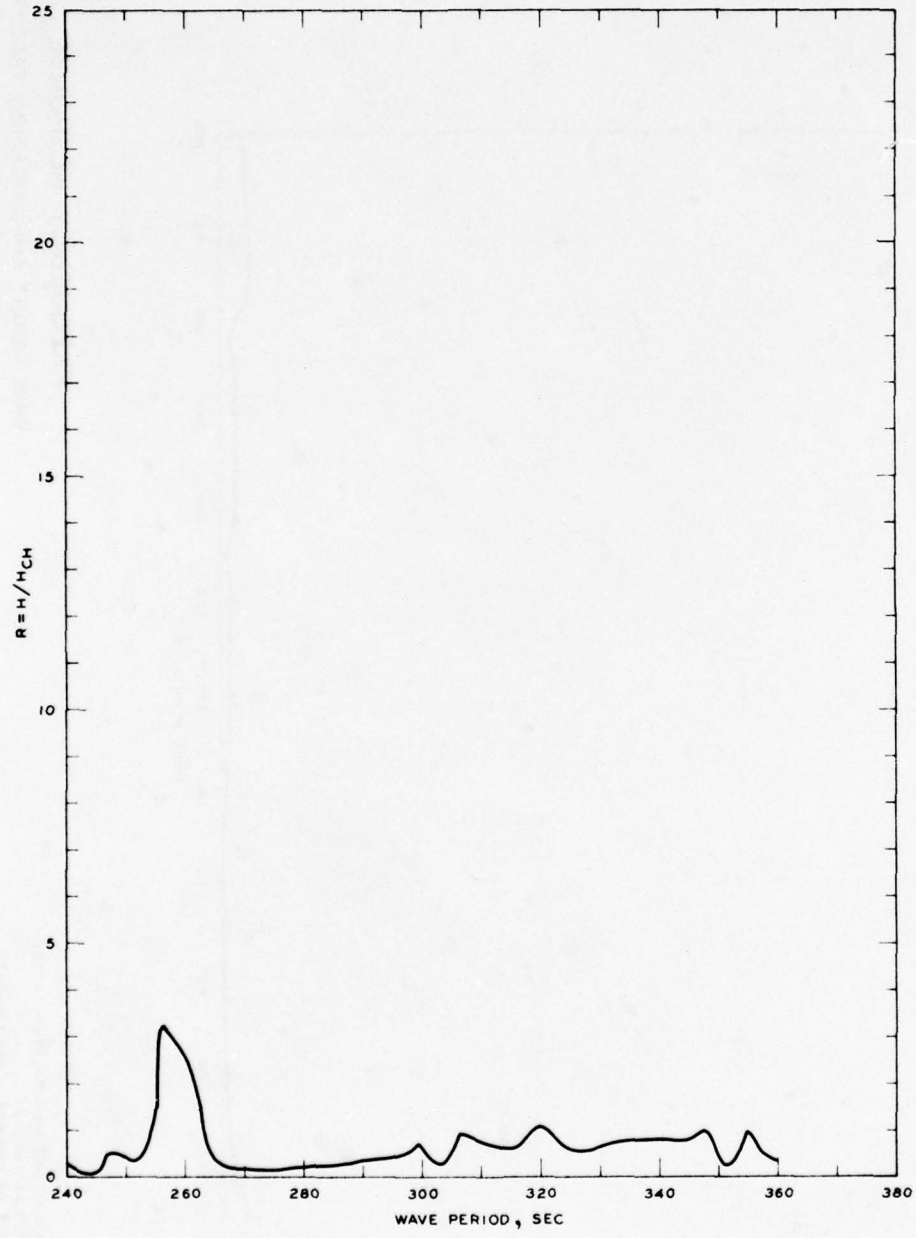

NOTE R = WAVE-HEIGHT AMPLIFICATION FACTOR
H = WAVE HEIGHT, FT
H_{CH} = WAVE HEIGHT FOR CLOSED HARBOR, FT

FREQUENCY RESPONSE

WAVE-HEIGHT AMPLIFICATION FACTOR
STA LA-11, GRID 4A

PLATE 71

PLATE 72

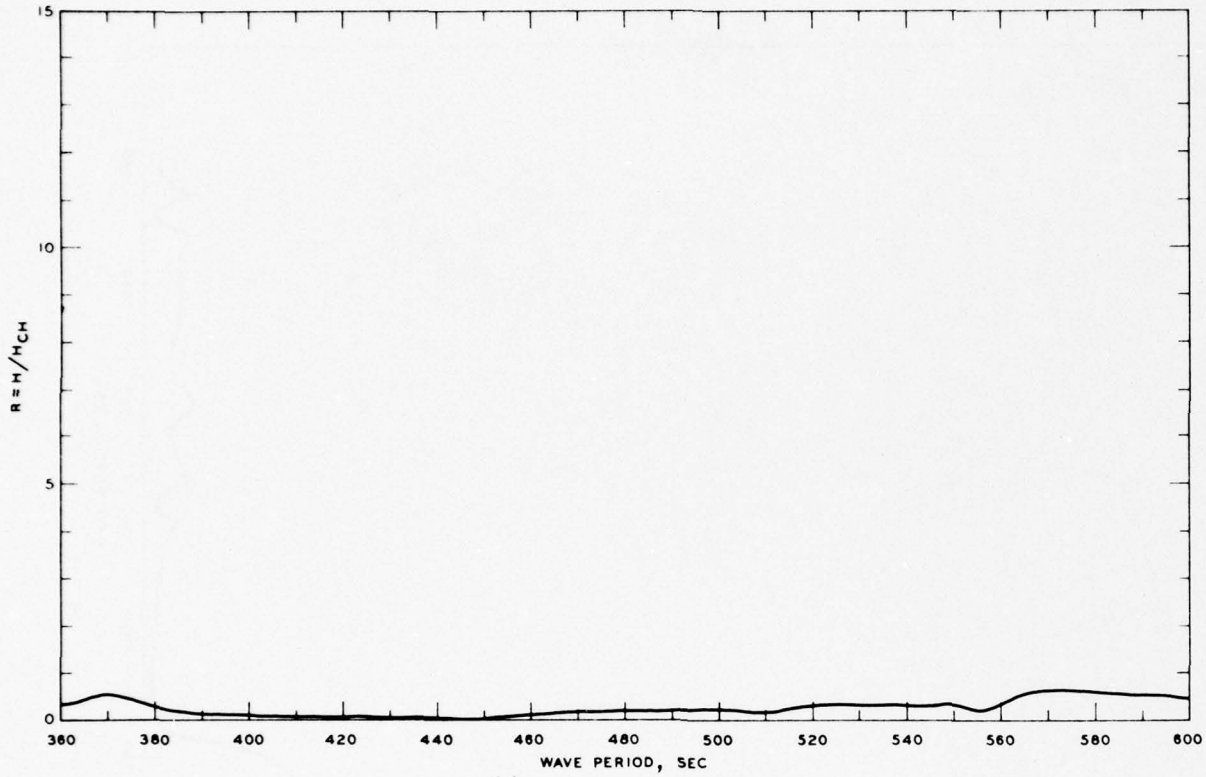

NOTE: R = WAVE-HEIGHT AMPLIFICATION FACTOR
H = WAVE HEIGHT, FT
H_{CH} = WAVE HEIGHT FOR CLOSED HARBOR, FT

FREQUENCY RESPONSE

WAVE-HEIGHT AMPLIFICATION FACTOR
STA LA-11, GRID 5A

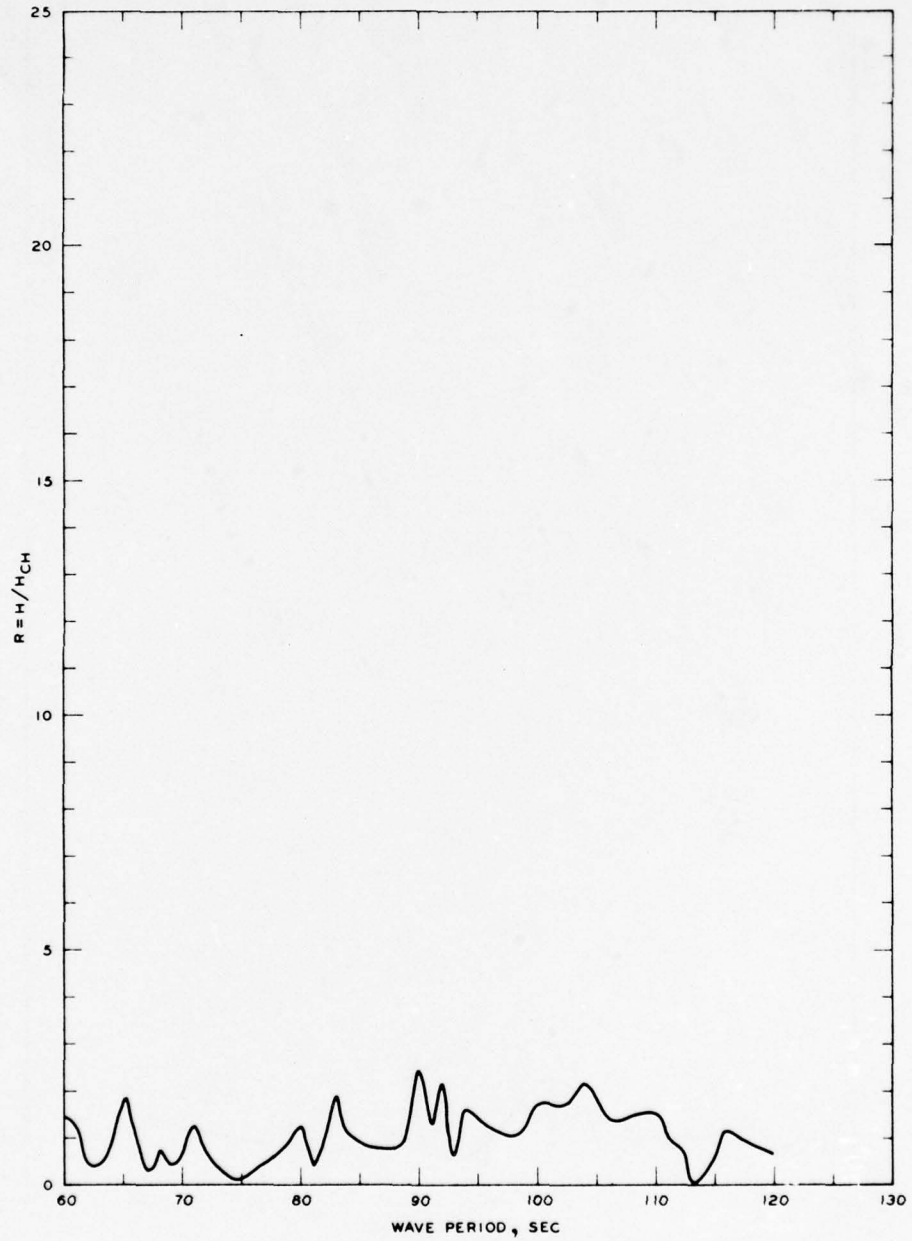

NOTE R = WAVE-HEIGHT AMPLIFICATION FACTOR
H = WAVE HEIGHT, FT
H_{CH} = WAVE HEIGHT FOR CLOSED HARBOR, FT

FREQUENCY RESPONSE

WAVE-HEIGHT AMPLIFICATION FACTOR
STA LA-12, GRID 1A

PLATE 73

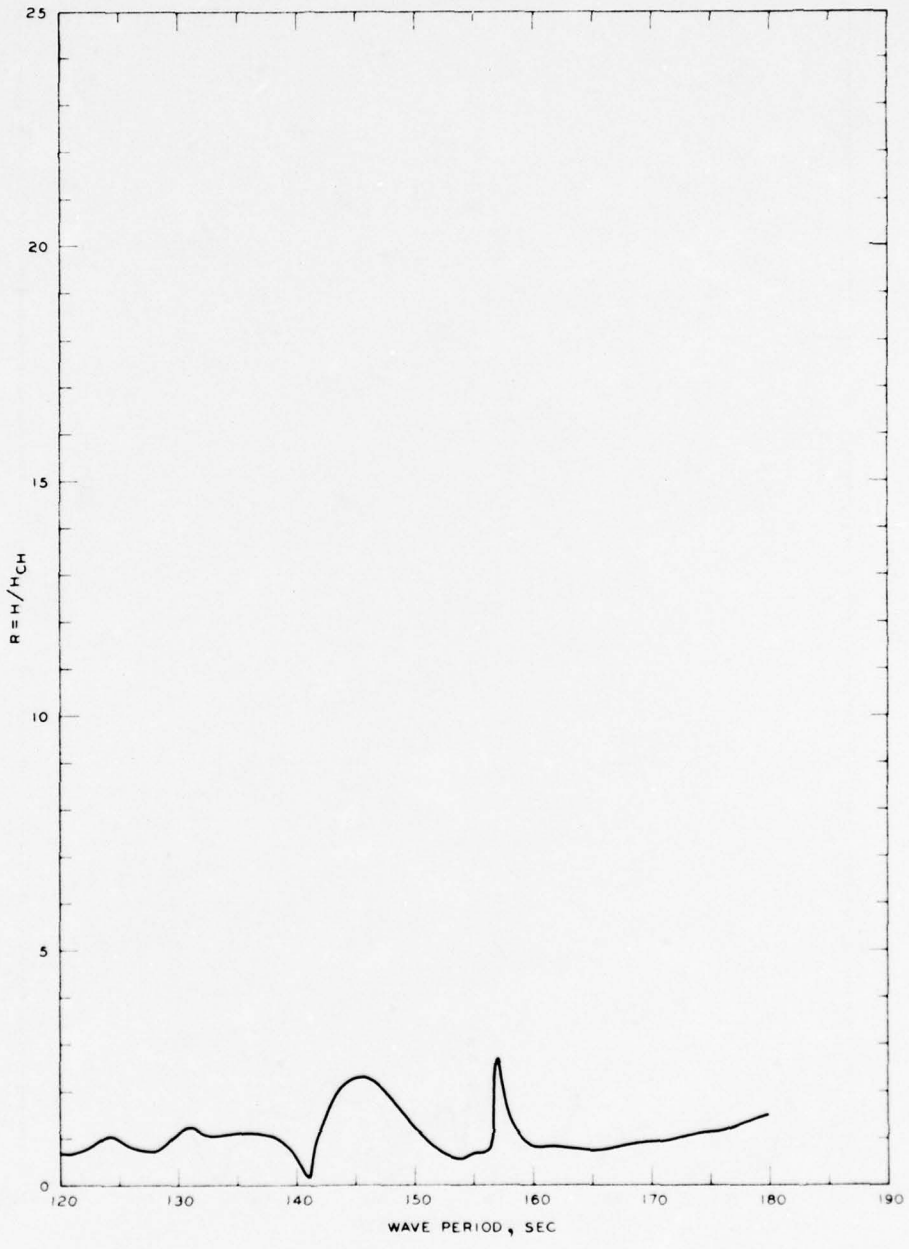

NOTE R = WAVE-HEIGHT AMPLIFICATION FACTOR
H = WAVE HEIGHT, FT
H_{CH} = WAVE HEIGHT FOR CLOSED HARBOR, FT

FREQUENCY RESPONSE

WAVE-HEIGHT AMPLIFICATION FACTOR
STA LA-12, GRID 2A

PLATE 74

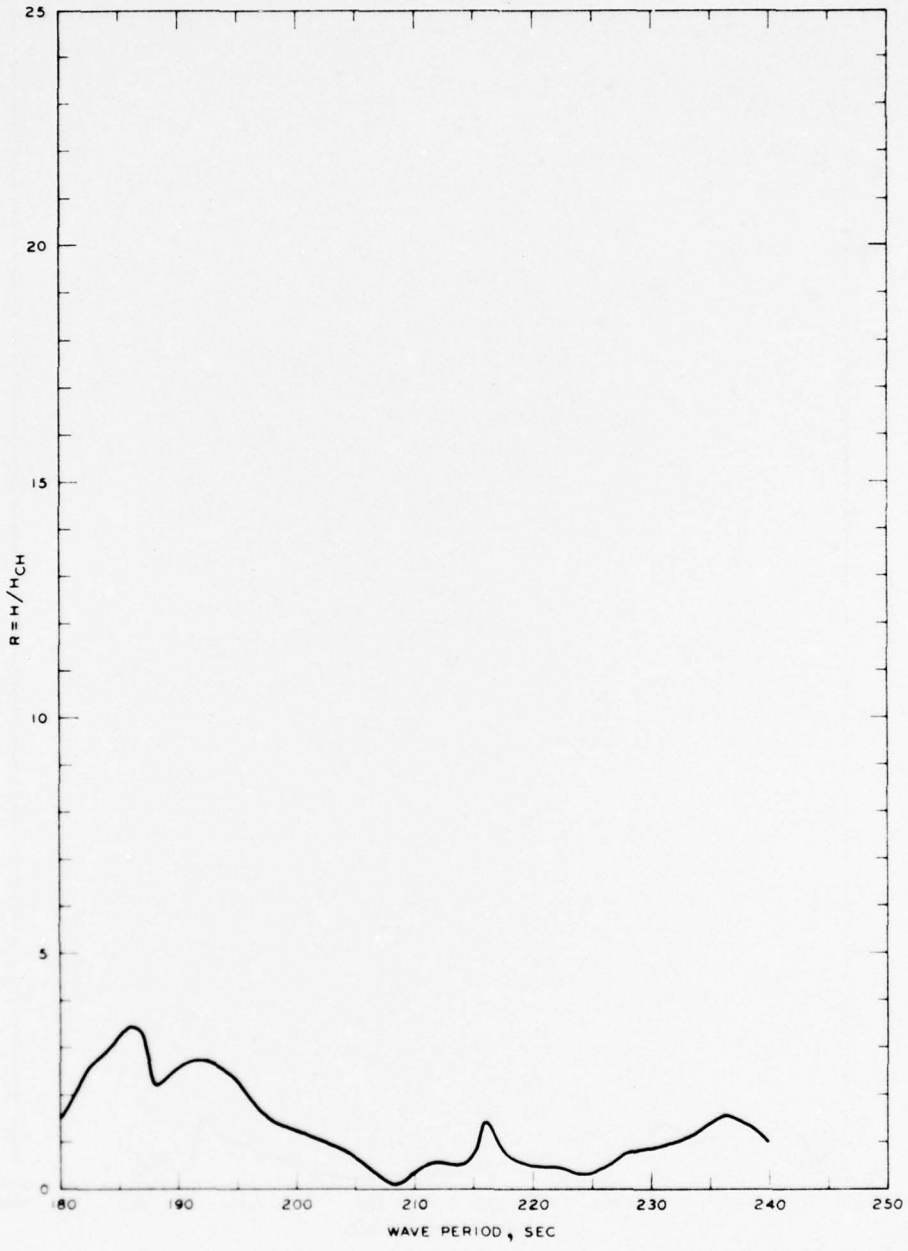

NOTE R = WAVE-HEIGHT AMPLIFICATION FACTOR
H = WAVE HEIGHT, FT
H_{CH} = WAVE HEIGHT FOR CLOSED HARBOR, FT

FREQUENCY RESPONSE

WAVE-HEIGHT AMPLIFICATION FACTOR
STA LA-12, GRID 3A

PLATE 75

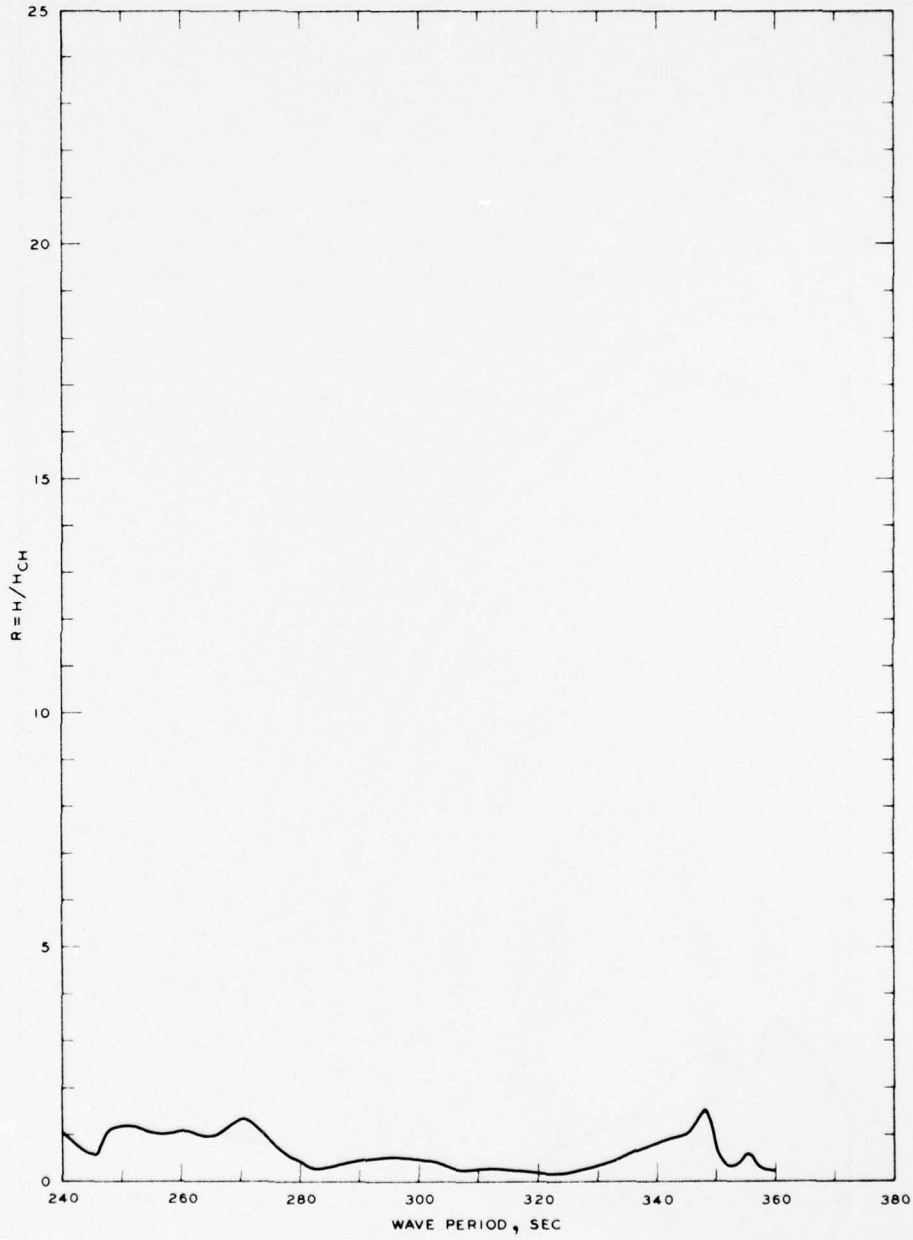

NOTE R = WAVE-HEIGHT AMPLIFICATION FACTOR
H = WAVE HEIGHT, FT
H_{CH} = WAVE HEIGHT FOR CLOSED HARBOR, FT

FREQUENCY RESPONSE

WAVE-HEIGHT AMPLIFICATION FACTOR
STA LA-12, GRID 4A

PLATE 76

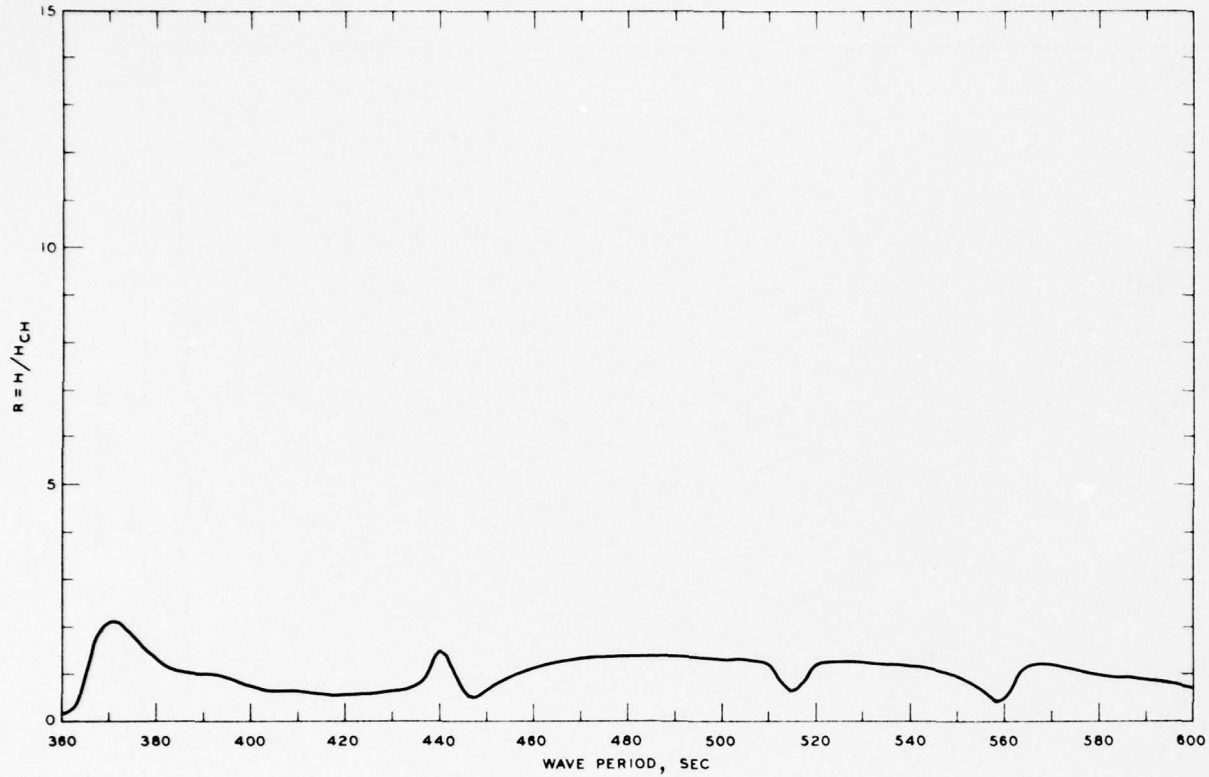

LEGEND

——— GRID 5

— — — GRID 5A

NOTE: R = WAVE-HEIGHT AMPLIFICATION FACTOR
H = WAVE HEIGHT, FT
H_{CH} = WAVE HEIGHT FOR CLOSED HARBOR, FT

FREQUENCY RESPONSE

WAVE-HEIGHT AMPLIFICATION FACTOR
STA LA-12, GRID 5A

PLATE 77

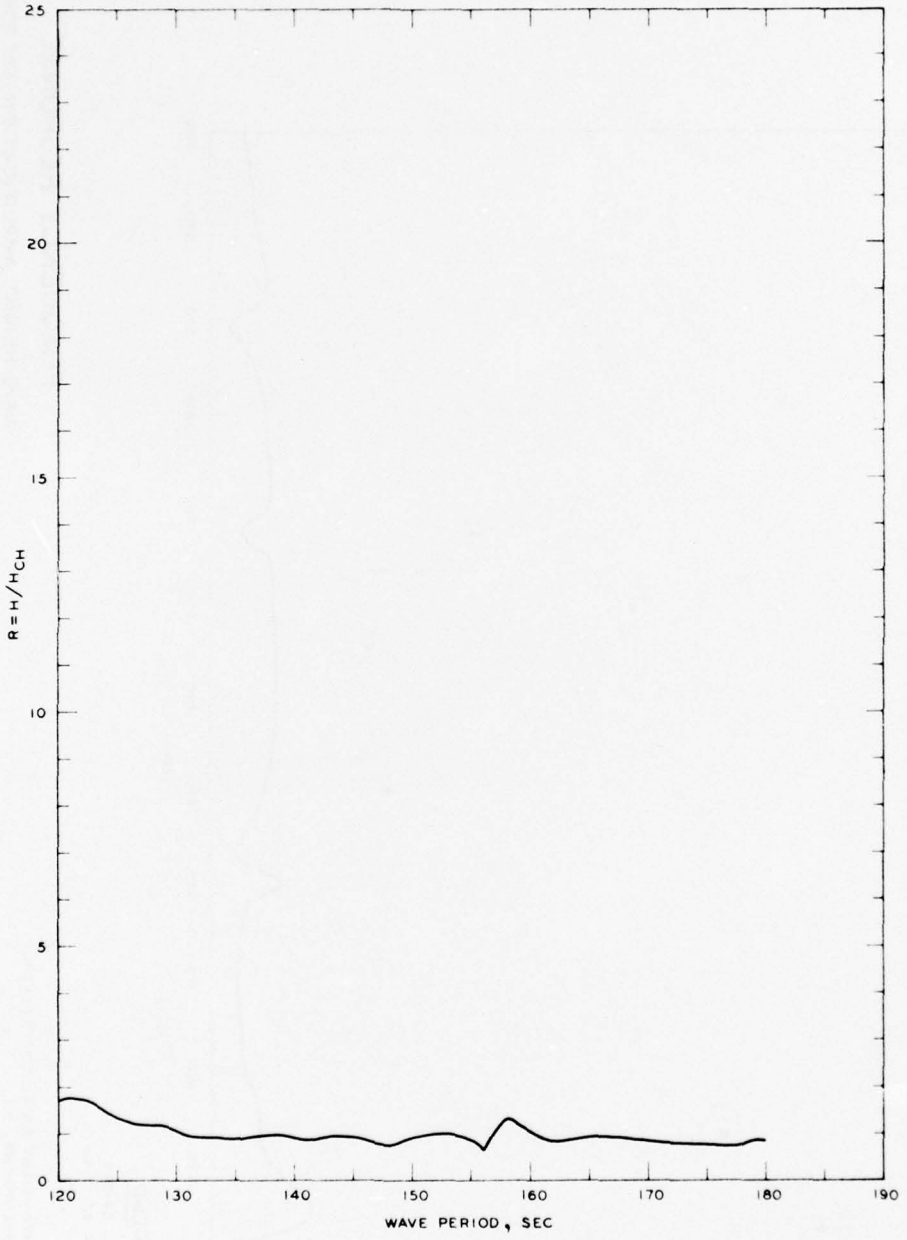

NOTE R = WAVE-HEIGHT AMPLIFICATION FACTOR
H = WAVE HEIGHT, FT
H_{CH} = WAVE HEIGHT FOR CLOSED HARBOR, FT

FREQUENCY RESPONSE

WAVE-HEIGHT AMPLIFICATION FACTOR
STA LA-13, GRID 2A

PLATE 78

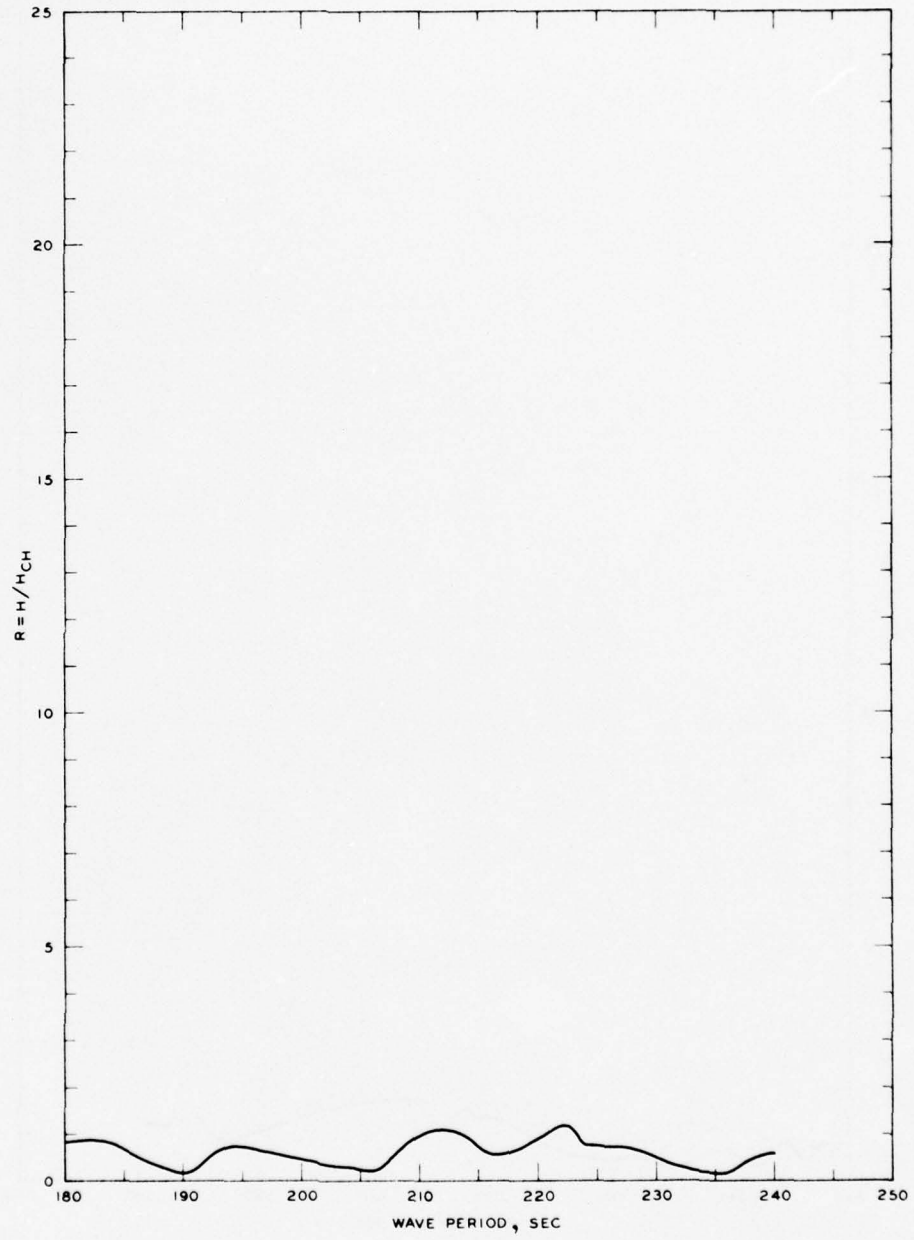

NOTE R = WAVE-HEIGHT AMPLIFICATION FACTOR
H = WAVE HEIGHT, FT
H_{CH} = WAVE HEIGHT FOR CLOSED HARBOR, FT

FREQUENCY RESPONSE

WAVE-HEIGHT AMPLIFICATION FACTOR
STA LA-13, GRID 3A

PLATE 79

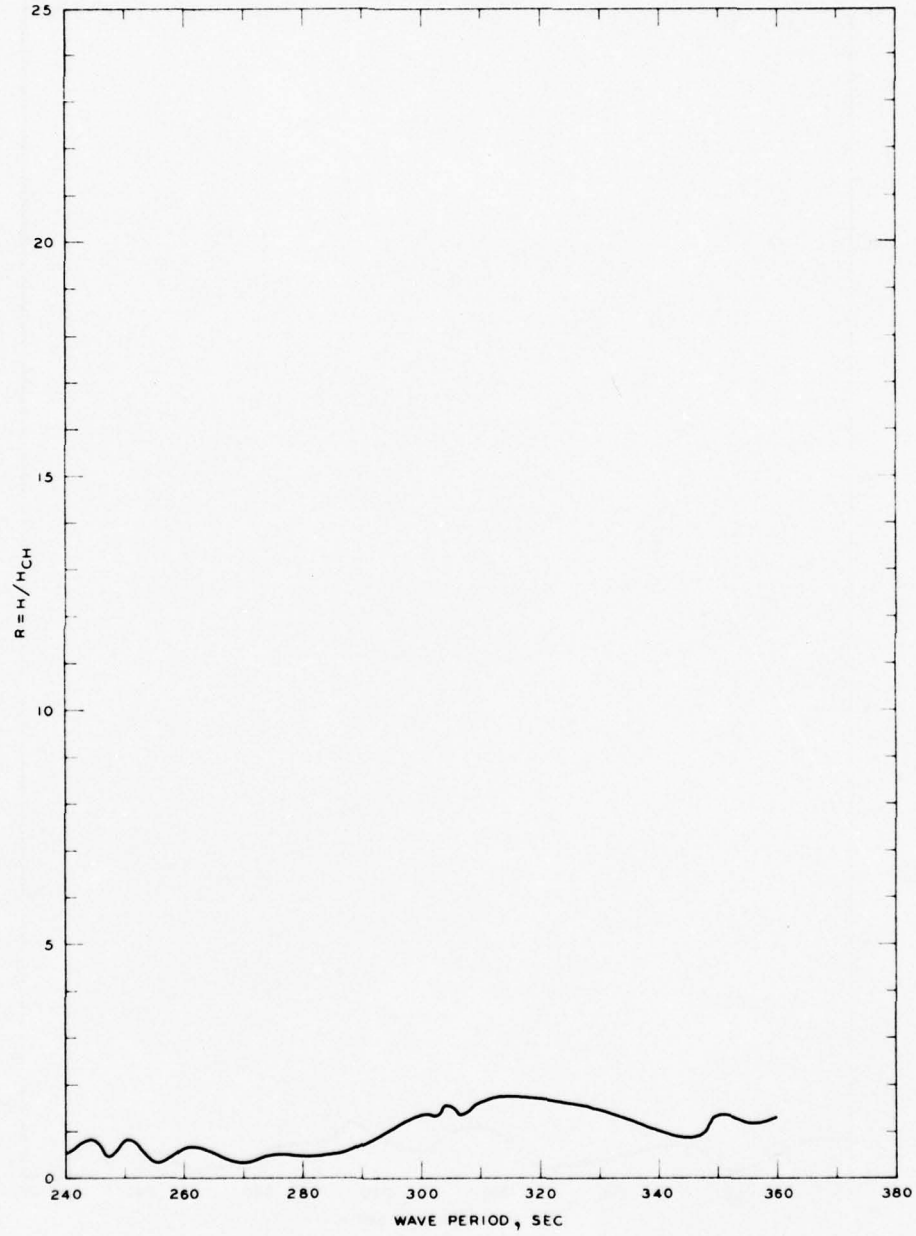

NOTE R = WAVE-HEIGHT AMPLIFICATION FACTOR
H = WAVE HEIGHT, FT
H_{CH} = WAVE HEIGHT FOR CLOSED HARBOR, FT

FREQUENCY RESPONSE

WAVE-HEIGHT AMPLIFICATION FACTOR
STA LA-13, GRID 4A

PLATE 80

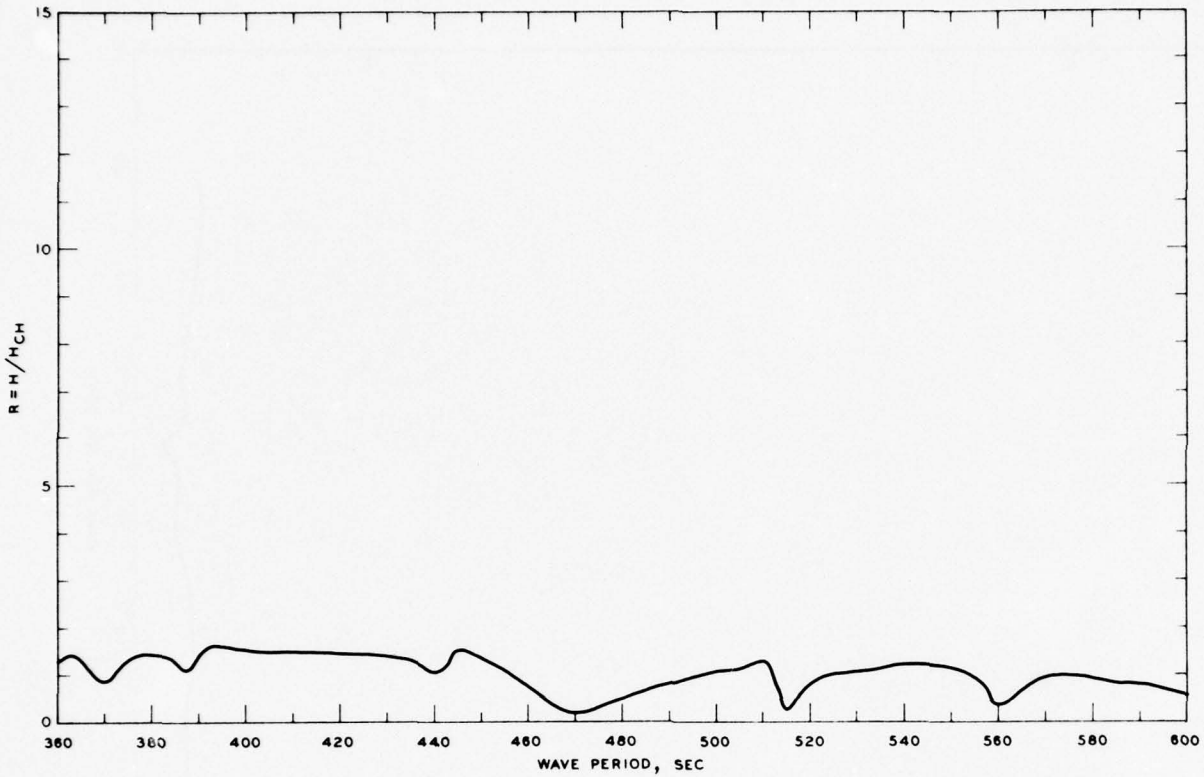

NOTE: R = WAVE-HEIGHT AMPLIFICATION FACTOR
H = WAVE HEIGHT, FT
H_{CH} = WAVE HEIGHT FOR CLOSED HARBOR, FT

FREQUENCY RESPONSE

WAVE-HEIGHT AMPLIFICATION FACTOR
STA LA-13, GRID 5A

PLATE 81

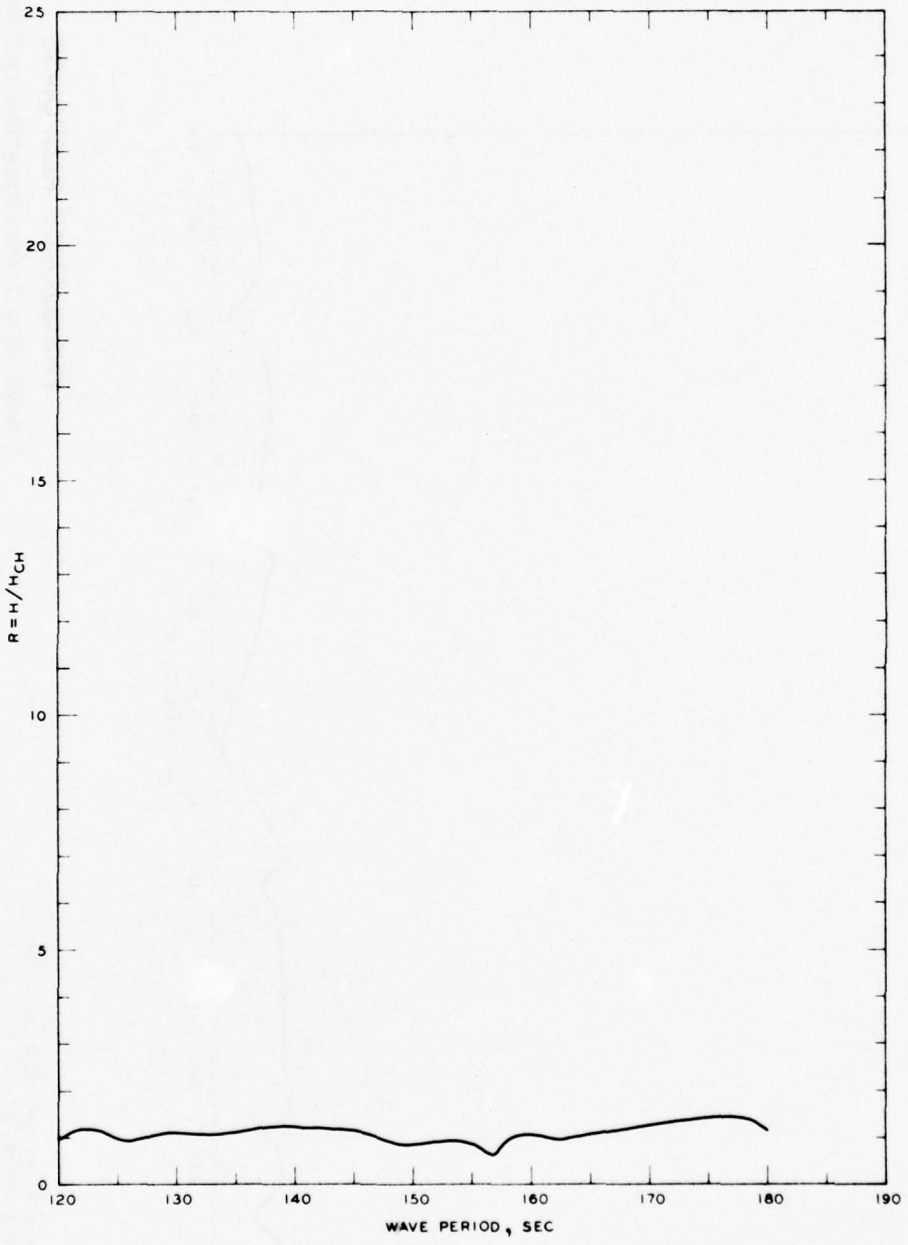

NOTE R = WAVE-HEIGHT AMPLIFICATION FACTOR
H = WAVE HEIGHT, FT
H_{CH} = WAVE HEIGHT FOR CLOSED HARBOR, FT

FREQUENCY RESPONSE

WAVE-HEIGHT AMPLIFICATION FACTOR
STA LA-14, GRID 2A

PLATE 82

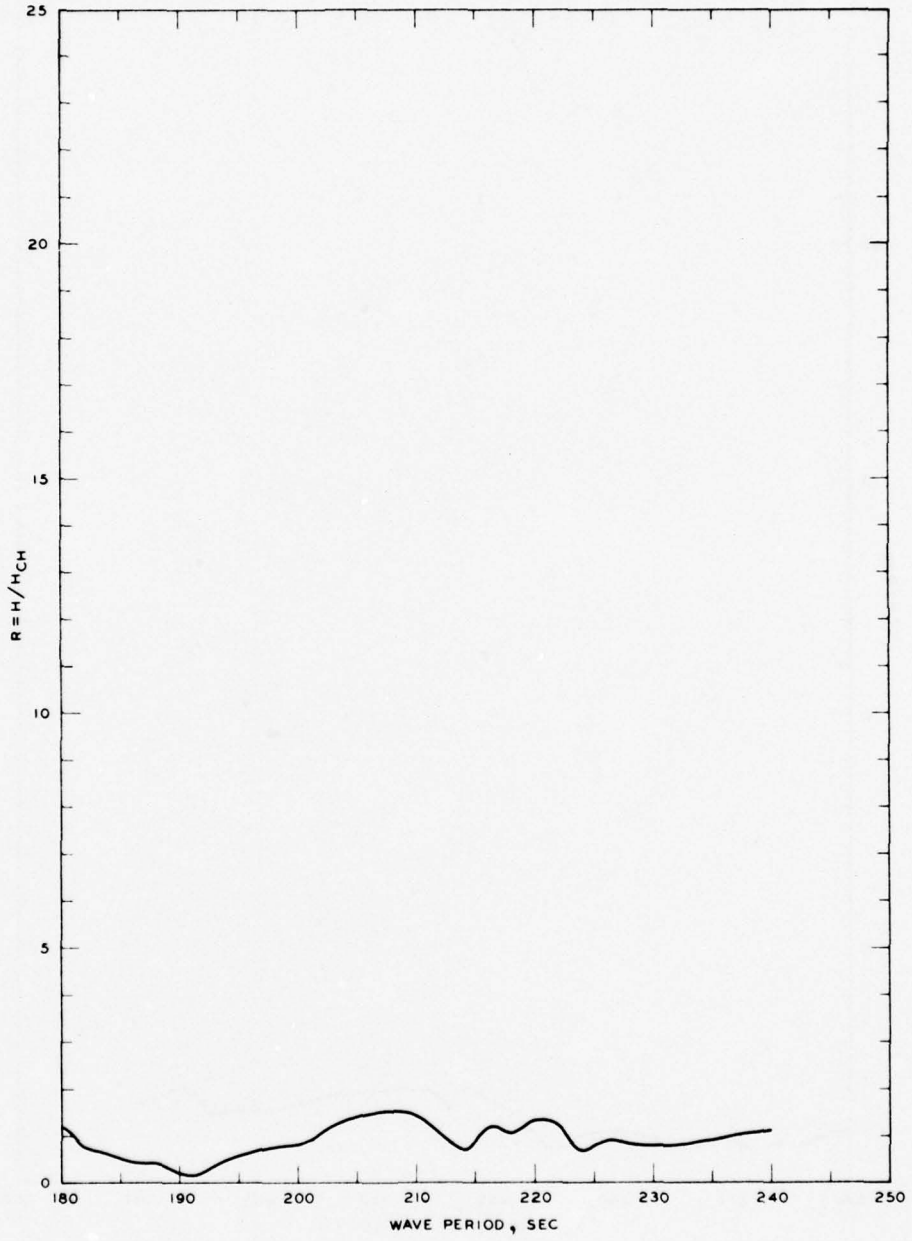

NOTE R = WAVE-HEIGHT AMPLIFICATION FACTOR
H = WAVE HEIGHT, FT
H_{CH} = WAVE HEIGHT FOR CLOSED HARBOR, FT

FREQUENCY RESPONSE

WAVE-HEIGHT AMPLIFICATION FACTOR
STA LA-14, GRID 3A

PLATE 83

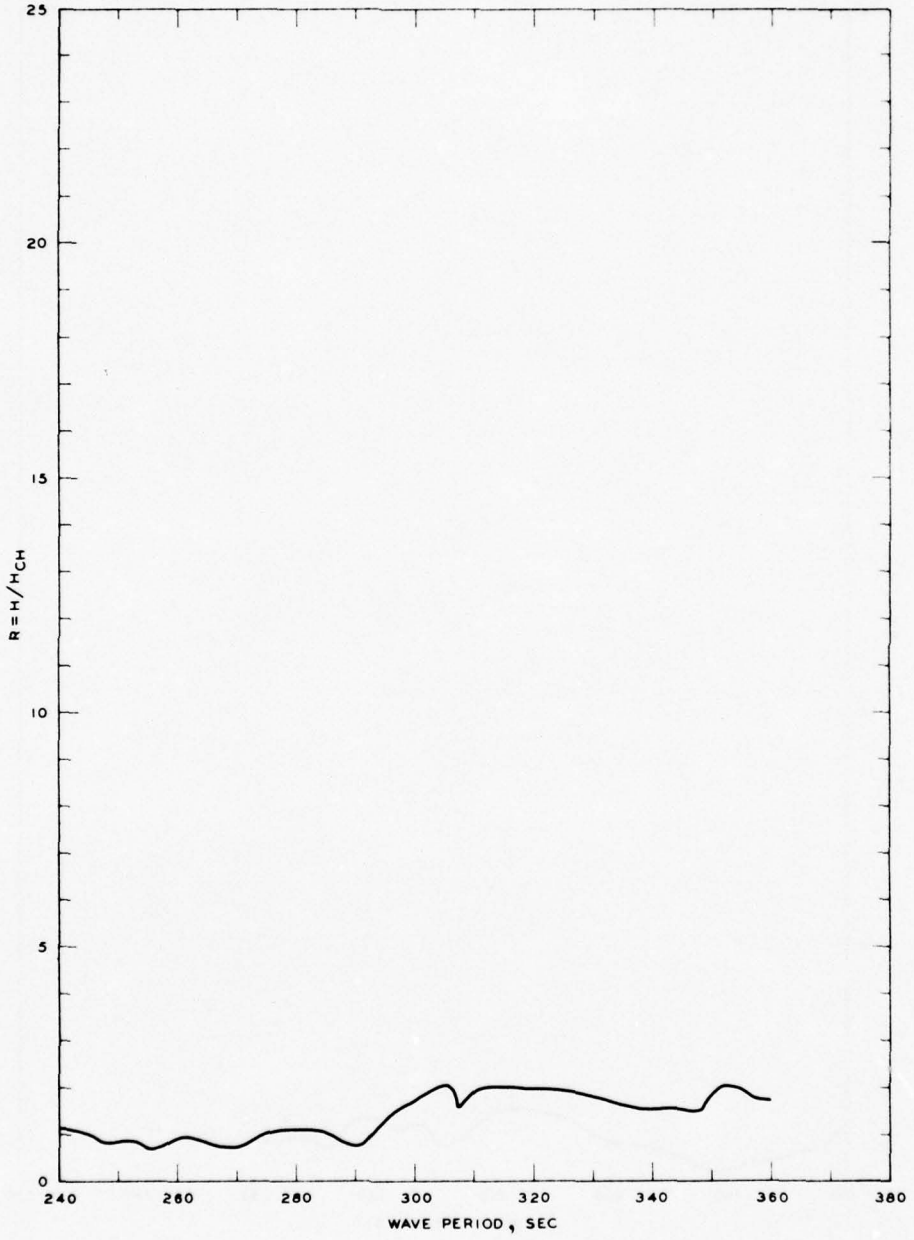

NOTE R = WAVE-HEIGHT AMPLIFICATION FACTOR
H = WAVE HEIGHT, FT
H_{CH} = WAVE HEIGHT FOR CLOSED HARBOR, FT

FREQUENCY RESPONSE

WAVE-HEIGHT AMPLIFICATION FACTOR
STA LA-14, GRID 4A

PLATE 84

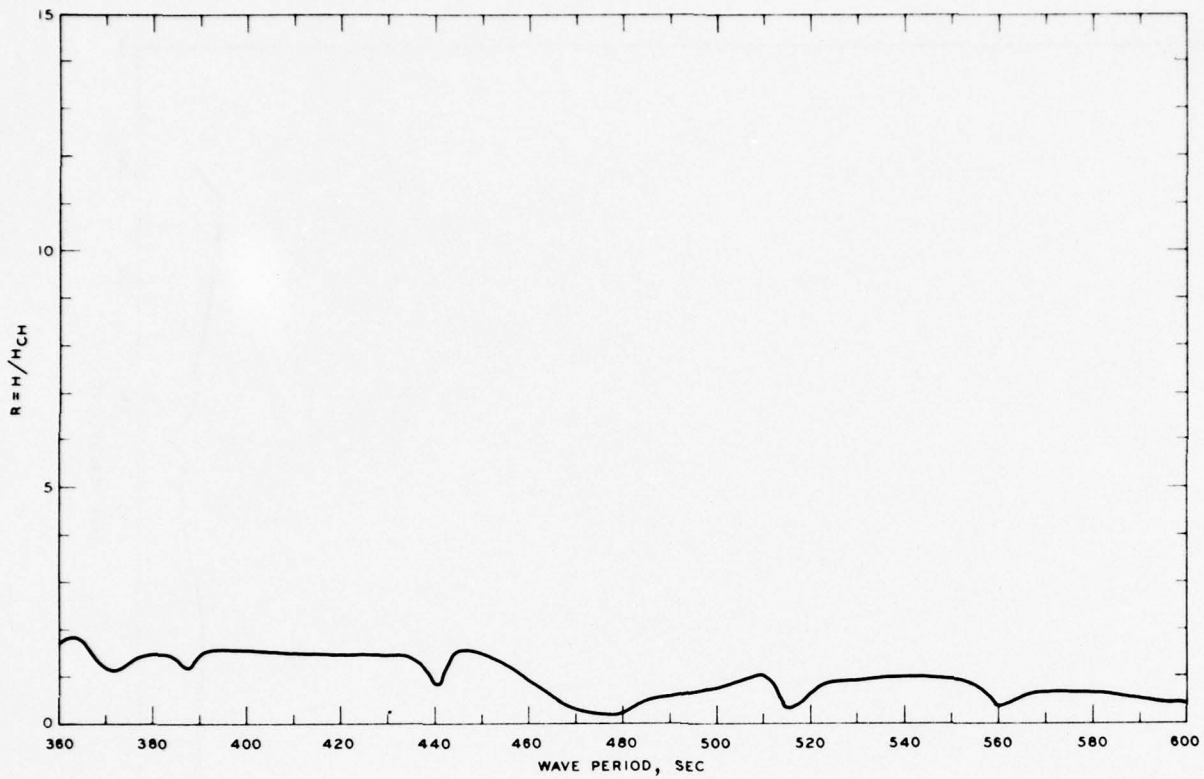

NOTE: R = WAVE-HEIGHT AMPLIFICATION FACTOR
H = WAVE HEIGHT, FT
H_{CH} = WAVE HEIGHT FOR CLOSED HARBOR, FT

FREQUENCY RESPONSE

WAVE-HEIGHT AMPLIFICATION FACTOR
STA LA-14, GRID 5A

PLATE 85

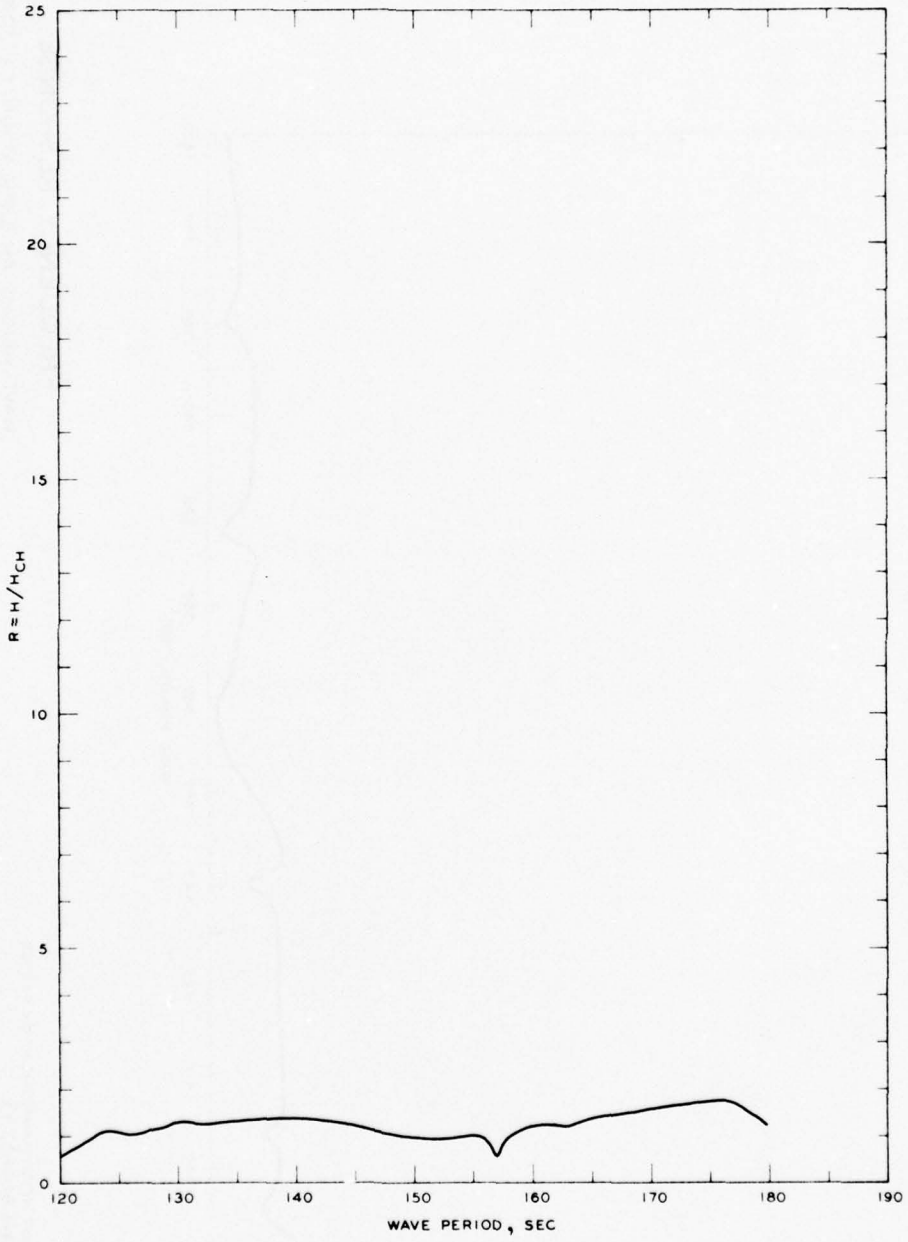

NOTE R = WAVE-HEIGHT AMPLIFICATION FACTOR
H = WAVE HEIGHT, FT
H_{CH} = WAVE HEIGHT FOR CLOSED HARBOR, FT

FREQUENCY RESPONSE

WAVE-HEIGHT AMPLIFICATION FACTOR
STA LA-15, GRID 2A

PLATE 86

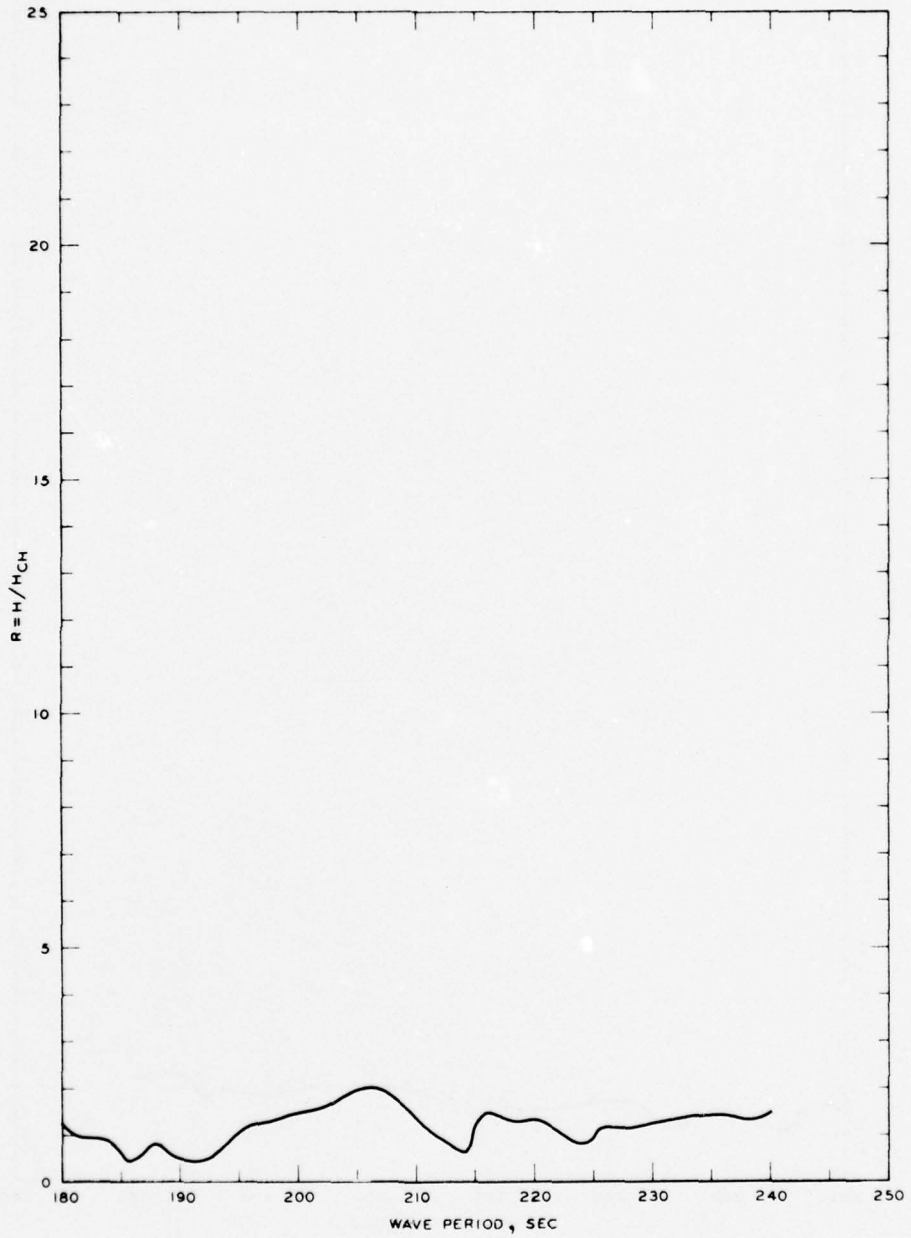

NOTE R = WAVE-HEIGHT AMPLIFICATION FACTOR
H = WAVE HEIGHT, FT
H_{CH} = WAVE HEIGHT FOR CLOSED HARBOR, FT

FREQUENCY RESPONSE

WAVE-HEIGHT AMPLIFICATION FACTOR
STA LA-15, GRID 3A

PLATE 87

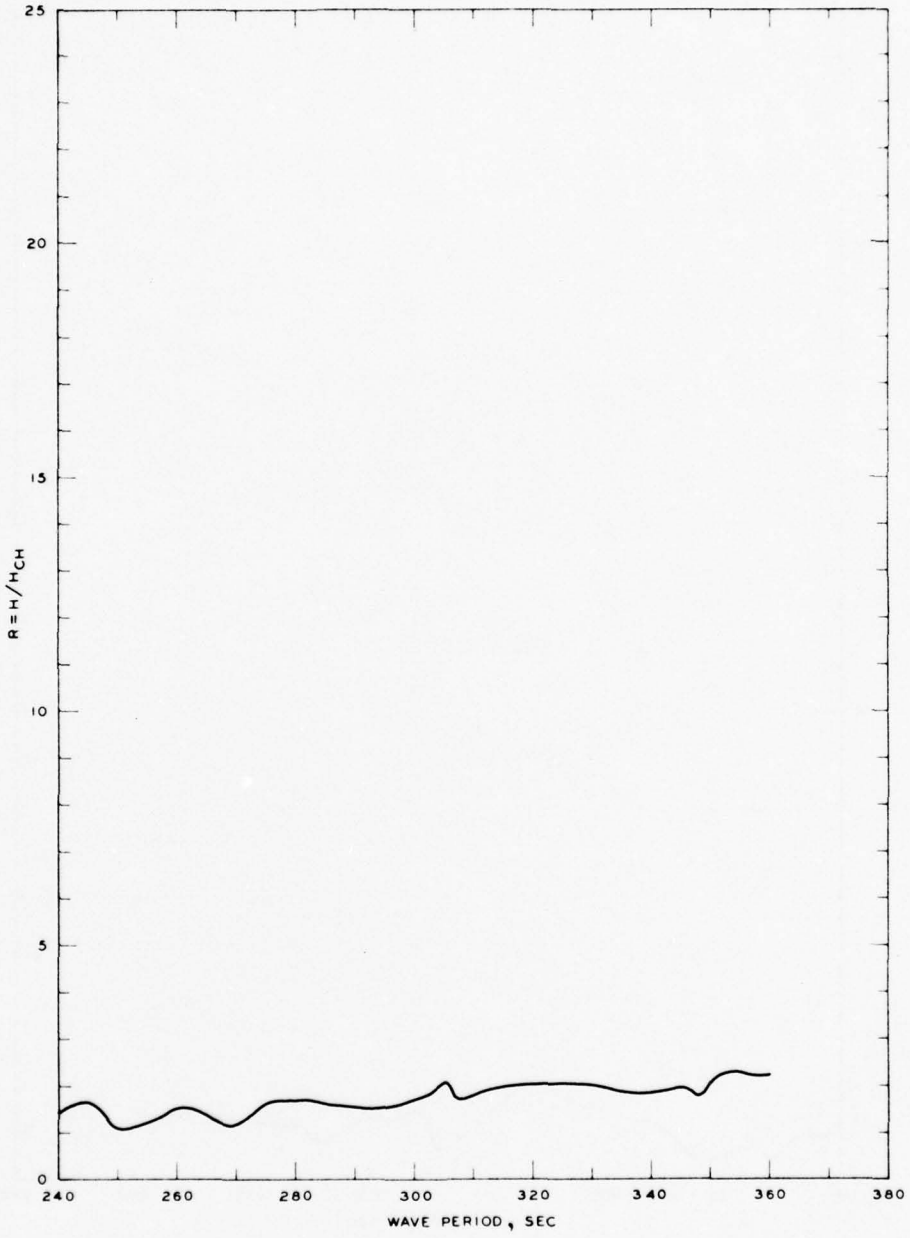

NOTE R = WAVE-HEIGHT AMPLIFICATION FACTOR
H = WAVE HEIGHT, FT
H_{CH} = WAVE HEIGHT FOR CLOSED HARBOR, FT

FREQUENCY RESPONSE

WAVE-HEIGHT AMPLIFICATION FACTOR
STA LA-15, GRID 4A

PLATE 88

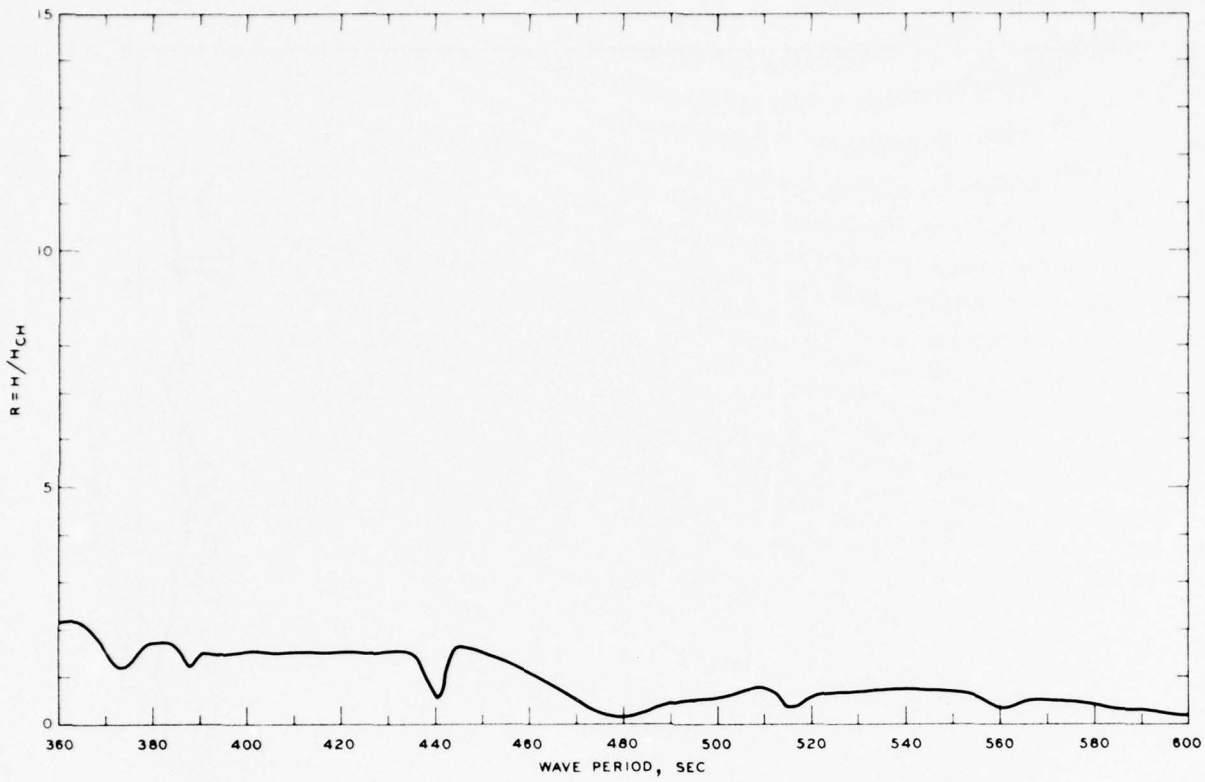

NOTE: R = WAVE-HEIGHT AMPLIFICATION FACTOR
H = WAVE HEIGHT, FT
H_{CH} = WAVE HEIGHT FOR CLOSED HARBOR, FT

FREQUENCY RESPONSE

WAVE-HEIGHT AMPLIFICATION FACTOR
STA LA-15, GRID 5A

PLATE 89

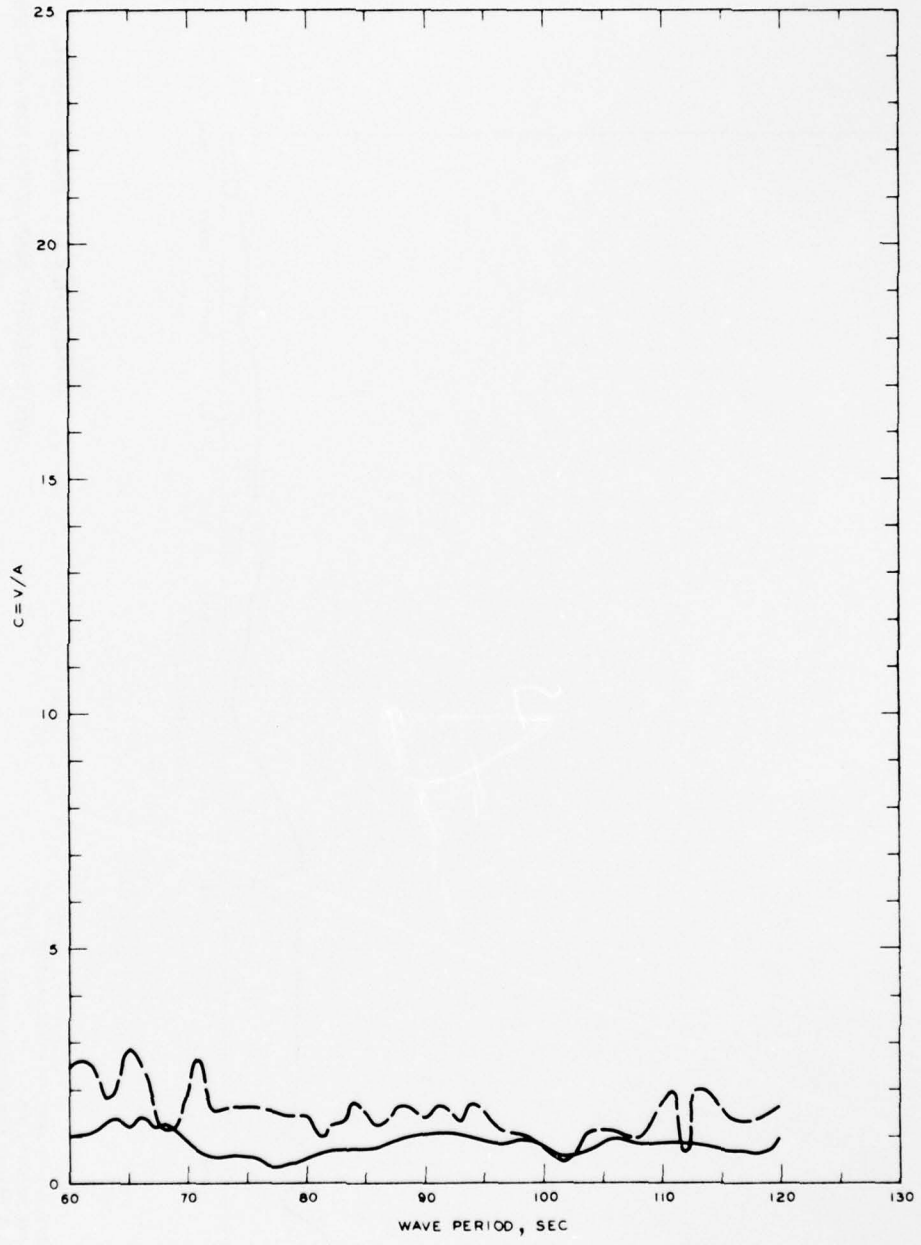

LEGEND

——— GRID 1

— — — GRID 1A

NOTE: C = NORMALIZED MAXIMUM CURRENT VELOCITY
V = CURRENT VELOCITY, FT/SEC
A = INCIDENT WAVE AMPLITUDE

FREQUENCY RESPONSE

NORMALIZED MAXIMUM CURRENT VELOCITY
GAGE 1, GRIDS 1 AND 1A

PLATE 90

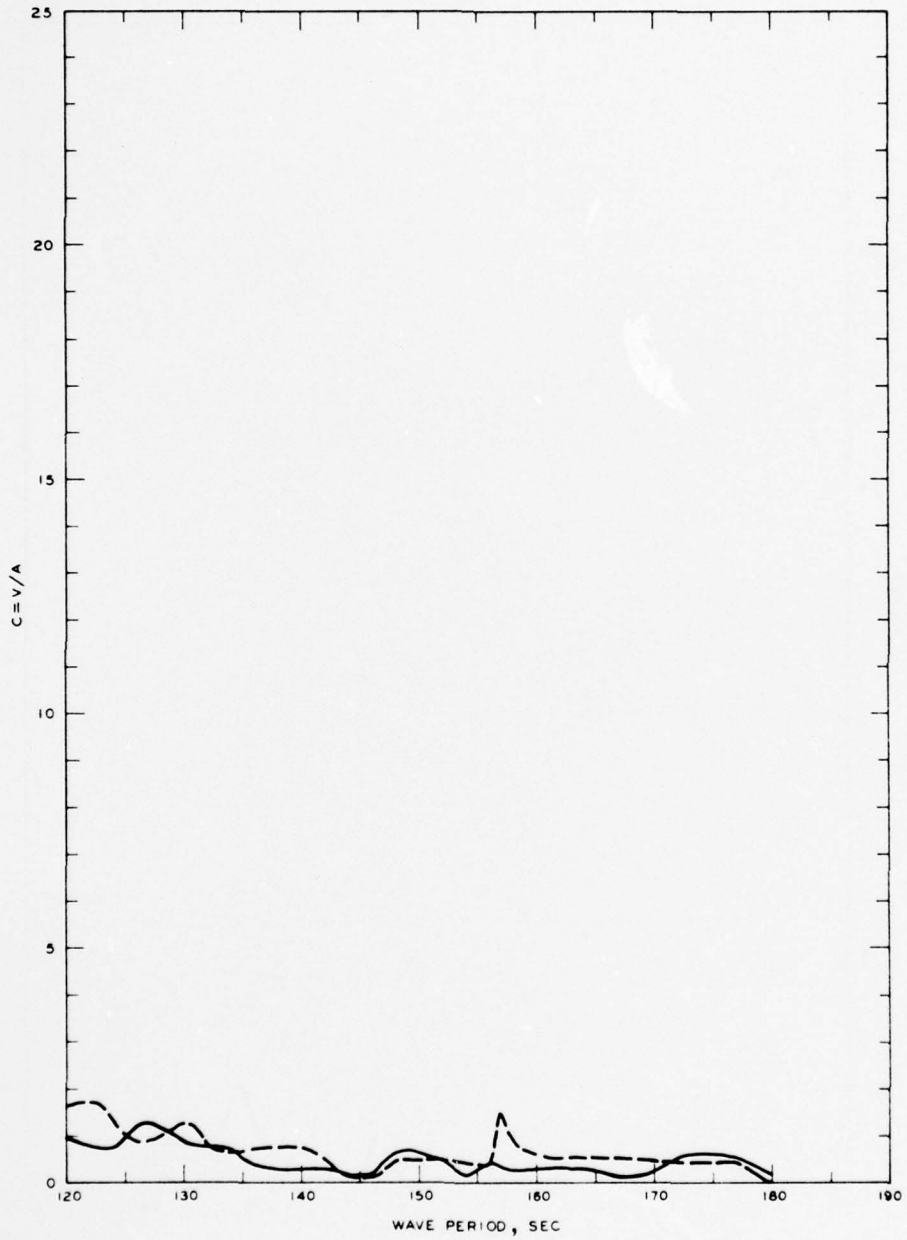

LEGEND

——— GRID 2

— — — GRID 2A

NOTE C = NORMALIZED MAXIMUM CURRENT VELOCITY
V = CURRENT VELOCITY, FT/SEC
A = INCIDENT WAVE AMPLITUDE

FREQUENCY RESPONSE

NORMALIZED MAXIMUM CURRENT VELOCITY
GAGE 1, GRIDS 2 AND 2A

PLATE 91

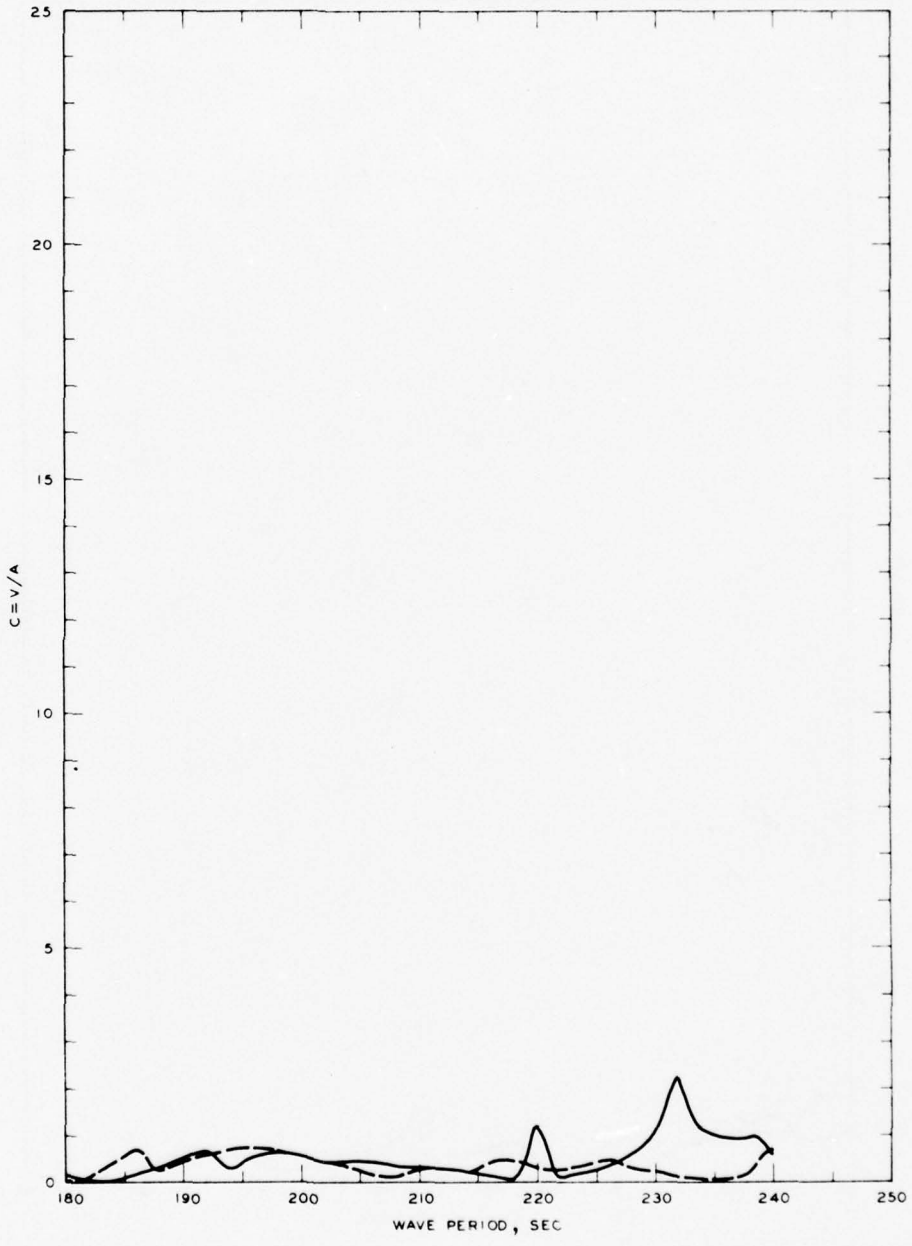

LEGEND

——— GRID 3

— — — GRID 3A

NOTE: C = NORMALIZED MAXIMUM CURRENT VELOCITY
V = CURRENT VELOCITY, FT/SEC
A = INCIDENT WAVE AMPLITUDE

FREQUENCY RESPONSE

NORMALIZED MAXIMUM CURRENT VELOCITY
GAGE 1, GRIDS 3 AND 3A

PLATE 92

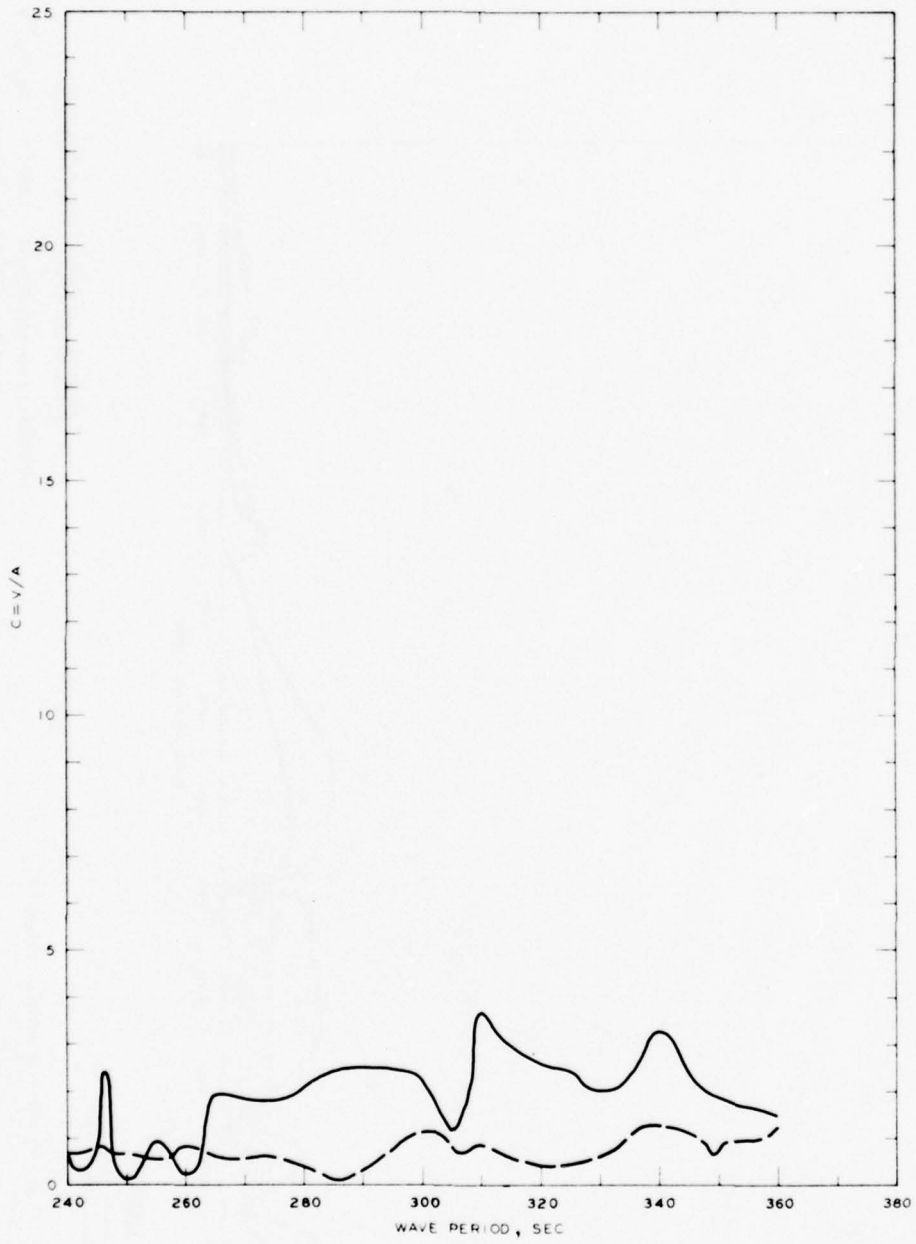

LEGEND

——— GRID 4

— — — GRID 4A

NOTE C = NORMALIZED MAXIMUM CURRENT VELOCITY
V = CURRENT VELOCITY, FT/SEC
A = INCIDENT WAVE AMPLITUDE

FREQUENCY RESPONSE

NORMALIZED MAXIMUM CURRENT VELOCITY
GAGE 1, GRIDS 4 AND 4A

PLATE 93

PLATE 94

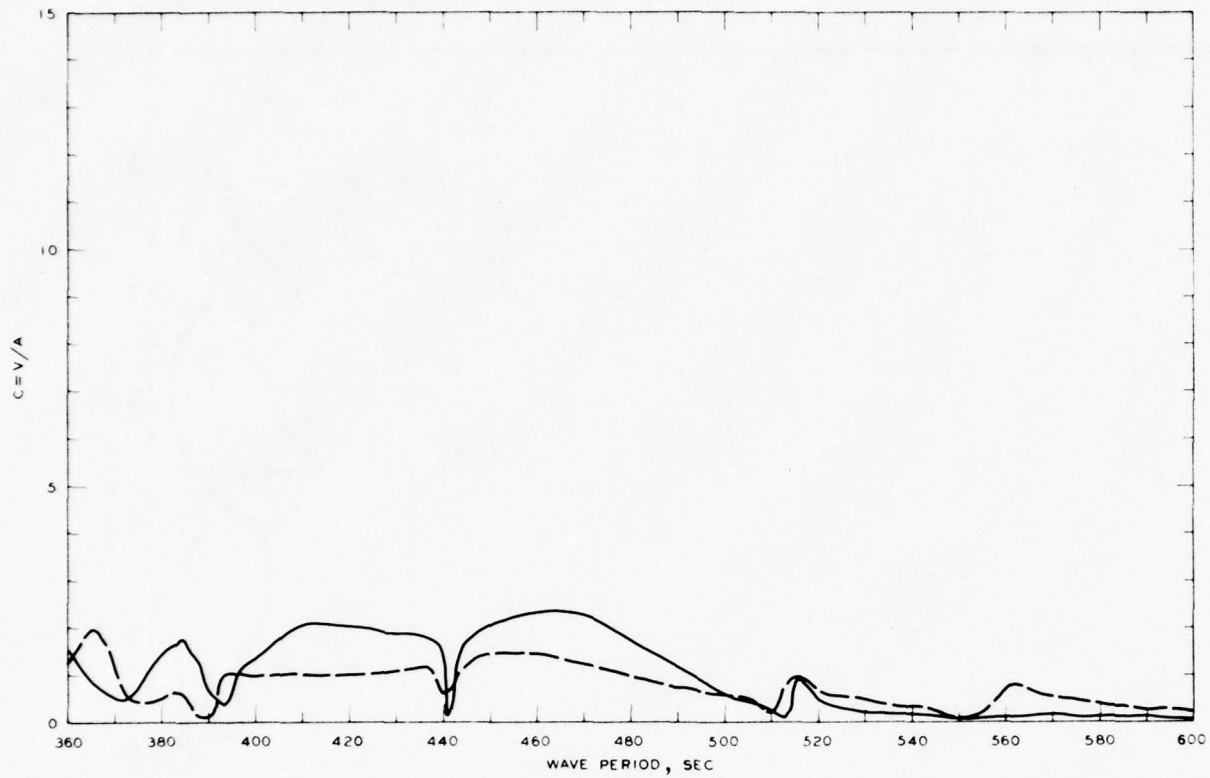

LEGEND

——— GRID 5

– – – GRID 5A

NOTE: C = NORMALIZED MAXIMUM CURRENT VELOCITY
V = CURRENT VELOCITY, FT/SEC
A = INCIDENT WAVE AMPLITUDE

FREQUENCY RESPONSE

NORMALIZED MAXIMUM CURRENT VELOCITY
GAGE 1, GRIDS 5 AND 5A

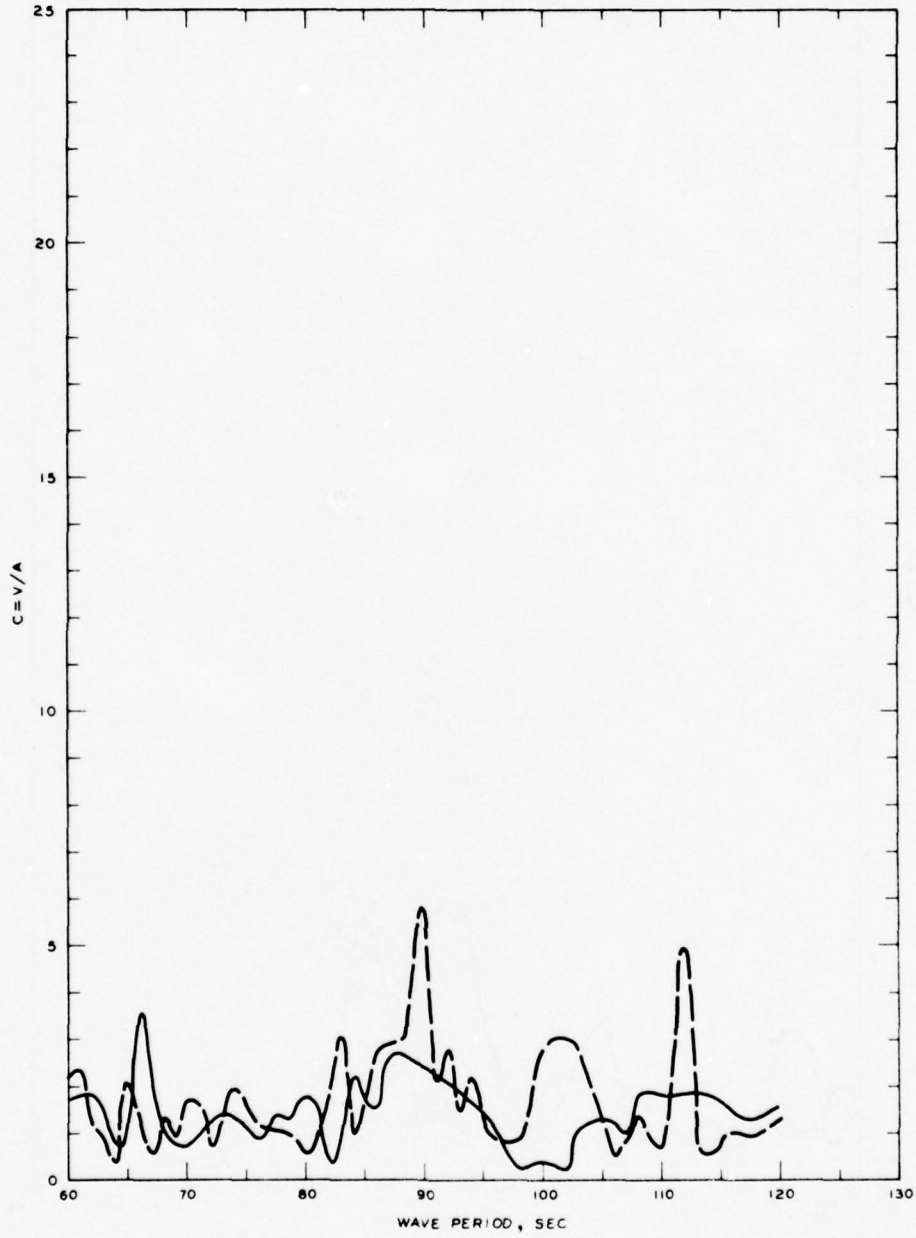

LEGEND

——— GRID 1

— — — GRID 1A

NOTE C = NORMALIZED MAXIMUM CURRENT VELOCITY
V = CURRENT VELOCITY, FT/SEC
A = INCIDENT WAVE AMPLITUDE

FREQUENCY RESPONSE

NORMALIZED MAXIMUM CURRENT VELOCITY
GAGE 2, GRIDS 1 AND 1A

PLATE 95

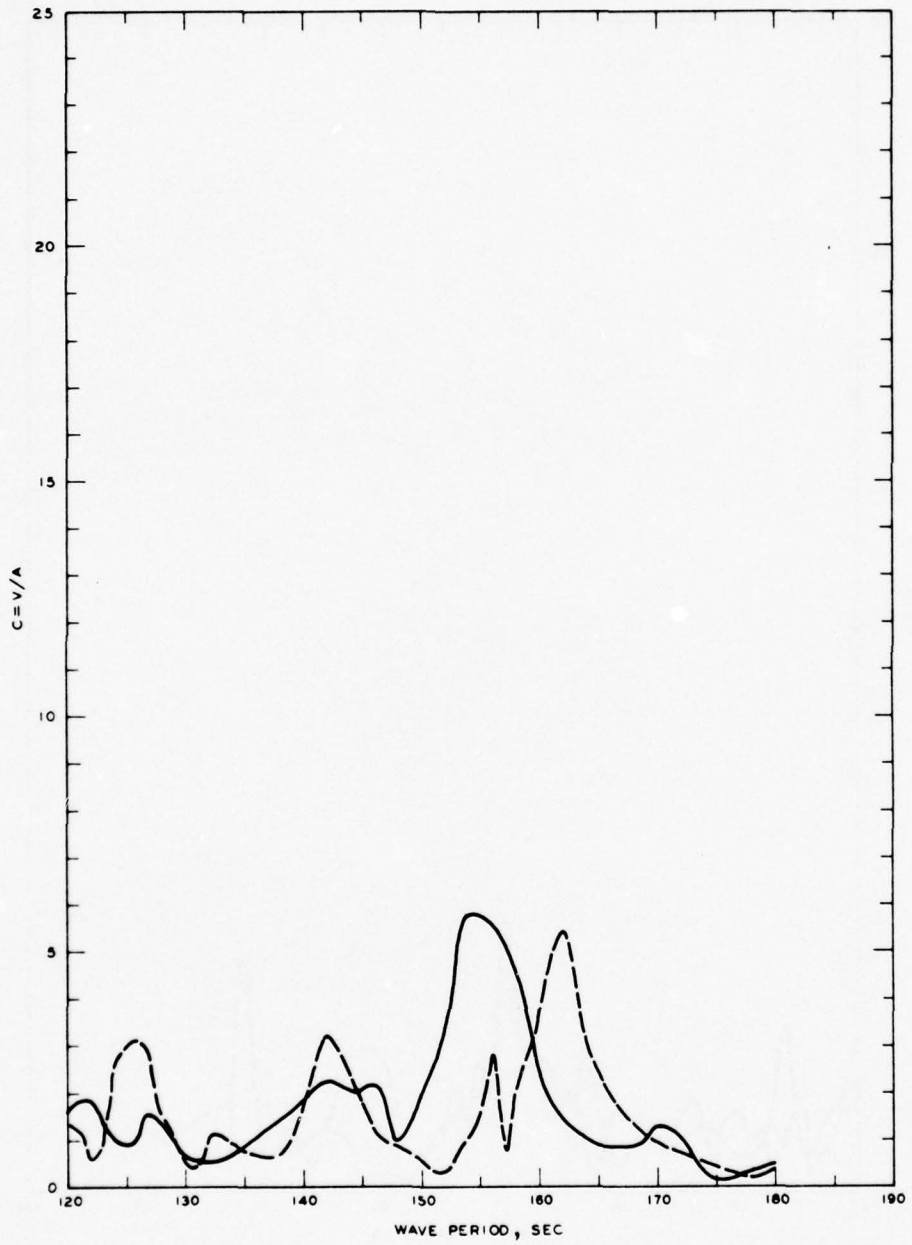

NOTE C = NORMALIZED MAXIMUM CURRENT VELOCITY
V = CURRENT VELOCITY, FT/SEC
A = INCIDENT WAVE AMPLITUDE

FREQUENCY RESPONSE

NORMALIZED MAXIMUM CURRENT VELOCITY
GAGE 2, GRIDS 2 AND 2A

PLATE 96

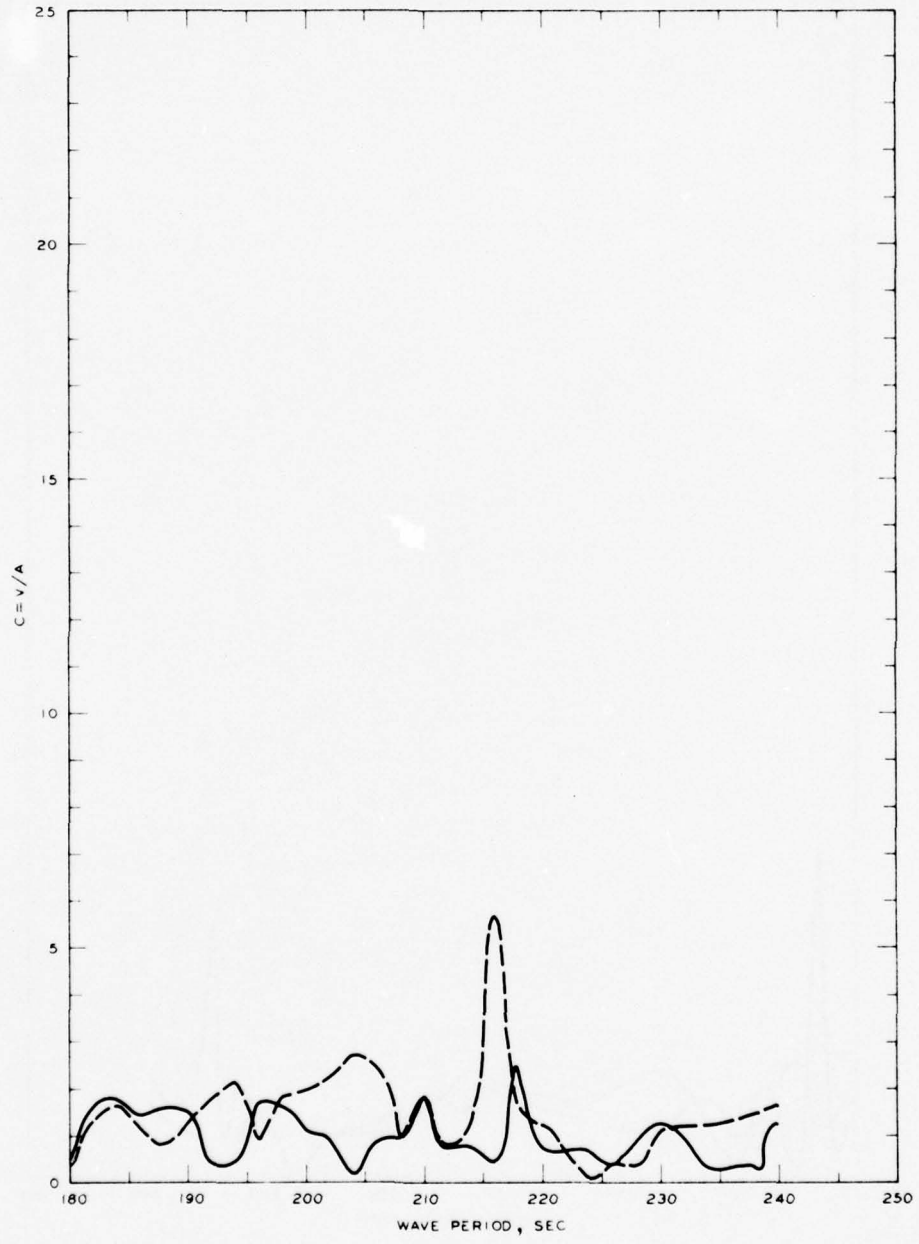

LEGEND

——— GRID 3

— — — GRID 3A

NOTE C = NORMALIZED MAXIMUM CURRENT VELOCITY
V = CURRENT VELOCITY, FT/SEC
A = INCIDENT WAVE AMPLITUDE

FREQUENCY RESPONSE

NORMALIZED MAXIMUM CURRENT VELOCITY
GAGE 2, GRIDS 3 AND 3A

PLATE 97

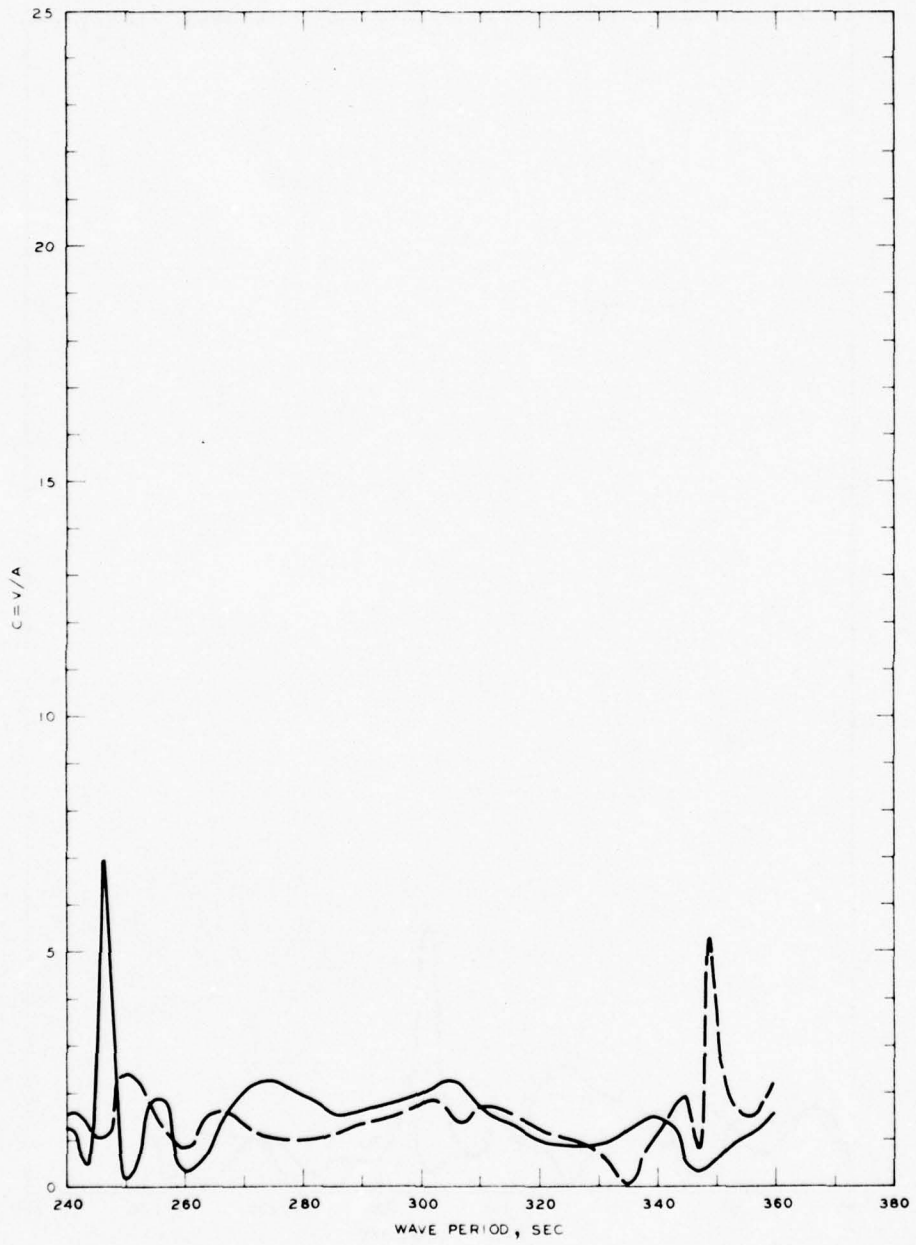

LEGEND

——— GRID 4

— — — GRID 4A

NOTE C = NORMALIZED MAXIMUM CURRENT VELOCITY
V = CURRENT VELOCITY, FT/SEC
A = INCIDENT WAVE AMPLITUDE

FREQUENCY RESPONSE

NORMALIZED MAXIMUM CURRENT VELOCITY
GAGE 2, GRIDS 4 AND 4A

PLATE 98

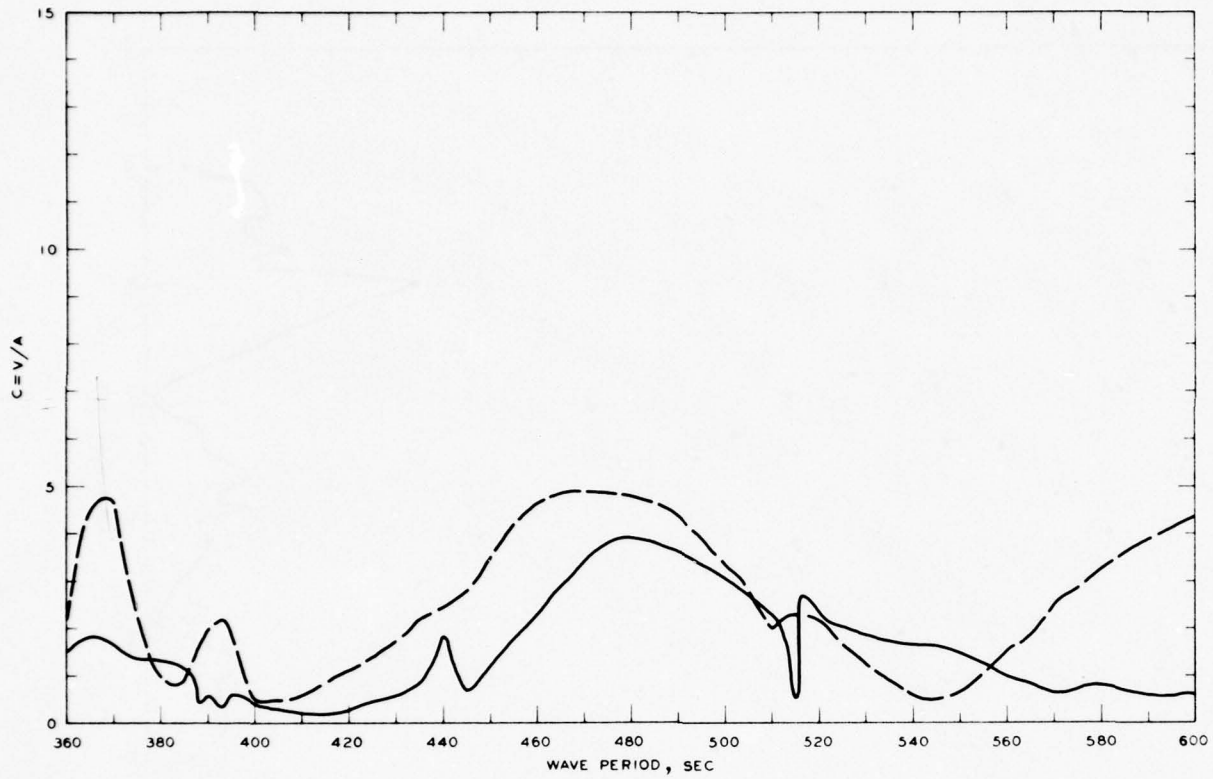

LEGEND

——— GRID 5

– – – GRID 5A

NOTE: C = NORMALIZED MAXIMUM CURRENT VELOCITY
V = CURRENT VELOCITY, FT/SEC
A = INCIDENT WAVE AMPLITUDE

FREQUENCY RESPONSE

NORMALIZED MAXIMUM CURRENT VELOCITY
GAGE 2, GRIDS 5 AND 5A

PLATE 99

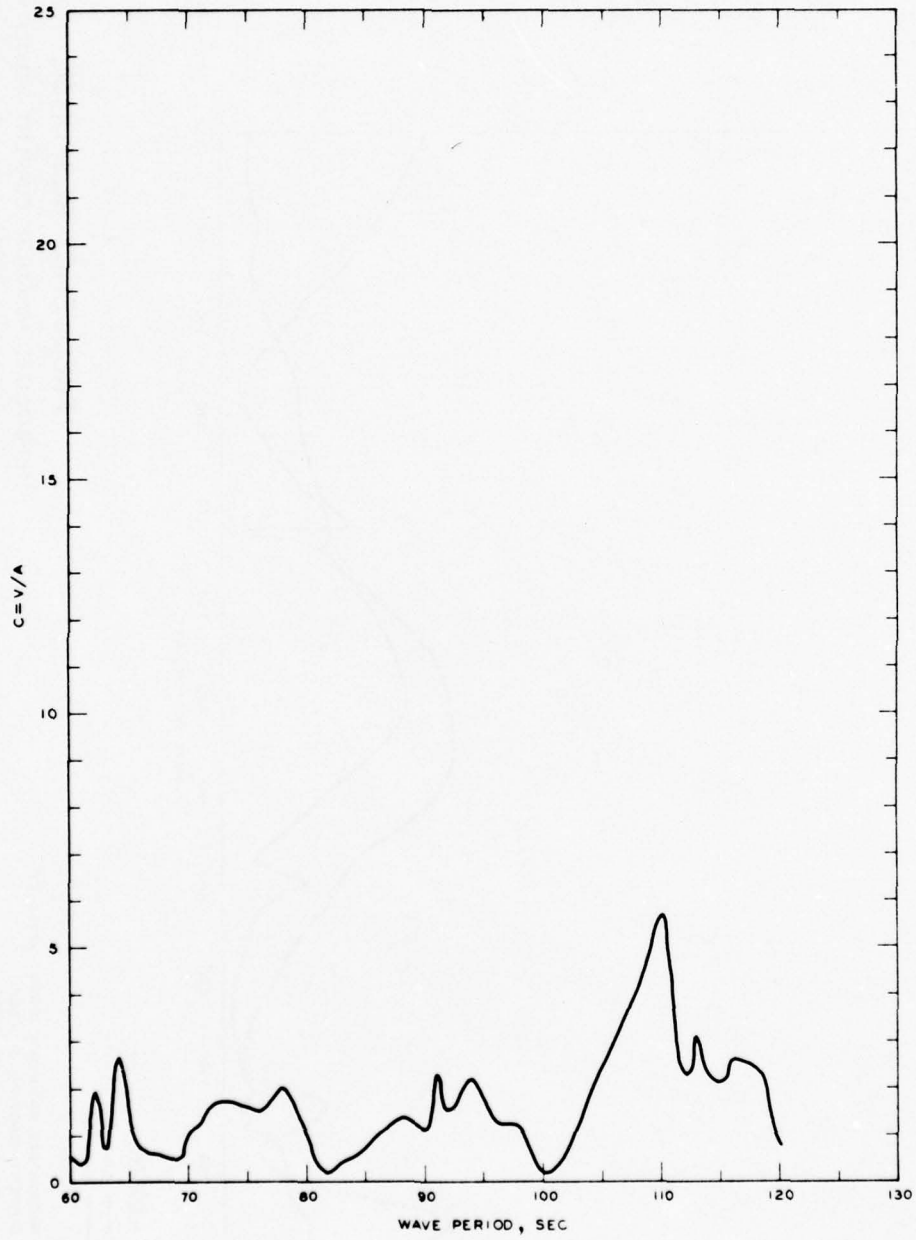

NOTE: C = NORMALIZED MAXIMUM CURRENT VELOCITY
V = CURRENT VELOCITY, FT/SEC
A = INCIDENT WAVE AMPLITUDE

FREQUENCY RESPONSE

NORMALIZED MAXIMUM CURRENT VELOCITY
STA 2, LNG SLIP, GRID 1A

PLATE 100

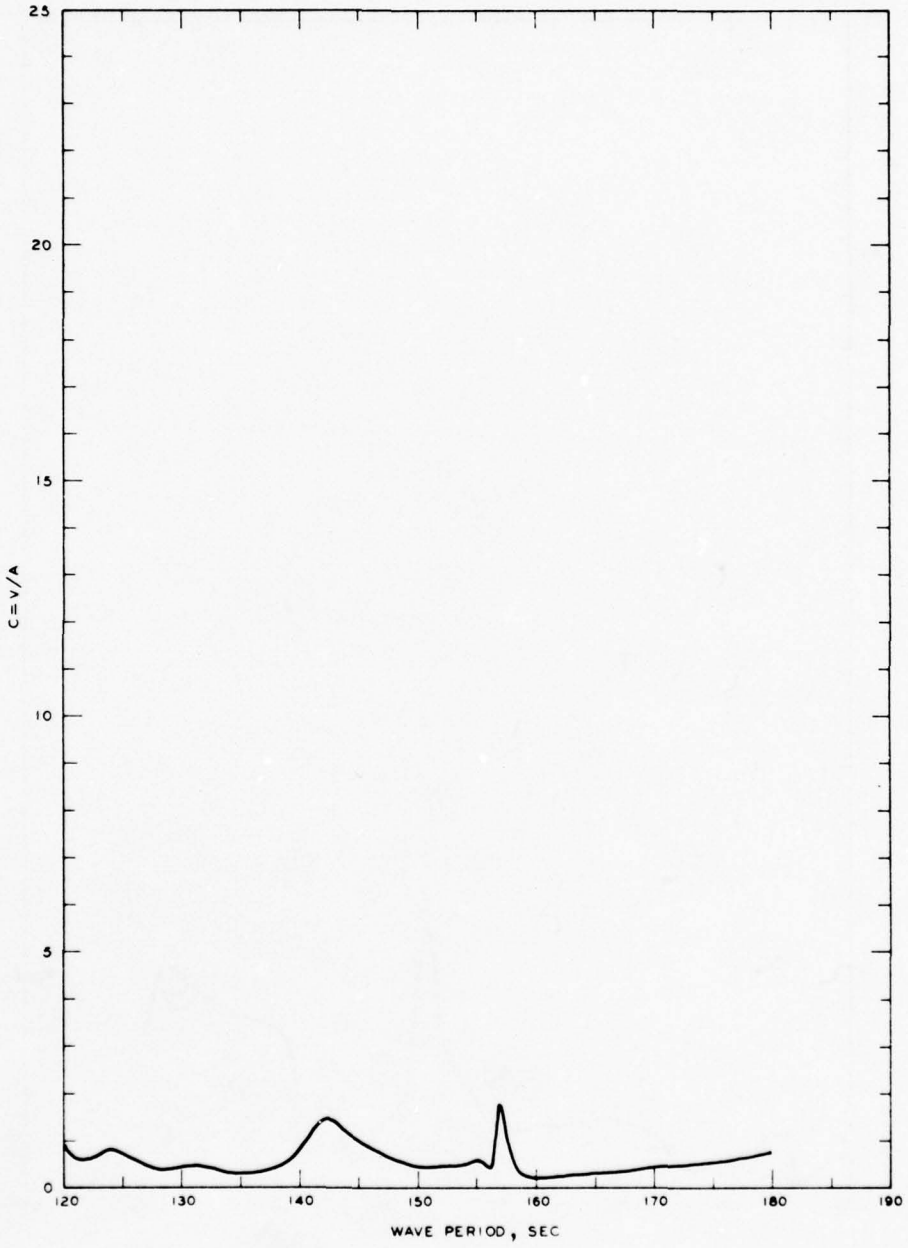

NOTE: C = NORMALIZED MAXIMUM CURRENT VELOCITY
V = CURRENT VELOCITY, FT/SEC
A = INCIDENT WAVE AMPLITUDE

FREQUENCY RESPONSE

NORMALIZED MAXIMUM CURRENT VELOCITY
STA 2, LNG SLIP, GRID 2A

PLATE 101

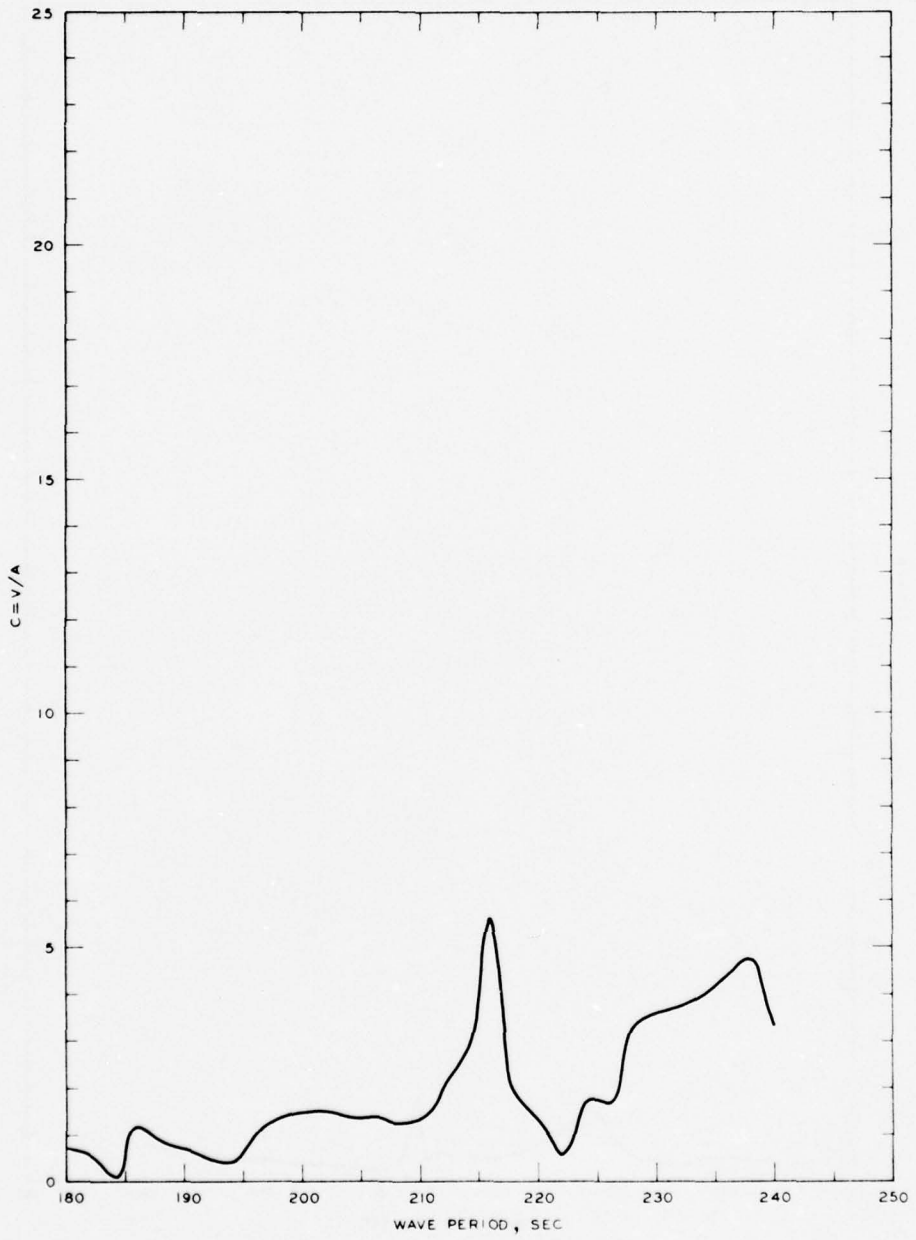

NOTE C = NORMALIZED MAXIMUM CURRENT VELOCITY
V = CURRENT VELOCITY, FT/SEC
A = INCIDENT WAVE AMPLITUDE

FREQUENCY RESPONSE

NORMALIZED MAXIMUM CURRENT VELOCITY
STA 2, LNG SLIP, GRID 3A

PLATE 102

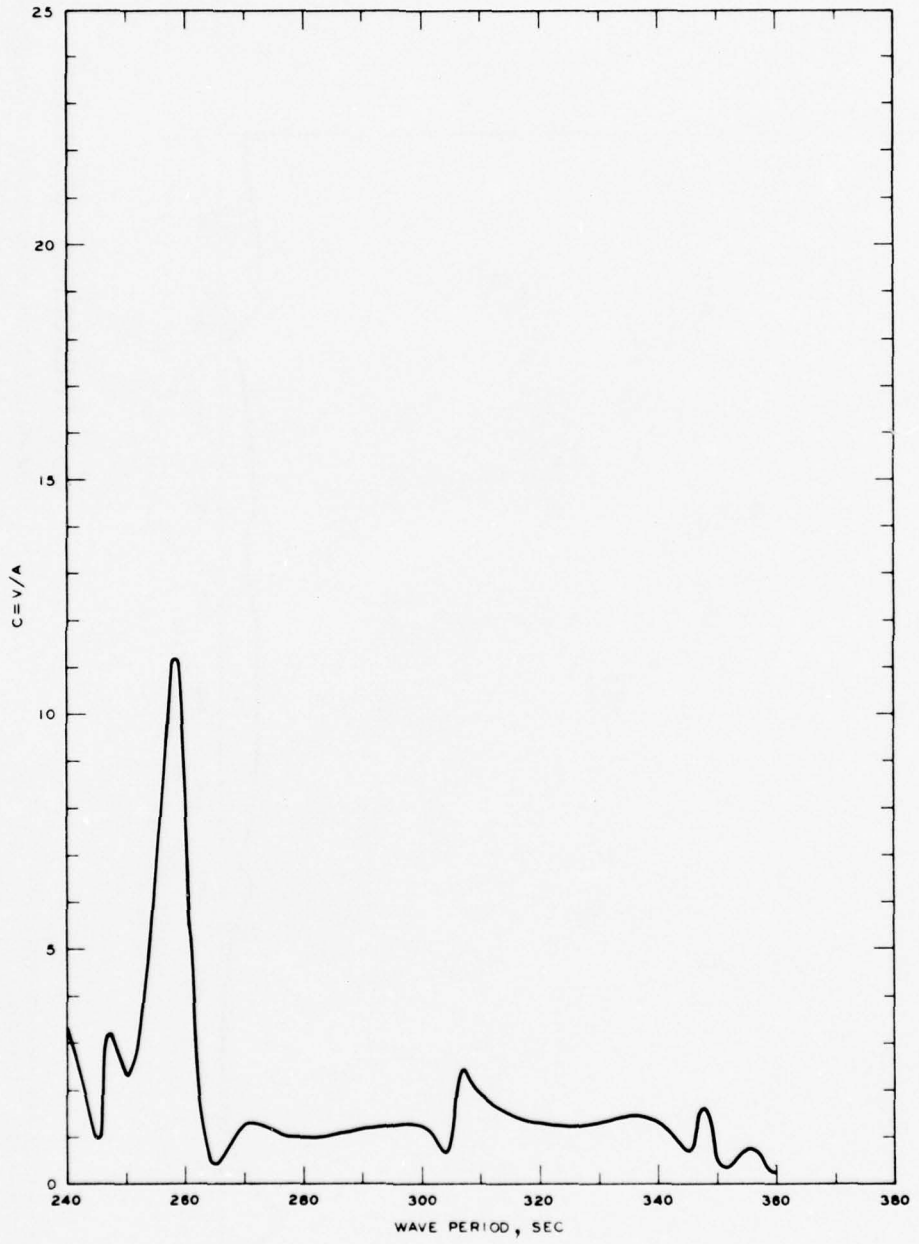

NOTE: C = NORMALIZED MAXIMUM CURRENT VELOCITY
V = CURRENT VELOCITY, FT/SEC
A = INCIDENT WAVE AMPLITUDE

FREQUENCY RESPONSE

NORMALIZED MAXIMUM CURRENT VELOCITY
STA 2, LNG SLIP, GRID 4A

PLATE 103

PLATE 104

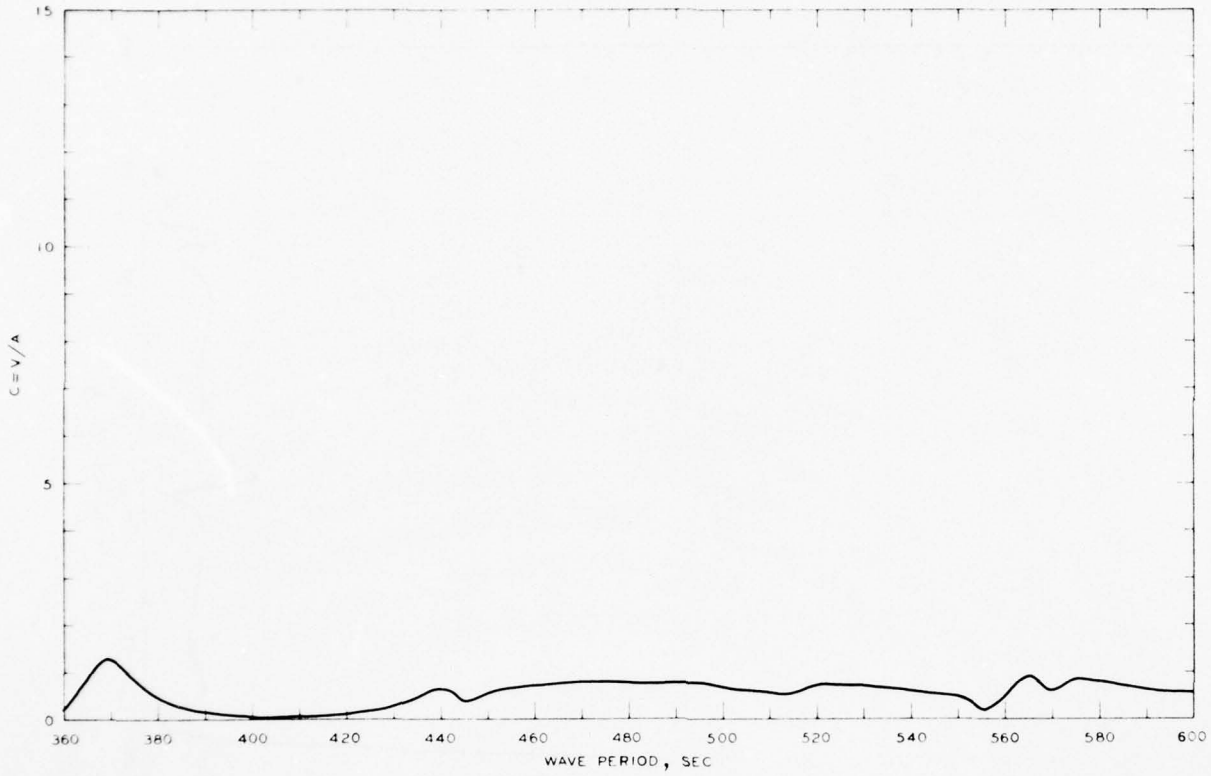

NOTE: C = NORMALIZED MAXIMUM CURRENT VELOCITY
V = CURRENT VELOCITY, FT/SEC
A = INCIDENT WAVE AMPLITUDE

FREQUENCY RESPONSE

NORMALIZED MAXIMUM CURRENT VELOCITY
STA 2, LNG SLIP, GRID 5A

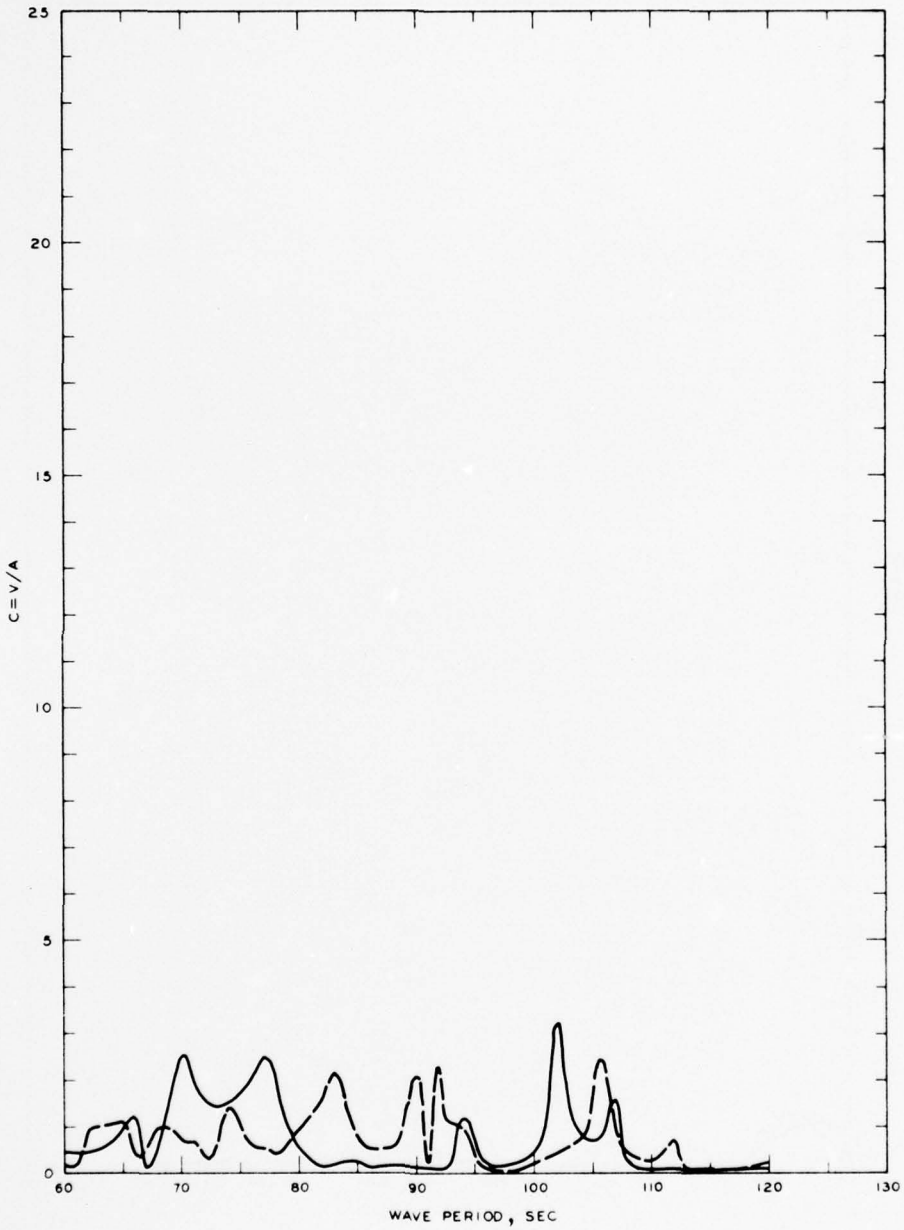

LEGEND

——— GRID 1

— — — GRID 1A

NOTE: C = NORMALIZED MAXIMUM CURRENT VELOCITY
V = CURRENT VELOCITY, FT/SEC
A = INCIDENT WAVE AMPLITUDE

FREQUENCY RESPONSE

NORMALIZED MAXIMUM CURRENT VELOCITY
STA LA-1, GRIDS 1 AND 1A

PLATE 105

LEGEND

——— GRID 2

– – – GRID 2A

NOTE: C = NORMALIZED MAXIMUM CURRENT VELOCITY
V = CURRENT VELOCITY, FT/SEC
A = INCIDENT WAVE AMPLITUDE

FREQUENCY RESPONSE

NORMALIZED MAXIMUM CURRENT VELOCITY
STA LA-1, GRIDS 2 AND 2A

PLATE 106

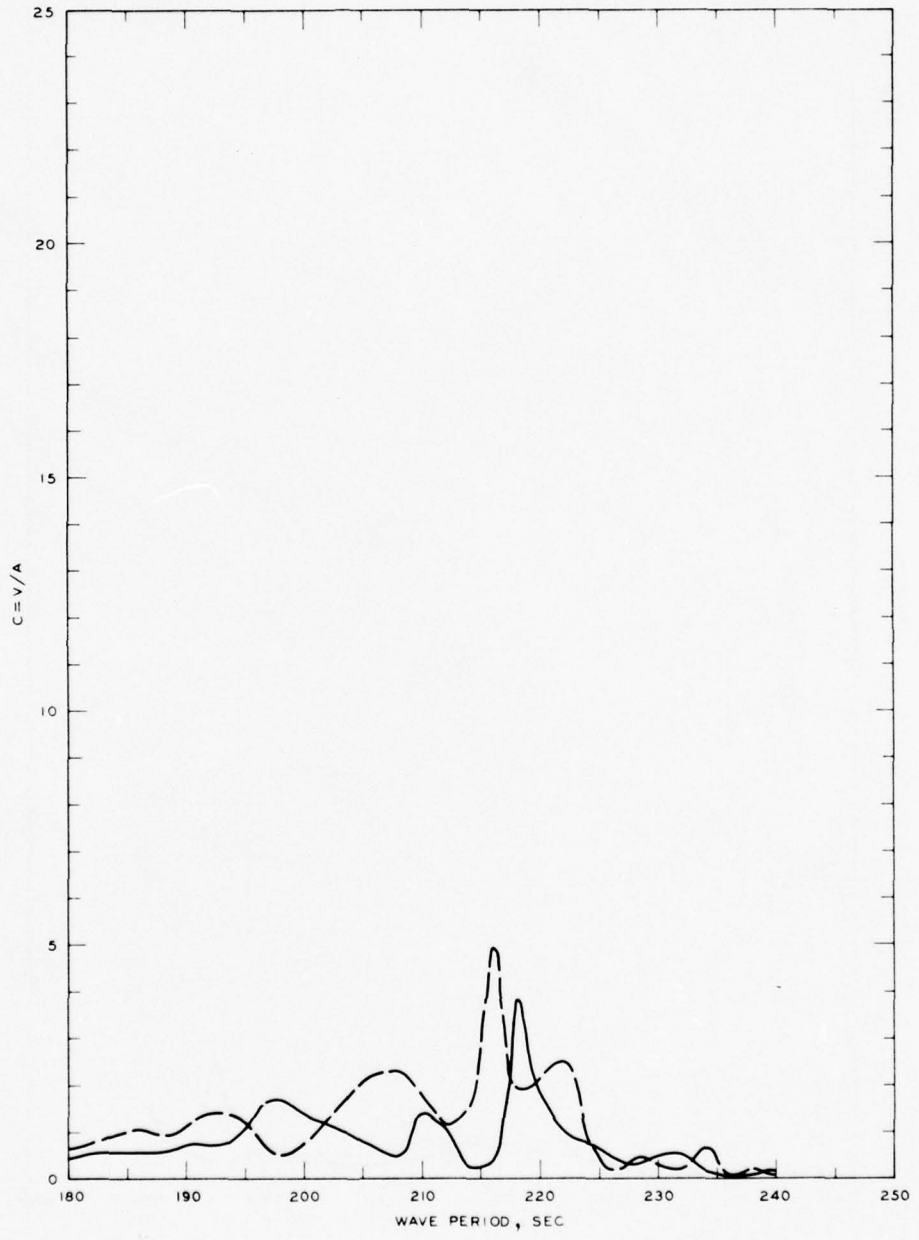

LEGEND

——— GRID 3

— — — GRID 3A

NOTE C = NORMALIZED MAXIMUM CURRENT VELOCITY
V = CURRENT VELOCITY, FT/SEC
A = INCIDENT WAVE AMPLITUDE

FREQUENCY RESPONSE

NORMALIZED MAXIMUM CURRENT VELOCITY
STA LA-1, GRIDS 3 AND 3A

PLATE 107

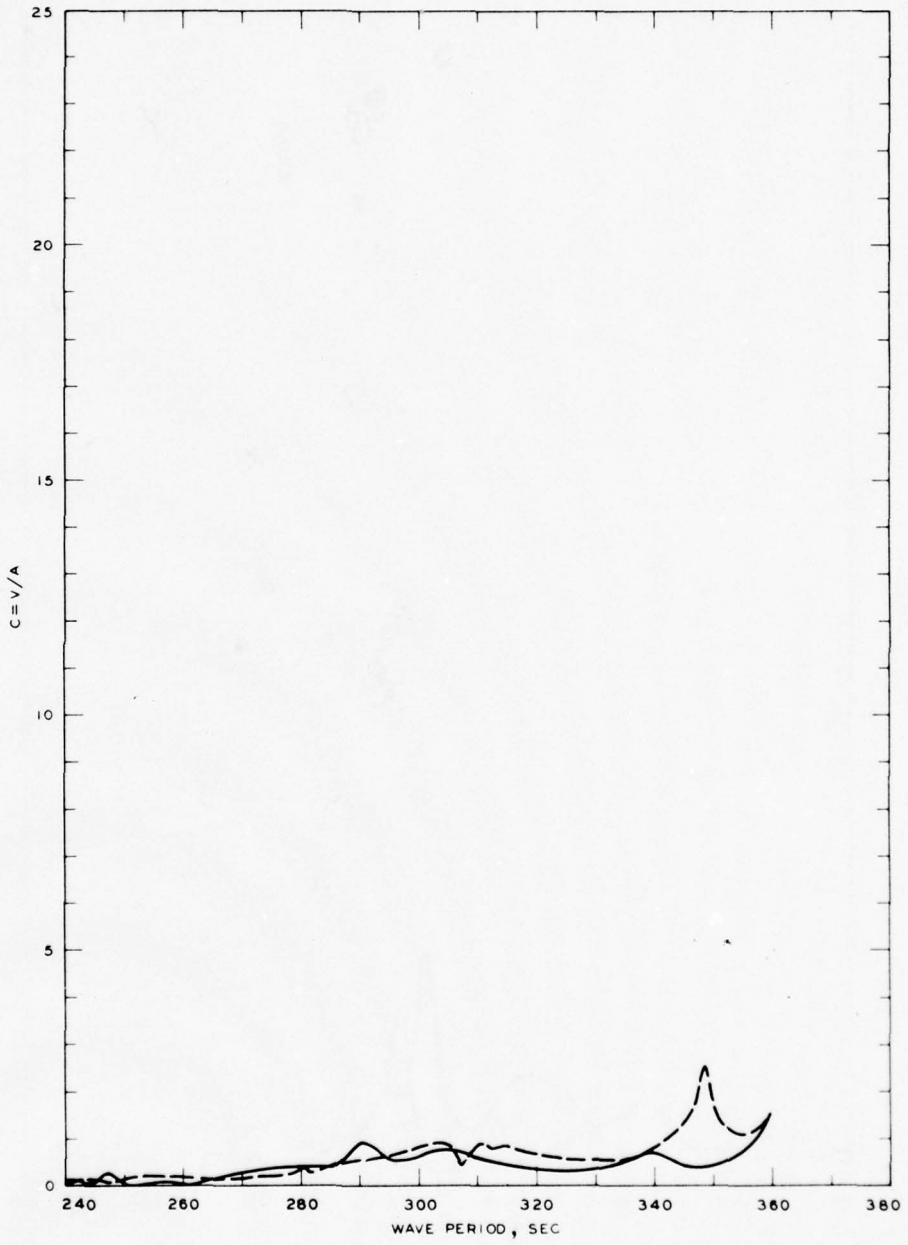

LEGEND

——— GRID 4

— — — GRID 4A

NOTE C = NORMALIZED MAXIMUM CURRENT VELOCITY
V = CURRENT VELOCITY, FT/SEC
A = INCIDENT WAVE AMPLITUDE

FREQUENCY RESPONSE

NORMALIZED MAXIMUM CURRENT VELOCITY
STA LA - 1, GRIDS 4 AND 4A

PLATE 108

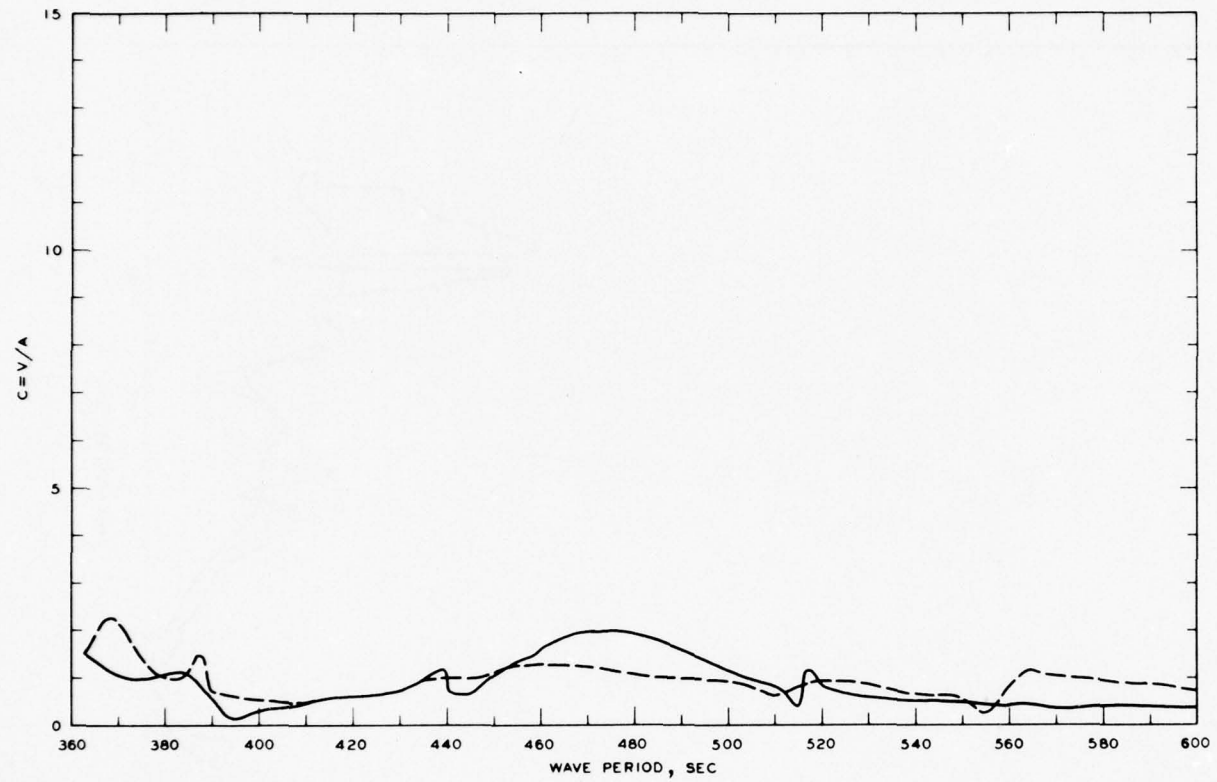

LEGEND

——— GRID 5

– – – GRID 5A

NOTE: C = NORMALIZED MAXIMUM CURRENT VELOCITY
V = CURRENT VELOCITY, FT/SEC
A = INCIDENT WAVE AMPLITUDE

FREQUENCY RESPONSE

NORMALIZED MAXIMUM CURRENT VELOCITY

STA LA-1, GRIDS 5 AND 5A

PLATE 109

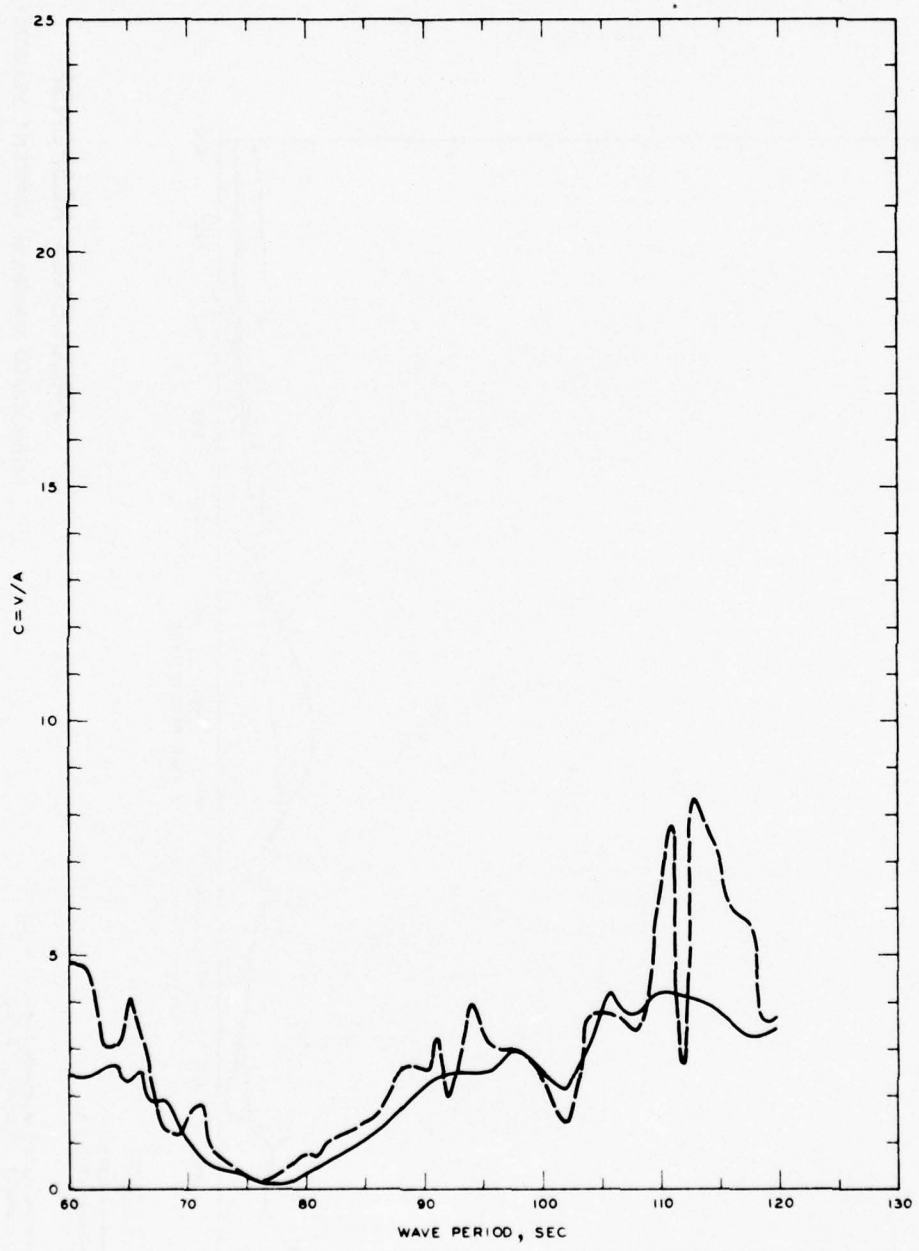

LEGEND

——— GRID 1

— — — GRID 1A

NOTE: C = NORMALIZED MAXIMUM CURRENT VELOCITY
V = CURRENT VELOCITY, FT/SEC
A = INCIDENT WAVE AMPLITUDE

FREQUENCY RESPONSE

NORMALIZED MAXIMUM CURRENT VELOCITY
STA LA-3, GRIDS 1 AND 1A

PLATE 110

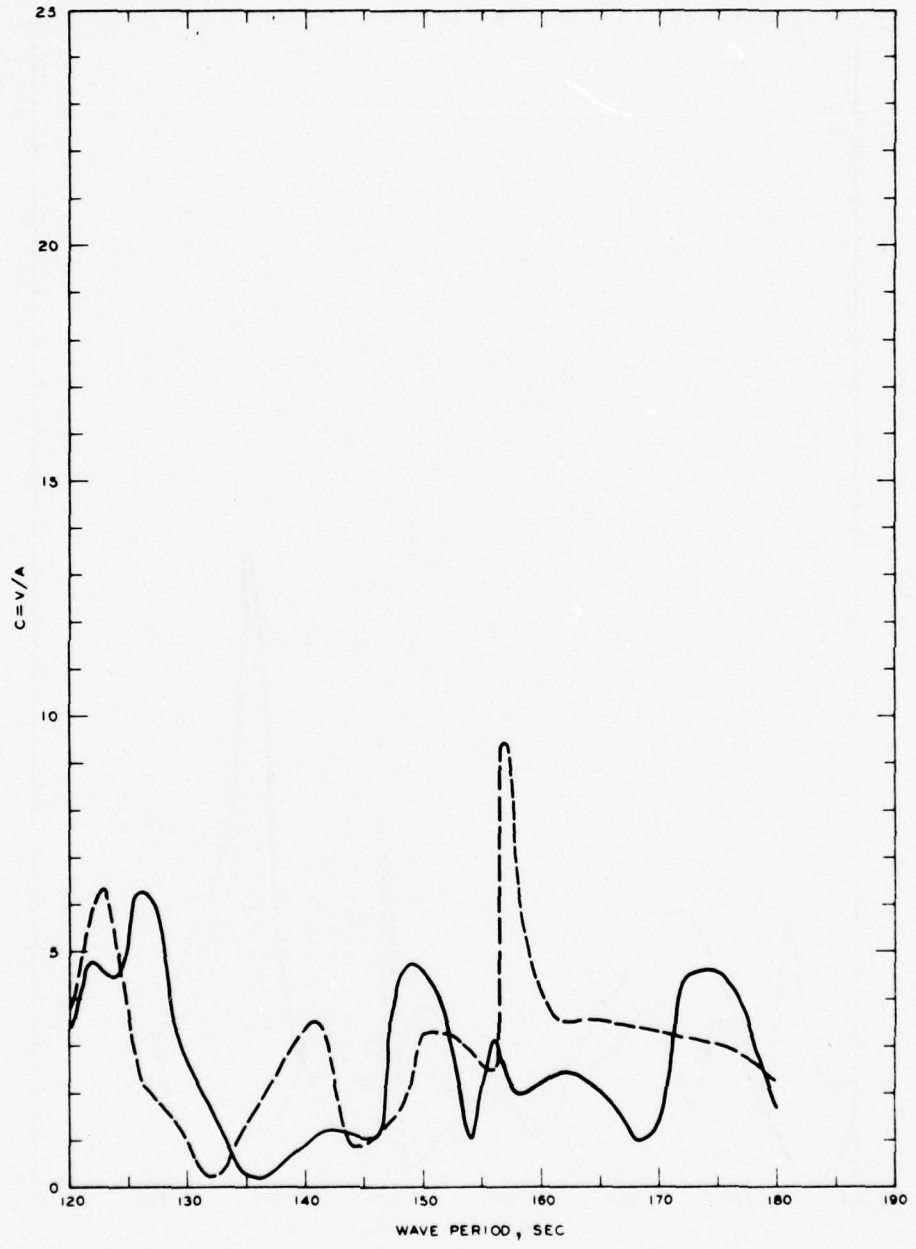

LEGEND

——— GRID 2

– – – GRID 2A

NOTE: C = NORMALIZED MAXIMUM CURRENT VELOCITY
V = CURRENT VELOCITY, FT/SEC
A = INCIDENT WAVE AMPLITUDE

FREQUENCY RESPONSE

NORMALIZED MAXIMUM CURRENT VELOCITY
STA LA- 3, GRIDS 2 AND 2A

PLATE 111

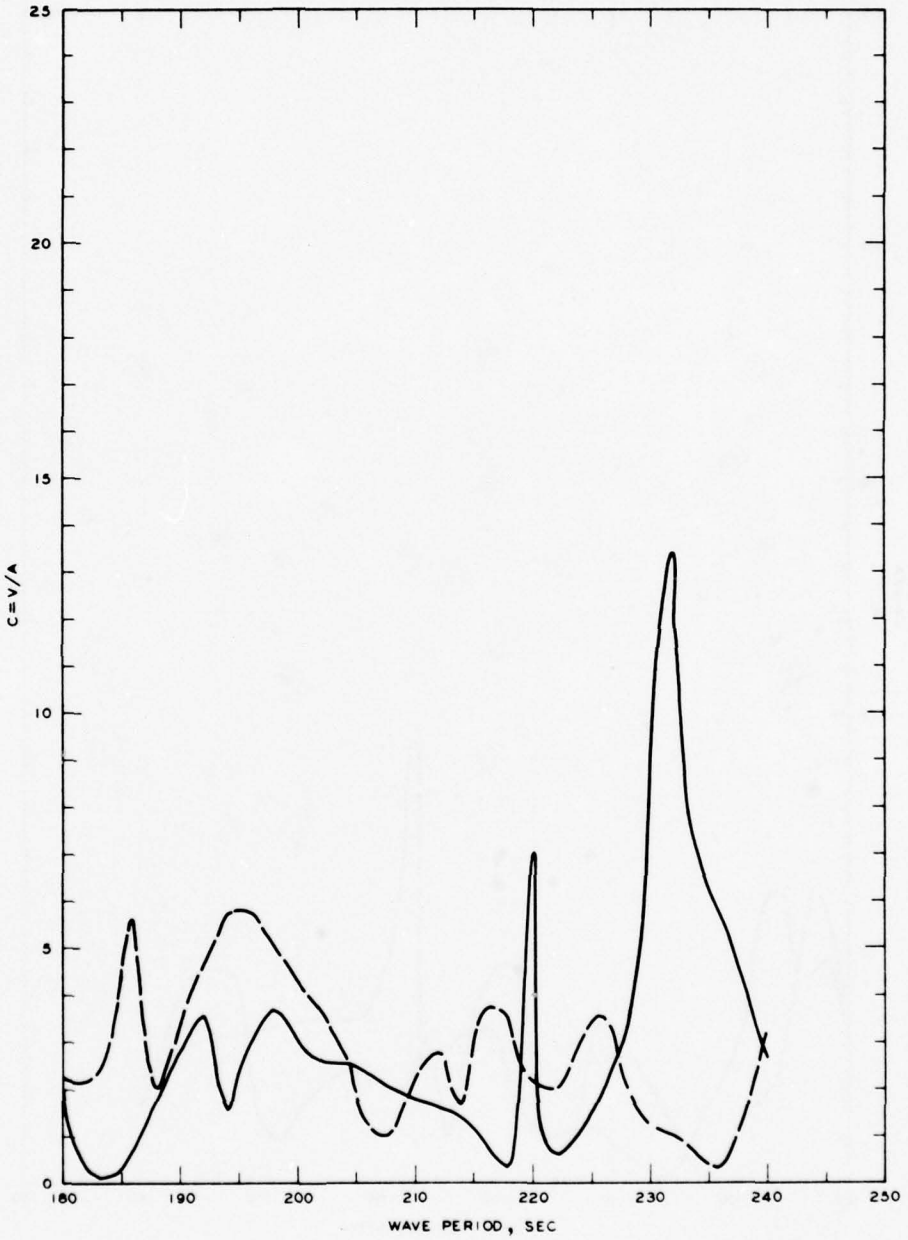

LEGEND

——— GRID 3

— — — GRID 3A

NOTE: C = NORMALIZED MAXIMUM CURRENT VELOCITY
V = CURRENT VELOCITY, FT/SEC
A = INCIDENT WAVE AMPLITUDE

FREQUENCY RESPONSE

NORMALIZED MAXIMUM CURRENT VELOCITY
STA LA-3, GRIDS 3 AND 3A

PLATE 112

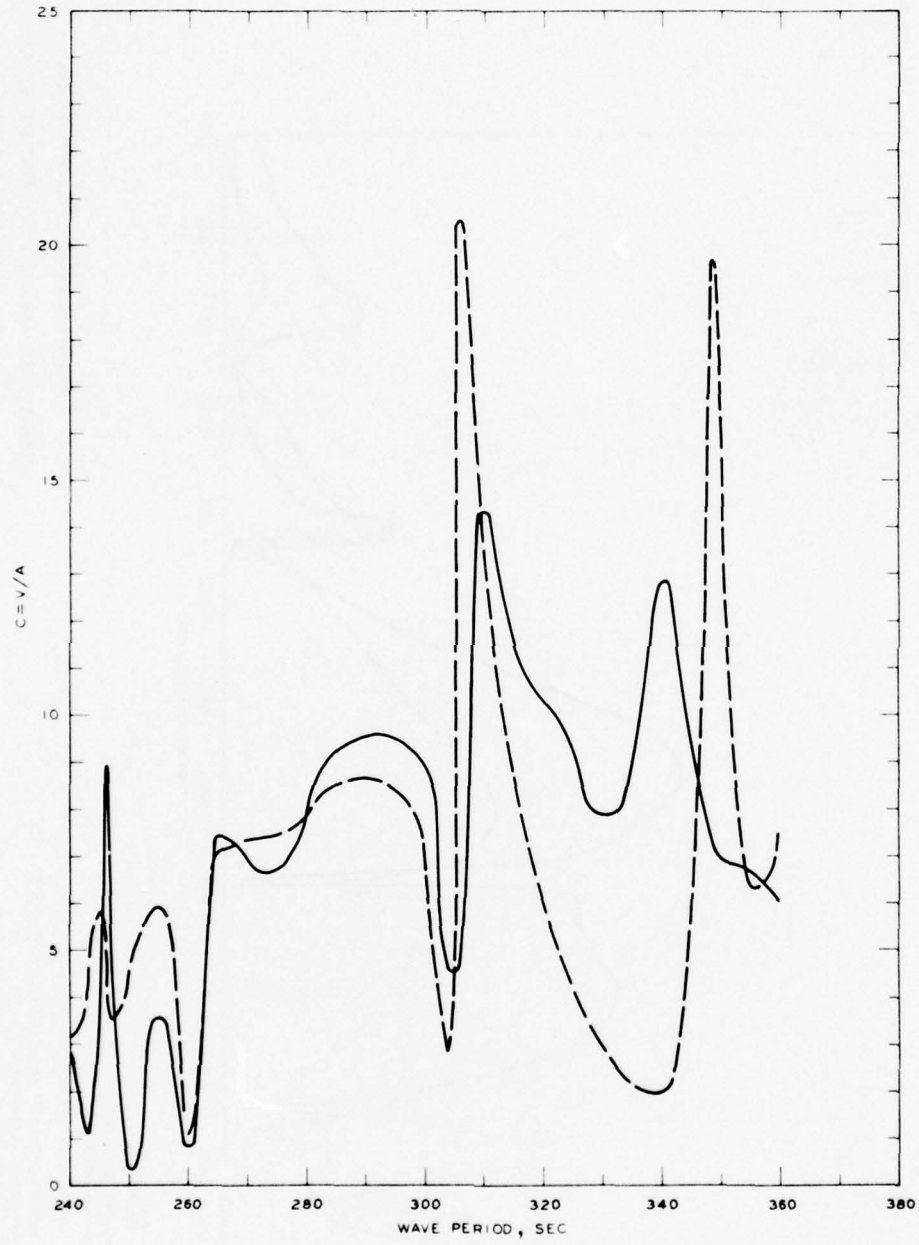

LEGEND

——— GRID 4

– – – GRID 4A

NOTE: C = NORMALIZED MAXIMUM CURRENT VELOCITY
V = CURRENT VELOCITY, FT/SEC
A = INCIDENT WAVE AMPLITUDE

FREQUENCY RESPONSE

NORMALIZED MAXIMUM CURRENT VELOCITY
STA LA-3, GRIDS 4 AND 4A

PLATE 113

PLATE 114

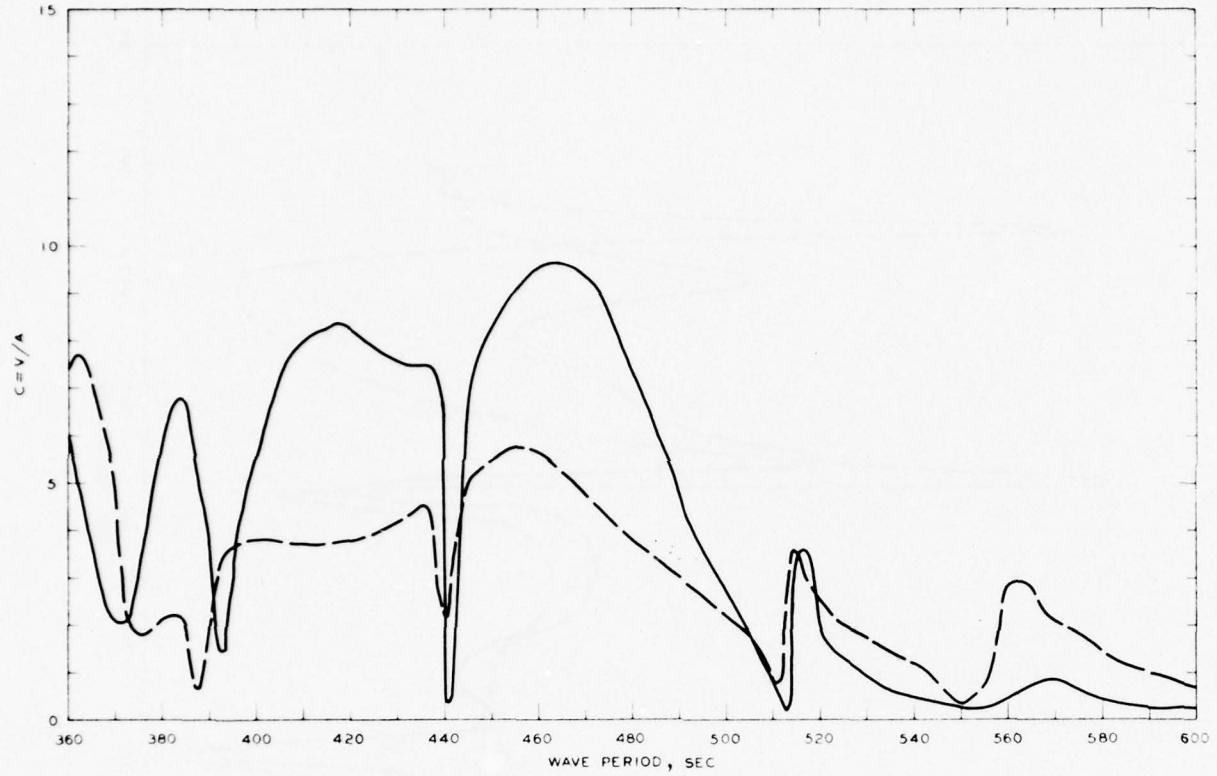

LEGEND

——— GRID 5

– – – GRID 5A

NOTE C = NORMALIZED MAXIMUM CURRENT VELOCITY
V = CURRENT VELOCITY, FT/SEC
A = INCIDENT WAVE AMPLITUDE

FREQUENCY RESPONSE

NORMALIZED MAXIMUM CURRENT VELOCITY
STA LA-3, GRIDS 5 AND 5A

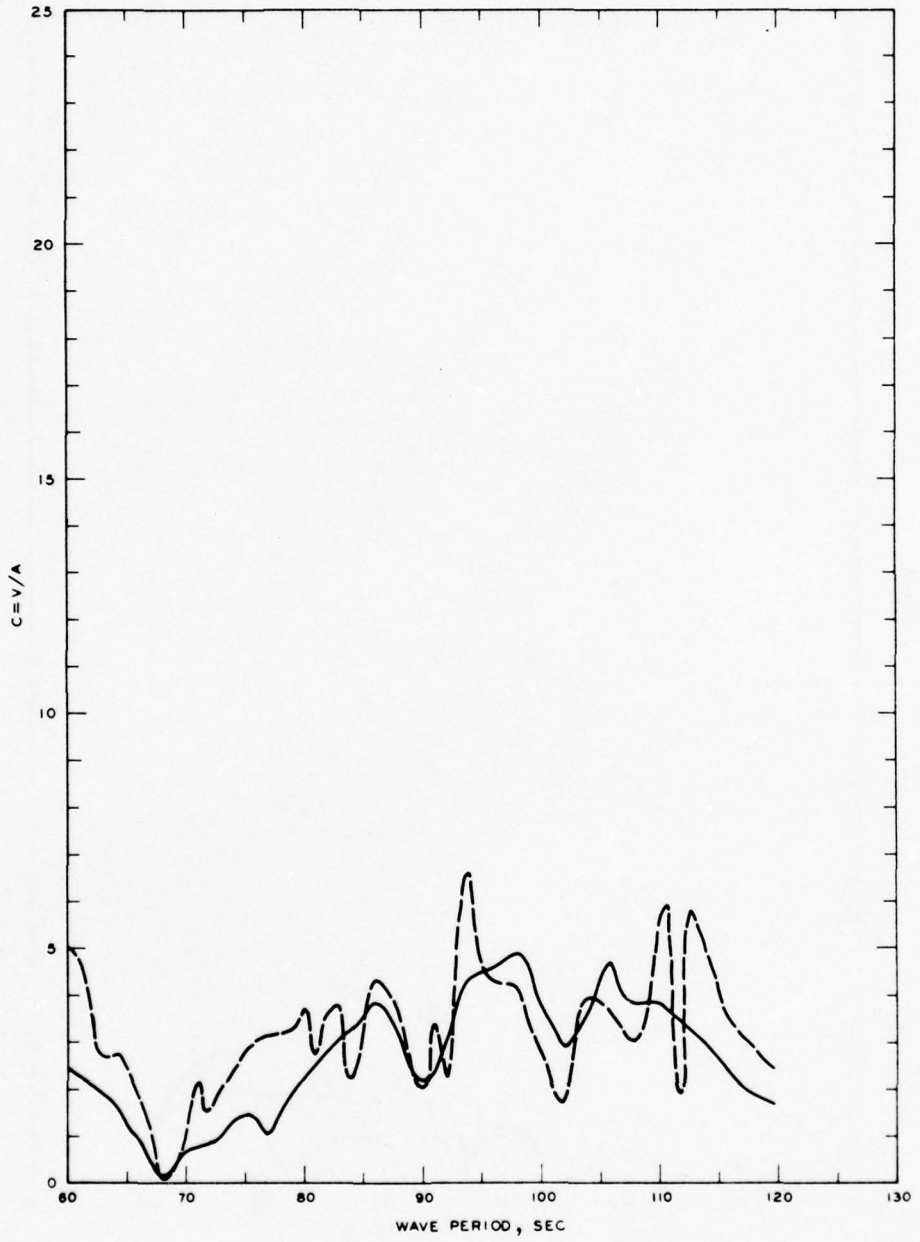

LEGEND

——— GRID 1
– – – GRID 1A

NOTE: C = NORMALIZED MAXIMUM CURRENT VELOCITY
V = CURRENT VELOCITY, FT/SEC
A = INCIDENT WAVE AMPLITUDE

FREQUENCY RESPONSE

NORMALIZED MAXIMUM CURRENT VELOCITY
STA LA-4, GRIDS 1 AND 1A

PLATE 115

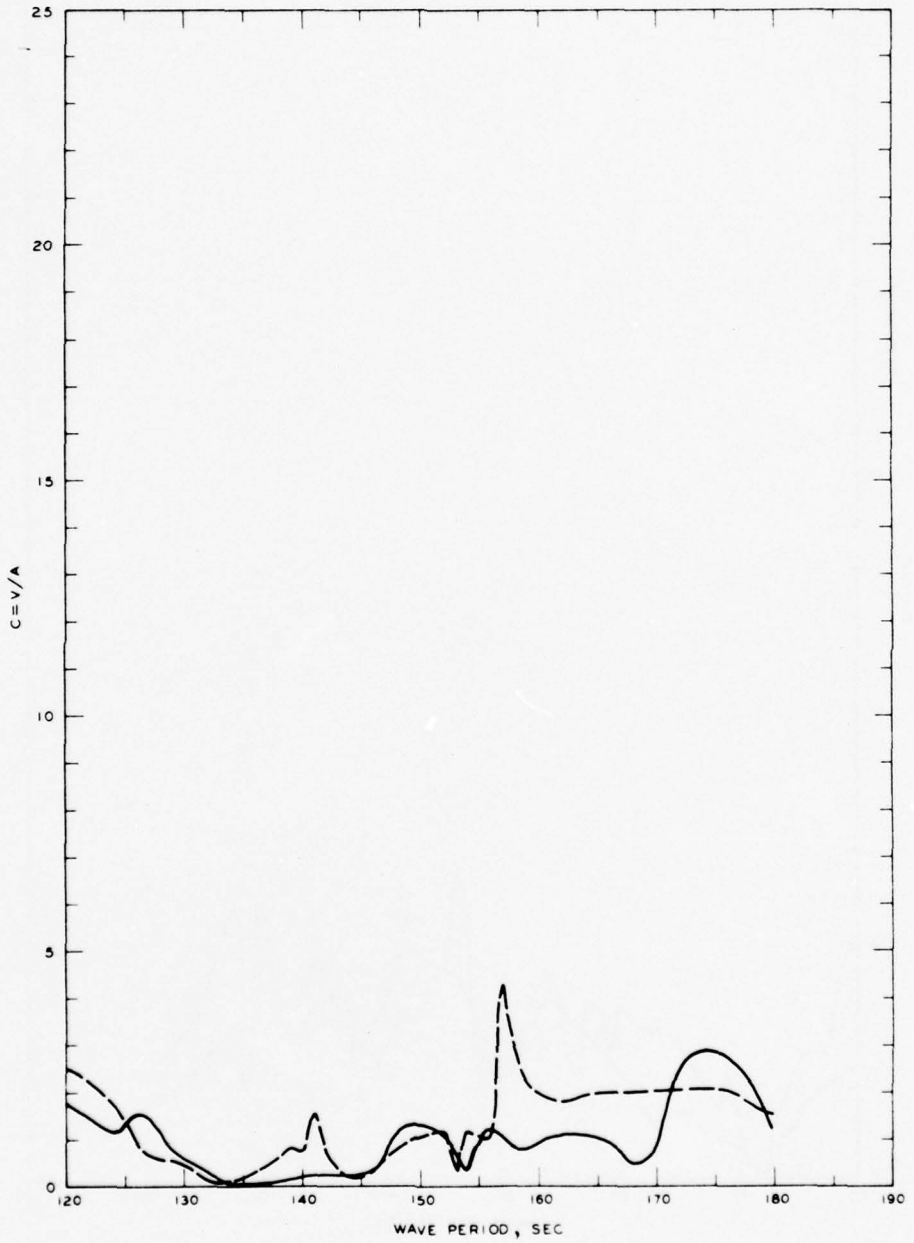

LEGEND

——— GRID 2

– – – GRID 2A

NOTE: C = NORMALIZED MAXIMUM CURRENT VELOCITY
V = CURRENT VELOCITY, FT/SEC
A = INCIDENT WAVE AMPLITUDE

FREQUENCY RESPONSE

NORMALIZED MAXIMUM CURRENT VELOCITY
STA LA- 4, GRIDS 2 AND 2A

PLATE 116

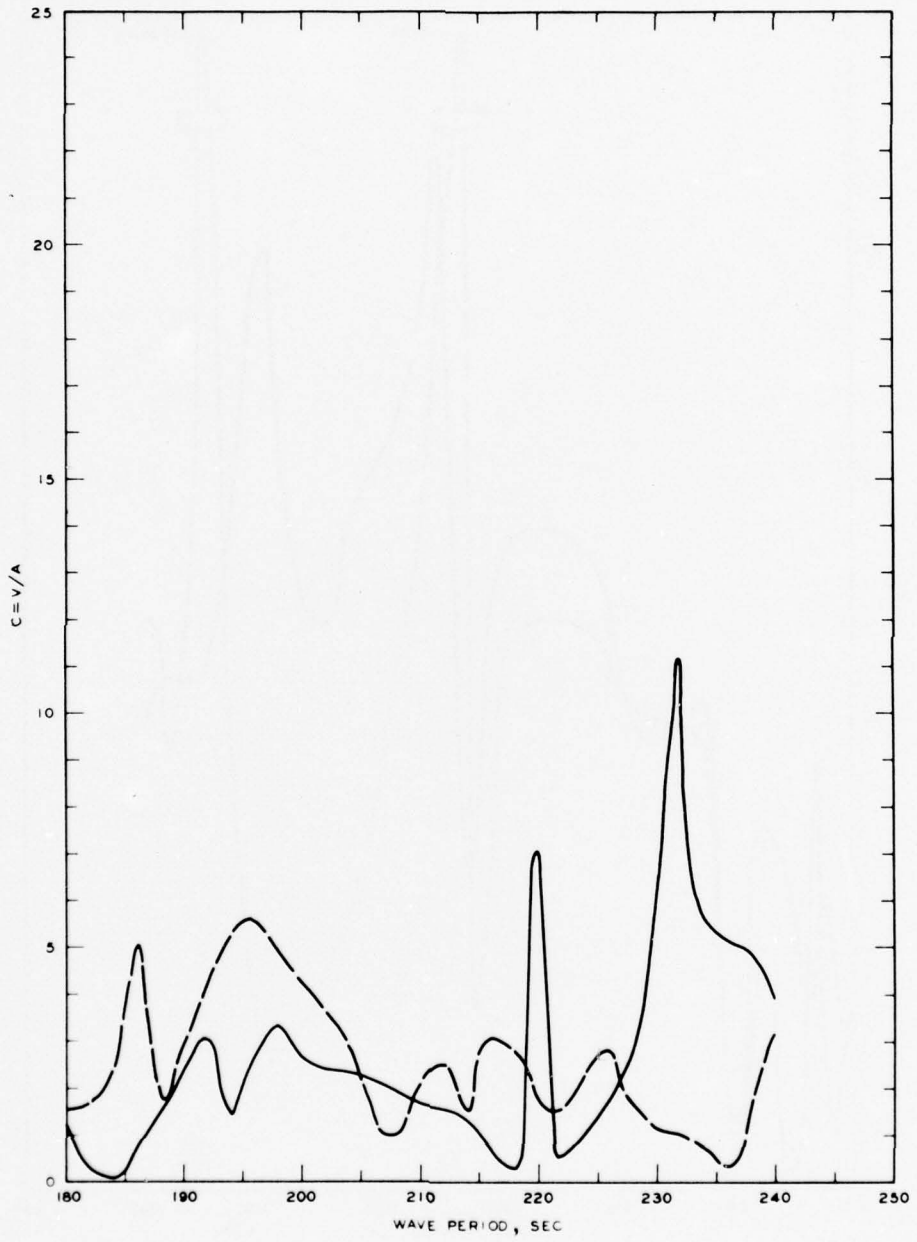

LEGEND

——— GRID 3

— — — GRID 3A

NOTE C = NORMALIZED MAXIMUM CURRENT VELOCITY
V = CURRENT VELOCITY, FT/SEC
A = INCIDENT WAVE AMPLITUDE

FREQUENCY RESPONSE

NORMALIZED MAXIMUM CURRENT VELOCITY
STA LA-4, GRIDS 3 AND 3A

PLATE 117

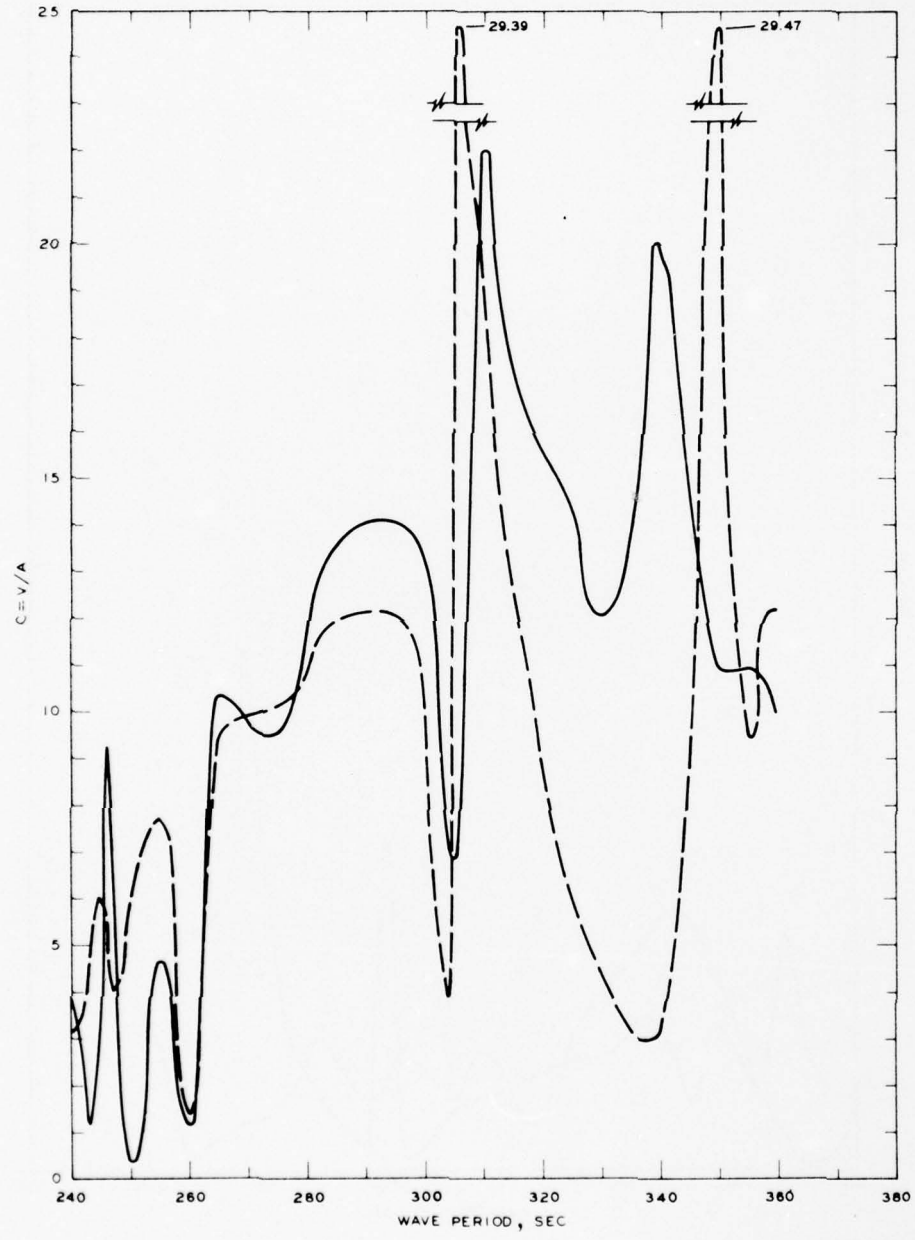

NOTE: C = NORMALIZED MAXIMUM CURRENT VELOCITY
V = CURRENT VELOCITY, FT/SEC
A = INCIDENT WAVE AMPLITUDE

FREQUENCY RESPONSE

NORMALIZED MAXIMUM CURRENT VELOCITY
STA LA-4, GRIDS 4 AND 4A

PLATE 118

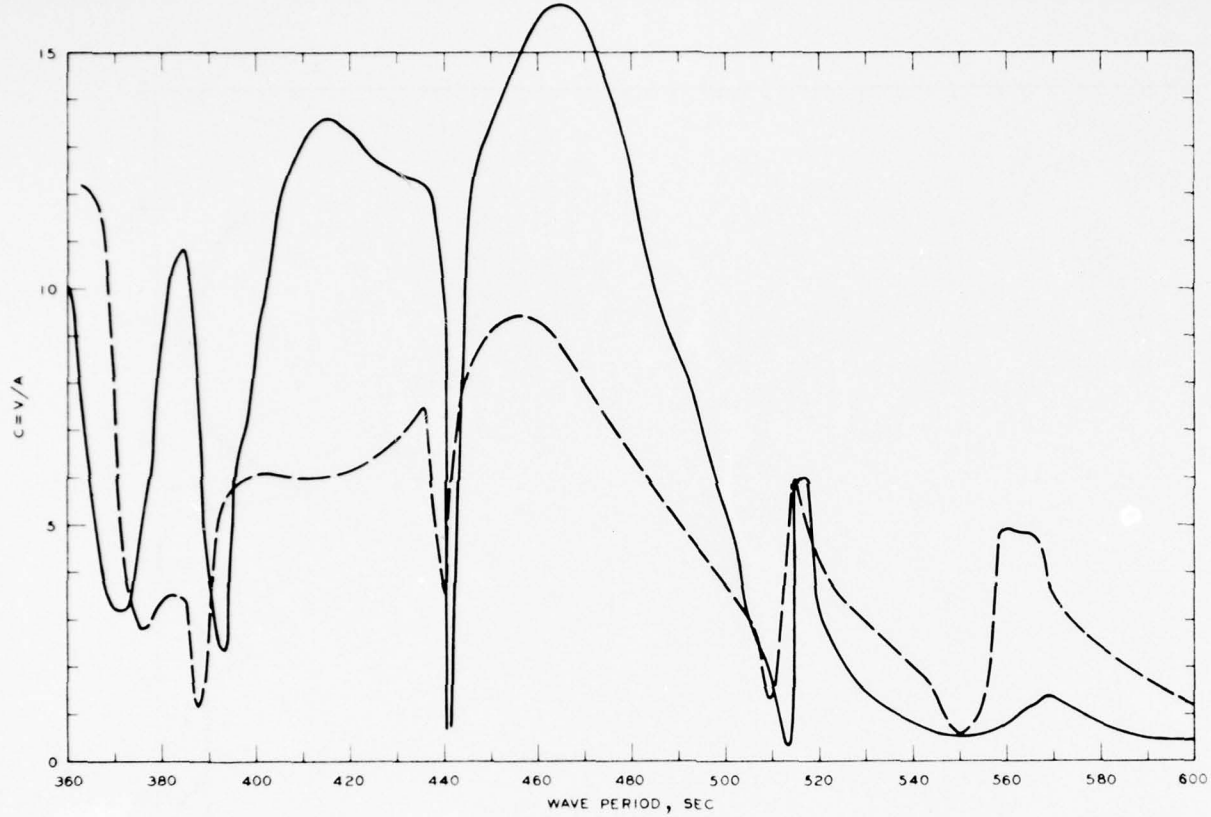

LEGEND

——— GRID 5

— — — GRID 5A

NOTE: C = NORMALIZED MAXIMUM CURRENT VELOCITY
V = CURRENT VELOCITY, FT/SEC
A = INCIDENT WAVE AMPLITUDE

FREQUENCY RESPONSE

NORMALIZED MAXIMUM CURRENT VELOCITY
STA LA-4, GRIDS 5 AND 5A

PLATE 119

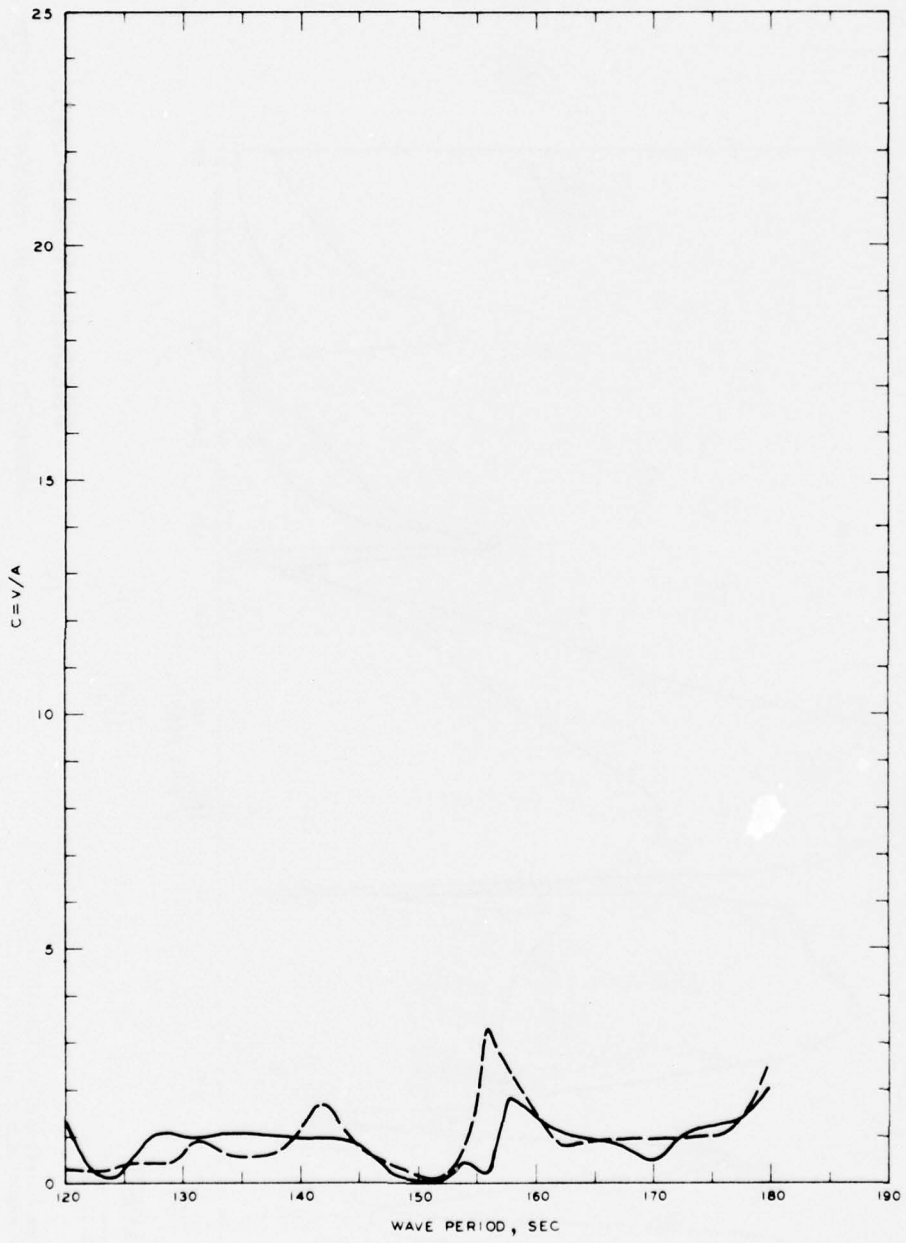

LEGEND

——— GRID 2

– – – GRID 2A

NOTE C = NORMALIZED MAXIMUM CURRENT VELOCITY
V = CURRENT VELOCITY, FT/SEC
A = INCIDENT WAVE AMPLITUDE

FREQUENCY RESPONSE

NORMALIZED MAXIMUM CURRENT VELOCITY
STA LA-5, GRIDS 2 AND 2A

PLATE 120

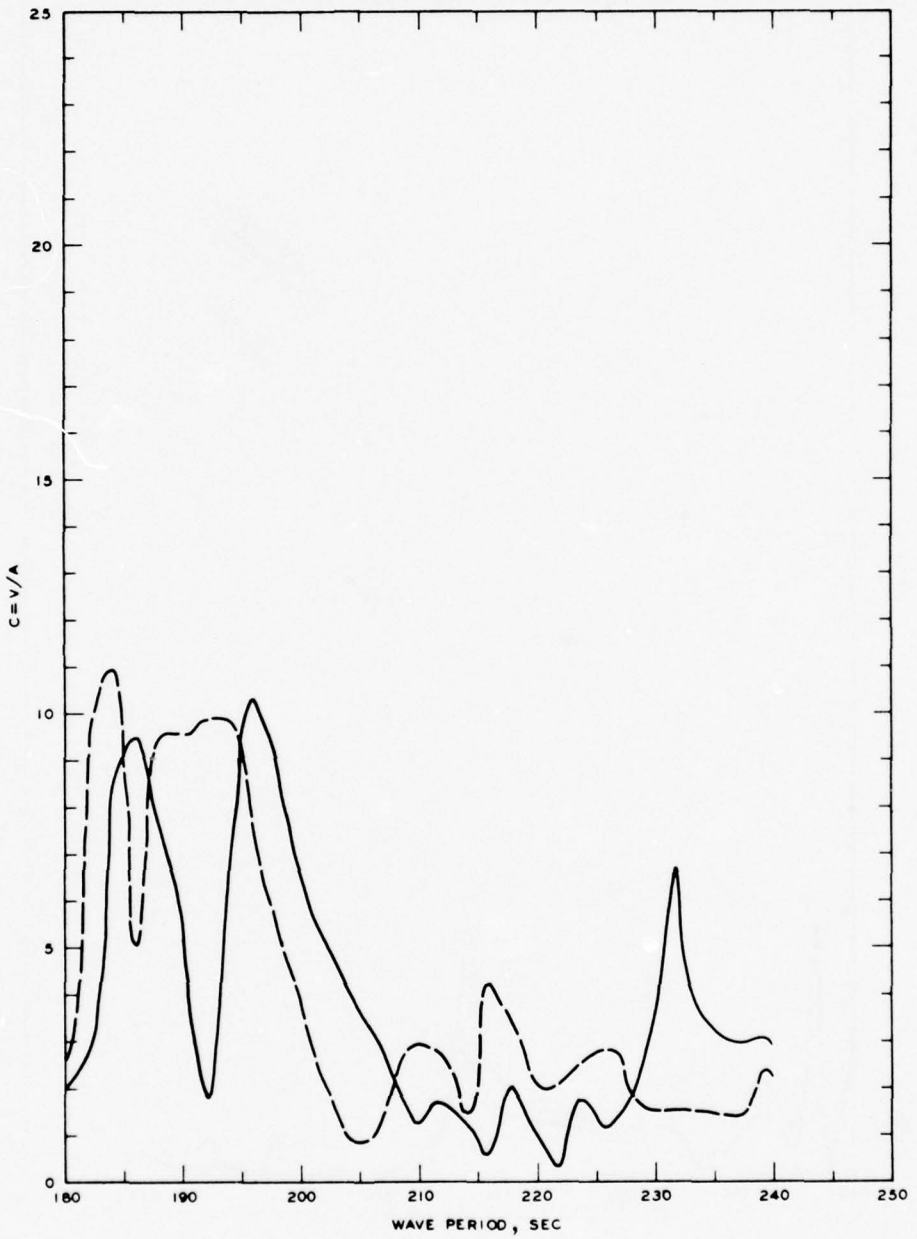

LEGEND

——— GRID 3

– – – GRID 3A

NOTE: C = NORMALIZED MAXIMUM CURRENT VELOCITY
V = CURRENT VELOCITY, FT/SEC
A = INCIDENT WAVE AMPLITUDE

FREQUENCY RESPONSE

NORMALIZED MAXIMUM CURRENT VELOCITY
STA LA-5, GRIDS 3 AND 3A

PLATE 121

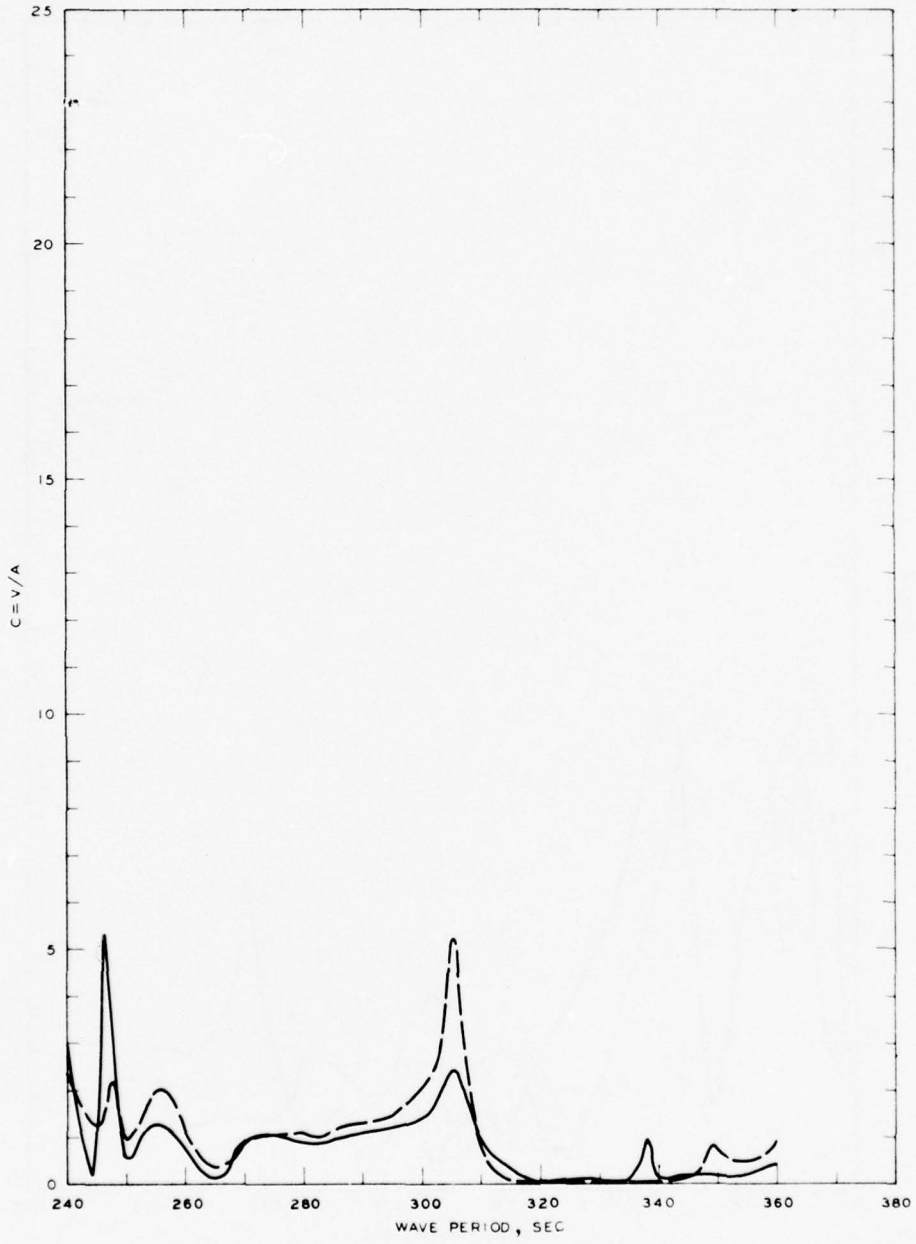

LEGEND

——— GRID 4

— — — GRID 4A

NOTE C = NORMALIZED MAXIMUM CURRENT VELOCITY
V = CURRENT VELOCITY, FT/SEC
A = INCIDENT WAVE AMPLITUDE

FREQUENCY RESPONSE

NORMALIZED MAXIMUM CURRENT VELOCITY
STA LA-5, GRIDS 4 AND 4A

PLATE 122

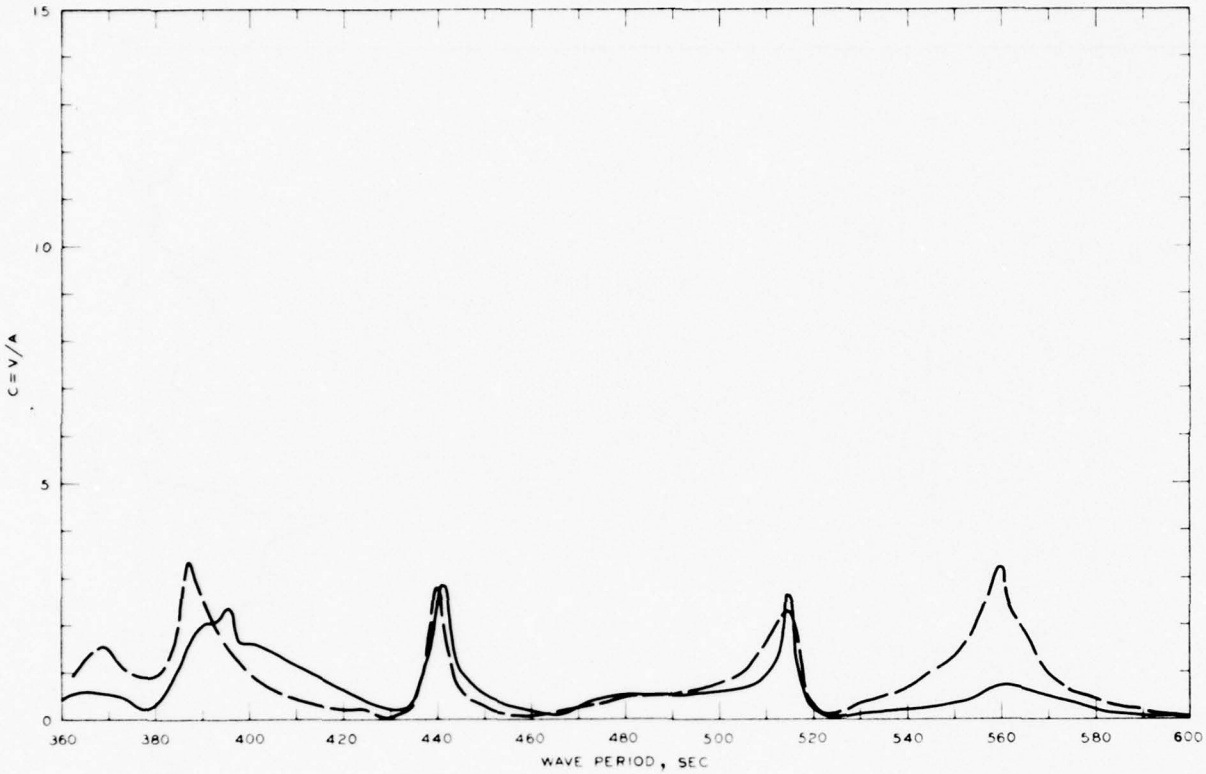

LEGEND

——— GRID 5

— — — GRID 5A

NOTE C = NORMALIZED MAXIMUM CURRENT VELOCITY
V = CURRENT VELOCITY, FT/SEC
A = INCIDENT WAVE AMPLITUDE

FREQUENCY RESPONSE

NORMALIZED MAXIMUM CURRENT VELOCITY
STA LA-5, GRIDS 5 AND 5A

PLATE 123

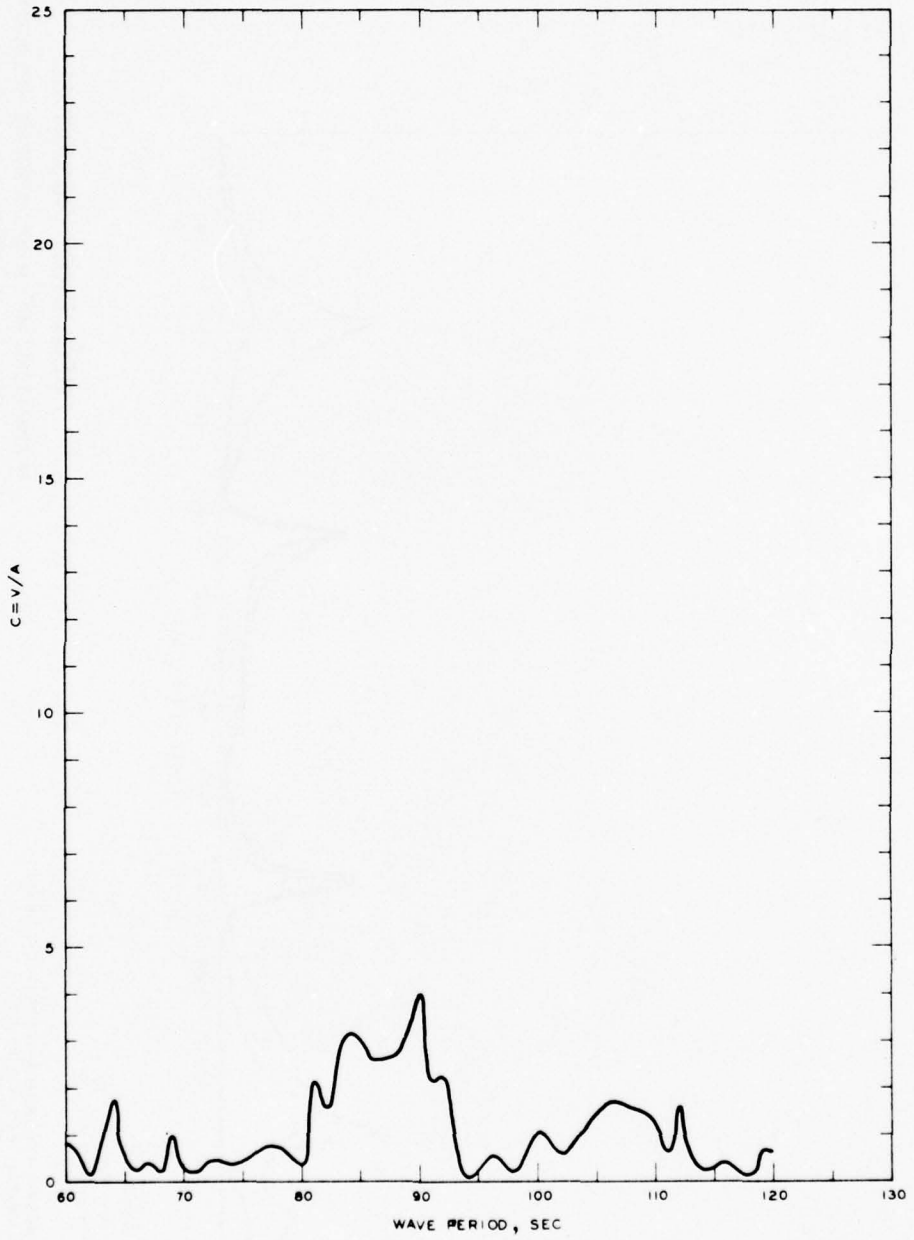

NOTE: C = NORMALIZED MAXIMUM CURRENT VELOCITY
V = CURRENT VELOCITY, FT/SEC
A = INCIDENT WAVE AMPLITUDE

FREQUENCY RESPONSE

NORMALIZED MAXIMUM CURRENT VELOCITY
STA LA-6, GRID 1A

PLATE 124

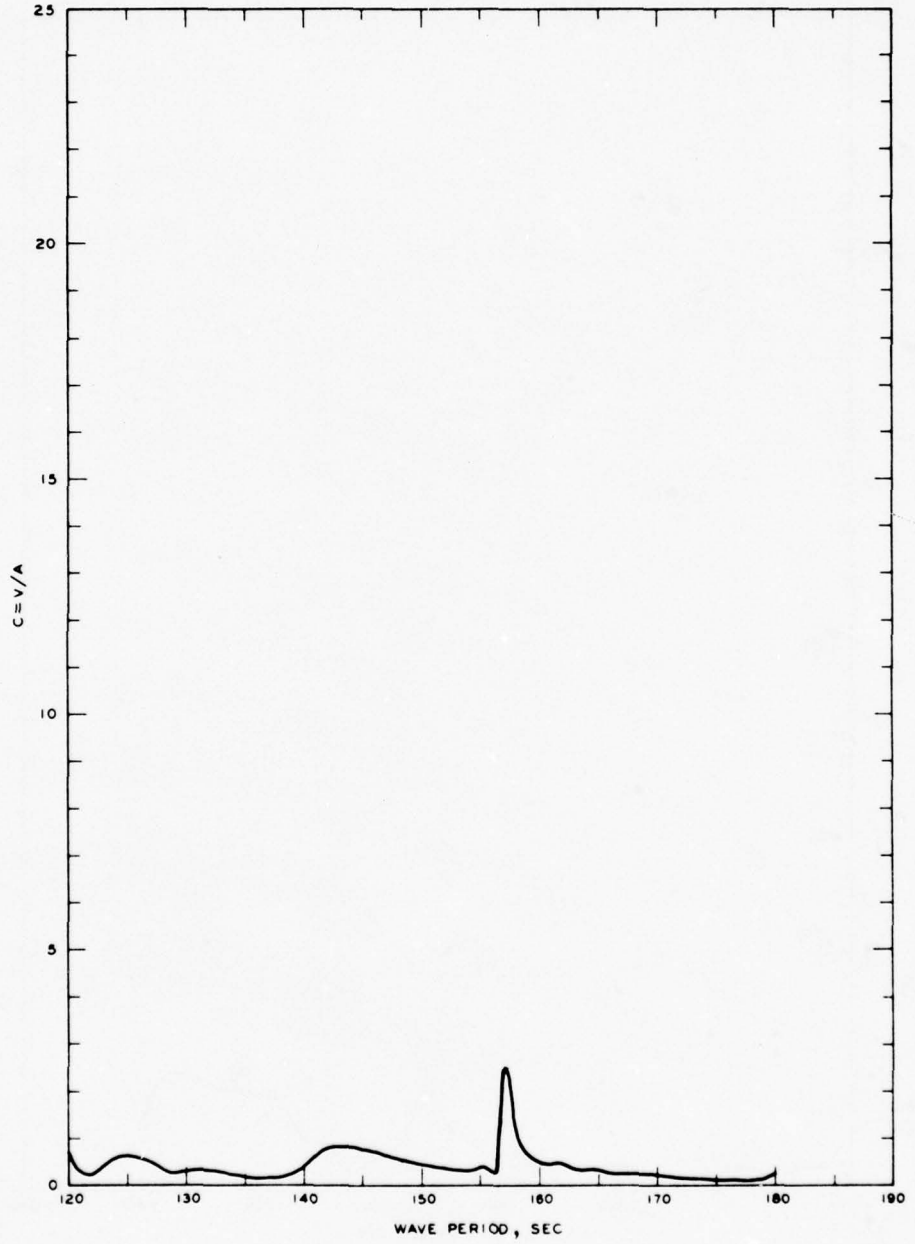

NOTE: C = NORMALIZED MAXIMUM CURRENT VELOCITY
V = CURRENT VELOCITY, FT/SEC
A = INCIDENT WAVE AMPLITUDE

FREQUENCY RESPONSE

NORMALIZED MAXIMUM CURRENT VELOCITY
STA LA-6, GRID 2A

PLATE 125

NOTE: C = NORMALIZED MAXIMUM CURRENT VELOCITY
V = CURRENT VELOCITY, FT/SEC
A = INCIDENT WAVE AMPLITUDE

FREQUENCY RESPONSE

NORMALIZED MAXIMUM CURRENT VELOCITY
STA LA-6, GRID 3A

PLATE 126

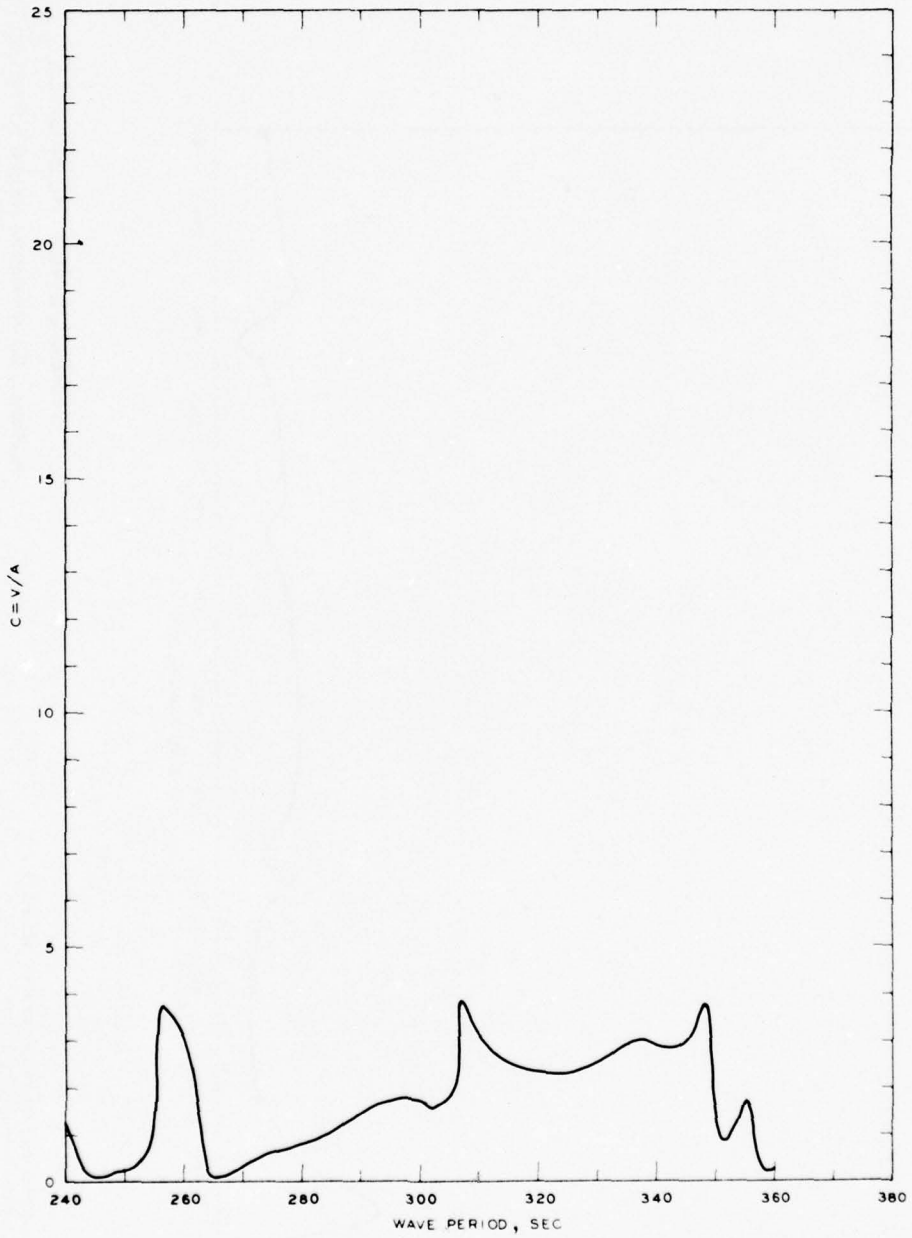

NOTE C = NORMALIZED MAXIMUM CURRENT VELOCITY
V = CURRENT VELOCITY, FT/SEC
A = INCIDENT WAVE AMPLITUDE

FREQUENCY RESPONSE

NORMALIZED MAXIMUM CURRENT VELOCITY
STA LA-6, GRID 4A

PLATE 127

PLATE 128

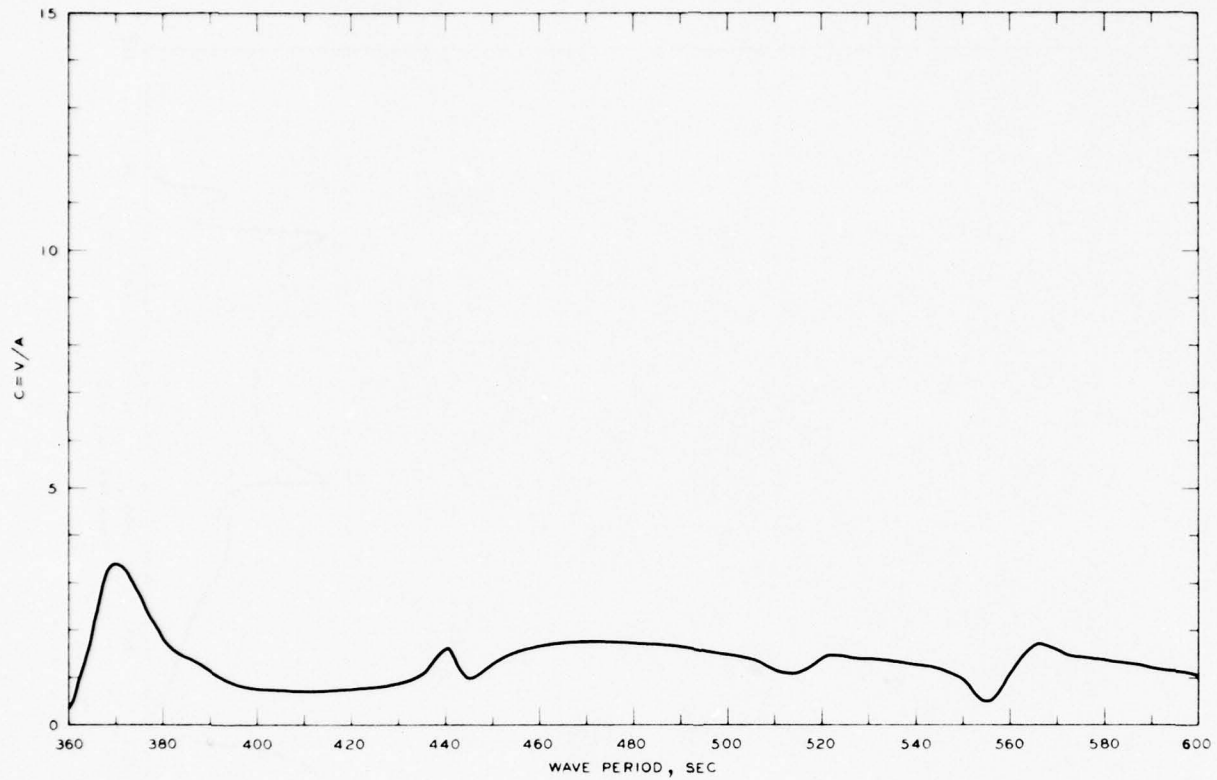

NOTE: C = NORMALIZED MAXIMUM CURRENT VELOCITY
V = CURRENT VELOCITY, FT/SEC
A = INCIDENT WAVE AMPLITUDE

FREQUENCY RESPONSE

NORMALIZED MAXIMUM CURRENT VELOCITY
STA LA-6, GRID 5A

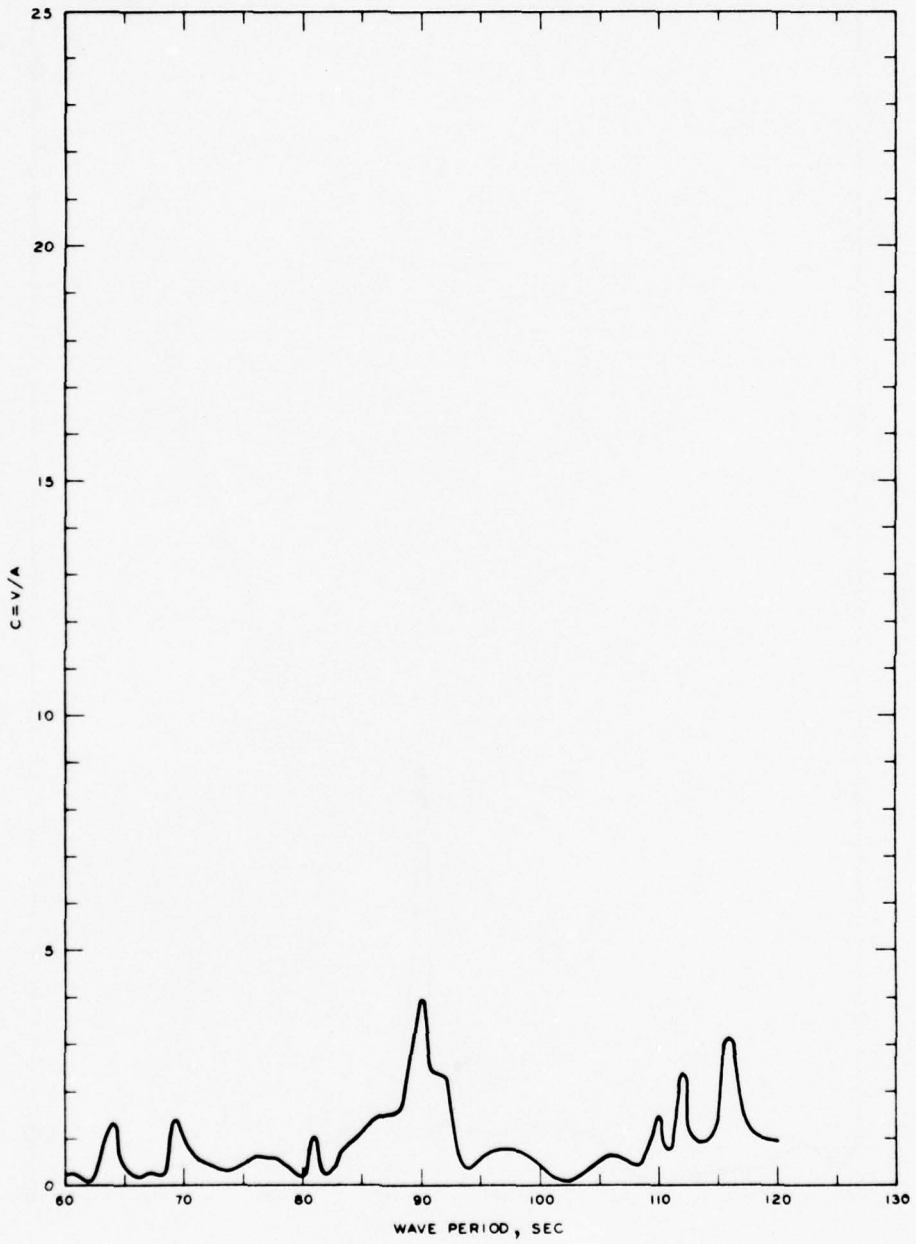

NOTE: C = NORMALIZED MAXIMUM CURRENT VELOCITY
V = CURRENT VELOCITY, FT/SEC
A = INCIDENT WAVE AMPLITUDE

FREQUENCY RESPONSE

NORMALIZED MAXIMUM CURRENT VELOCITY
STA LA-7, GRID 1A

PLATE 129

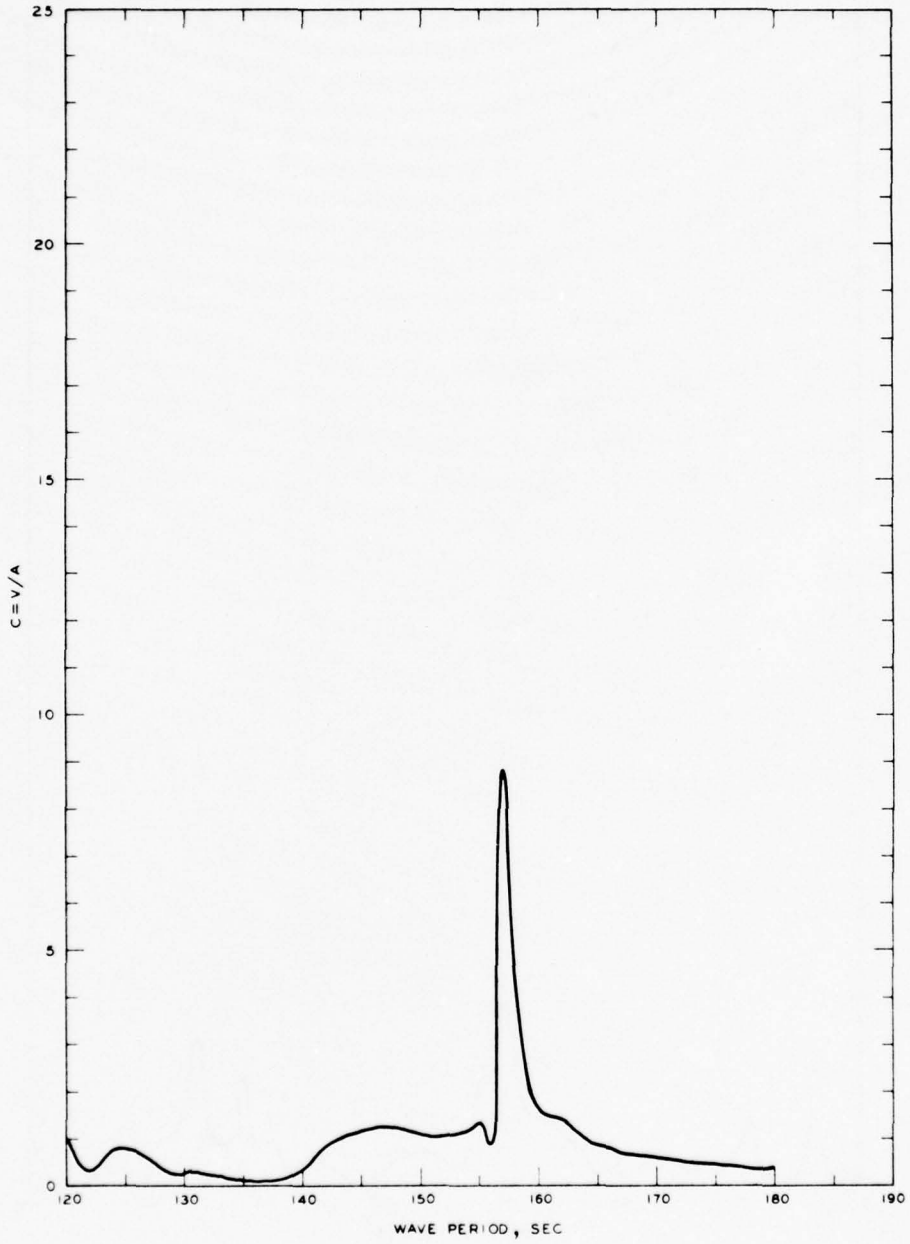

NOTE C = NORMALIZED MAXIMUM CURRENT VELOCITY
V = CURRENT VELOCITY, FT/SEC
A = INCIDENT WAVE AMPLITUDE

FREQUENCY RESPONSE

NORMALIZED MAXIMUM CURRENT VELOCITY
STA LA-7, GRID 2A

PLATE 130

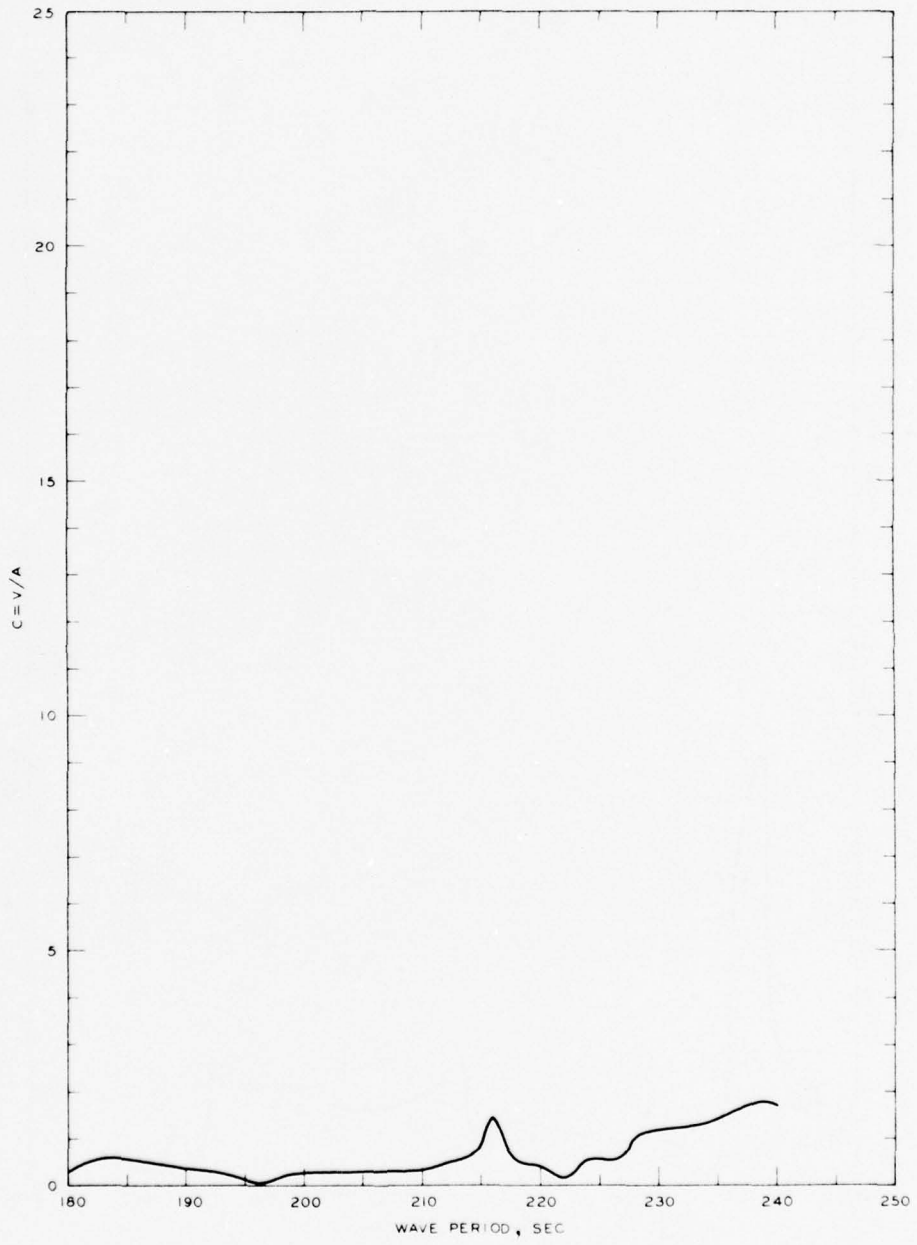

NOTE C = NORMALIZED MAXIMUM CURRENT VELOCITY
V = CURRENT VELOCITY, FT/SEC
A = INCIDENT WAVE AMPLITUDE

FREQUENCY RESPONSE

NORMALIZED MAXIMUM CURRENT VELOCITY
STA LA- 7, GRID 3A

PLATE 131

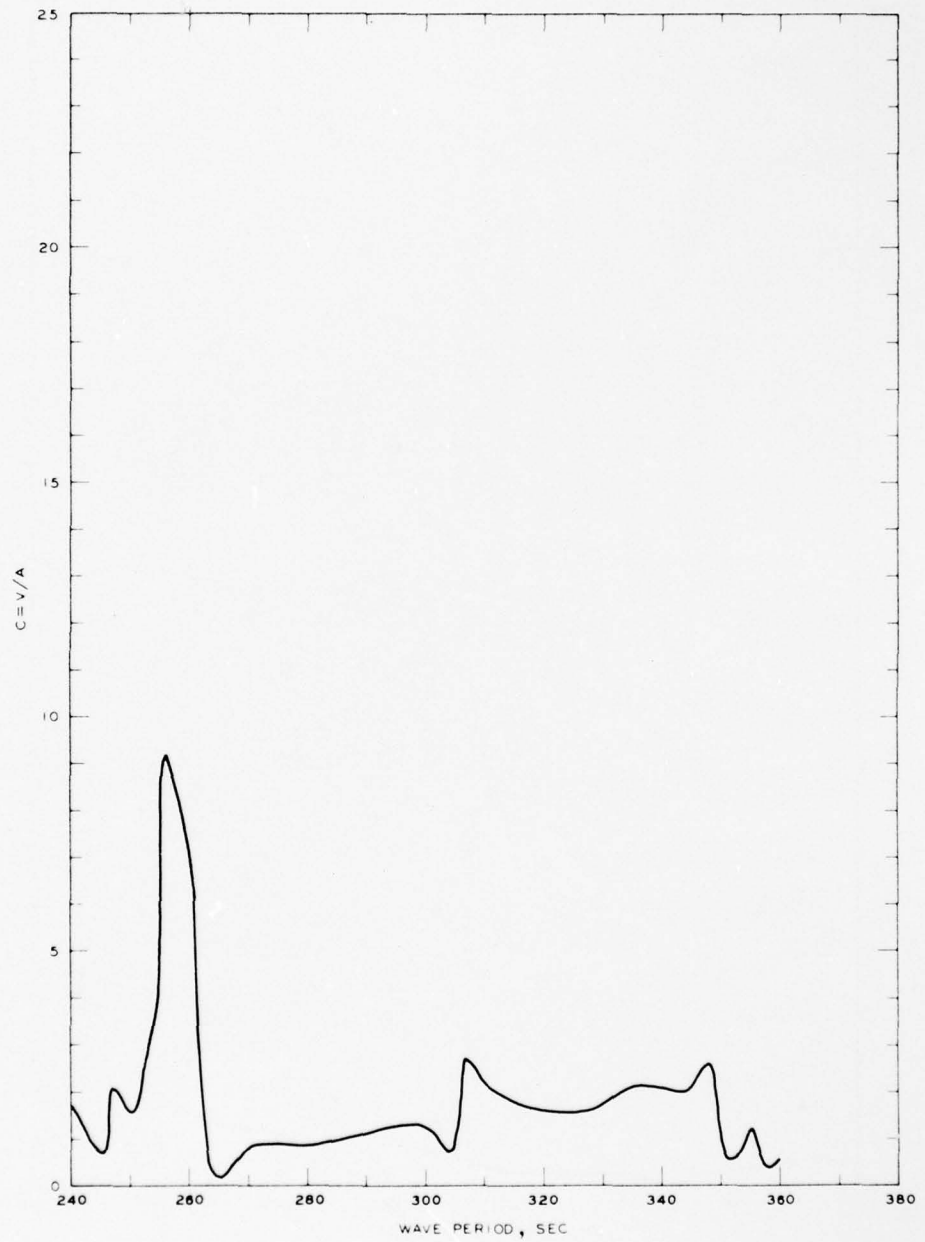

NOTE C = NORMALIZED MAXIMUM CURRENT VELOCITY
V = CURRENT VELOCITY, FT/SEC
A = INCIDENT WAVE AMPLITUDE

FREQUENCY RESPONSE

NORMALIZED MAXIMUM CURRENT VELOCITY
STA LA-7, GRID 4A

PLATE 132

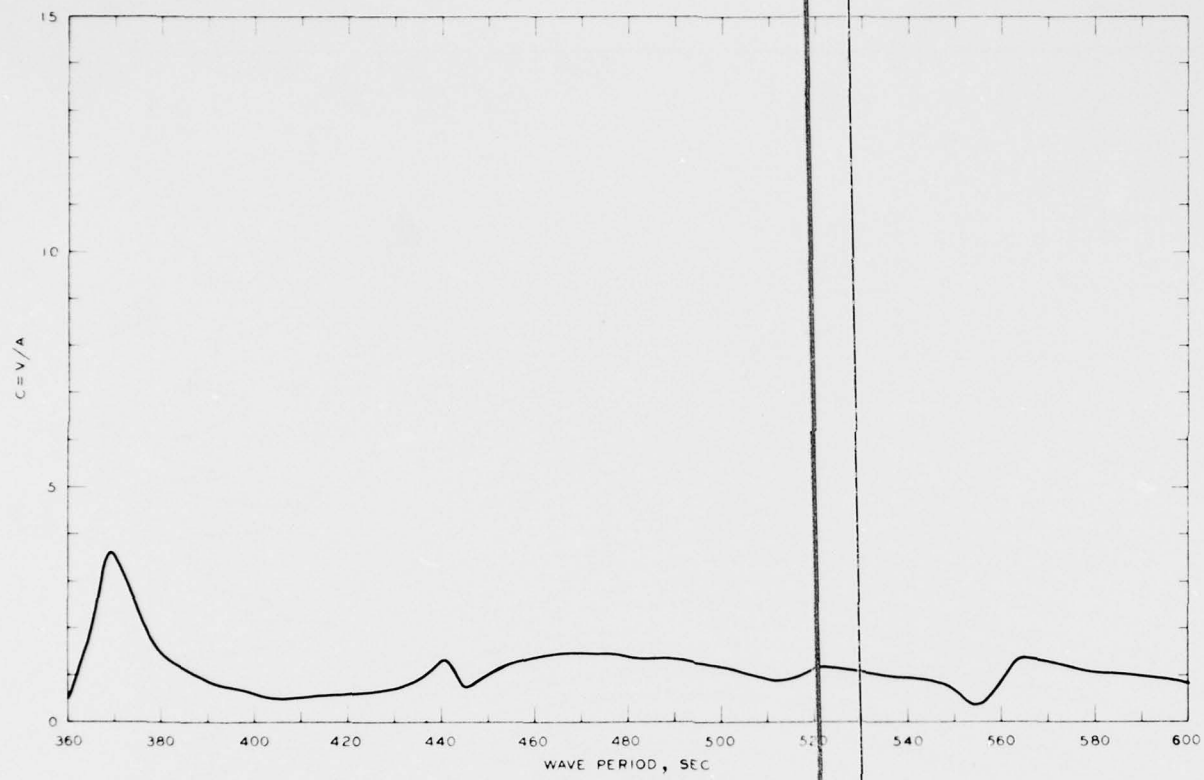

NOTE C = NORMALIZED MAXIMUM CURRENT VELOCITY
V = CURRENT VELOCITY, FT/SEC
A = INCIDENT WAVE AMPLITUDE

FREQUENCY RESPONSE

NORMALIZED MAXIMUM CURRENT VELOCITY
STA LA-7, GRID 5A

PLATE 133

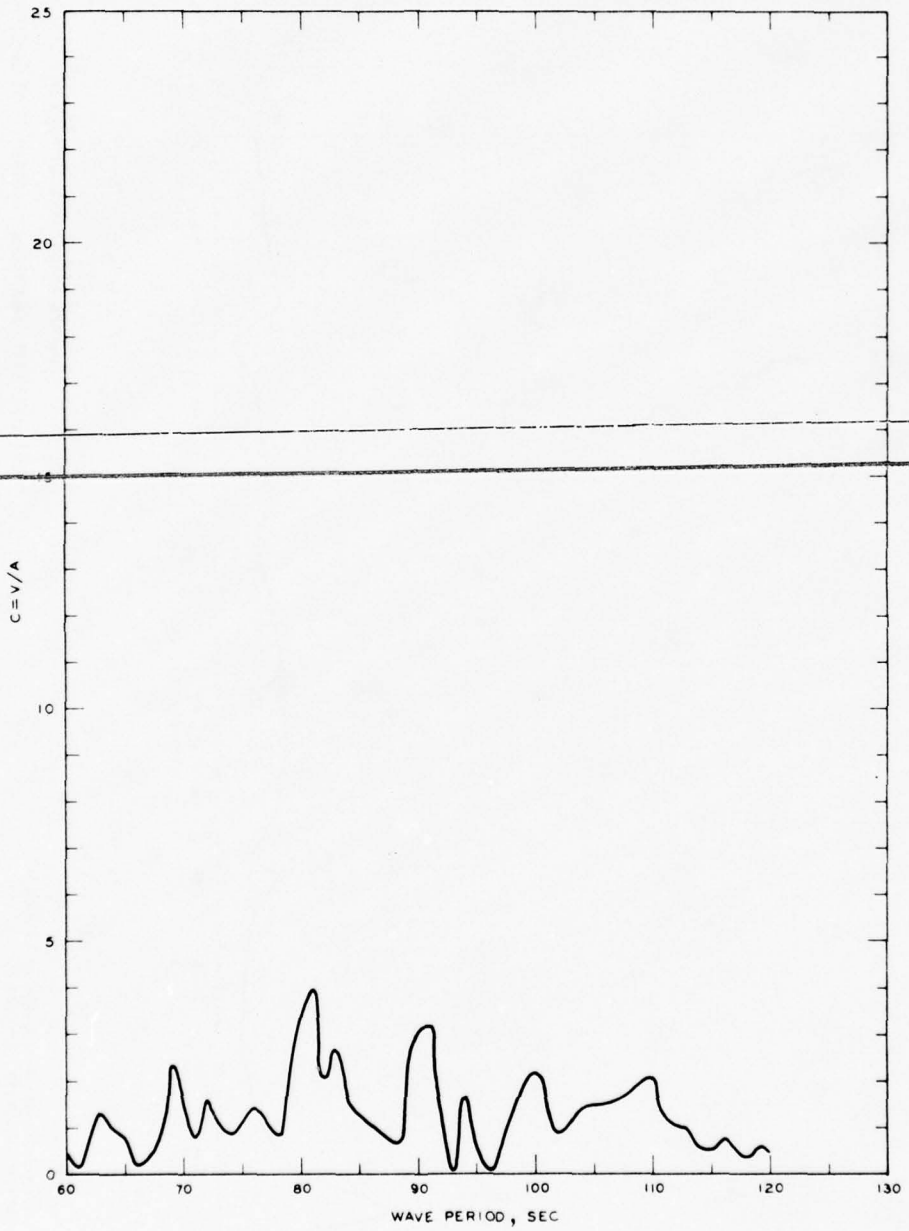

NOTE C = NORMALIZED MAXIMUM CURRENT VELOCITY
V = CURRENT VELOCITY, FT/SEC
A = INCIDENT WAVE AMPLITUDE

FREQUENCY RESPONSE

NORMALIZED MAXIMUM CURRENT VELOCITY
STA LA-8, GRID 1A

PLATE 134

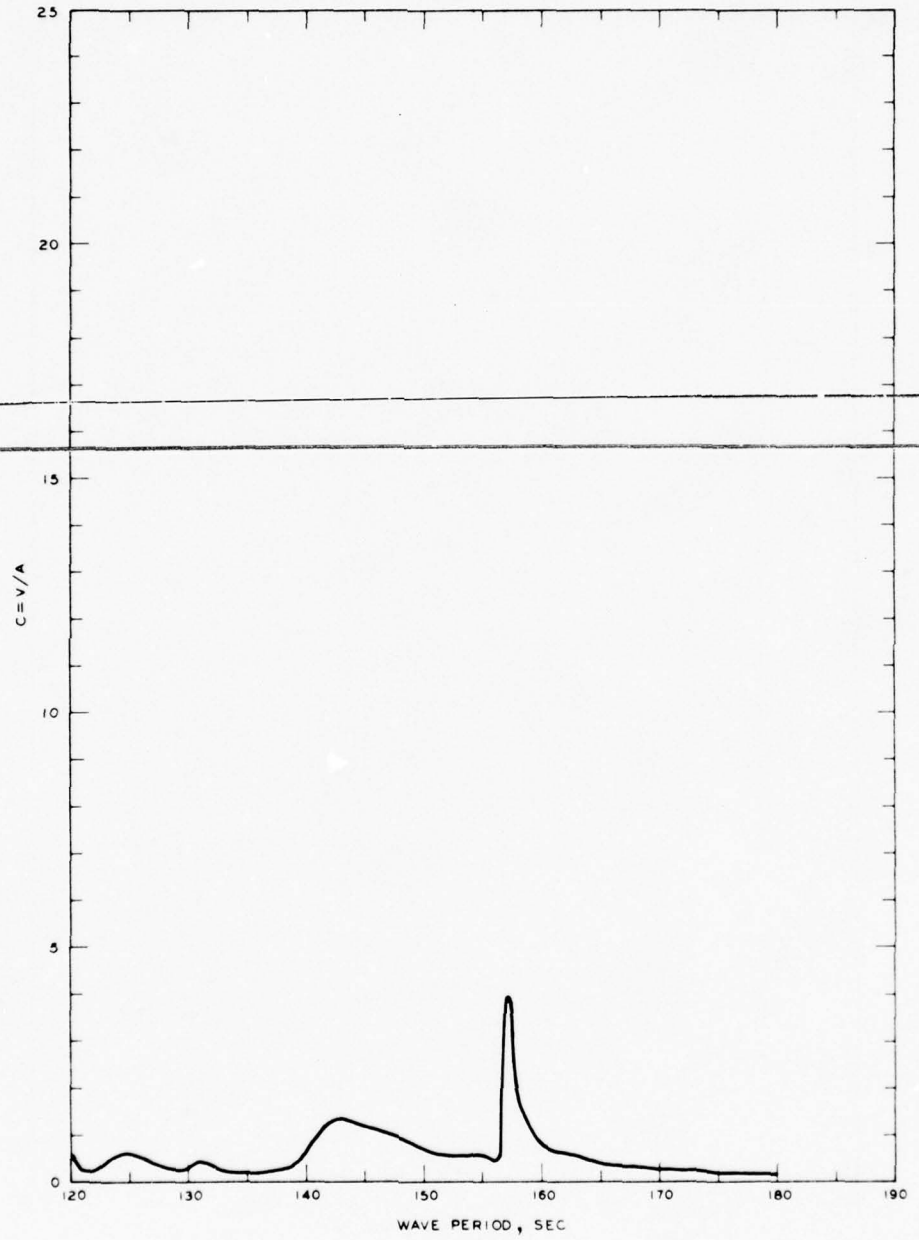

NOTE C = NORMALIZED MAXIMUM CURRENT VELOCITY
V = CURRENT VELOCITY, FT/SEC
A = INCIDENT WAVE AMPLITUDE

FREQUENCY RESPONSE

NORMALIZED MAXIMUM CURRENT VELOCITY
STA LA-8, GRID 2A

PLATE 135

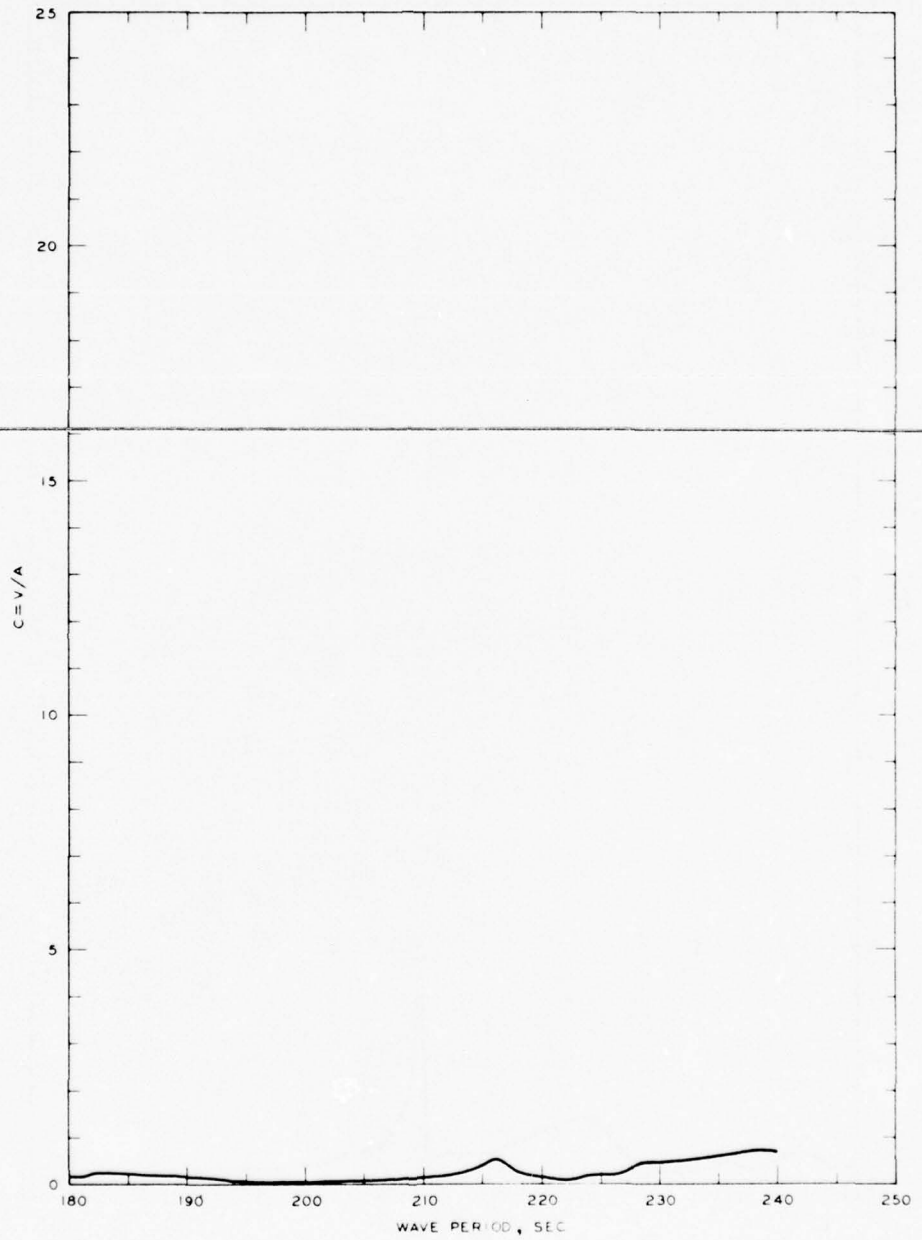

NOTE C = NORMALIZED MAXIMUM CURRENT VELOCITY
V = CURRENT VELOCITY, FT/SEC
A = INCIDENT WAVE AMPLITUDE

FREQUENCY RESPONSE

NORMALIZED MAXIMUM CURRENT VELOCITY
STA LA-8, GRID 3A

PLATE 136

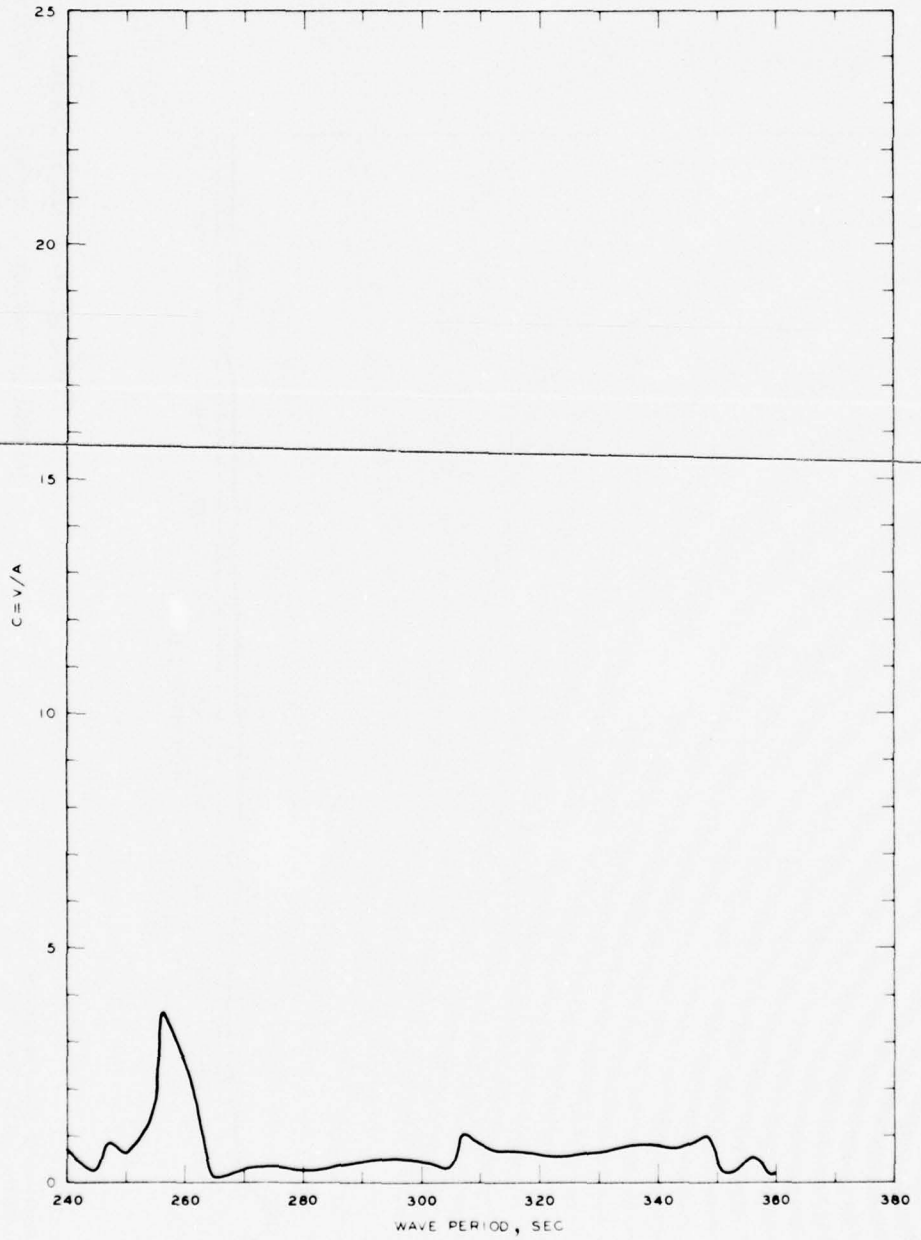

NOTE C = NORMALIZED MAXIMUM CURRENT VELOCITY
V = CURRENT VELOCITY, FT/SEC
A = INCIDENT WAVE AMPLITUDE

FREQUENCY RESPONSE

NORMALIZED MAXIMUM CURRENT VELOCITY
STA LA-8, GRID 4A

PLATE 137

PLATE 138

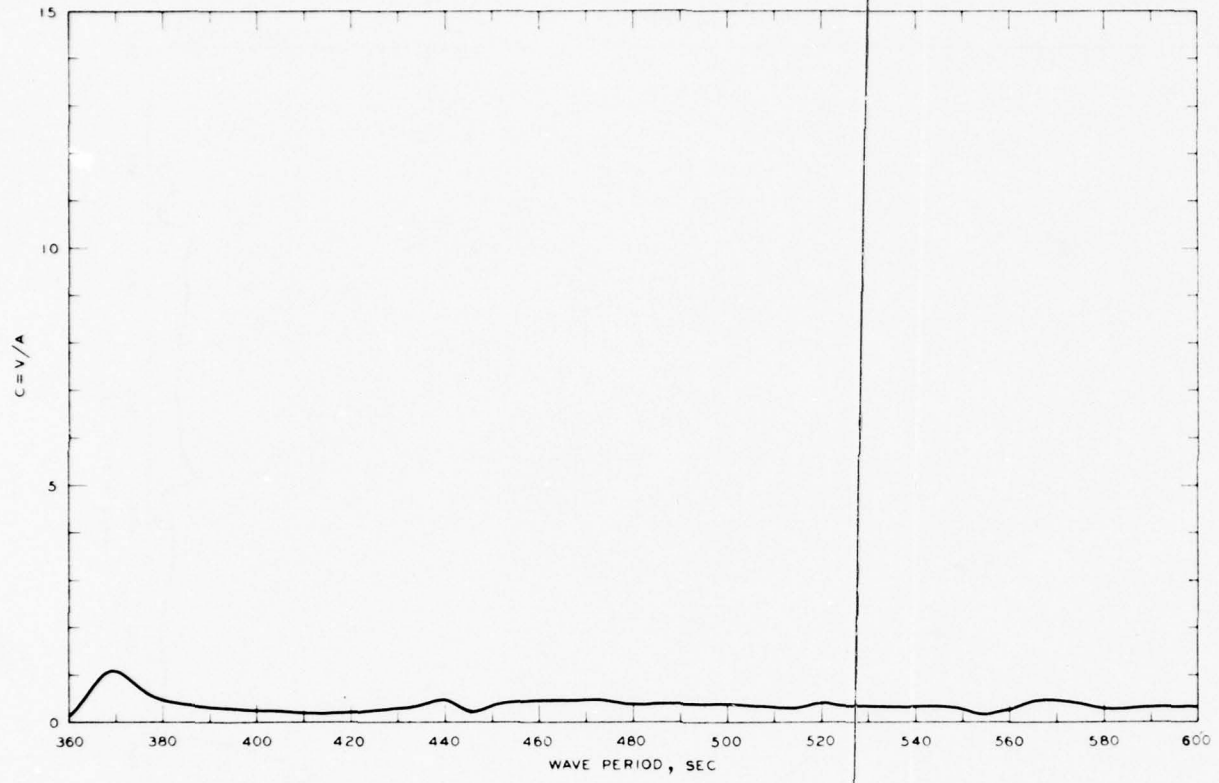

NOTE C = NORMALIZED MAXIMUM CURRENT VELOCITY
V = CURRENT VELOCITY, FT/SEC
A = INCIDENT WAVE AMPLITUDE

FREQUENCY RESPONSE

NORMALIZED MAXIMUM CURRENT VELOCITY
STA LA-8, GRID 5A

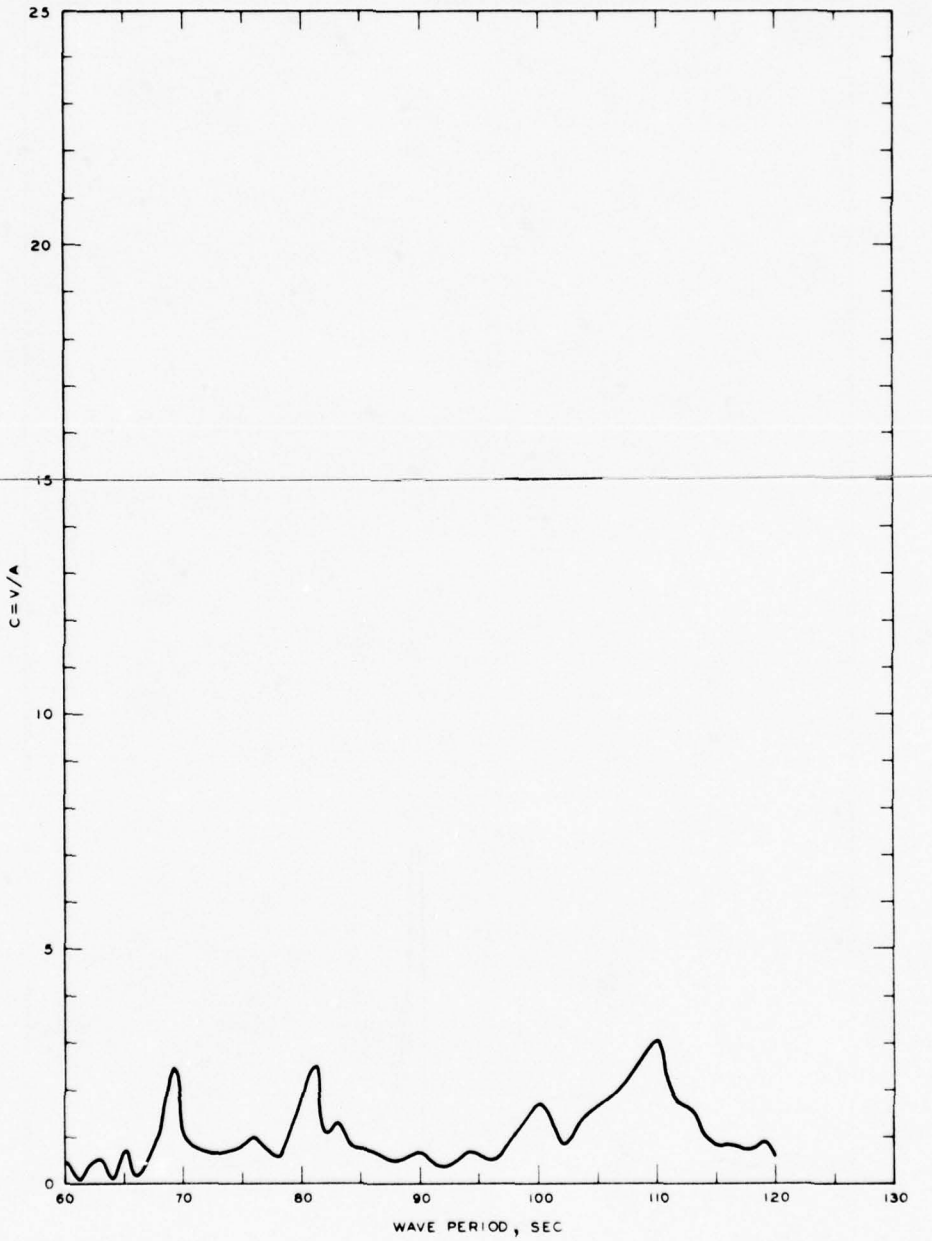

NOTE: C = NORMALIZED MAXIMUM CURRENT VELOCITY
V = CURRENT VELOCITY, FT/SEC
A = INCIDENT WAVE AMPLITUDE

FREQUENCY RESPONSE

NORMALIZED MAXIMUM CURRENT VELOCITY
STA LA-9, GRID 1A

PLATE 139

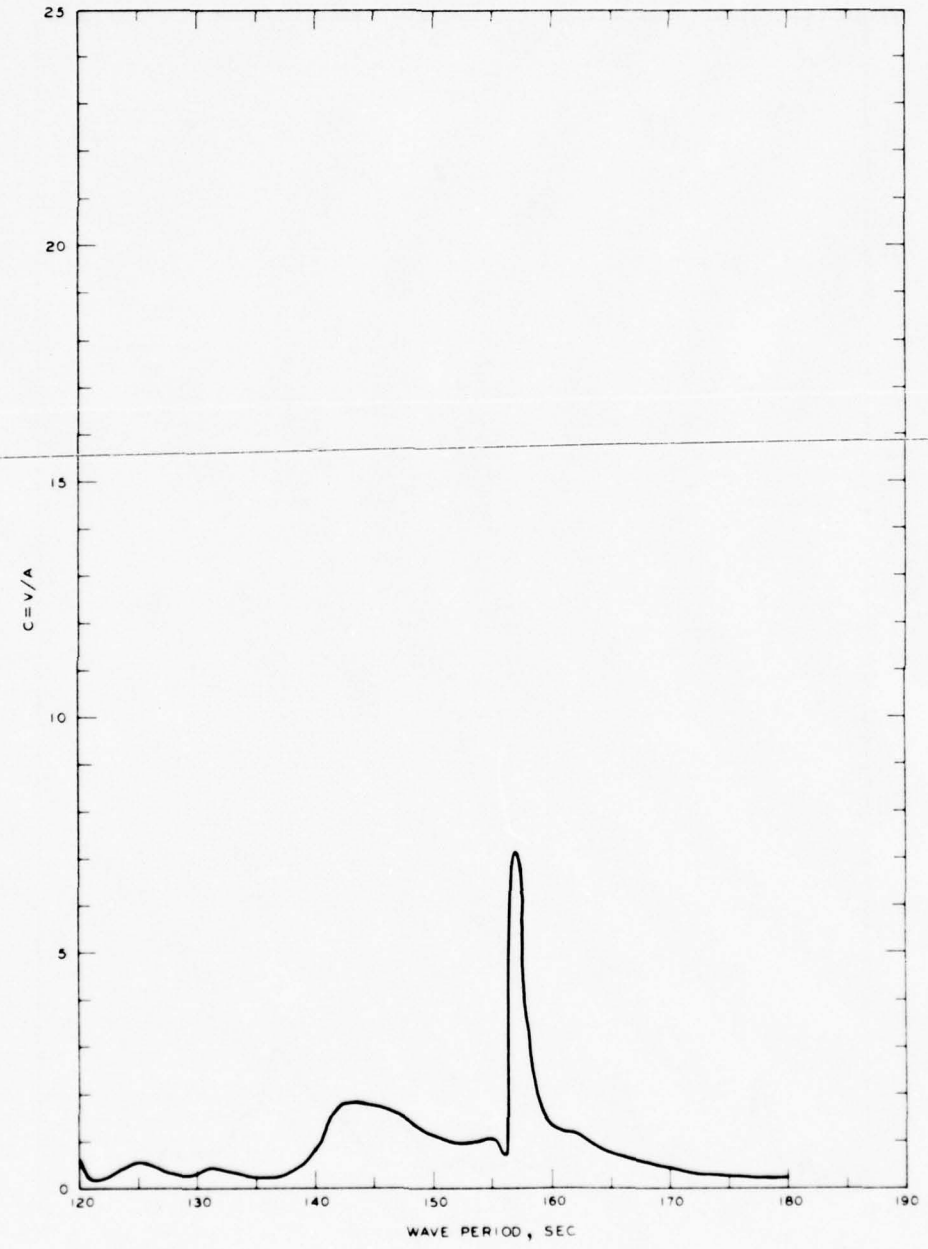

NOTE C = NORMALIZED MAXIMUM CURRENT VELOCITY
V = CURRENT VELOCITY, FT/SEC
A = INCIDENT WAVE AMPLITUDE

FREQUENCY RESPONSE

NORMALIZED MAXIMUM CURRENT VELOCITY
STA LA-9, GRID 2A

PLATE 140

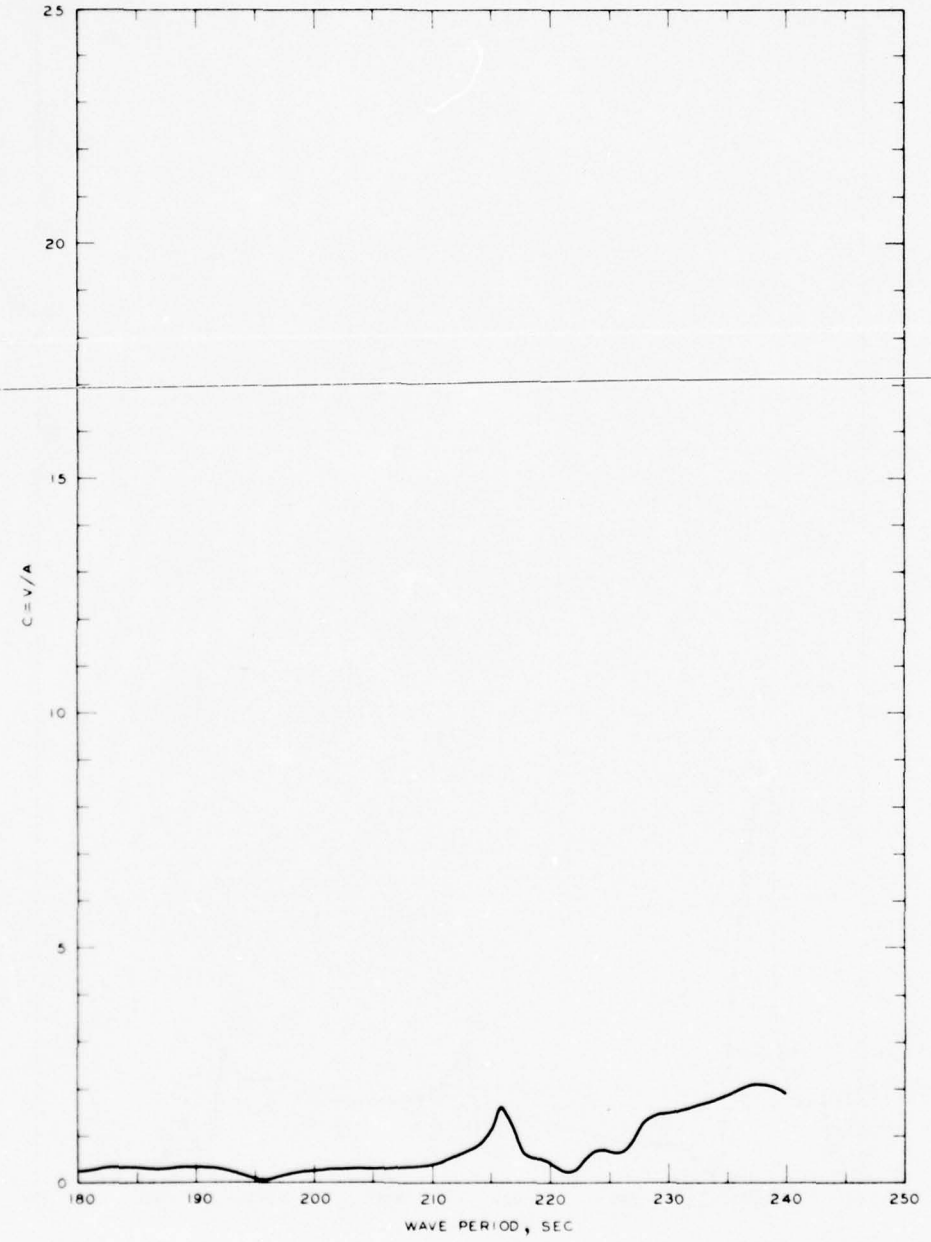

NOTE C = NORMALIZED MAXIMUM CURRENT VELOCITY
V = CURRENT VELOCITY, FT/SEC
A = INCIDENT WAVE AMPLITUDE

FREQUENCY RESPONSE

NORMALIZED MAXIMUM CURRENT VELOCITY
STA LA-9, GRID 3A

PLATE 141

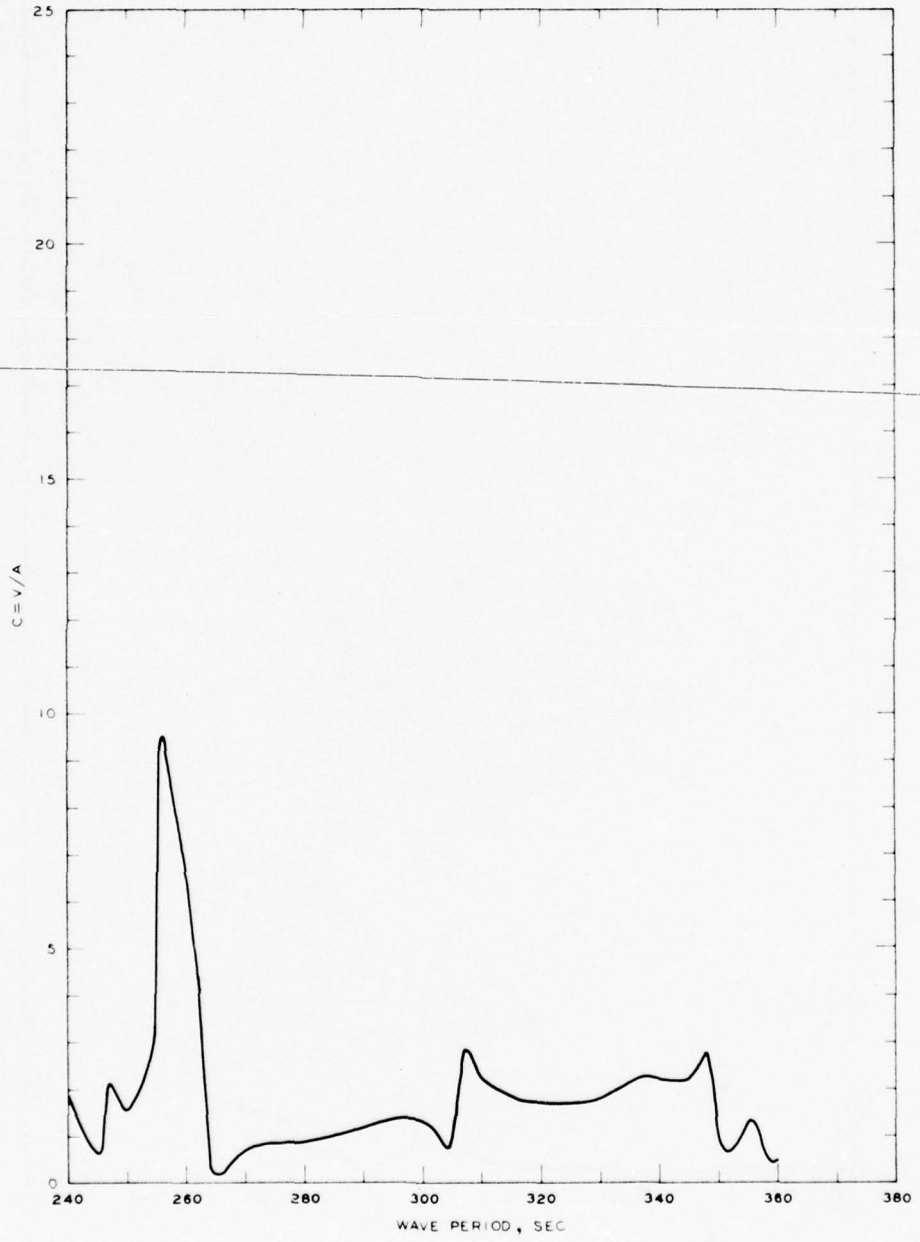

NOTE C = NORMALIZED MAXIMUM CURRENT VELOCITY
V = CURRENT VELOCITY, FT/SEC
A = INCIDENT WAVE AMPLITUDE

FREQUENCY RESPONSE

NORMALIZED MAXIMUM CURRENT VELOCITY
STA LA-9, GRID 4A

PLATE 142

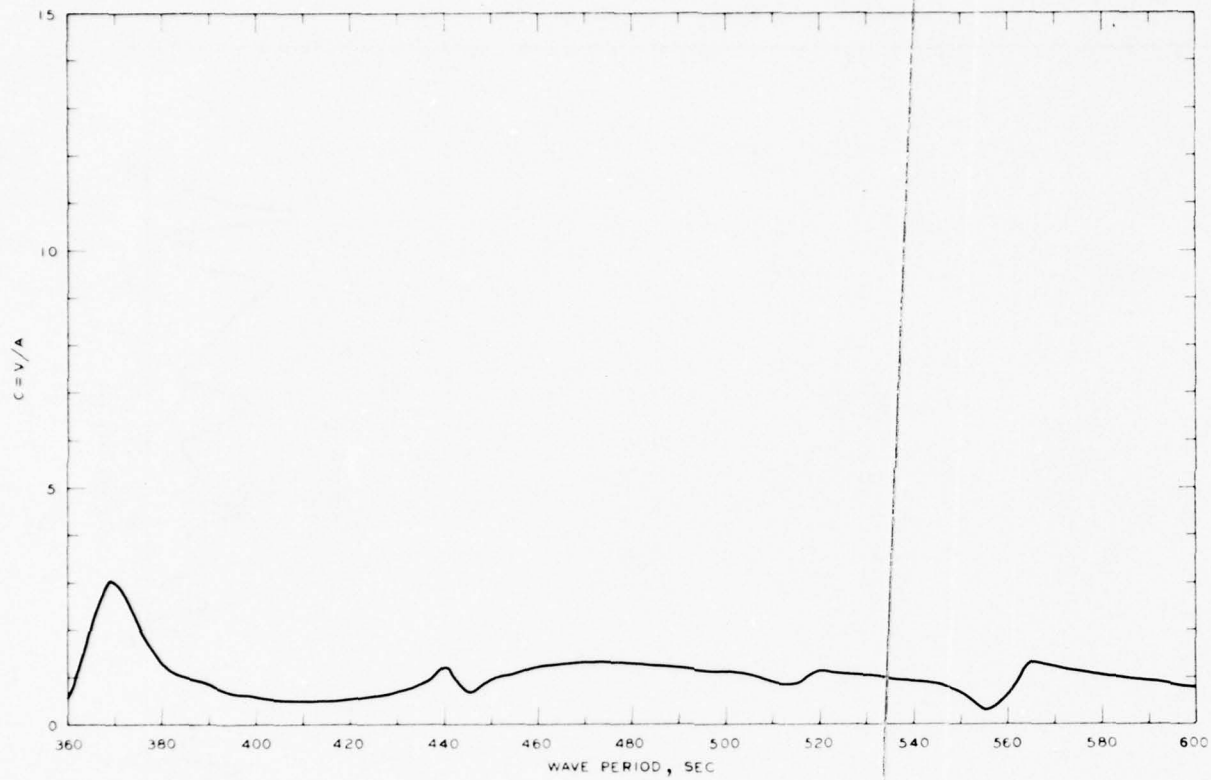

NOTE C = NORMALIZED MAXIMUM CURRENT VELOCITY
V = CURRENT VELOCITY, FT/SEC
A = INCIDENT WAVE AMPLITUDE

FREQUENCY RESPONSE

NORMALIZED MAXIMUM CURRENT VELOCITY
STA LA-9, GRID 5A

PLATE 143

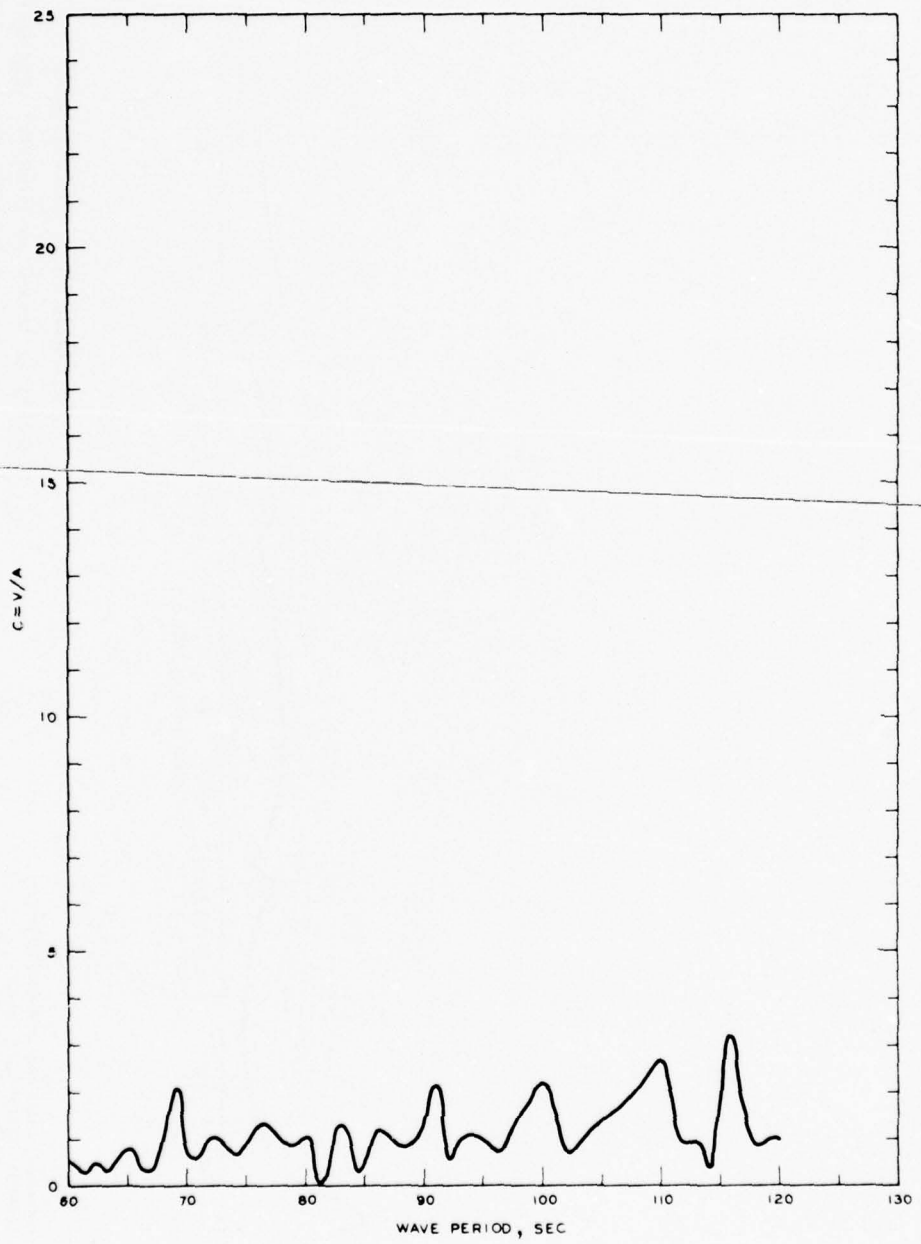

NOTE: C = NORMALIZED MAXIMUM CURRENT VELOCITY
V = CURRENT VELOCITY, FT/SEC
A = INCIDENT WAVE AMPLITUDE

FREQUENCY RESPONSE

NORMALIZED MAXIMUM CURRENT VELOCITY
STA LA-10, GRID 1A

PLATE 144

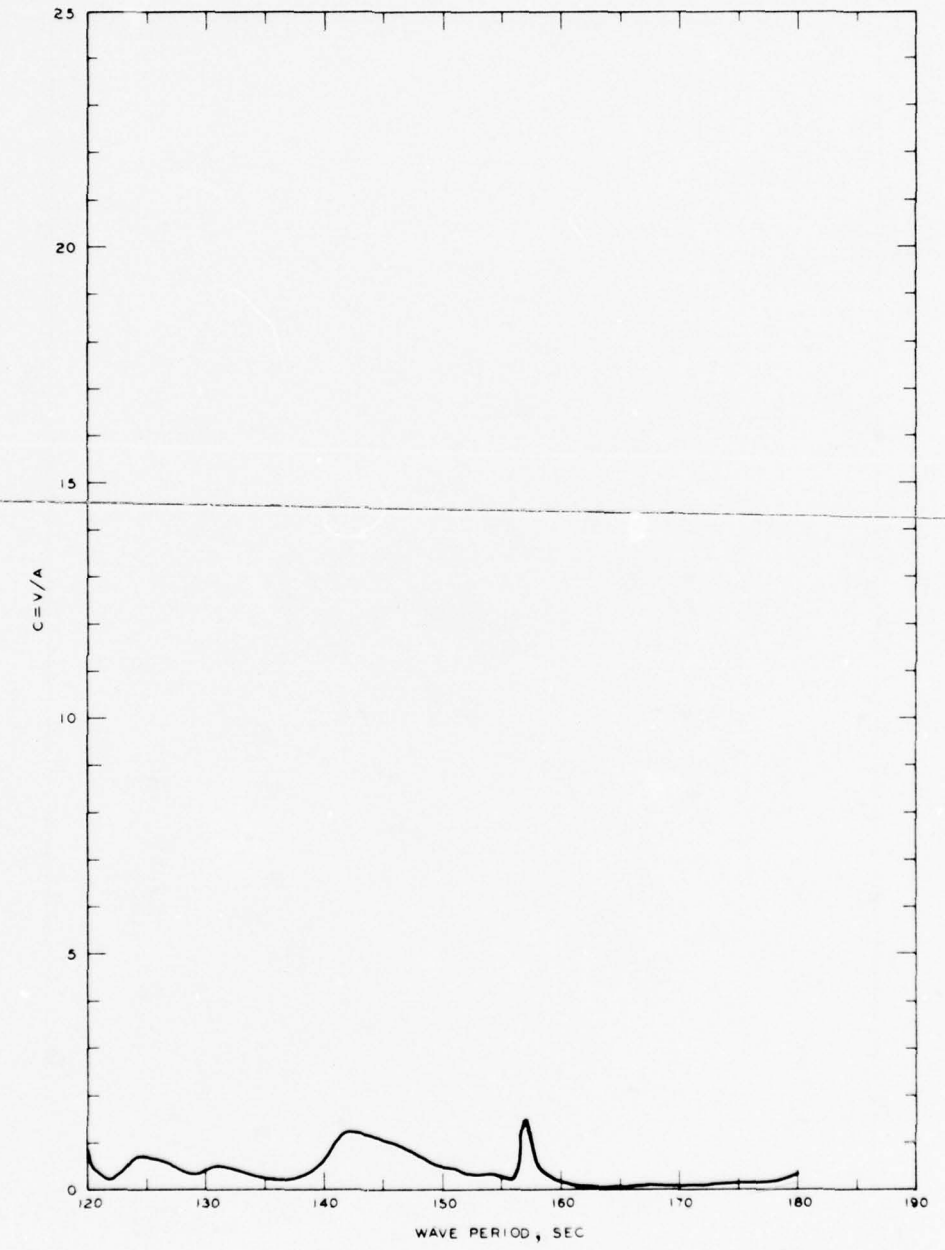

NOTE: C = NORMALIZED MAXIMUM CURRENT VELOCITY
V = CURRENT VELOCITY, FT/SEC
A = INCIDENT WAVE AMPLITUDE

FREQUENCY RESPONSE

NORMALIZED MAXIMUM CURRENT VELOCITY
STA LA-10, GRID 2A

PLATE 145

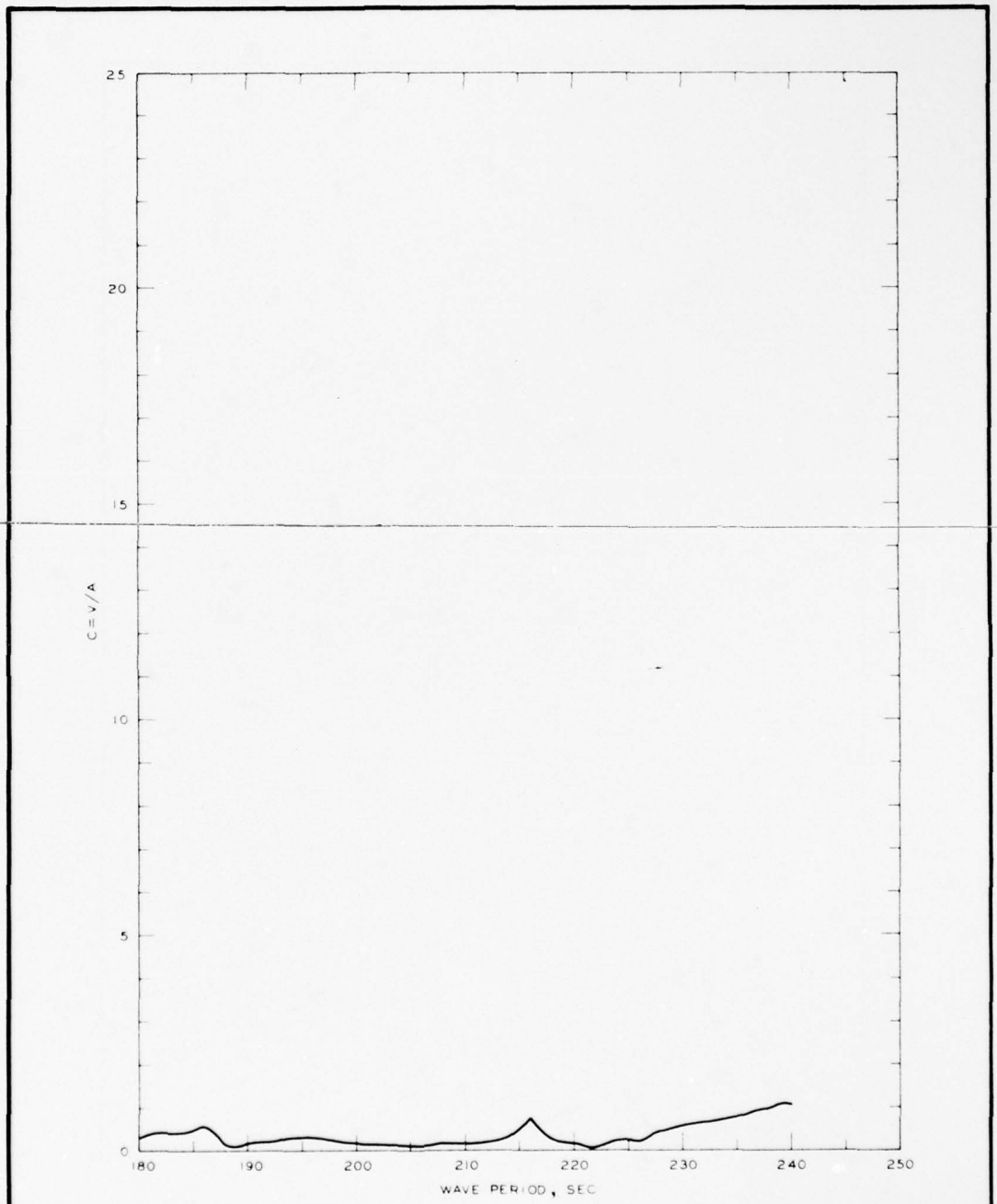

NOTE C = NORMALIZED MAXIMUM CURRENT VELOCITY
V = CURRENT VELOCITY, FT/SEC
A = INCIDENT WAVE AMPLITUDE

FREQUENCY RESPONSE

NORMALIZED MAXIMUM CURRENT VELOCITY
STA LA-10, GRID 3A

PLATE 146

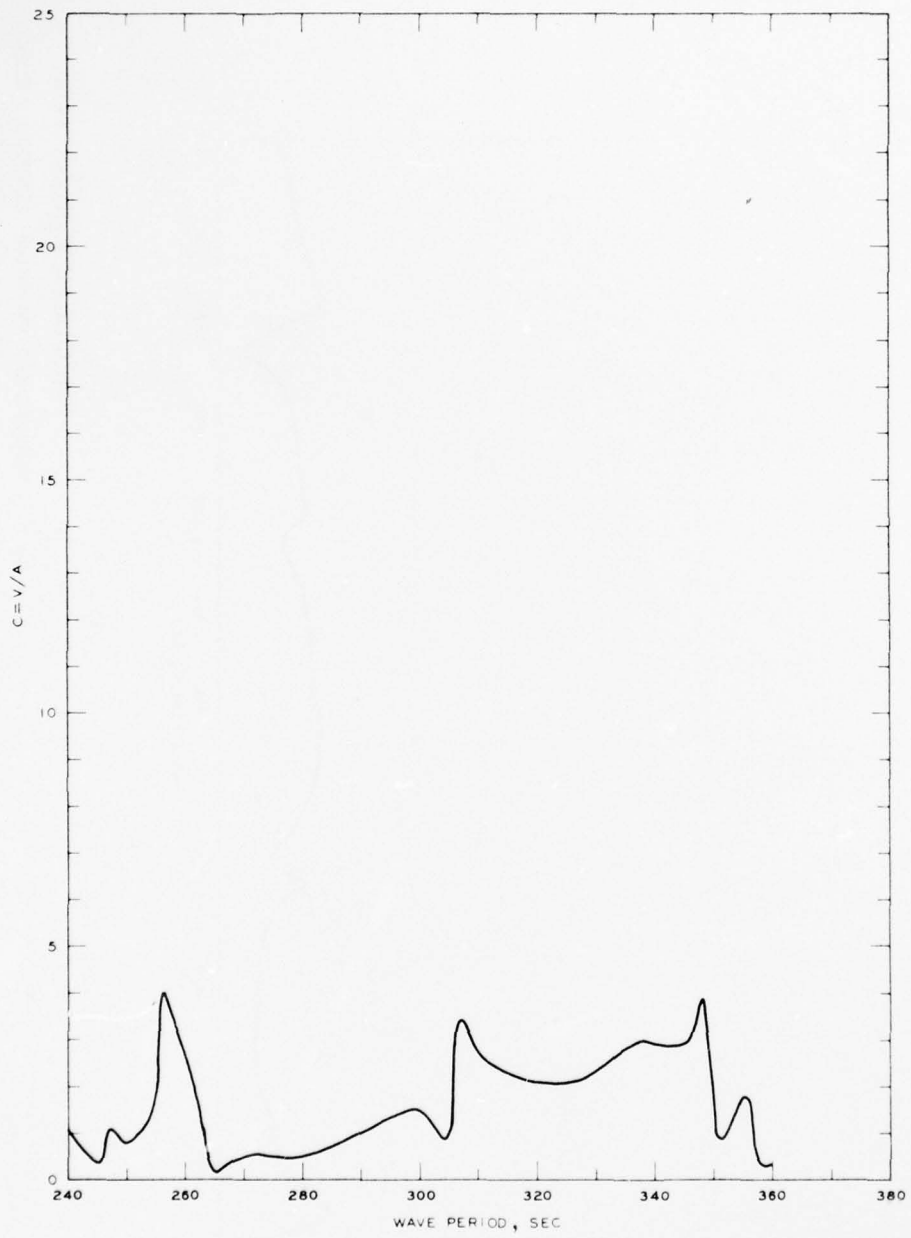

NOTE C = NORMALIZED MAXIMUM CURRENT VELOCITY
V = CURRENT VELOCITY, FT/SEC
A = INCIDENT WAVE AMPLITUDE

FREQUENCY RESPONSE

NORMALIZED MAXIMUM CURRENT VELOCITY
STA LA-10, GRID 4A

PLATE 147

PLATE 148

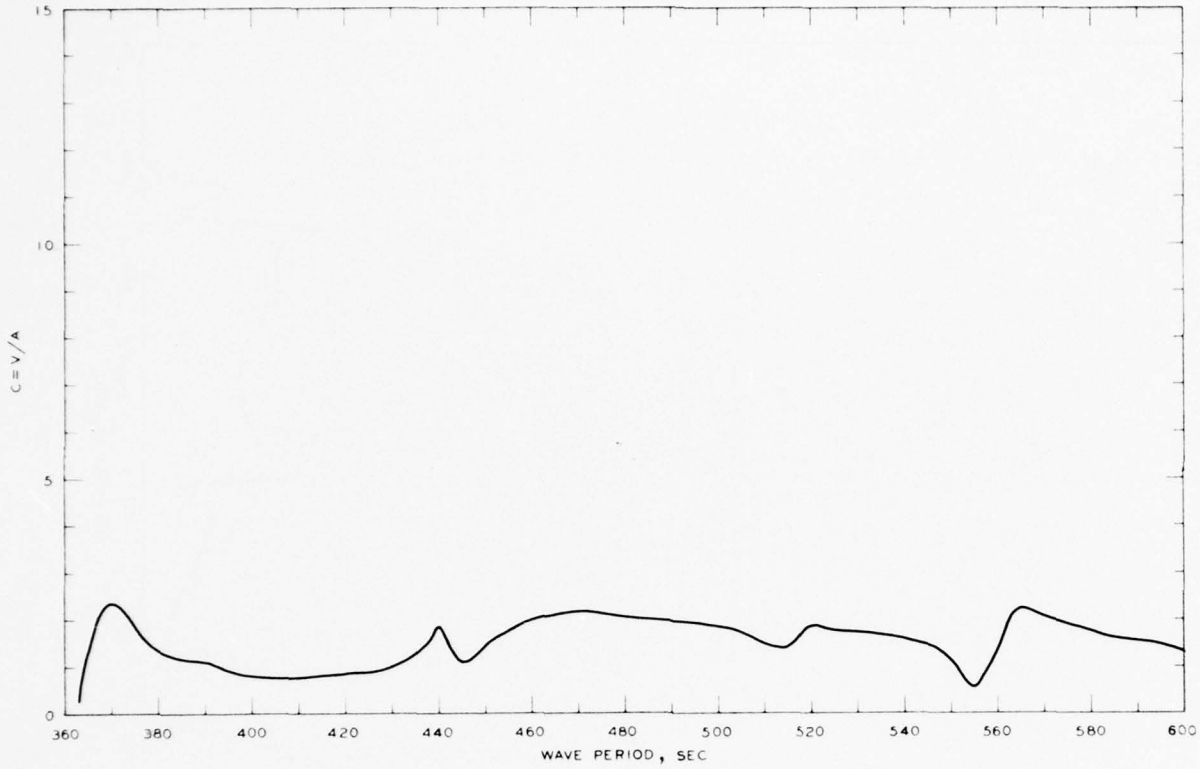

NOTE: C = NORMALIZED MAXIMUM CURRENT VELOCITY
V = CURRENT VELOCITY, FT / SEC
A = INCIDENT WAVE AMPLITUDE

FREQUENCY RESPONSE

NORMALIZED MAXIMUM CURRENT VELOCITY
STA LA-10, GRID 5A

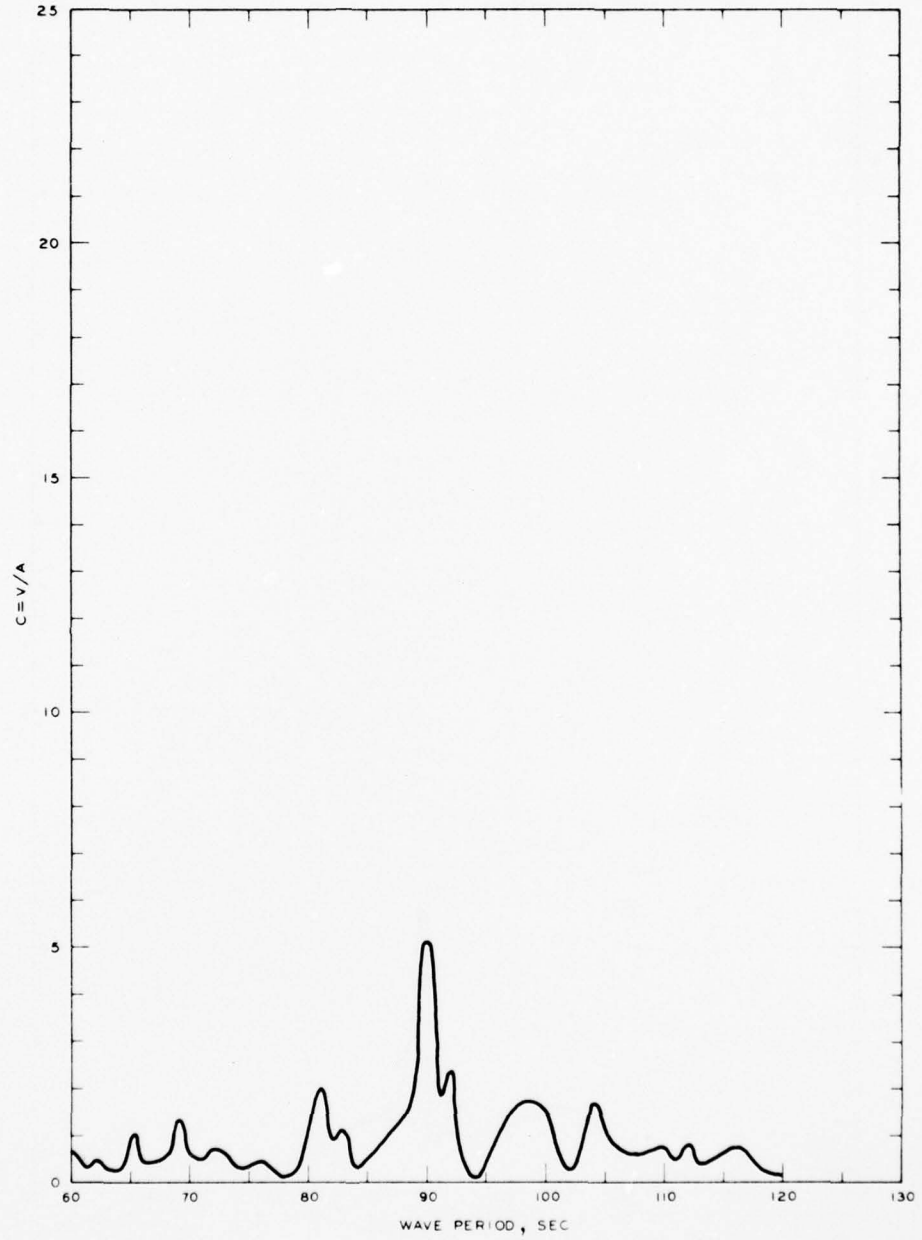

NOTE C = NORMALIZED MAXIMUM CURRENT VELOCITY
V = CURRENT VELOCITY, FT/SEC
A = INCIDENT WAVE AMPLITUDE

FREQUENCY RESPONSE

NORMALIZED MAXIMUM CURRENT VELOCITY
STA LA-11, GRID 1A

PLATE 149

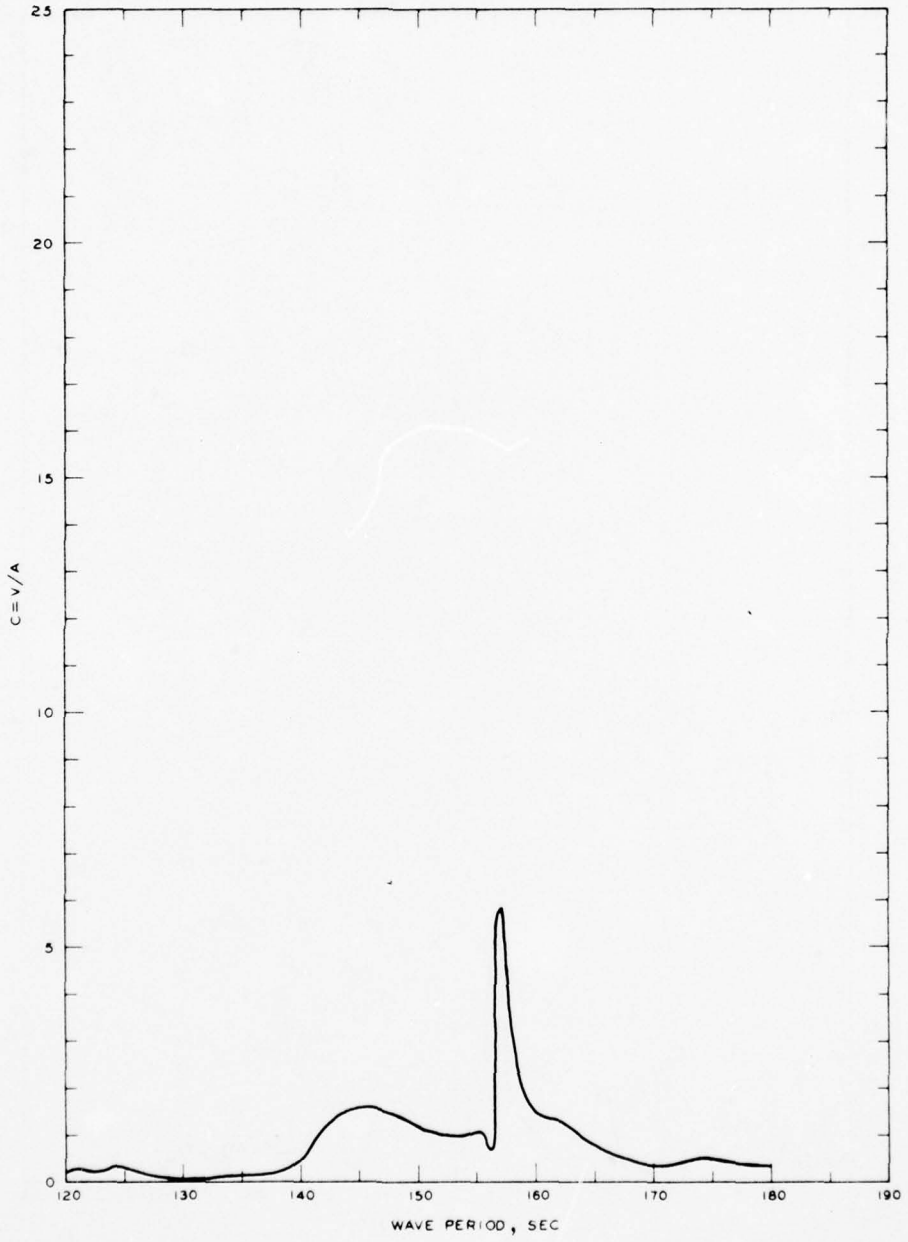

NOTE: C = NORMALIZED MAXIMUM CURRENT VELOCITY
V = CURRENT VELOCITY, FT/SEC
A = INCIDENT WAVE AMPLITUDE

FREQUENCY RESPONSE

NORMALIZED MAXIMUM CURRENT VELOCITY
STA LA-11, GRID 2A

PLATE 150

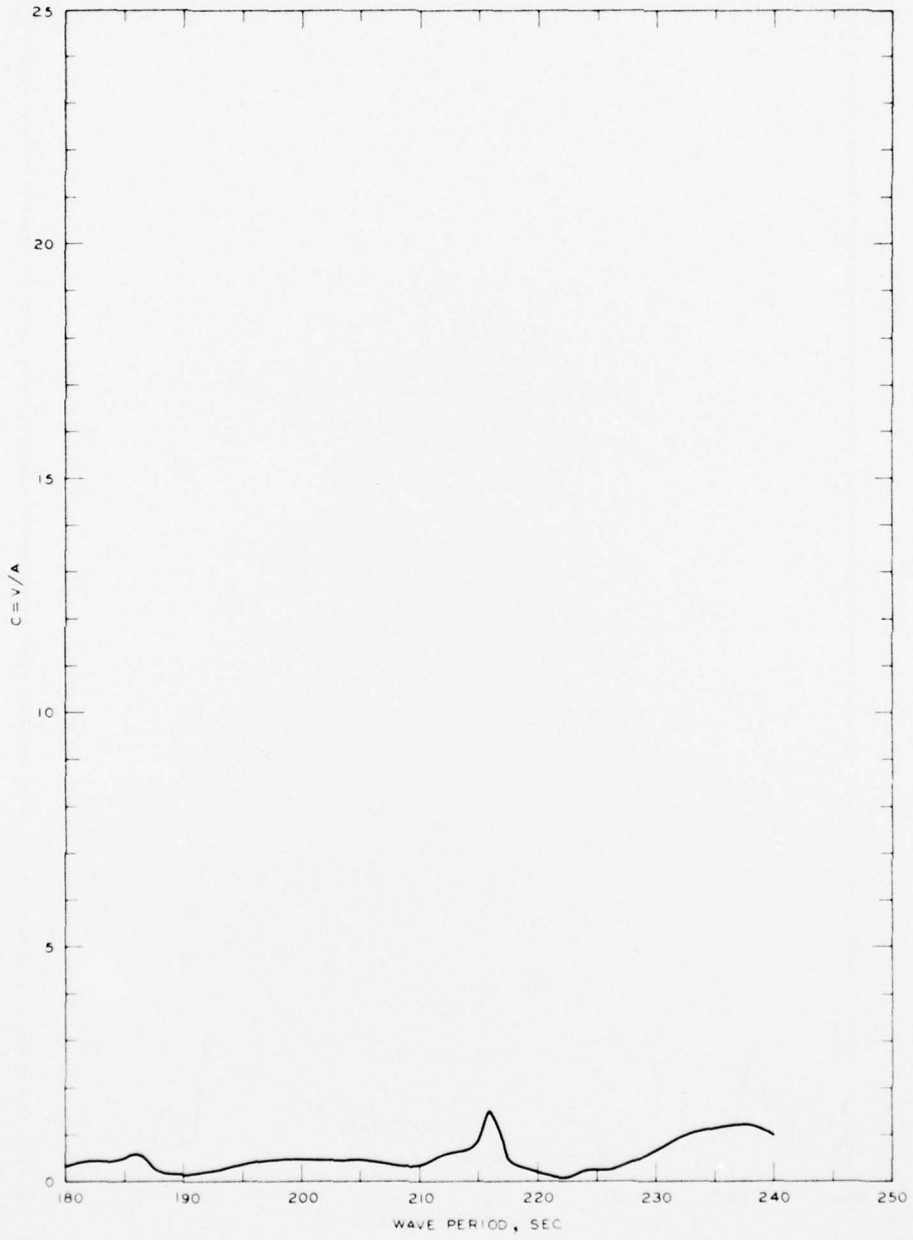

NOTE C = NORMALIZED MAXIMUM CURRENT VELOCITY
V = CURRENT VELOCITY, FT/SEC
A = INCIDENT WAVE AMPLITUDE

FREQUENCY RESPONSE

NORMALIZED MAXIMUM CURRENT VELOCITY
STA LA-11, GRID 3A

PLATE 151

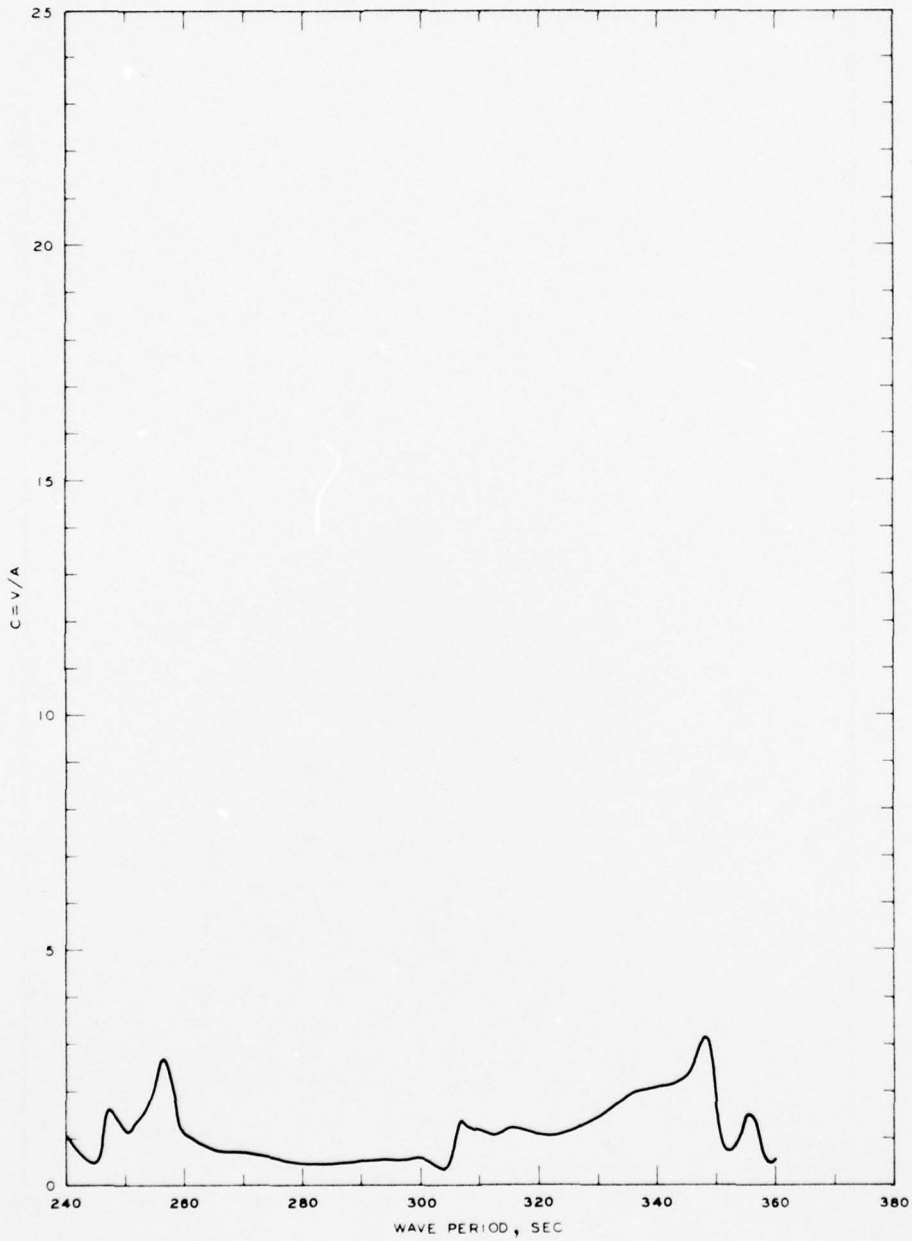

NOTE C = NORMALIZED MAXIMUM CURRENT VELOCITY
V = CURRENT VELOCITY, FT/SEC
A = INCIDENT WAVE AMPLITUDE

FREQUENCY RESPONSE

NORMALIZED MAXIMUM CURRENT VELOCITY
STA LA-11, GRID 4A

PLATE 152

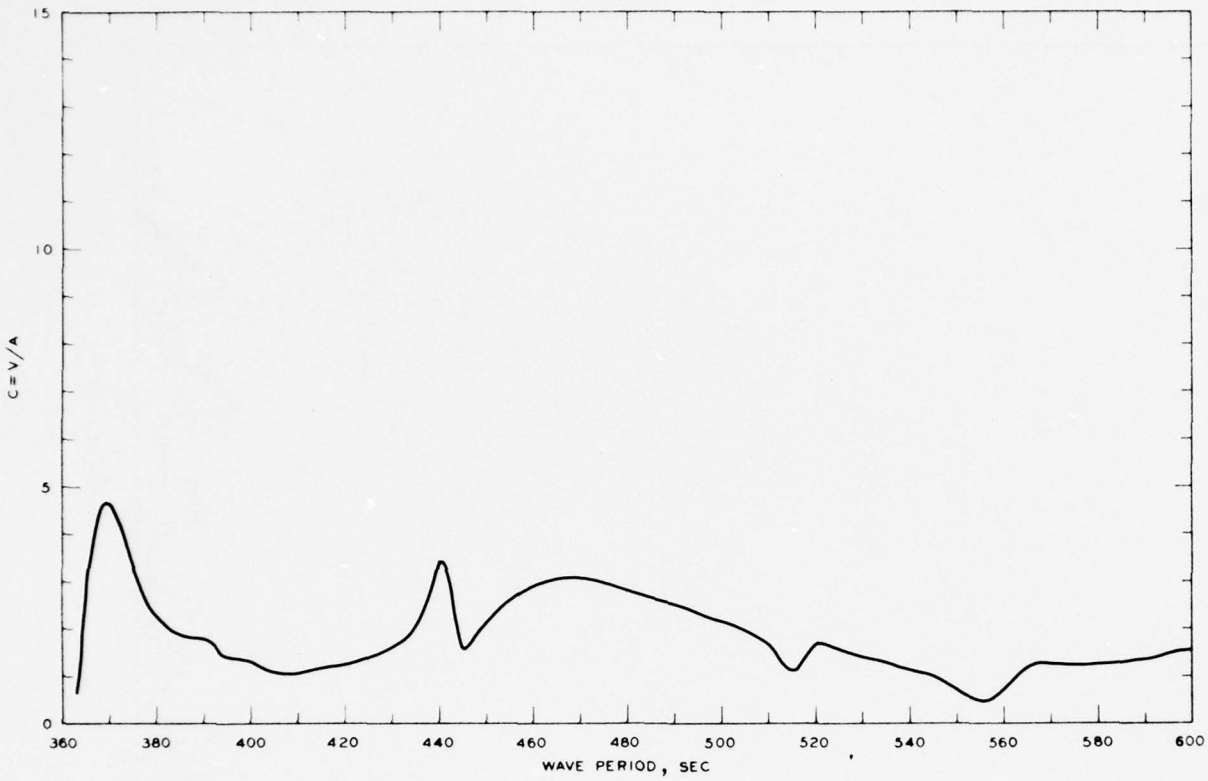

NOTE: C = NORMALIZED MAXIMUM CURRENT VELOCITY
V = CURRENT VELOCITY, FT/SEC
A = INCIDENT WAVE AMPLITUDE

FREQUENCY RESPONSE

NORMALIZED MAXIMUM CURRENT VELOCITY
STA LA-11, GRID 5A

PLATE 153

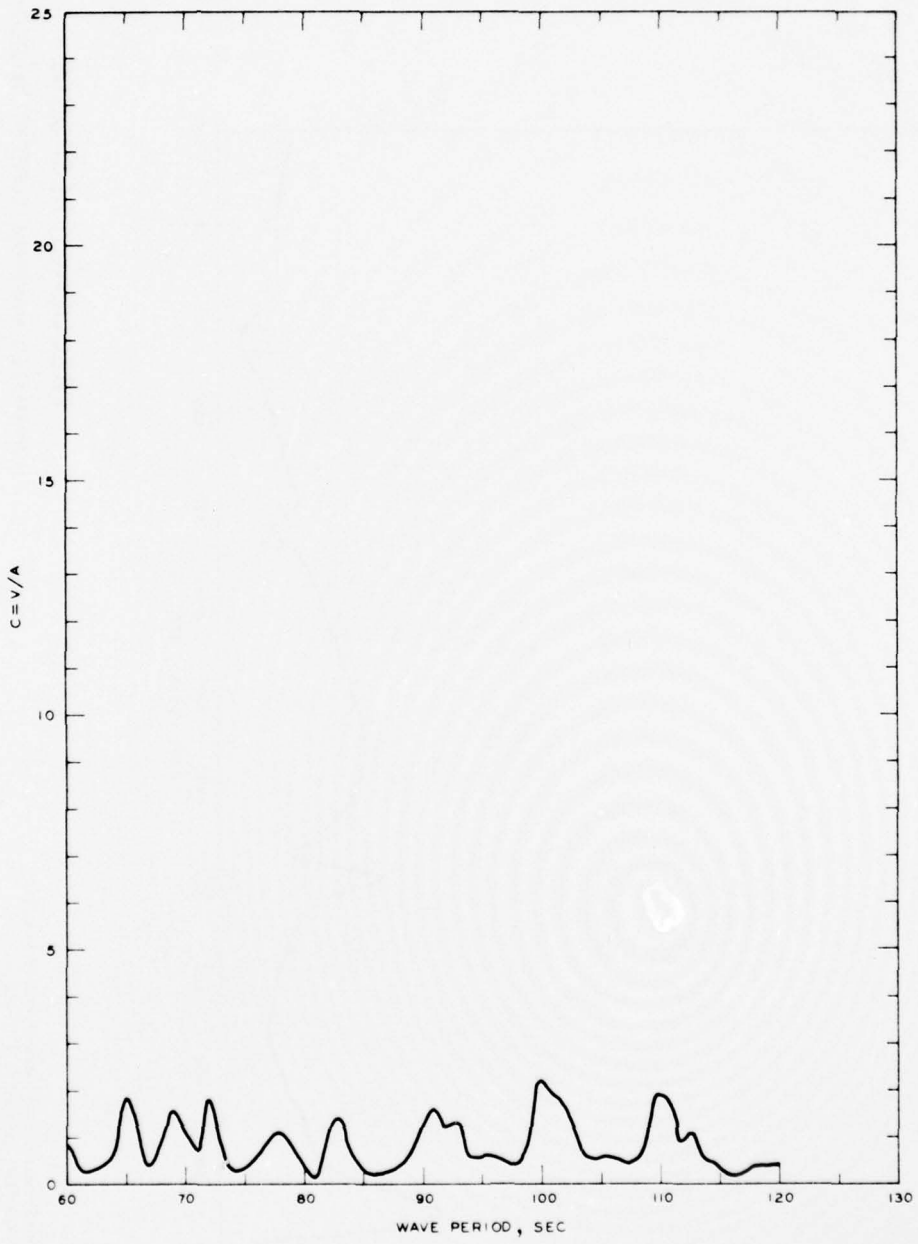

NOTE C = NORMALIZED MAXIMUM CURRENT VELOCITY
V = CURRENT VELOCITY, FT/SEC
A = INCIDENT WAVE AMPLITUDE

FREQUENCY RESPONSE

NORMALIZED MAXIMUM CURRENT VELOCITY
STA LA-12, GRID 1A

PLATE 154

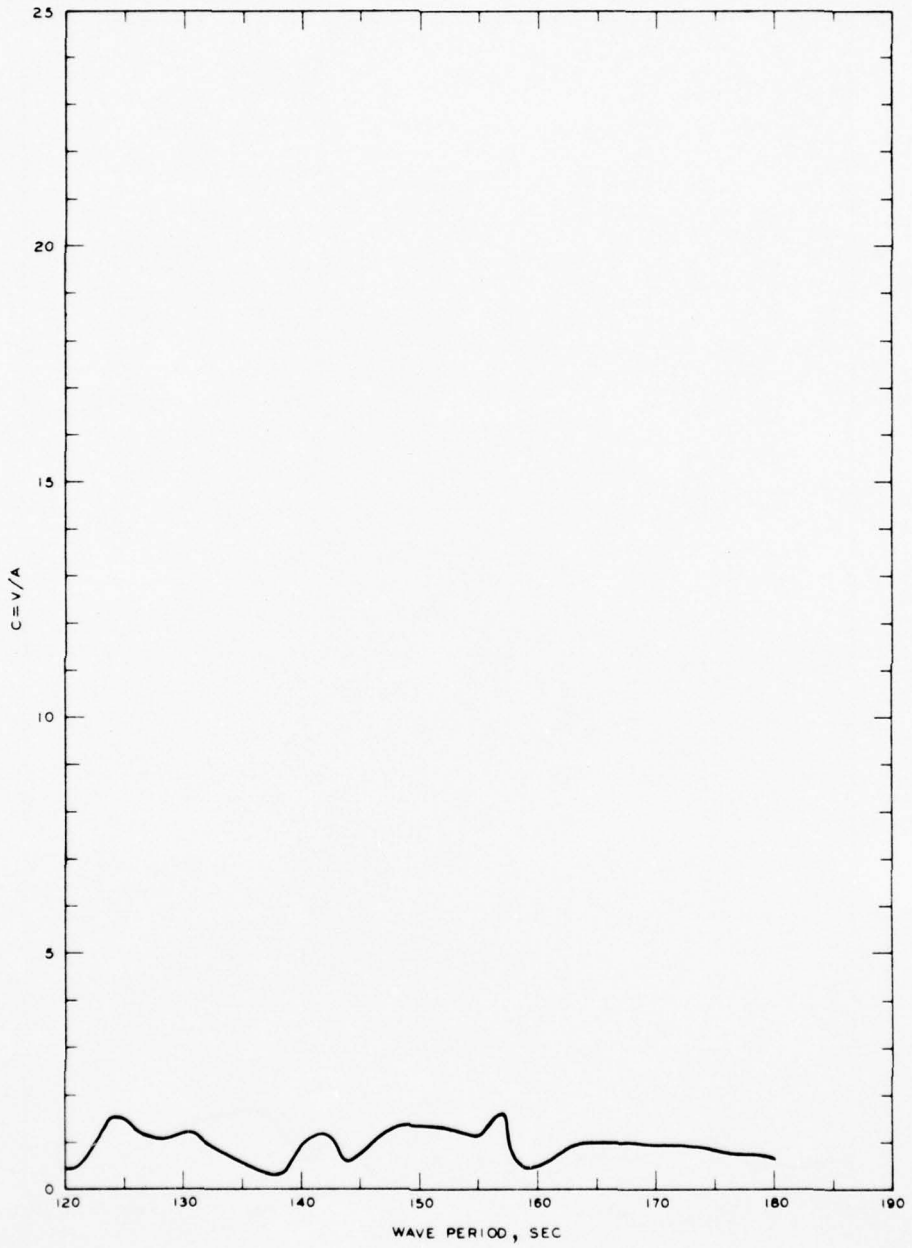

NOTE: C = NORMALIZED MAXIMUM CURRENT VELOCITY
V = CURRENT VELOCITY, FT/SEC
A = INCIDENT WAVE AMPLITUDE

FREQUENCY RESPONSE

NORMALIZED MAXIMUM CURRENT VELOCITY
STA LA-12, GRID 2A

PLATE 155

NOTE C = NORMALIZED MAXIMUM CURRENT VELOCITY
V = CURRENT VELOCITY, FT/SEC
A = INCIDENT WAVE AMPLITUDE

FREQUENCY RESPONSE

NORMALIZED MAXIMUM CURRENT VELOCITY
STA LA-12, GRID 3A

PLATE 156

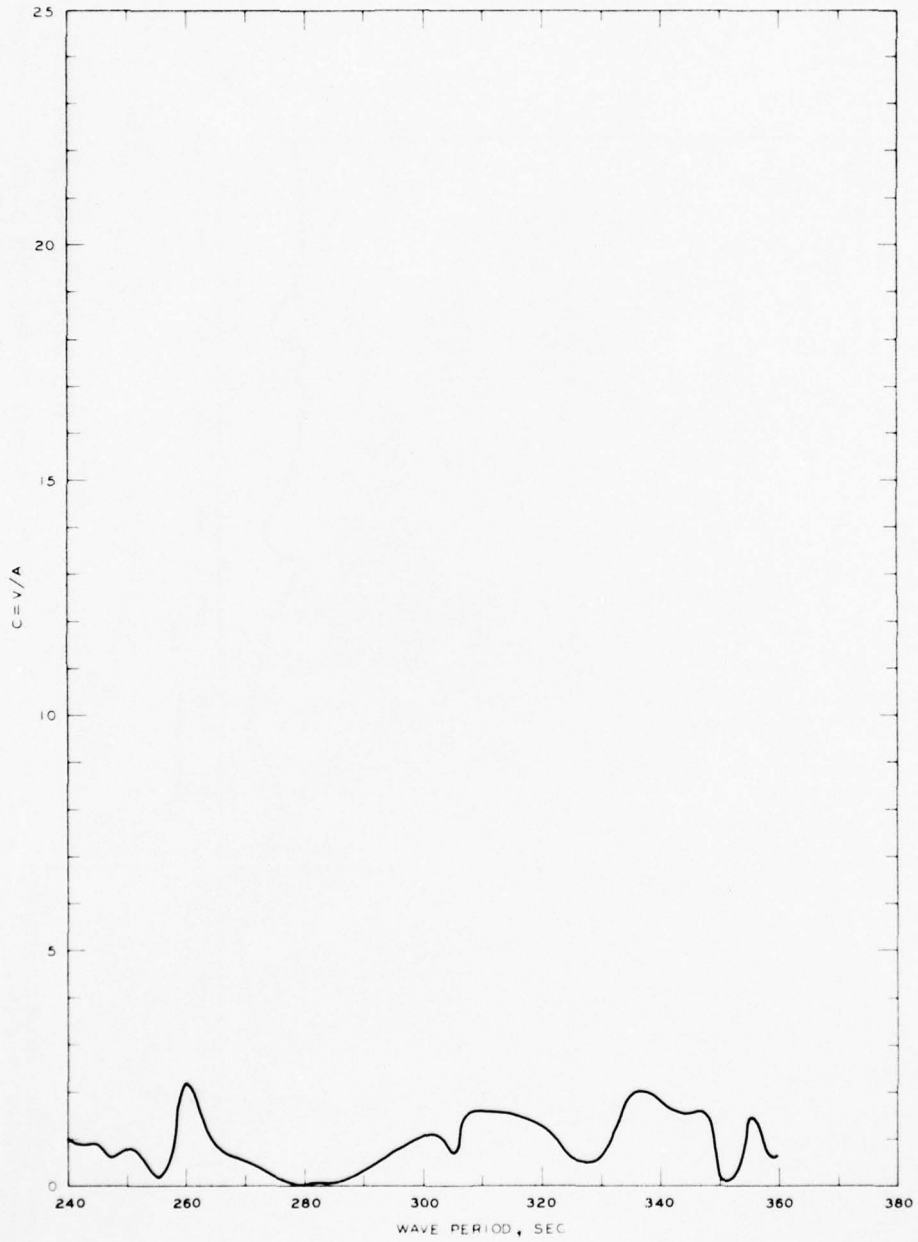

NOTE C = NORMALIZED MAXIMUM CURRENT VELOCITY
V = CURRENT VELOCITY, FT/SEC
A = INCIDENT WAVE AMPLITUDE

FREQUENCY RESPONSE

NORMALIZED MAXIMUM CURRENT VELOCITY
STA LA-12, GRID 4A

PLATE 157

PLATE 158

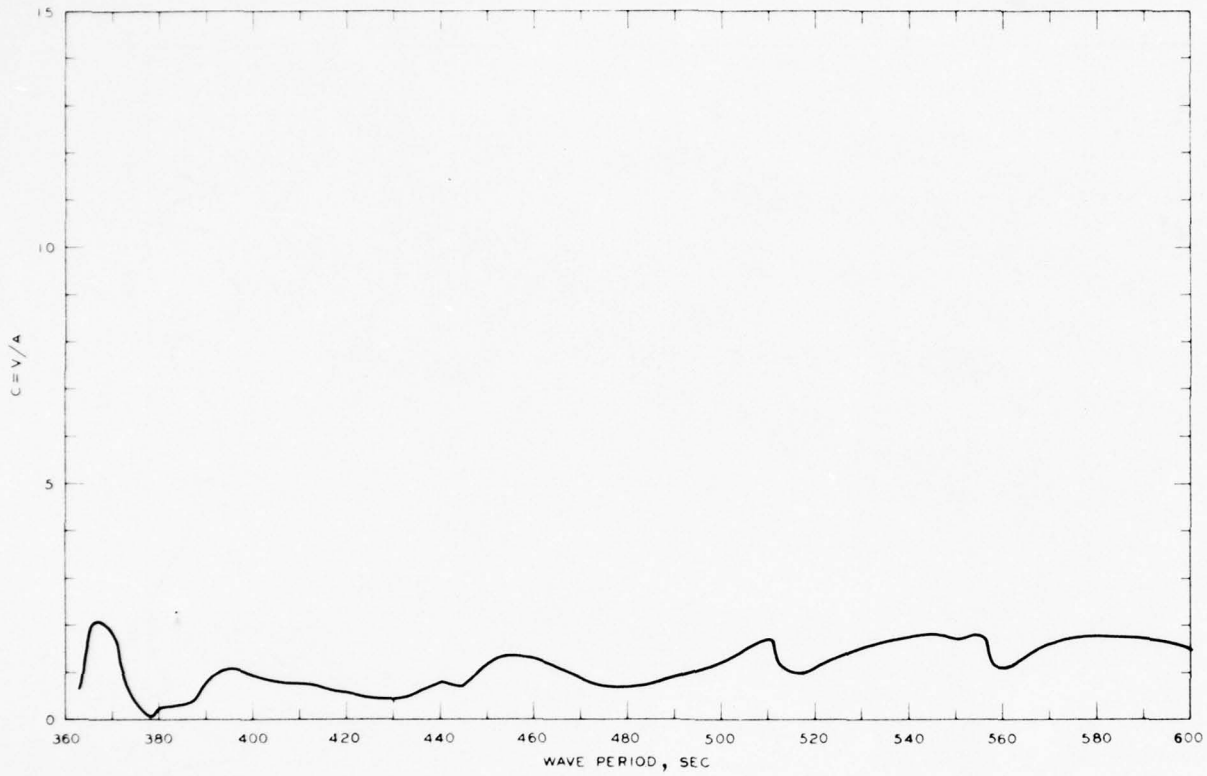

NOTE: C = NORMALIZED MAXIMUM CURRENT VELOCITY
V = CURRENT VELOCITY, FT/SEC
A = INCIDENT WAVE AMPLITUDE

FREQUENCY RESPONSE

NORMALIZED MAXIMUM CURRENT VELOCITY
STA LA-12, GRID 5A

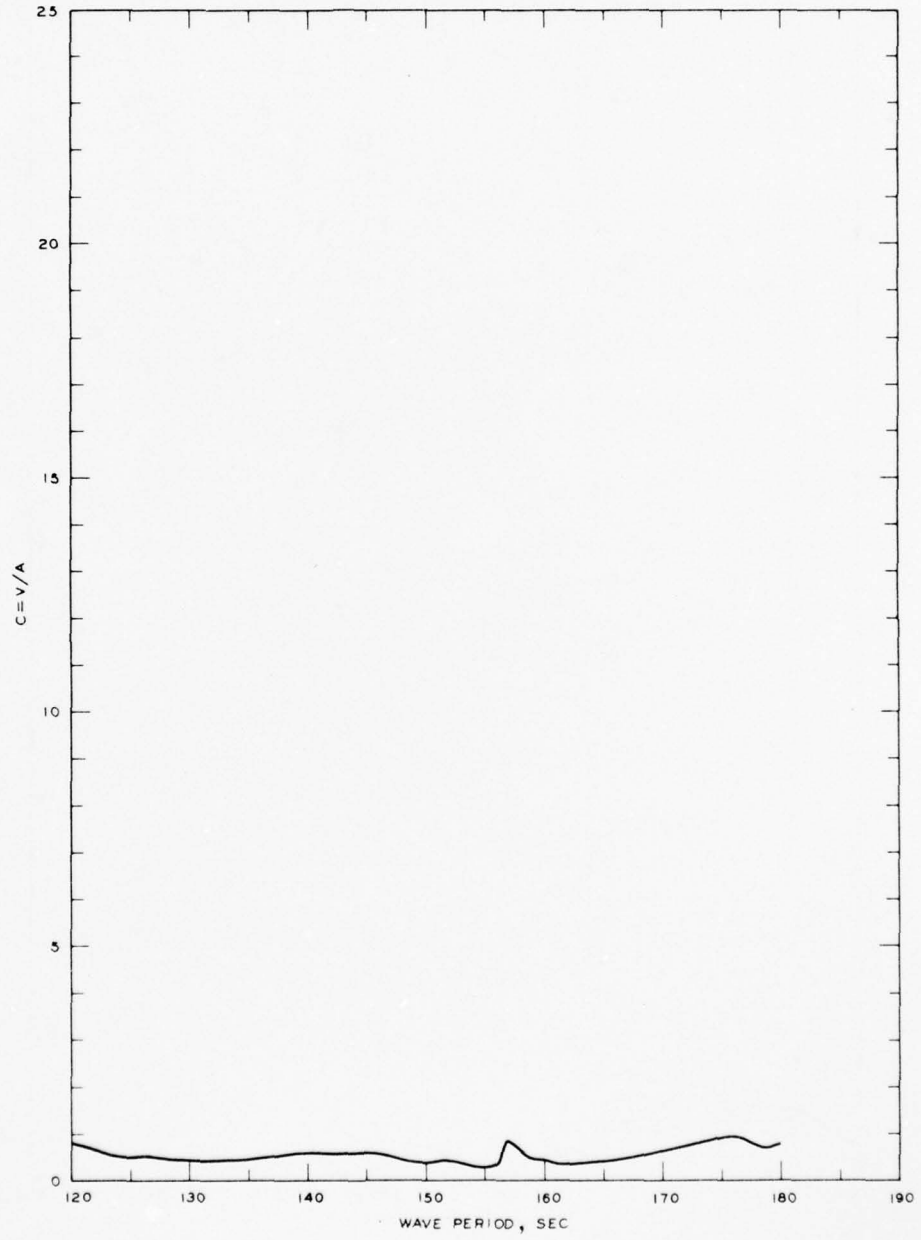

NOTE: C = NORMALIZED MAXIMUM CURRENT VELOCITY
V = CURRENT VELOCITY, FT/SEC
A = INCIDENT WAVE AMPLITUDE

FREQUENCY RESPONSE

NORMALIZED MAXIMUM CURRENT VELOCITY
STA LA-13, GRID 2A

PLATE 159

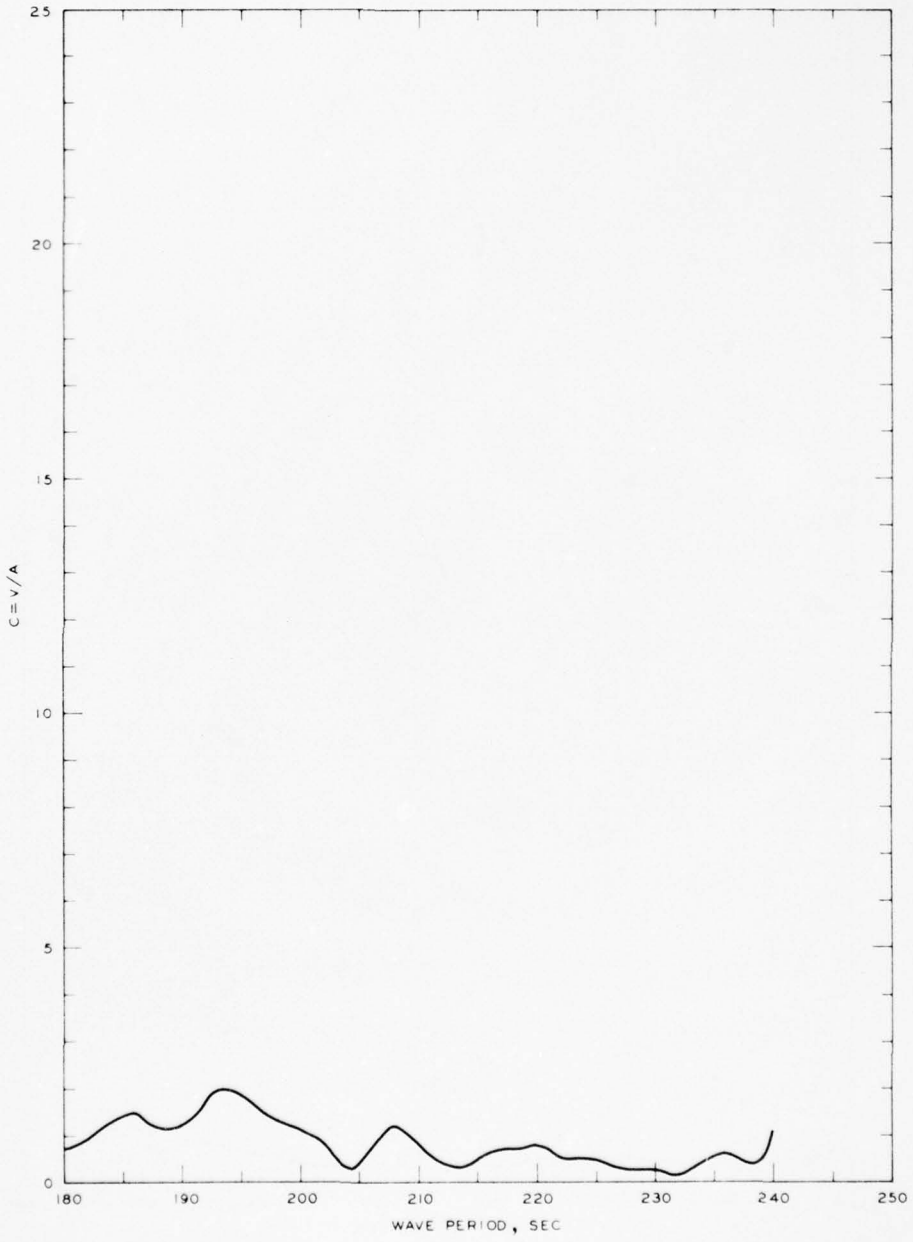

NOTE: C = NORMALIZED MAXIMUM CURRENT VELOCITY
V = CURRENT VELOCITY, FT/SEC
A = INCIDENT WAVE AMPLITUDE

FREQUENCY RESPONSE

NORMALIZED MAXIMUM CURRENT VELOCITY
STA LA-13, GRID 3A

PLATE 160

AD-A037 155 ARMY ENGINEER WATERWAYS EXPERIMENT STATION VICKSBURG MISS F/G 20/4
LOS ANGELES HARBOR NUMERICAL ANALYSIS OF HARBOR OSCILLATIONS.(U)
FEB 77 J R HOUSTON

UNCLASSIFIED WES-MP-H-77-2 NL

3 OF 3
AD
A037155

END

DATE
FILMED
4-77

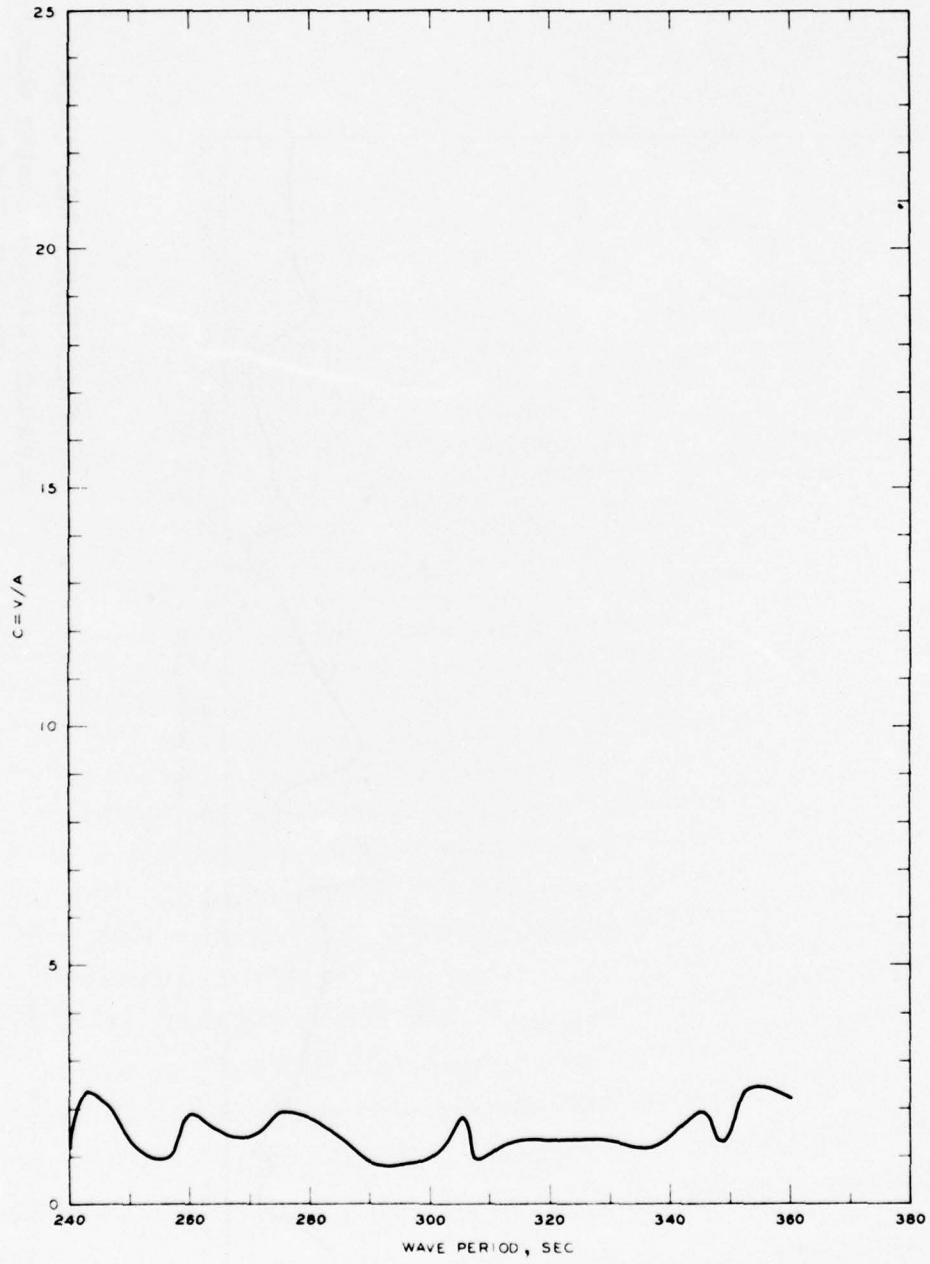

NOTE C = NORMALIZED MAXIMUM CURRENT VELOCITY
V = CURRENT VELOCITY, FT/SEC
A = INCIDENT WAVE AMPLITUDE

FREQUENCY RESPONSE

NORMALIZED MAXIMUM CURRENT VELOCITY
STA LA-13, GRID 4A

PLATE 161

PLATE 162

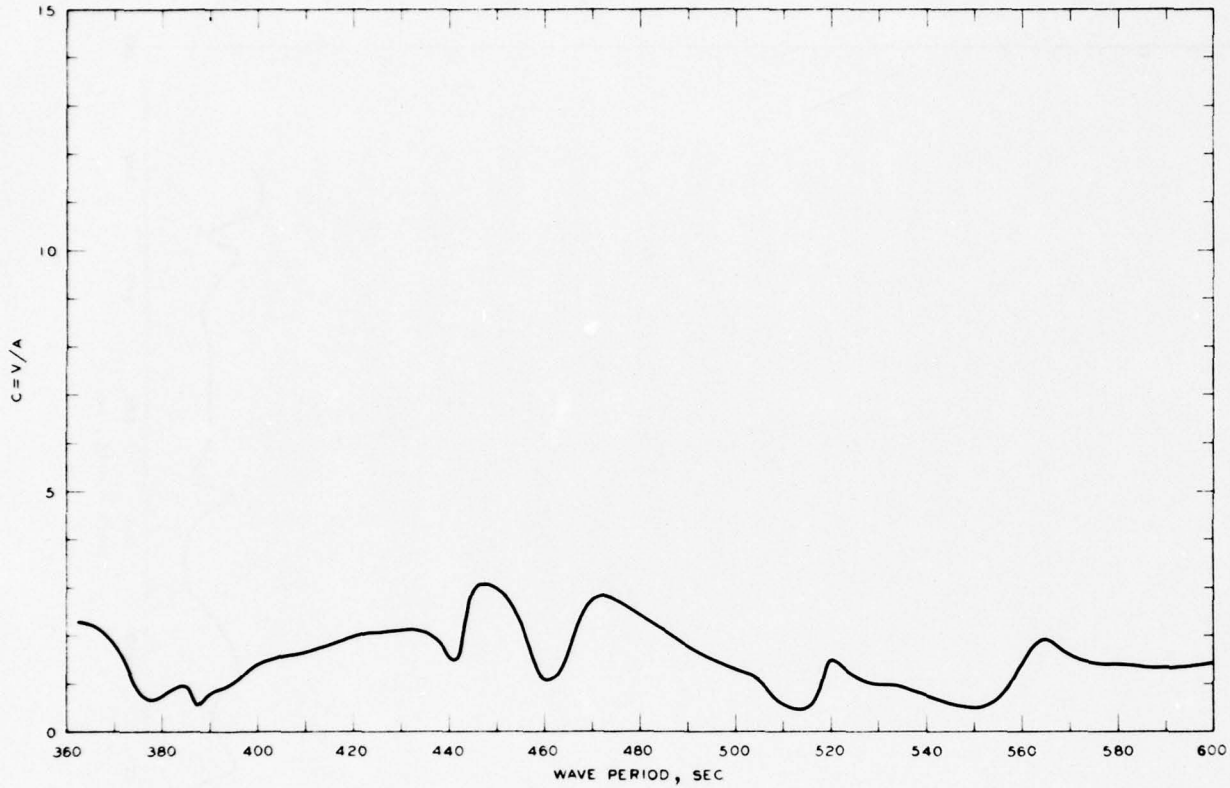

NOTE C = NORMALIZED MAXIMUM CURRENT VELOCITY
V = CURRENT VELOCITY, FT/SEC
A = INCIDENT WAVE AMPLITUDE

FREQUENCY RESPONSE

NORMALIZED MAXIMUM CURRENT VELOCITY
STA LA-13, GRID 5A

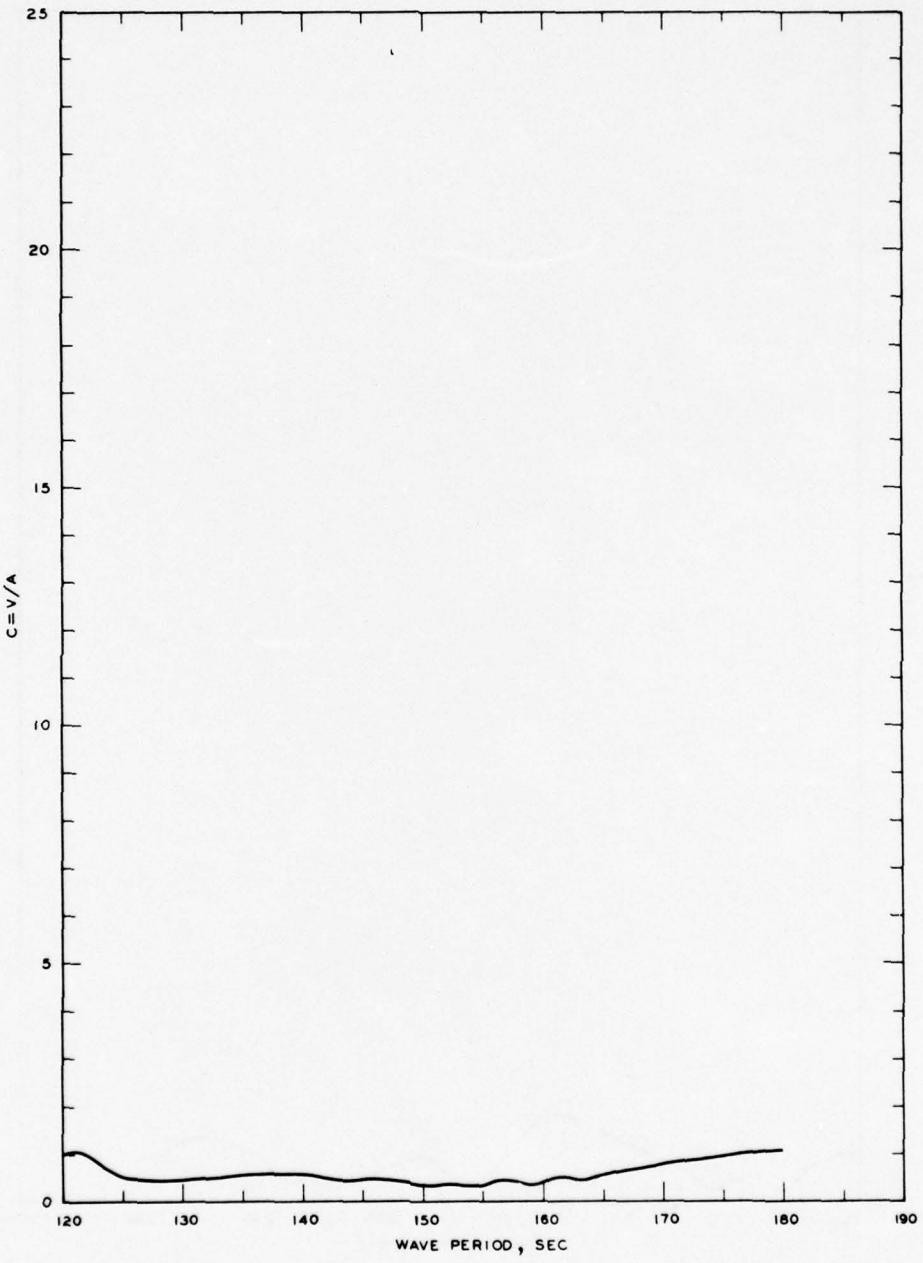

NOTE: C = NORMALIZED MAXIMUM CURRENT VELOCITY
V = CURRENT VELOCITY, FT/SEC
A = INCIDENT WAVE AMPLITUDE

FREQUENCY RESPONSE

NORMALIZED MAXIMUM CURRENT VELOCITY
STA LA-14, GRID 2A

PLATE 163

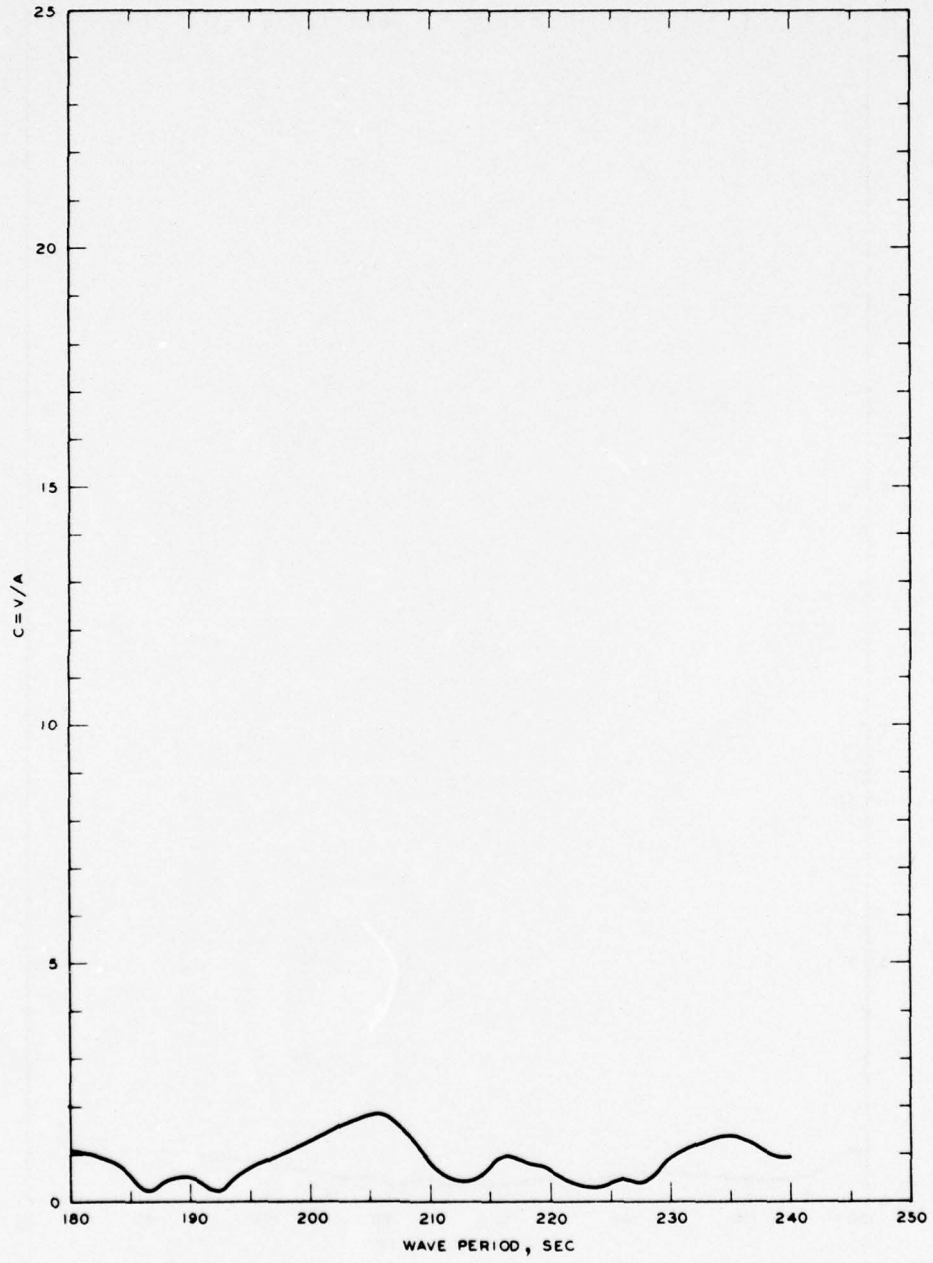

NOTE: C = NORMALIZED MAXIMUM CURRENT VELOCITY
V = CURRENT VELOCITY, FT/SEC
A = INCIDENT WAVE AMPLITUDE

FREQUENCY RESPONSE

NORMALIZED MAXIMUM CURRENT VELOCITY
STA LA-14, GRID 3A

PLATE 164

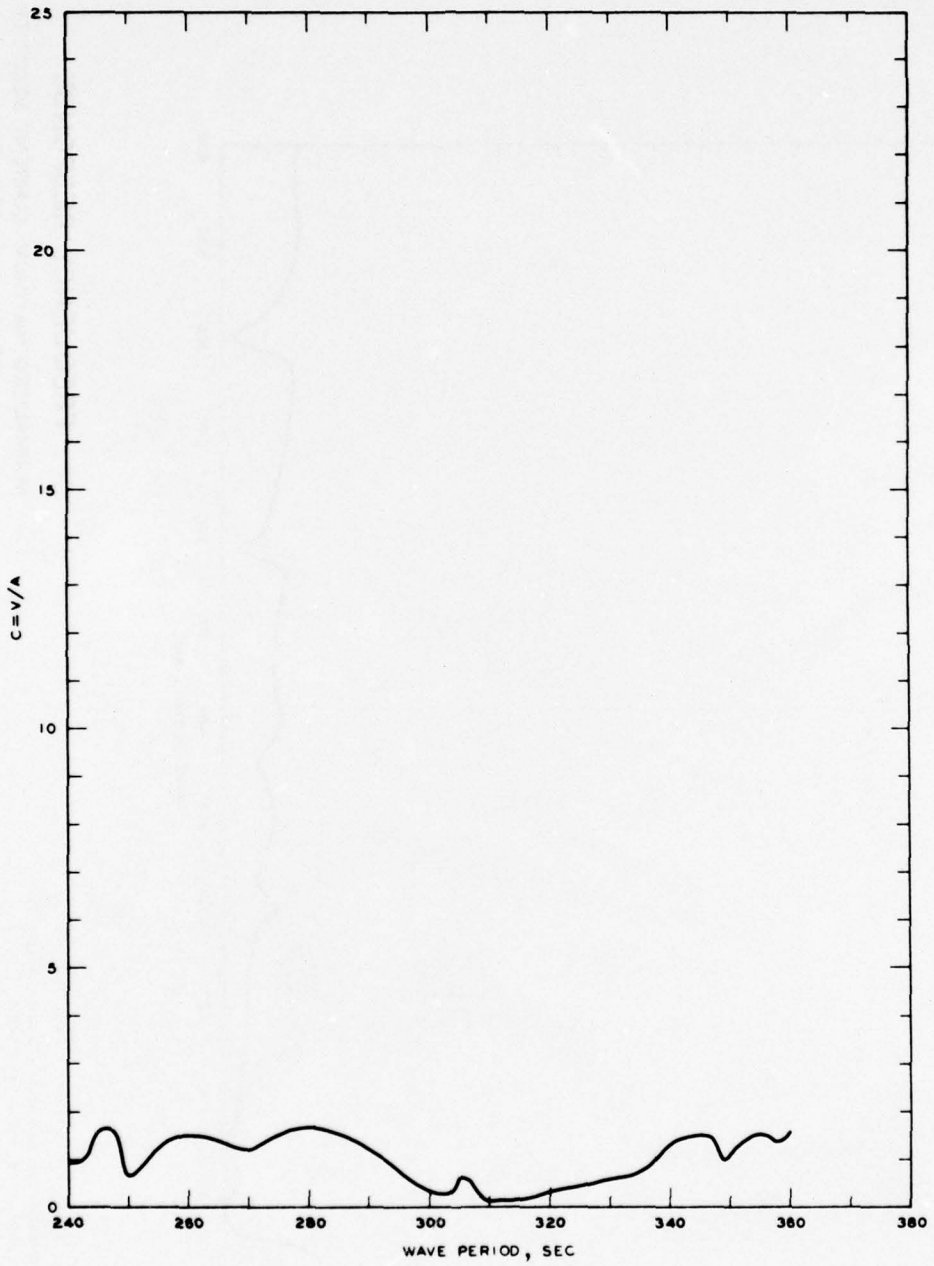

NOTE: C = NORMALIZED MAXIMUM CURRENT VELOCITY
V = CURRENT VELOCITY, FT/SEC
A = INCIDENT WAVE AMPLITUDE

FREQUENCY RESPONSE

NORMALIZED MAXIMUM CURRENT VELOCITY
STA LA-14, GRID 4A

PLATE 165

PLATE 166

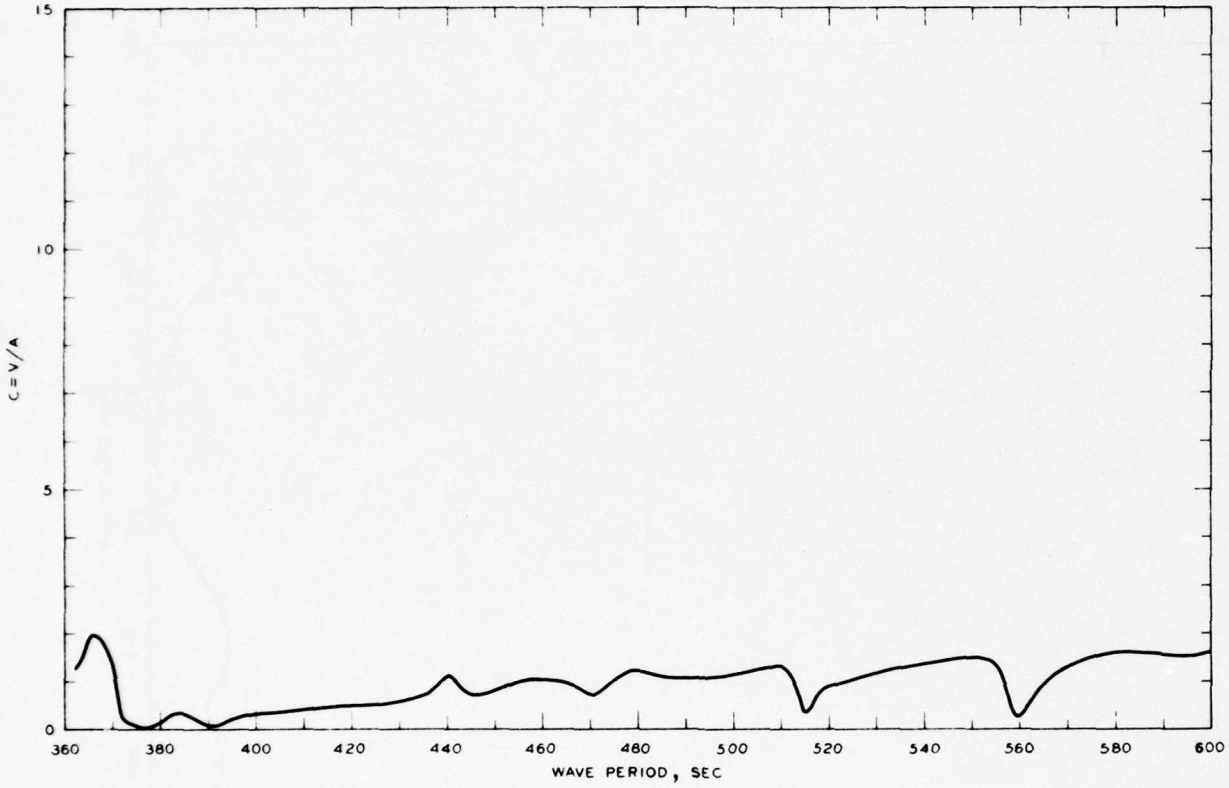

NOTE C = NORMALIZED MAXIMUM CURRENT VELOCITY
V = CURRENT VELOCITY, FT/SEC
A = INCIDENT WAVE AMPLITUDE

FREQUENCY RESPONSE

NORMALIZED MAXIMUM CURRENT VELOCITY
STA LA-14, GRID 5A

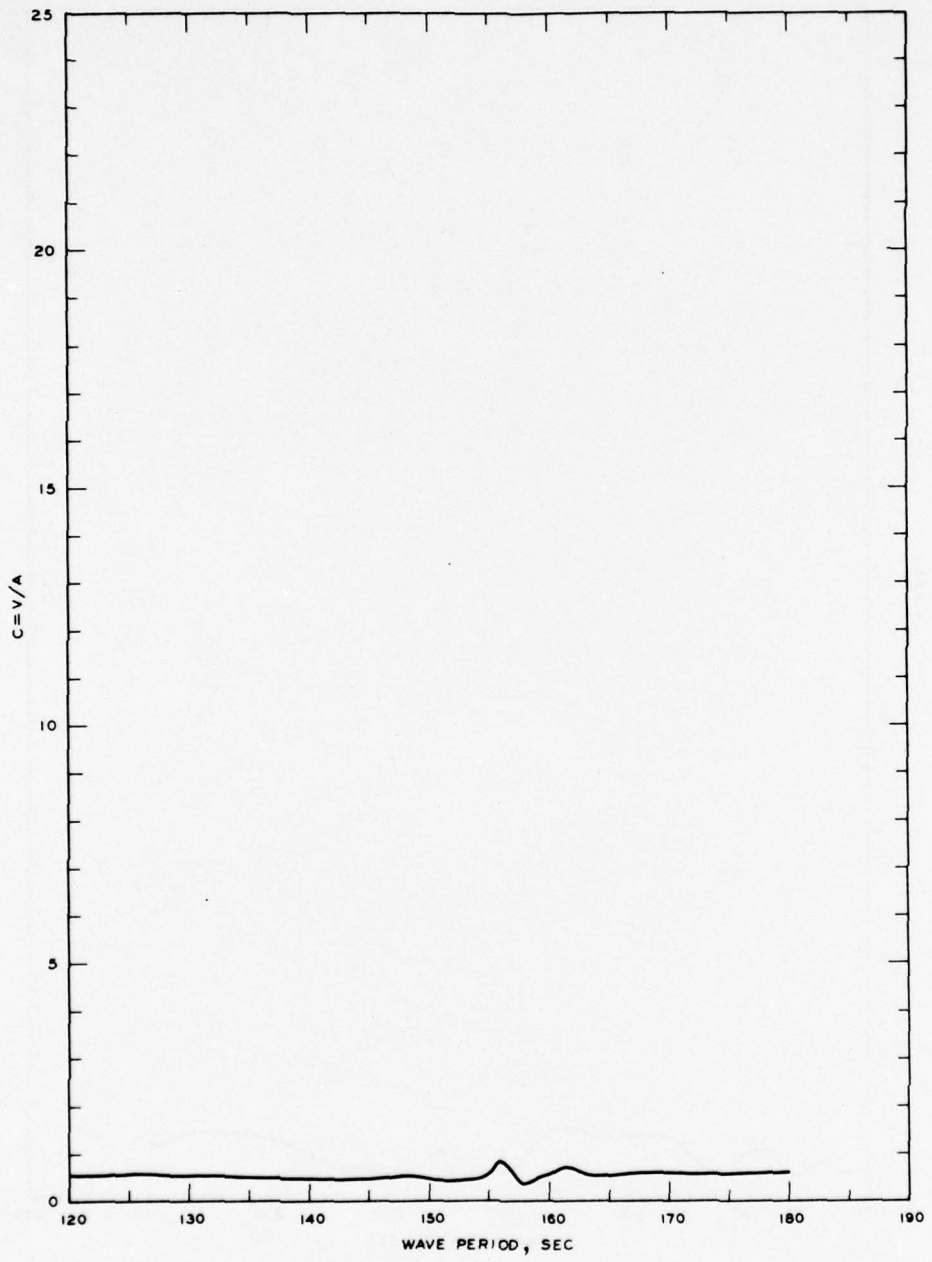

NOTE: C = NORMALIZED MAXIMUM CURRENT VELOCITY
V = CURRENT VELOCITY, FT/SEC
A = INCIDENT WAVE AMPLITUDE

FREQUENCY RESPONSE

NORMALIZED MAXIMUM CURRENT VELOCITY
STA LA-15, GRID 2A

PLATE 167

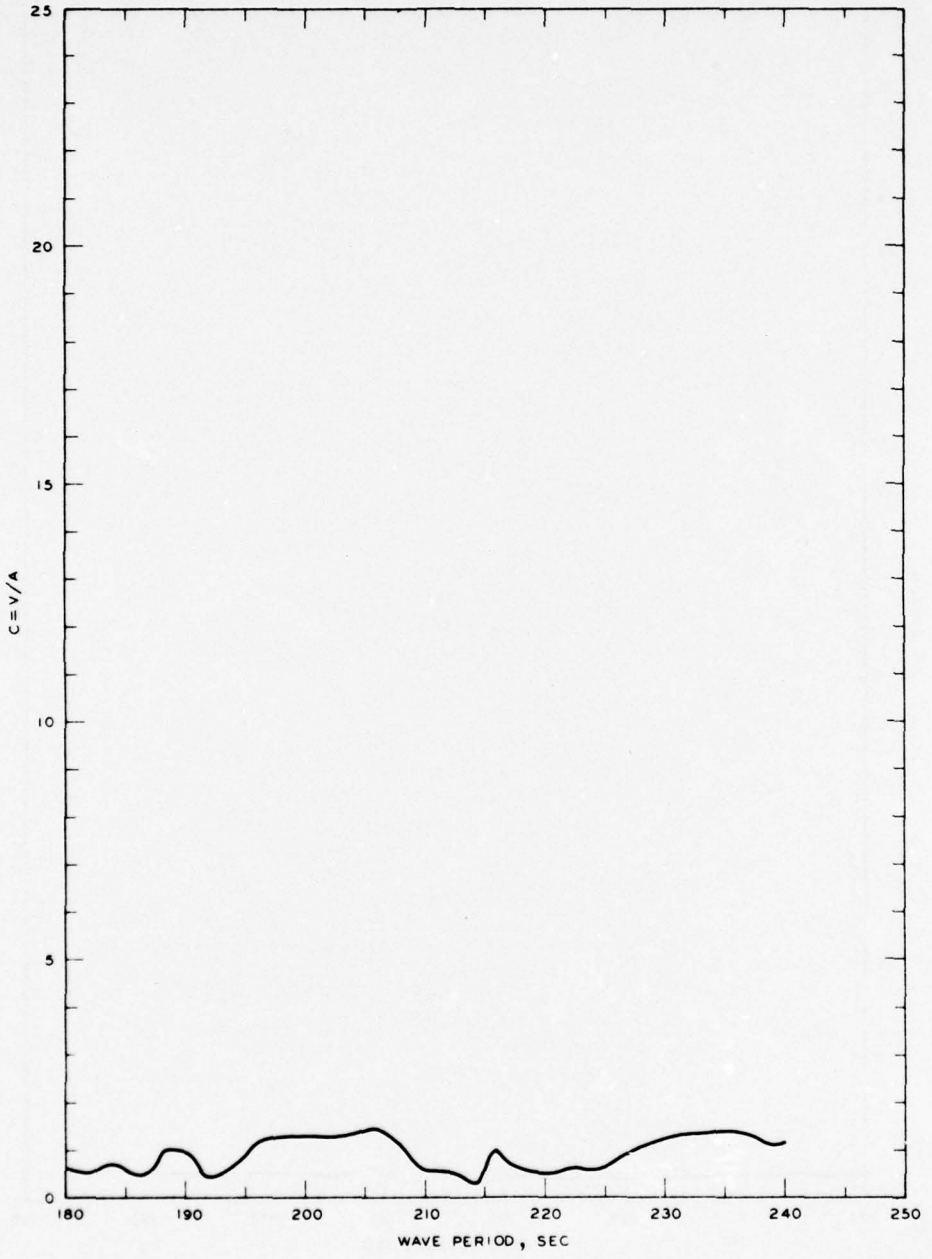

NOTE C = NORMALIZED MAXIMUM CURRENT VELOCITY
V = CURRENT VELOCITY, FT/SEC
A = INCIDENT WAVE AMPLITUDE

FREQUENCY RESPONSE

NORMALIZED MAXIMUM CURRENT VELOCITY
STA LA-15, GRID 3A

PLATE 168

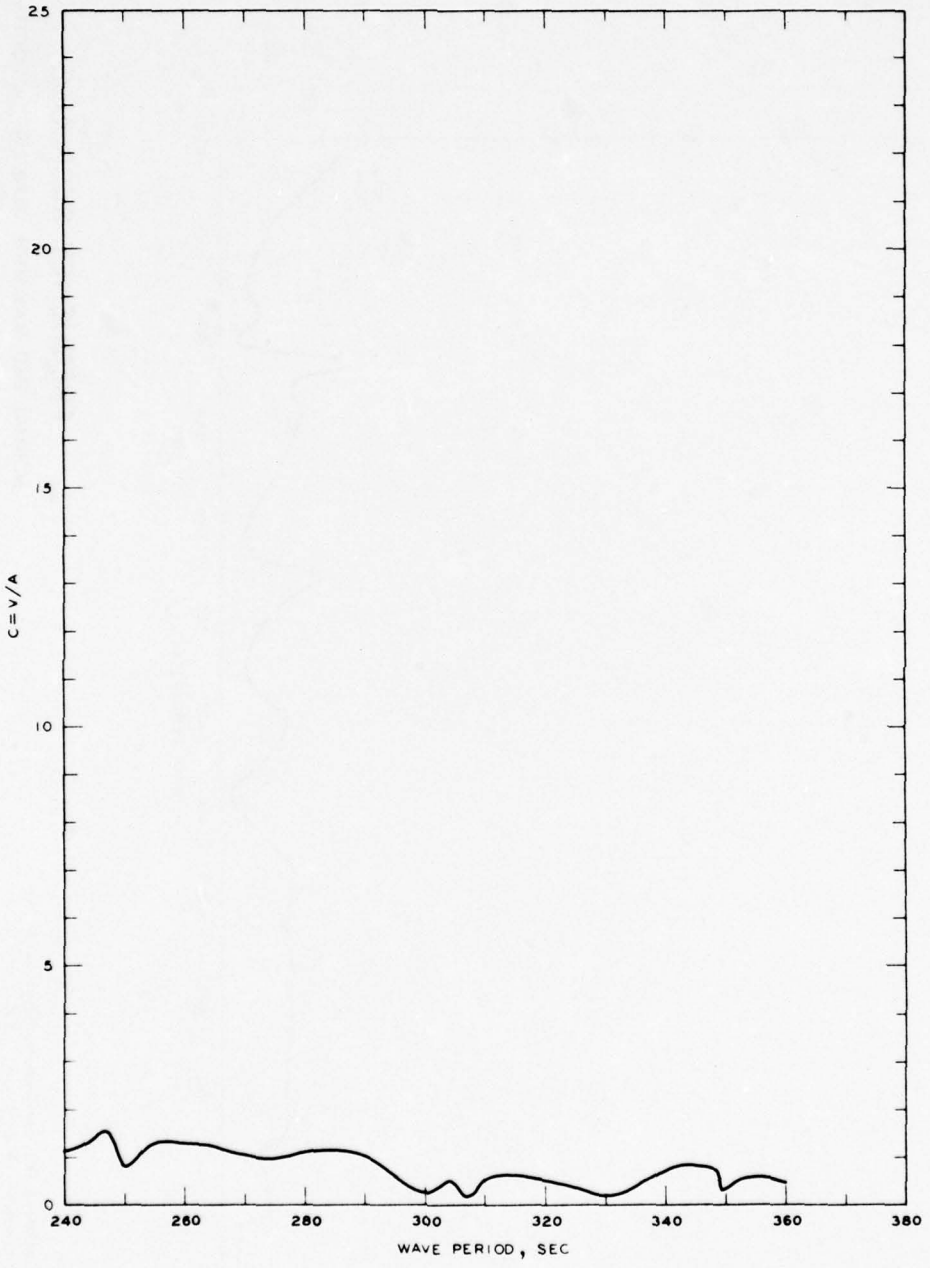

NOTE: C = NORMALIZED MAXIMUM CURRENT VELOCITY
V = CURRENT VELOCITY, FT/SEC
A = INCIDENT WAVE AMPLITUDE

FREQUENCY RESPONSE

NORMALIZED MAXIMUM CURRENT VELOCITY
STA LA-15, GRID 4A

PLATE 169

PLATE 170

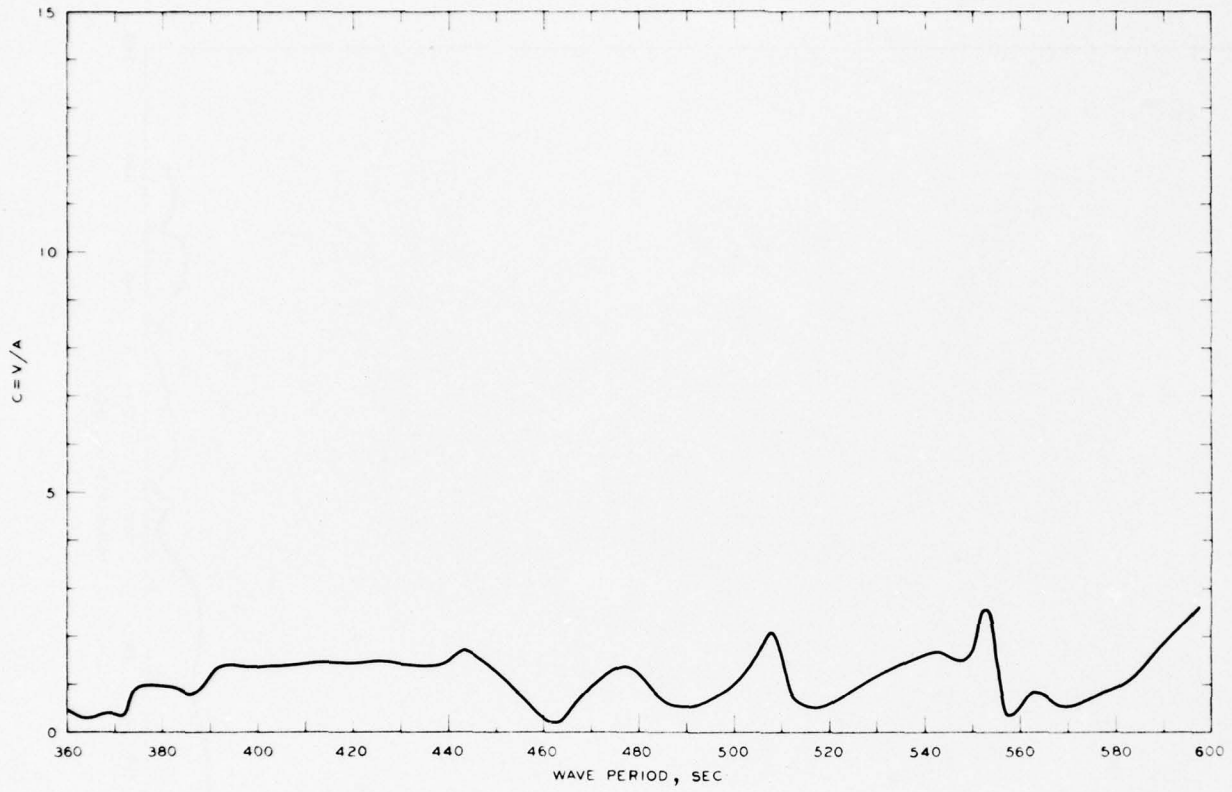

NOTE: C = NORMALIZED MAXIMUM CURRENT VELOCITY
V = CURRENT VELOCITY, FT / SEC
A = INCIDENT WAVE AMPLITUDE

FREQUENCY RESPONSE

NORMALIZED MAXIMUM CURRENT VELOCITY
STA LA-15, GRID 5A

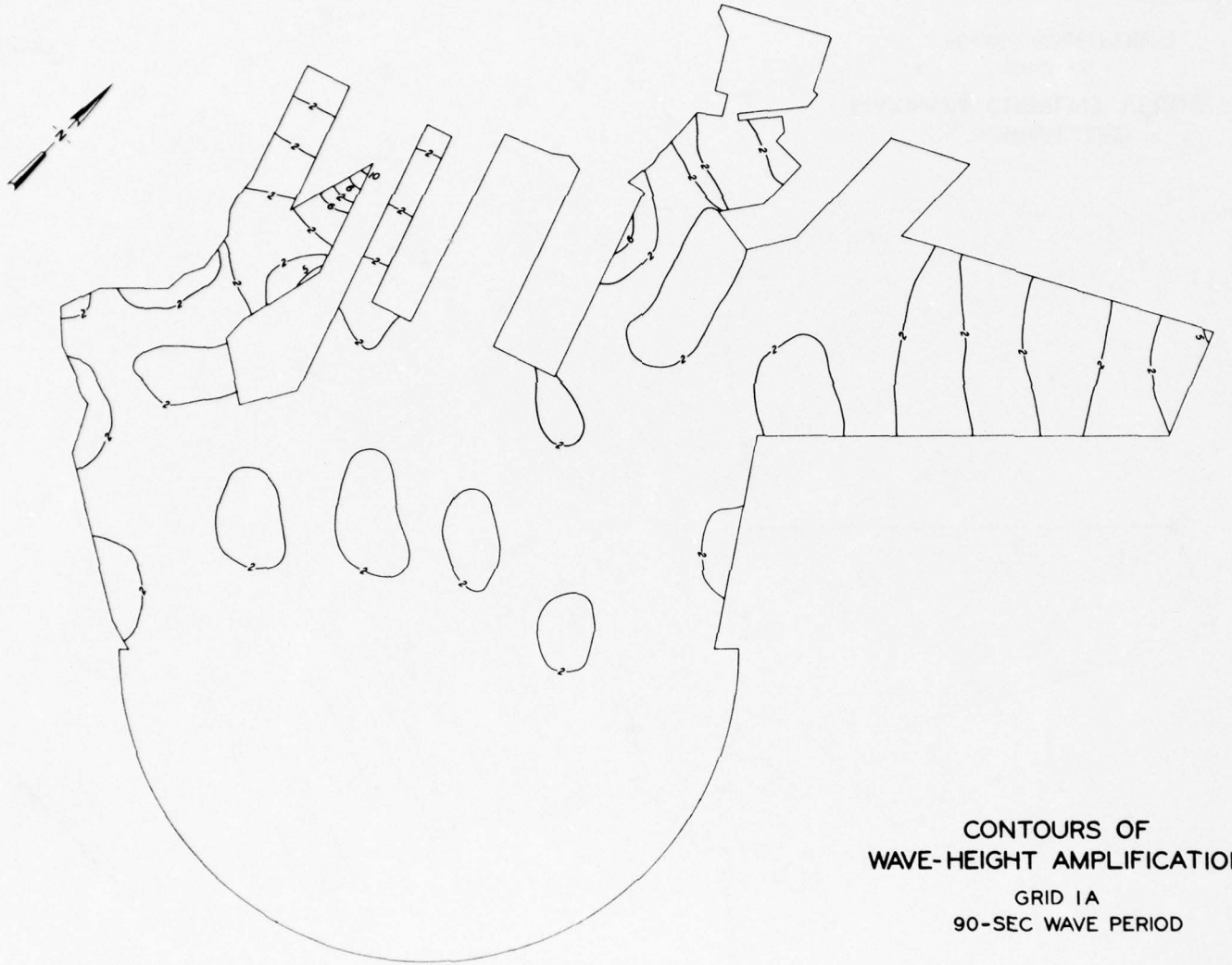

CONTOURS OF
WAVE-HEIGHT AMPLIFICATION

GRID 1A
90-SEC WAVE PERIOD

PLATE 171

PLATE 172

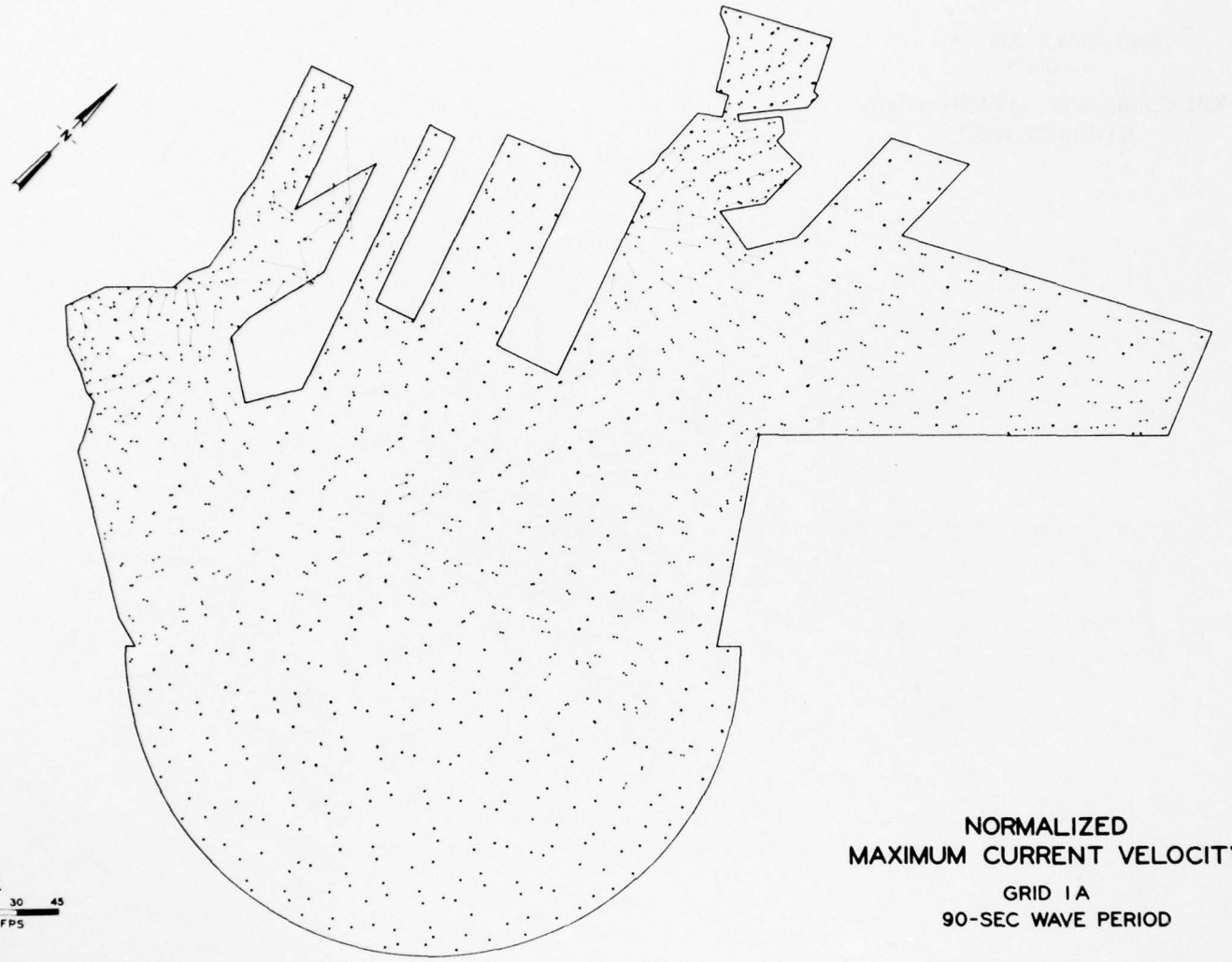

NORMALIZED
MAXIMUM CURRENT VELOCITY

GRID 1A
90-SEC WAVE PERIOD

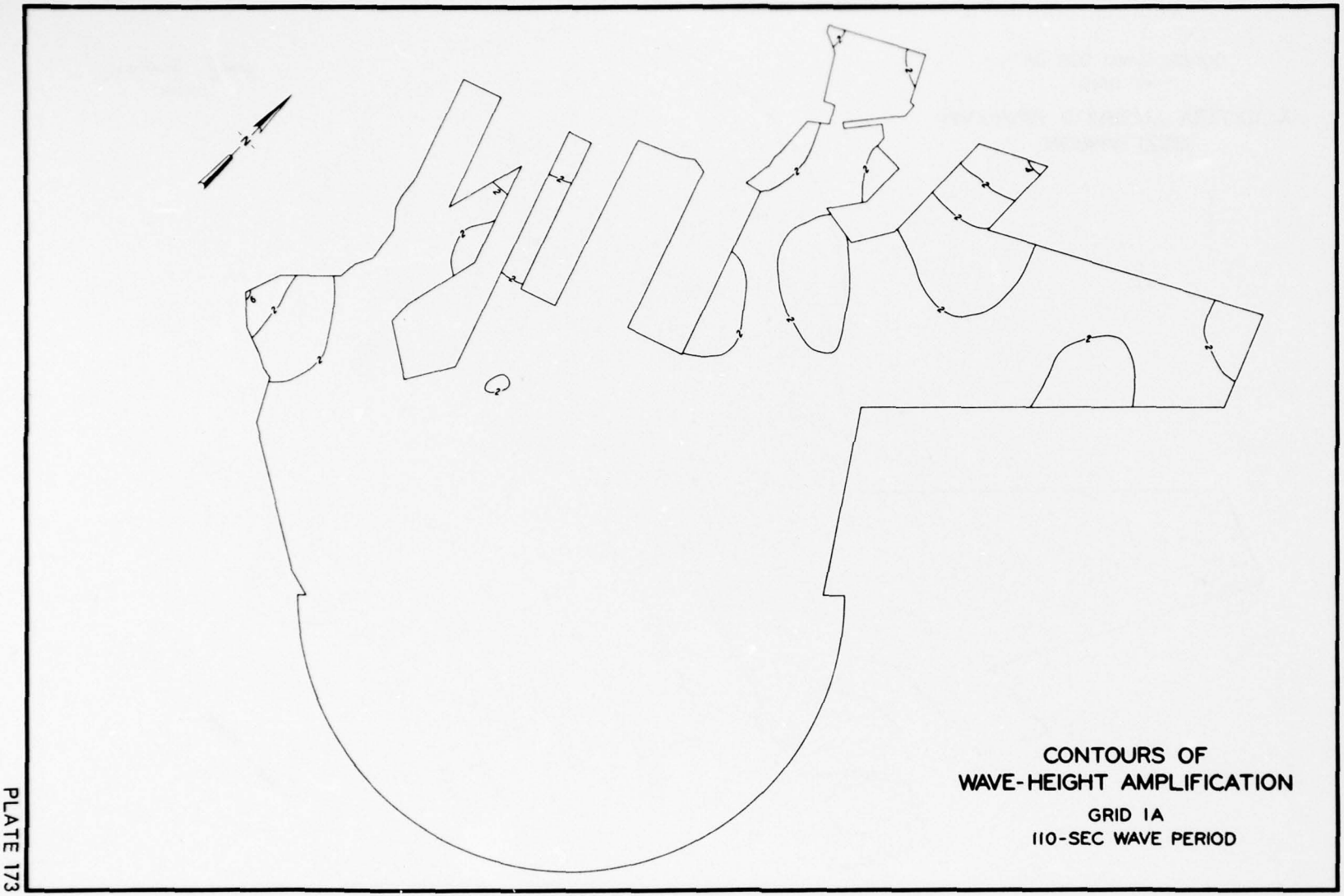
CONTOURS OF
WAVE-HEIGHT AMPLIFICATION
GRID 1A
110-SEC WAVE PERIOD

PLATE 173

PLATE 174

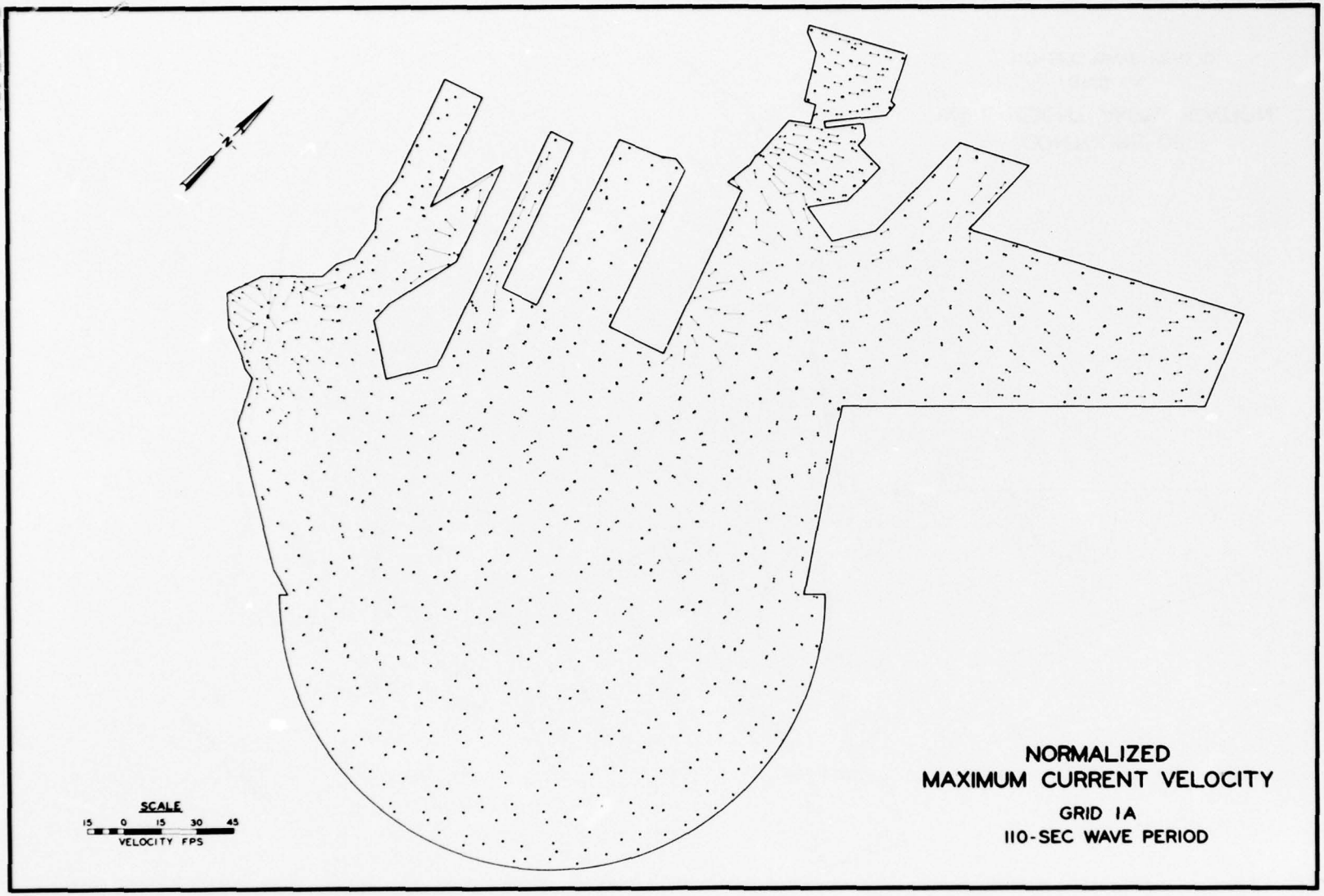

NORMALIZED
MAXIMUM CURRENT VELOCITY

GRID 1A
110-SEC WAVE PERIOD

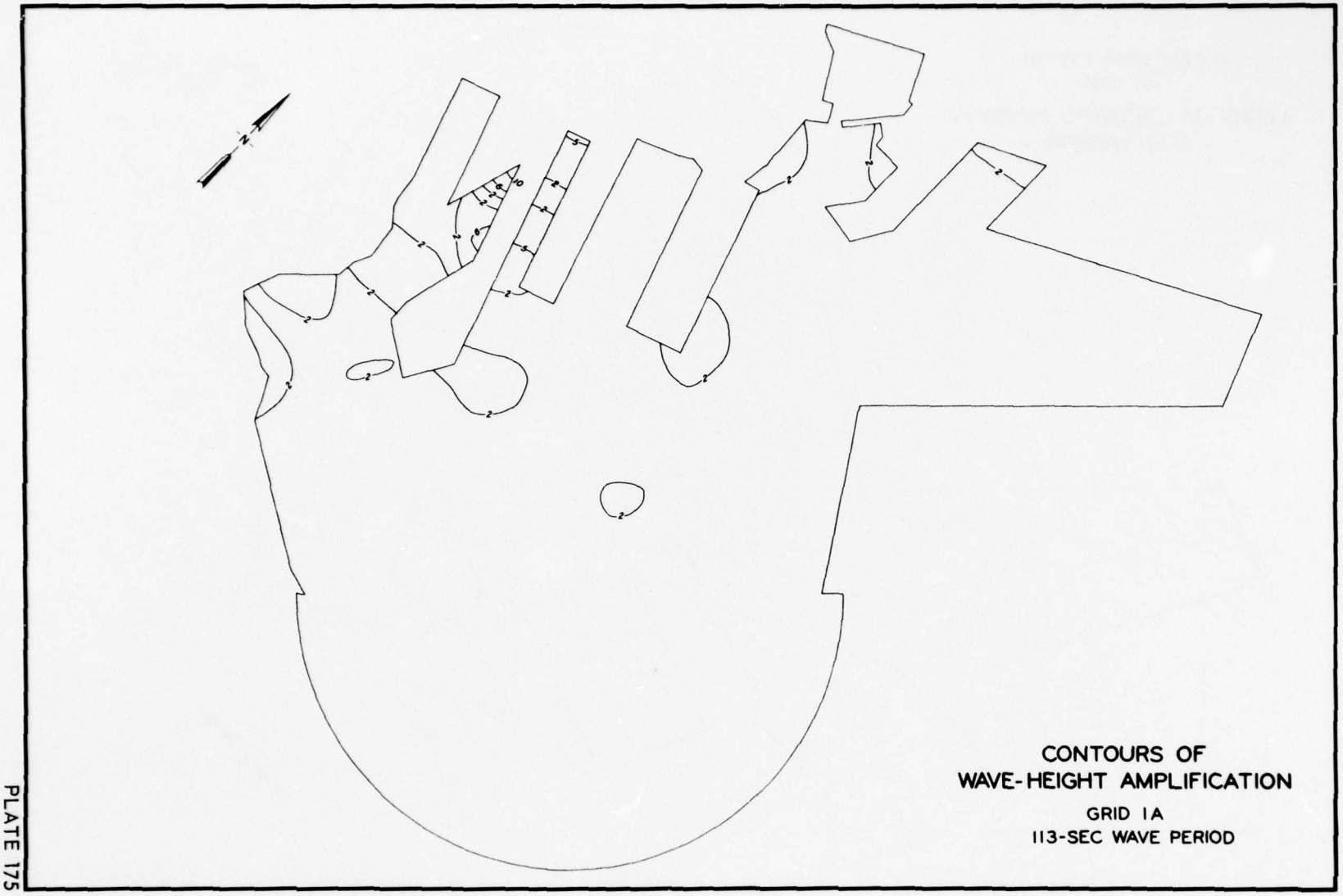

CONTOURS OF
WAVE-HEIGHT AMPLIFICATION

GRID 1A
113-SEC WAVE PERIOD

PLATE 175

PLATE 176

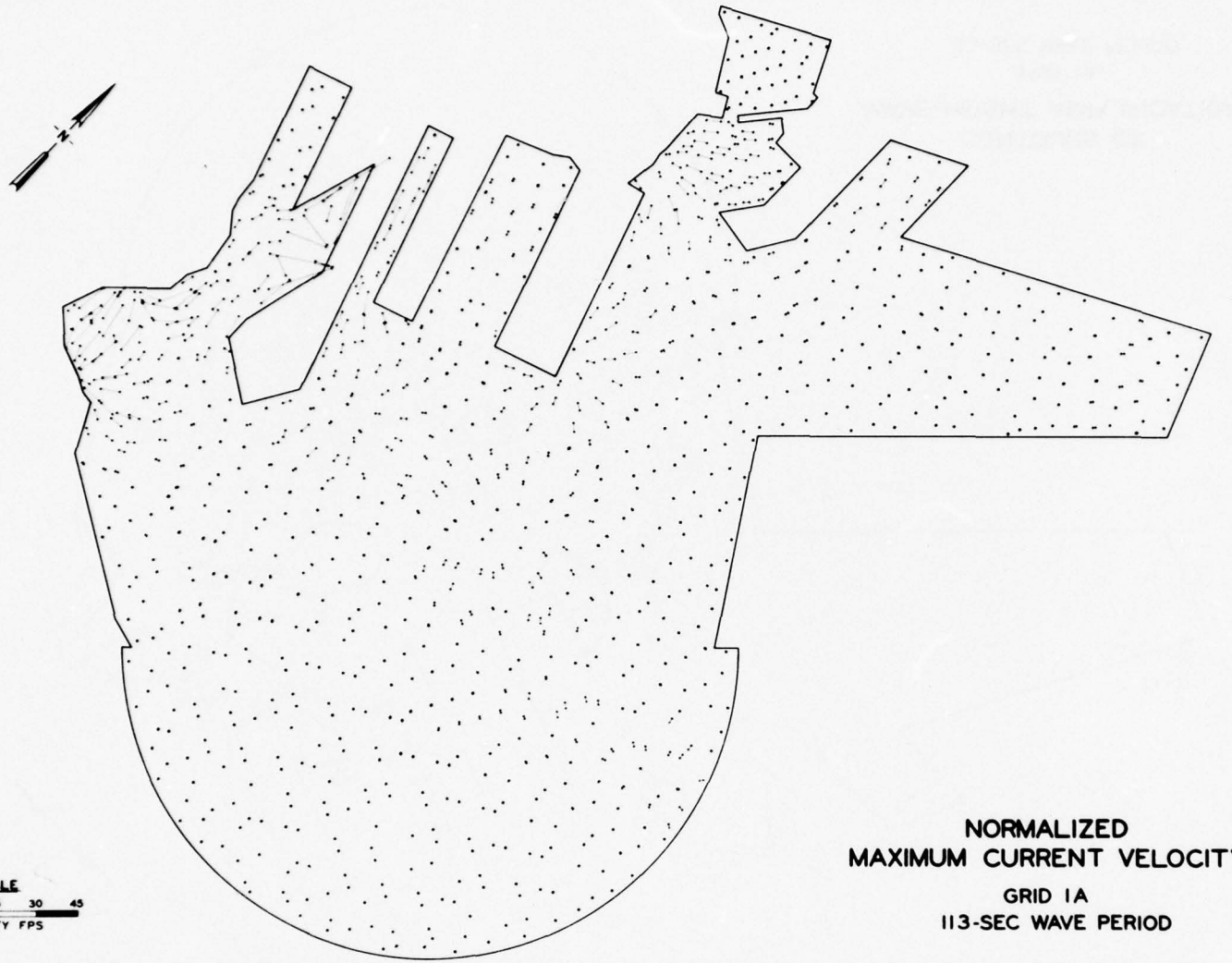

NORMALIZED
MAXIMUM CURRENT VELOCITY

GRID 1A
113-SEC WAVE PERIOD

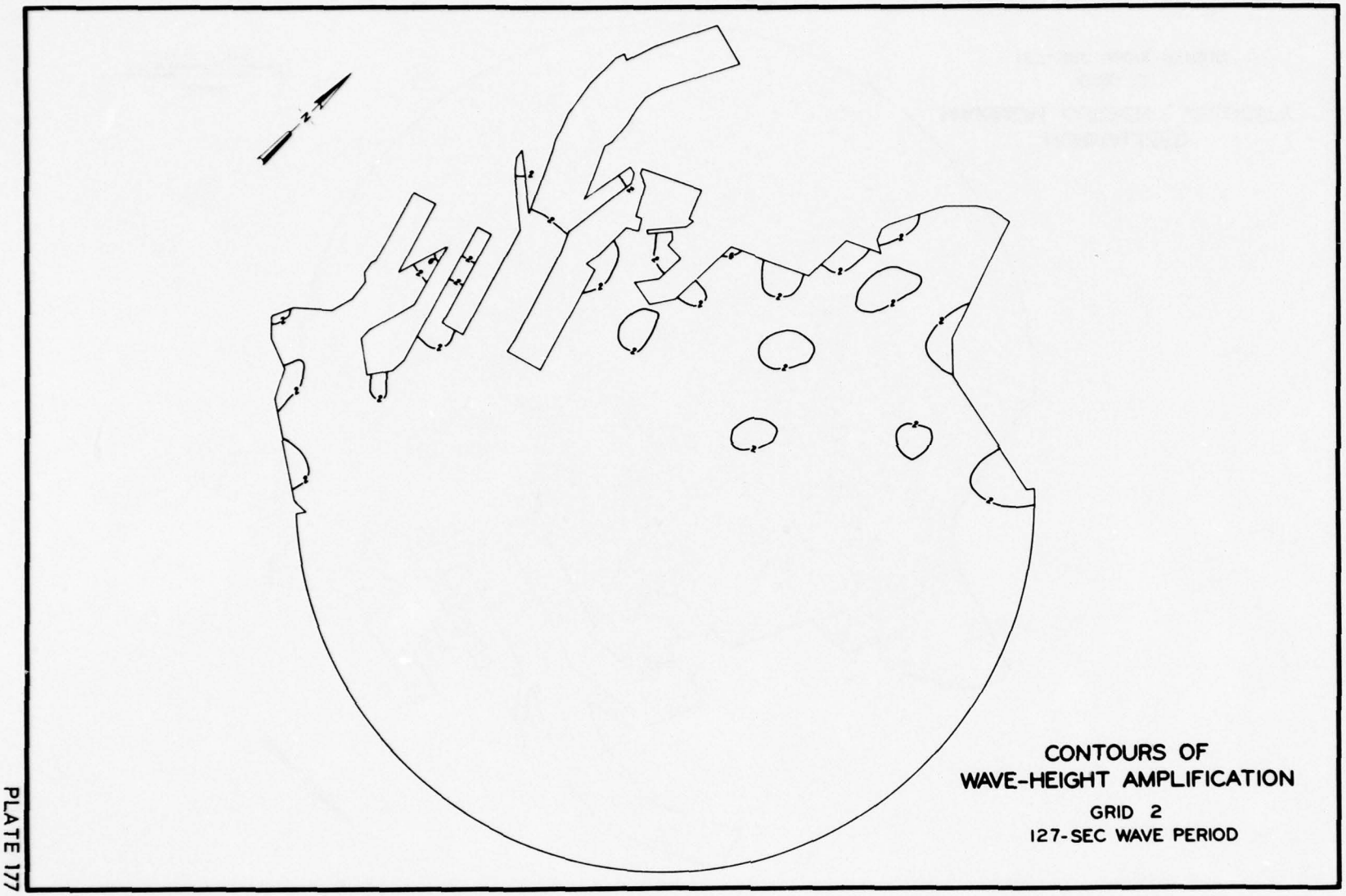

CONTOURS OF
WAVE-HEIGHT AMPLIFICATION

GRID 2
127-SEC WAVE PERIOD

PLATE 177

PLATE 178

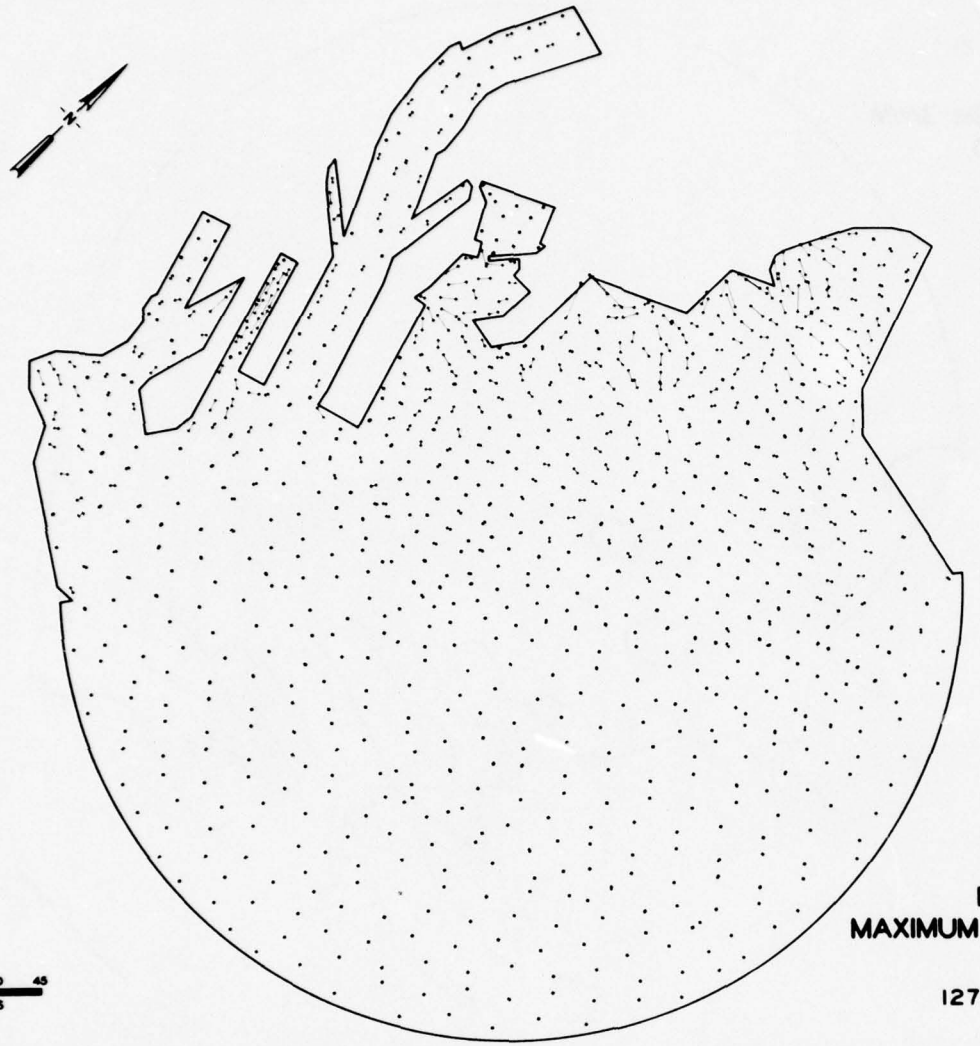

SCALE
15 0 15 30 45
VELOCITY FPS

NORMALIZED
MAXIMUM CURRENT VELOCITY

GRID 2
127-SEC WAVE PERIOD

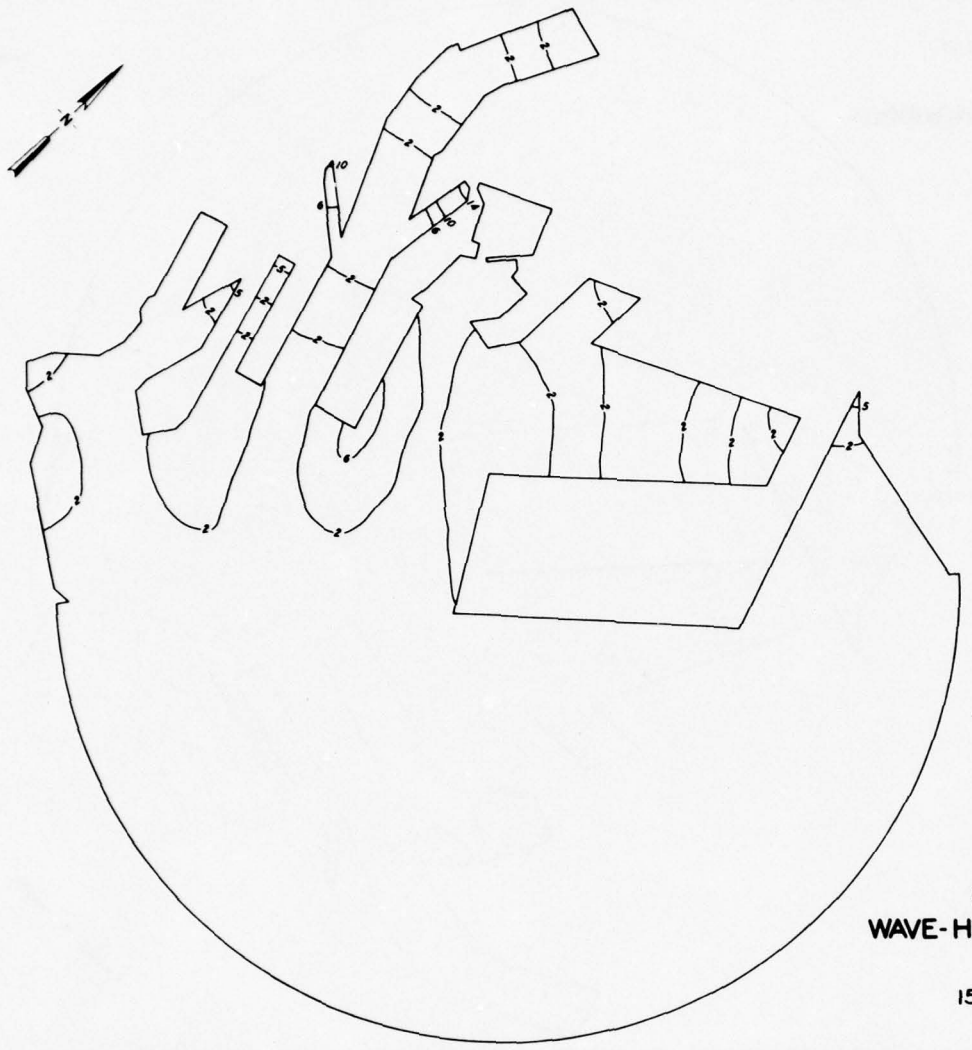

CONTOURS OF
WAVE-HEIGHT AMPLIFICATION

GRID 2A
157-SEC WAVE PERIOD

PLATE 179

PLATE 180

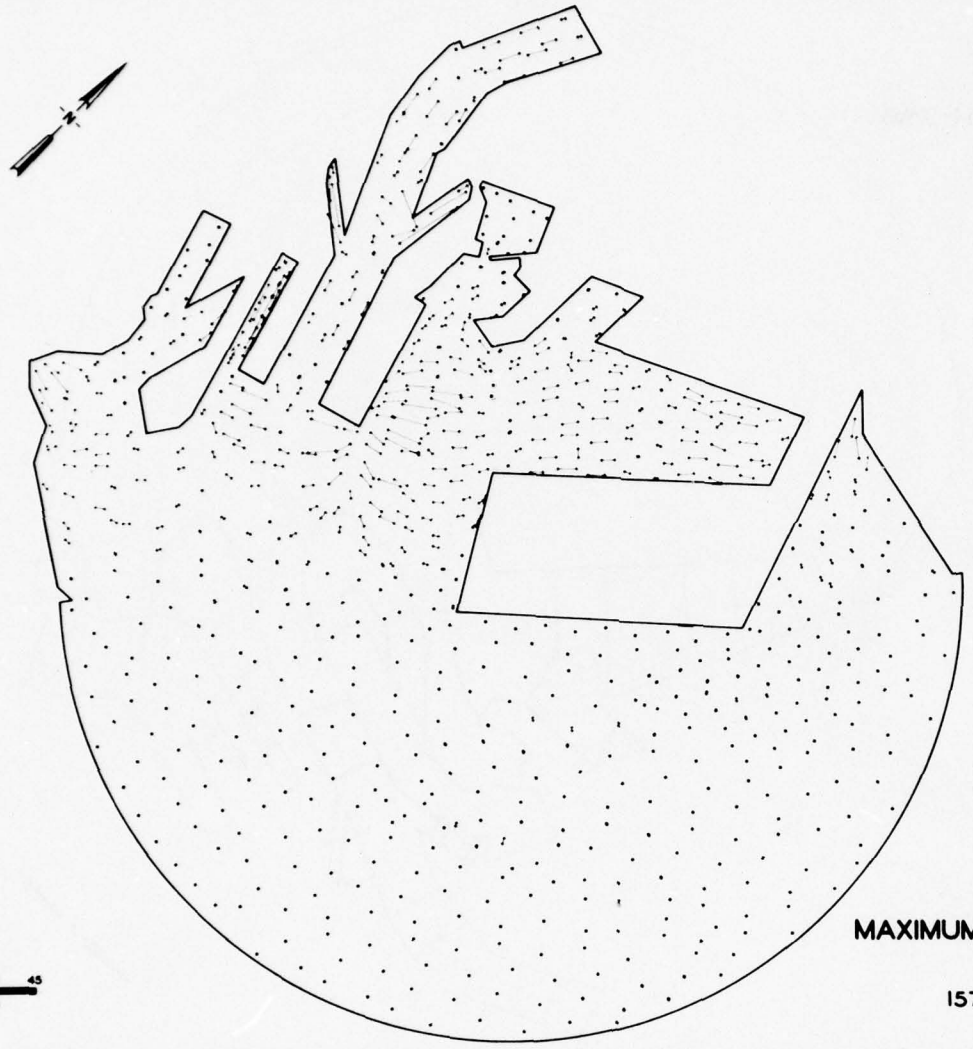

SCALE
15 0 15 30 45
VELOCITY FPS

NORMALIZED
MAXIMUM CURRENT VELOCITY

GRID 2A
157-SEC WAVE PERIOD

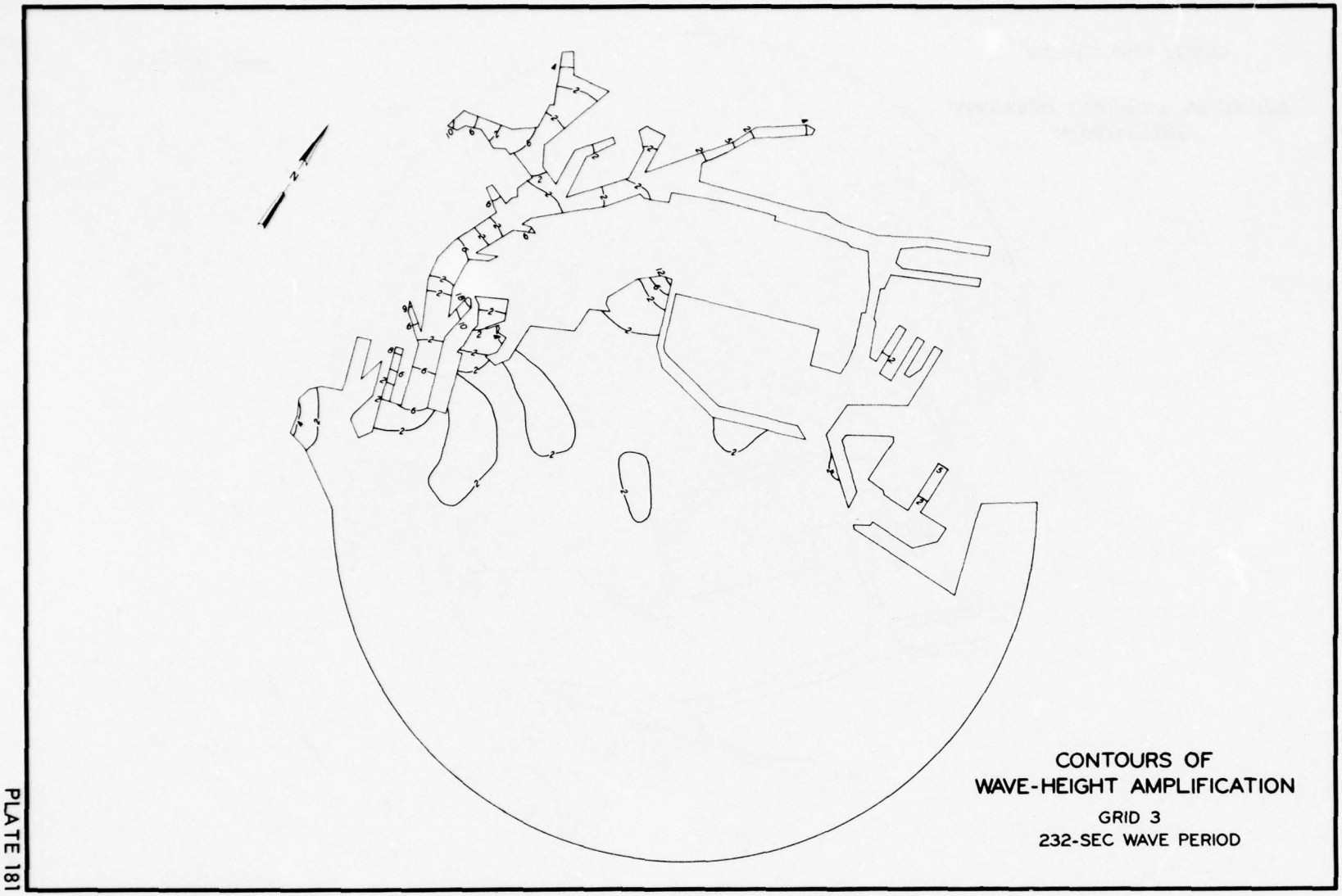

CONTOURS OF
WAVE-HEIGHT AMPLIFICATION
GRID 3
232-SEC WAVE PERIOD

PLATE 181

PLATE 182

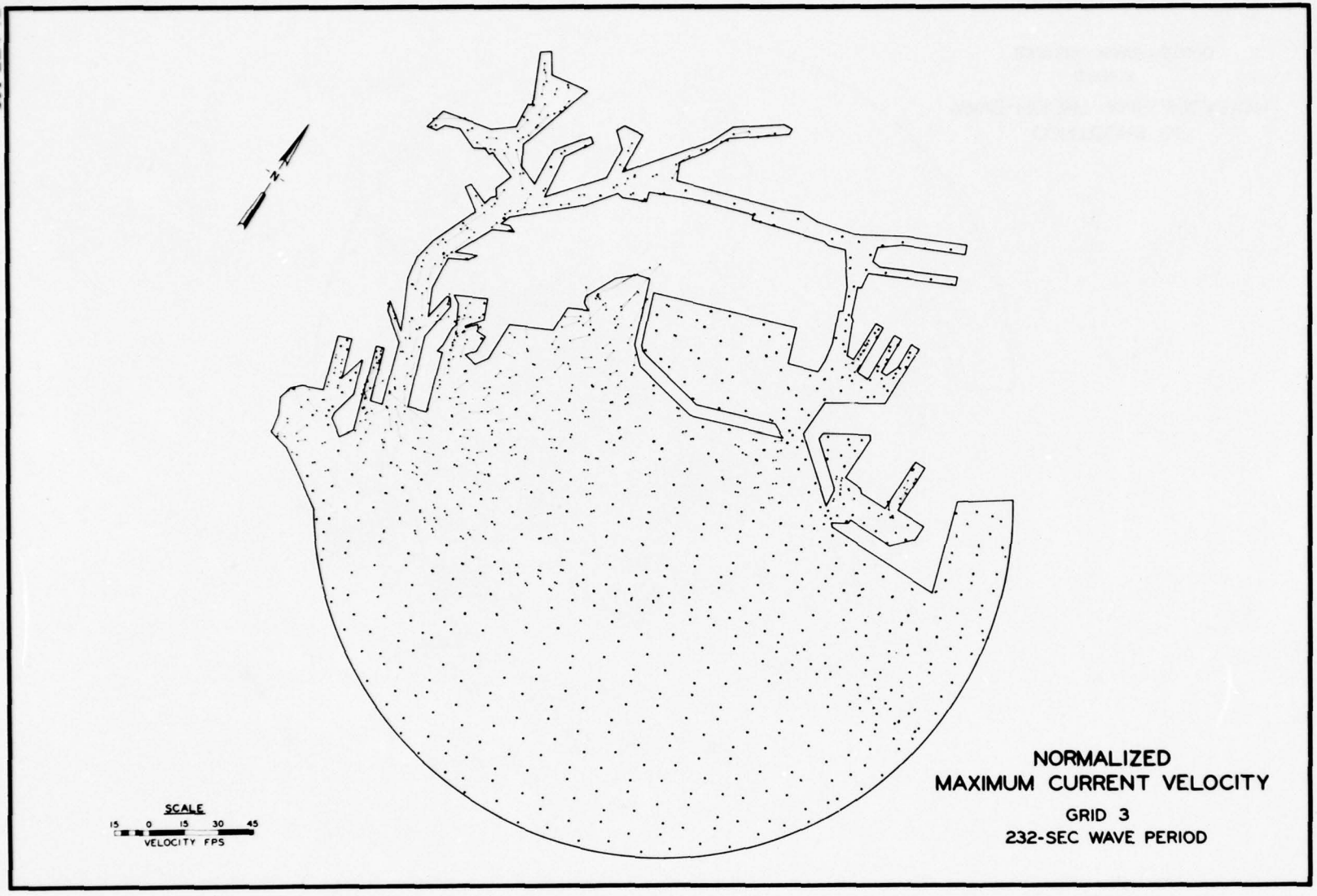

NORMALIZED
MAXIMUM CURRENT VELOCITY

GRID 3
232-SEC WAVE PERIOD

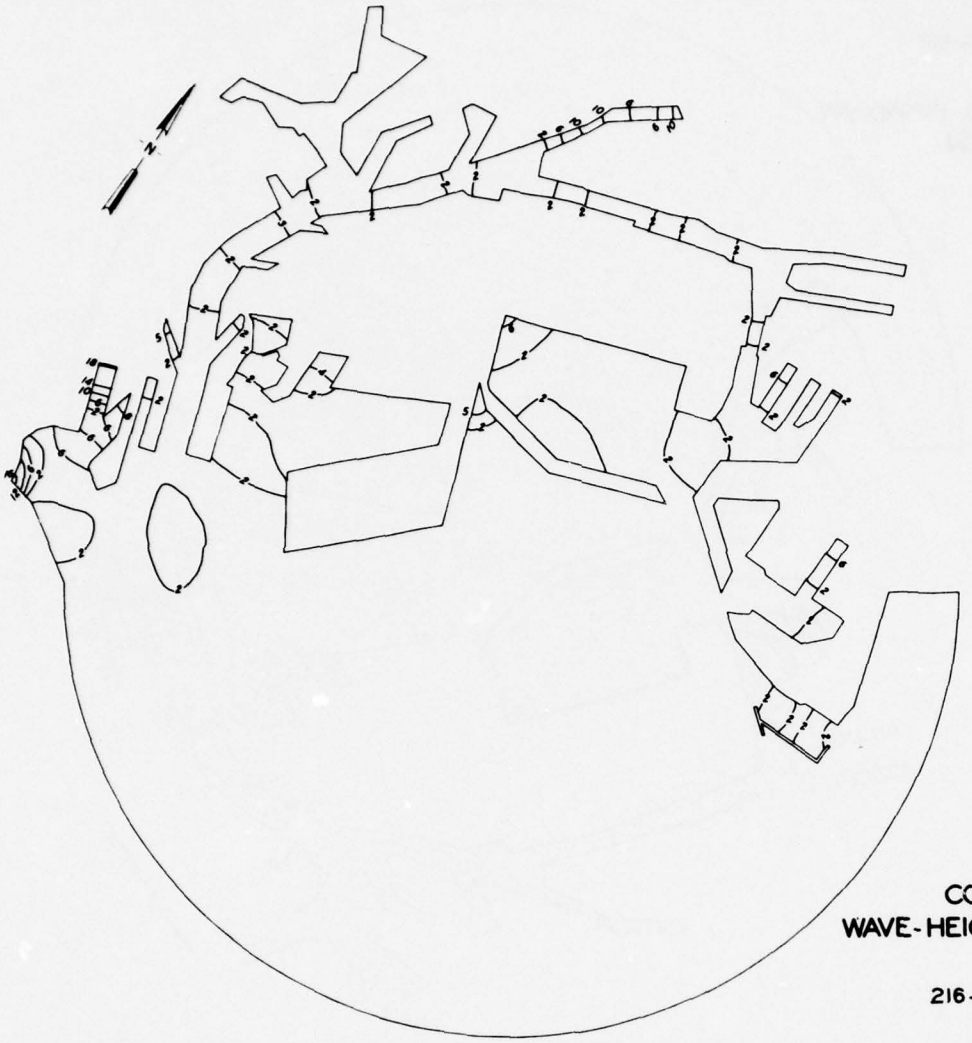

CONTOURS OF
WAVE-HEIGHT AMPLIFICATION

GRID 3A

216-SEC WAVE PERIOD

PLATE 183

PLATE 184

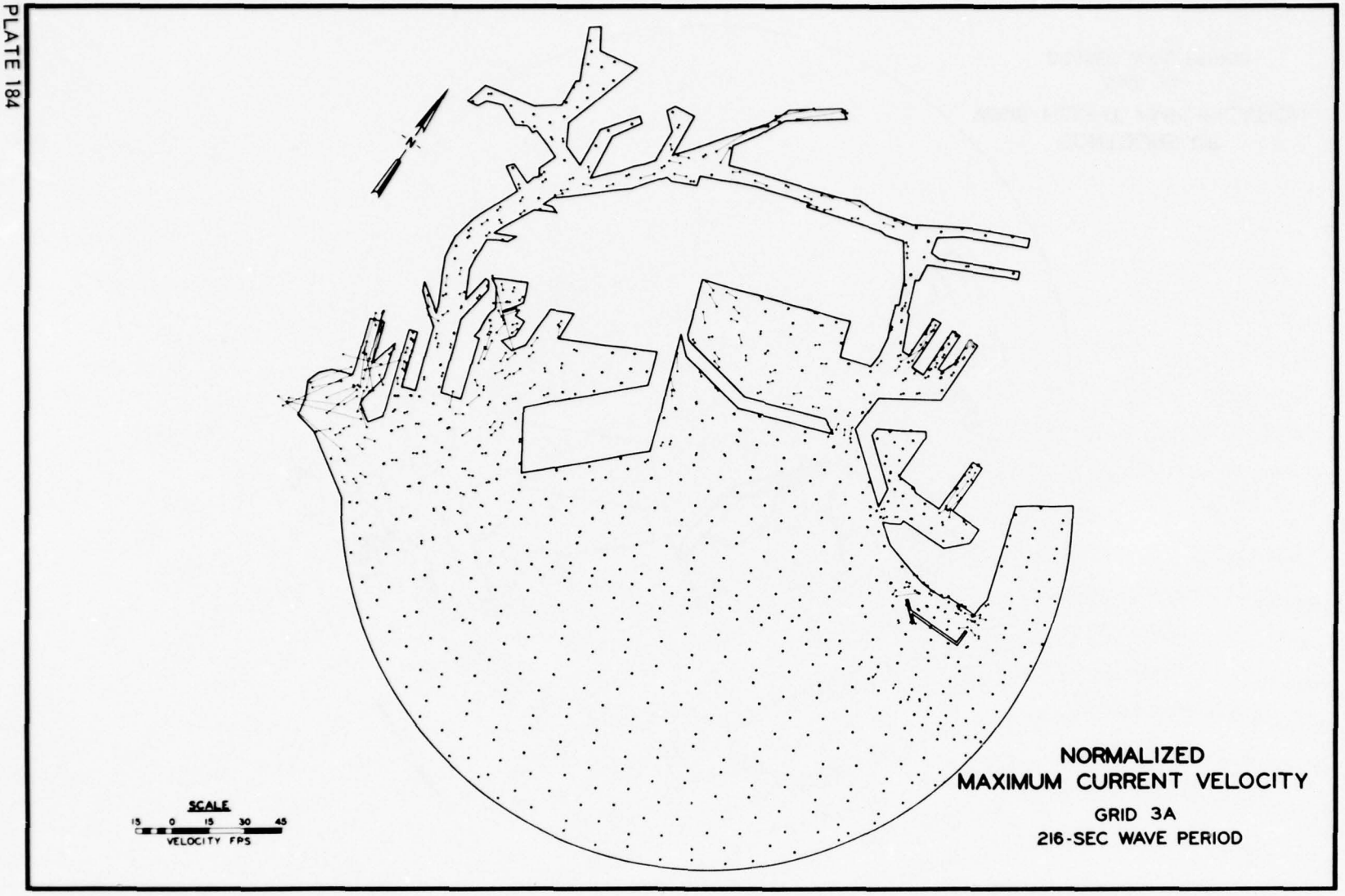

NORMALIZED
MAXIMUM CURRENT VELOCITY

GRID 3A

216-SEC WAVE PERIOD

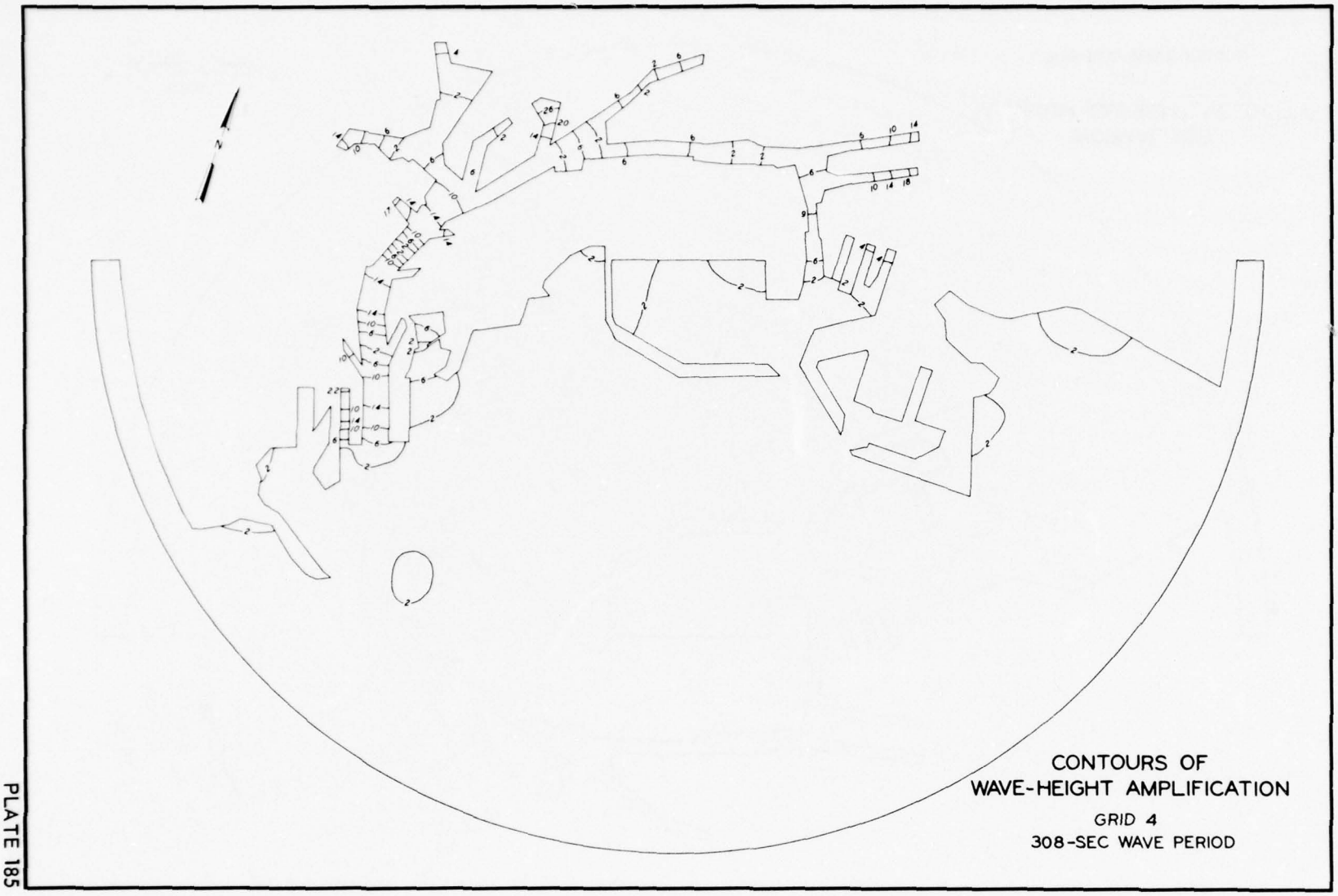

CONTOURS OF
WAVE-HEIGHT AMPLIFICATION

GRID 4
308-SEC WAVE PERIOD

PLATE 185

PLATE 186

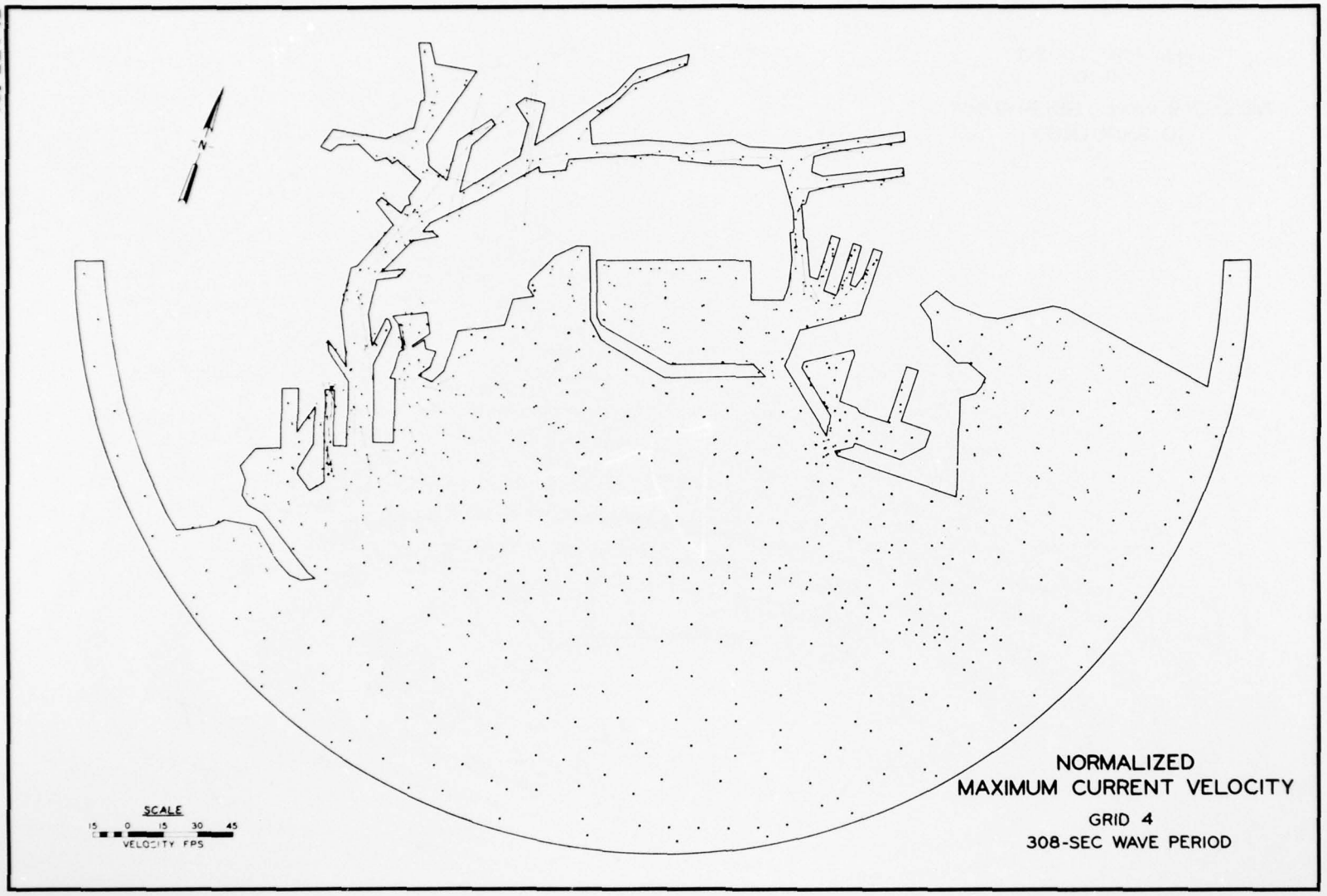

NORMALIZED
MAXIMUM CURRENT VELOCITY

GRID 4
308-SEC WAVE PERIOD

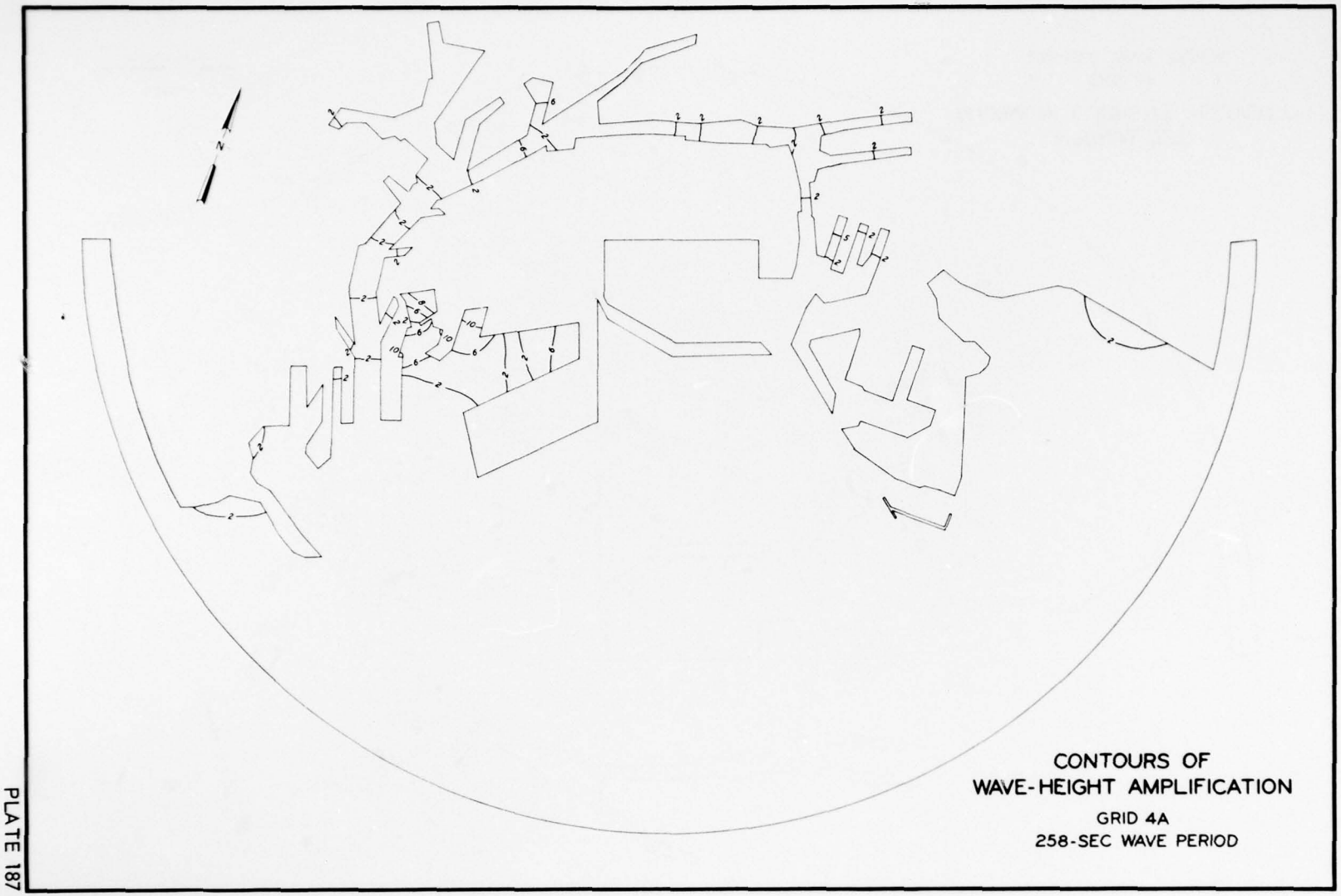

CONTOURS OF
WAVE-HEIGHT AMPLIFICATION

GRID 4A
258-SEC WAVE PERIOD

PLATE 187

PLATE 188

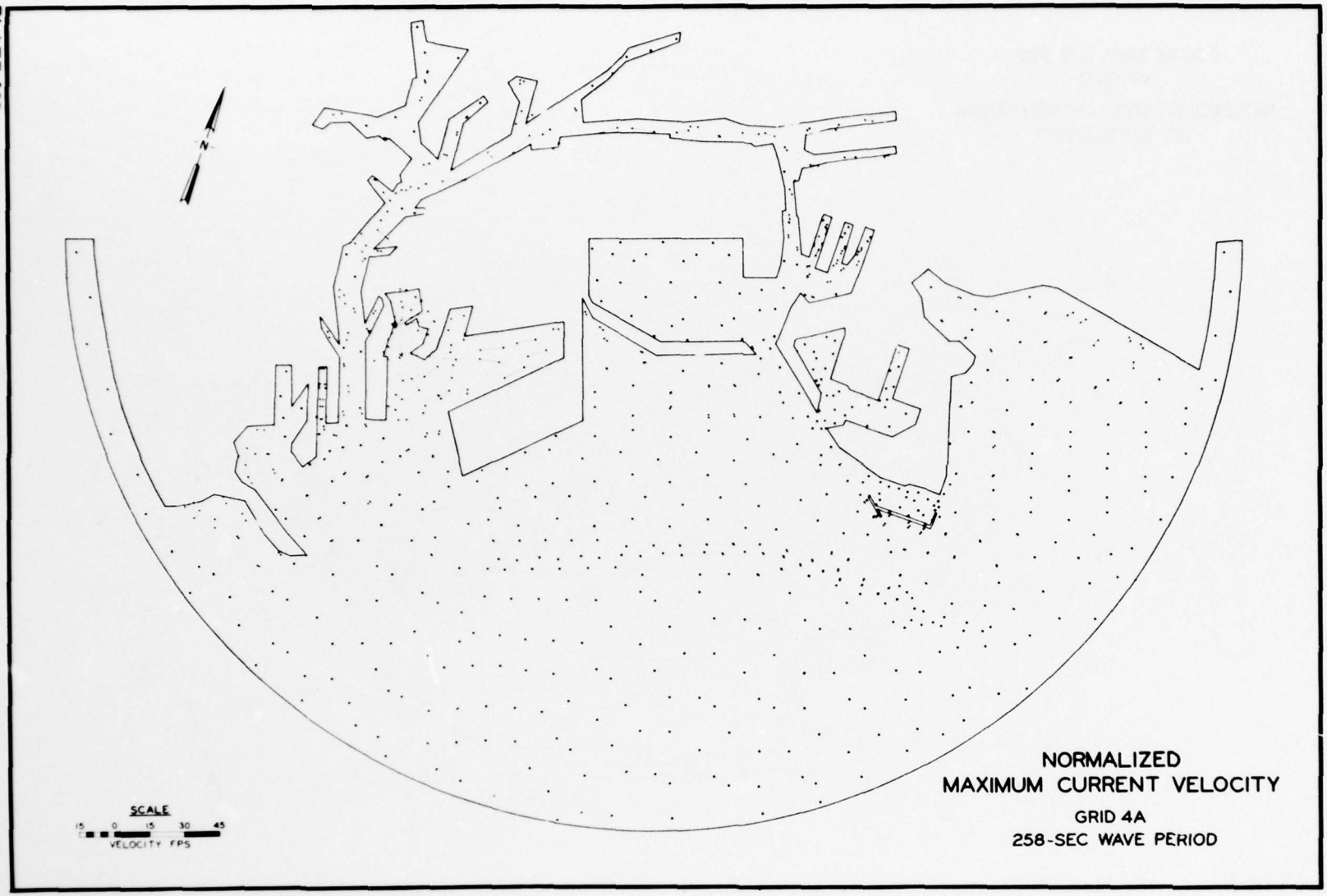

NORMALIZED
MAXIMUM CURRENT VELOCITY

GRID 4A
258-SEC WAVE PERIOD

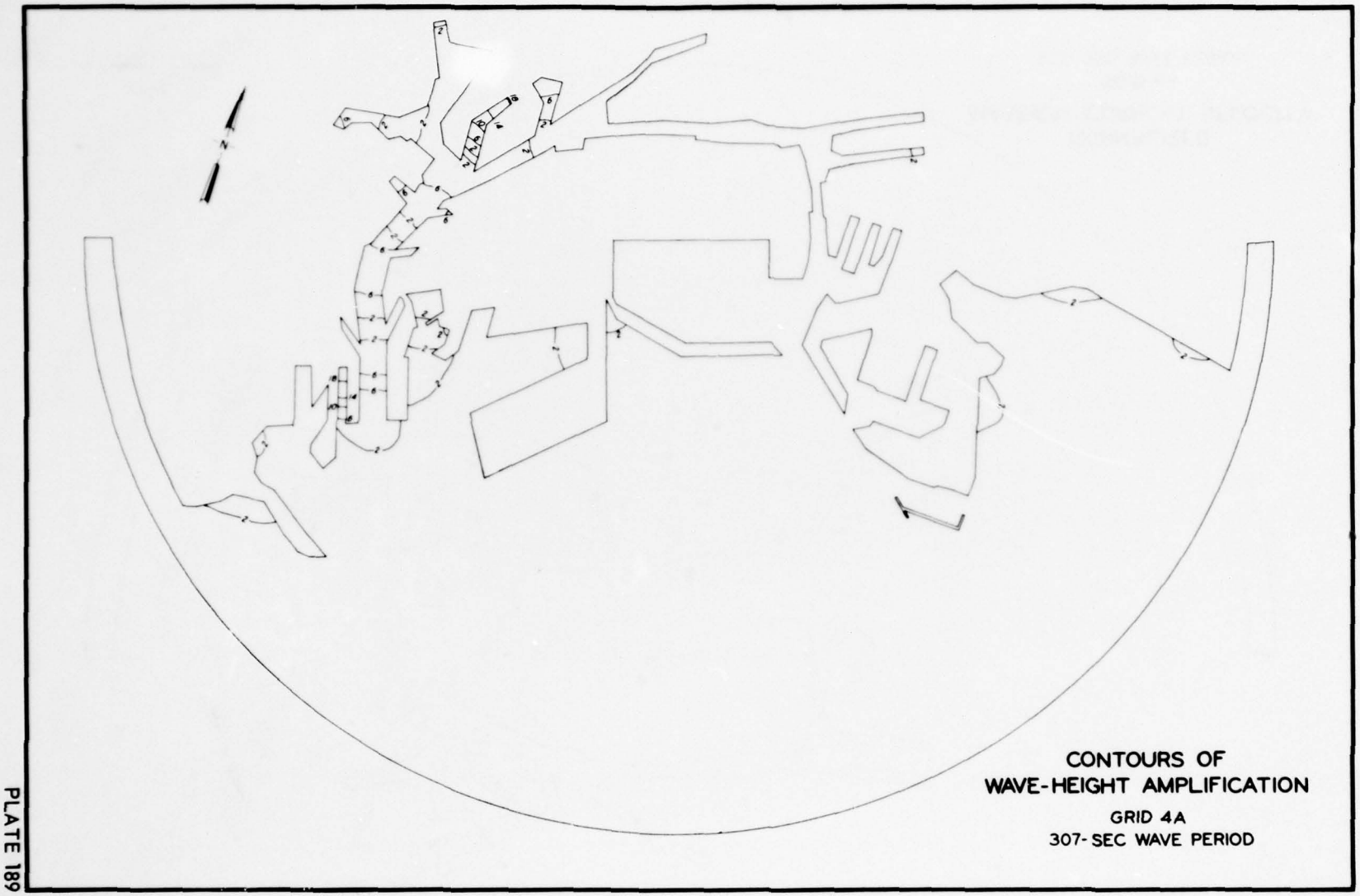

CONTOURS OF
WAVE-HEIGHT AMPLIFICATION

GRID 4A
307-SEC WAVE PERIOD

PLATE 189

PLATE 190

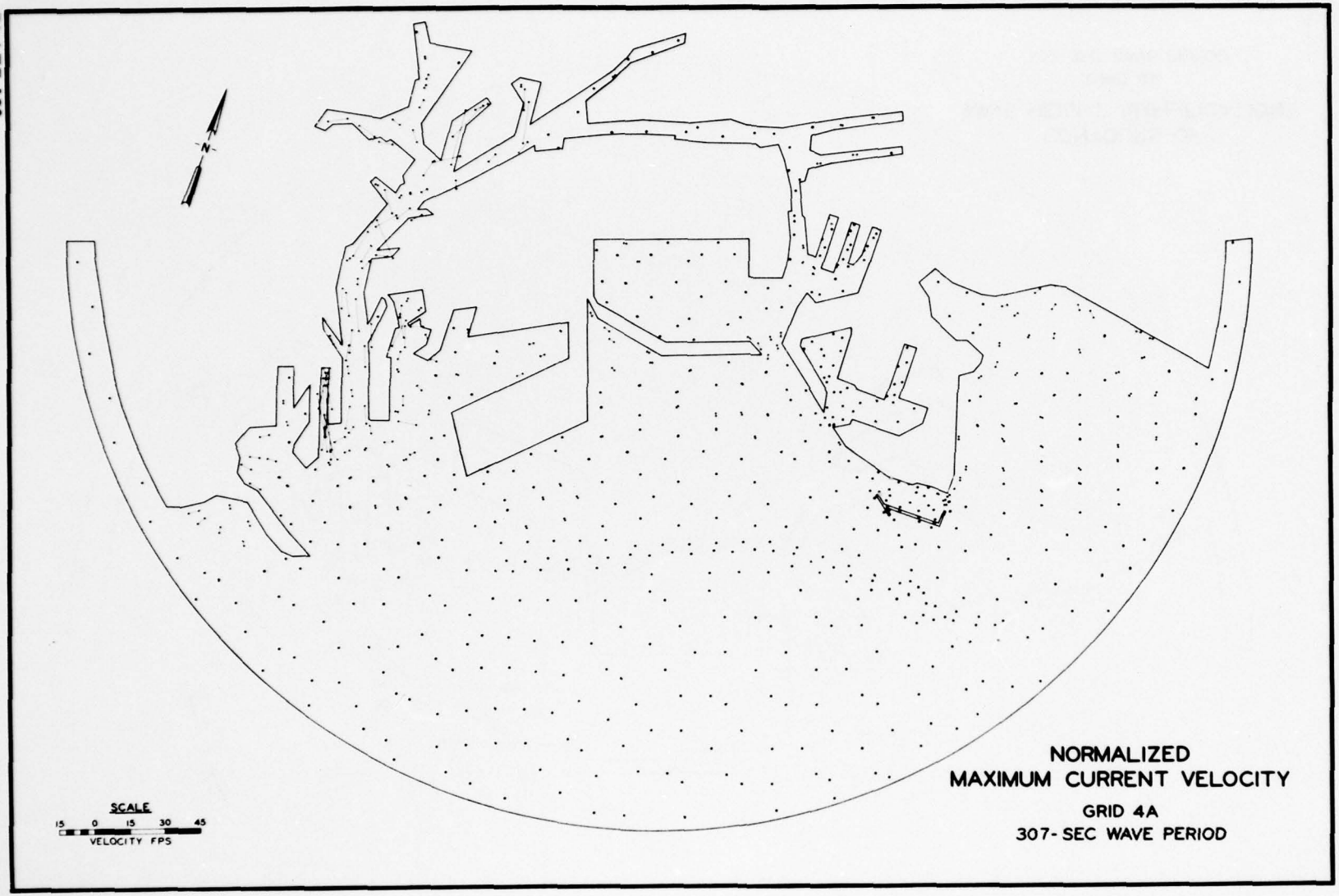

NORMALIZED
MAXIMUM CURRENT VELOCITY

GRID 4A
307-SEC WAVE PERIOD

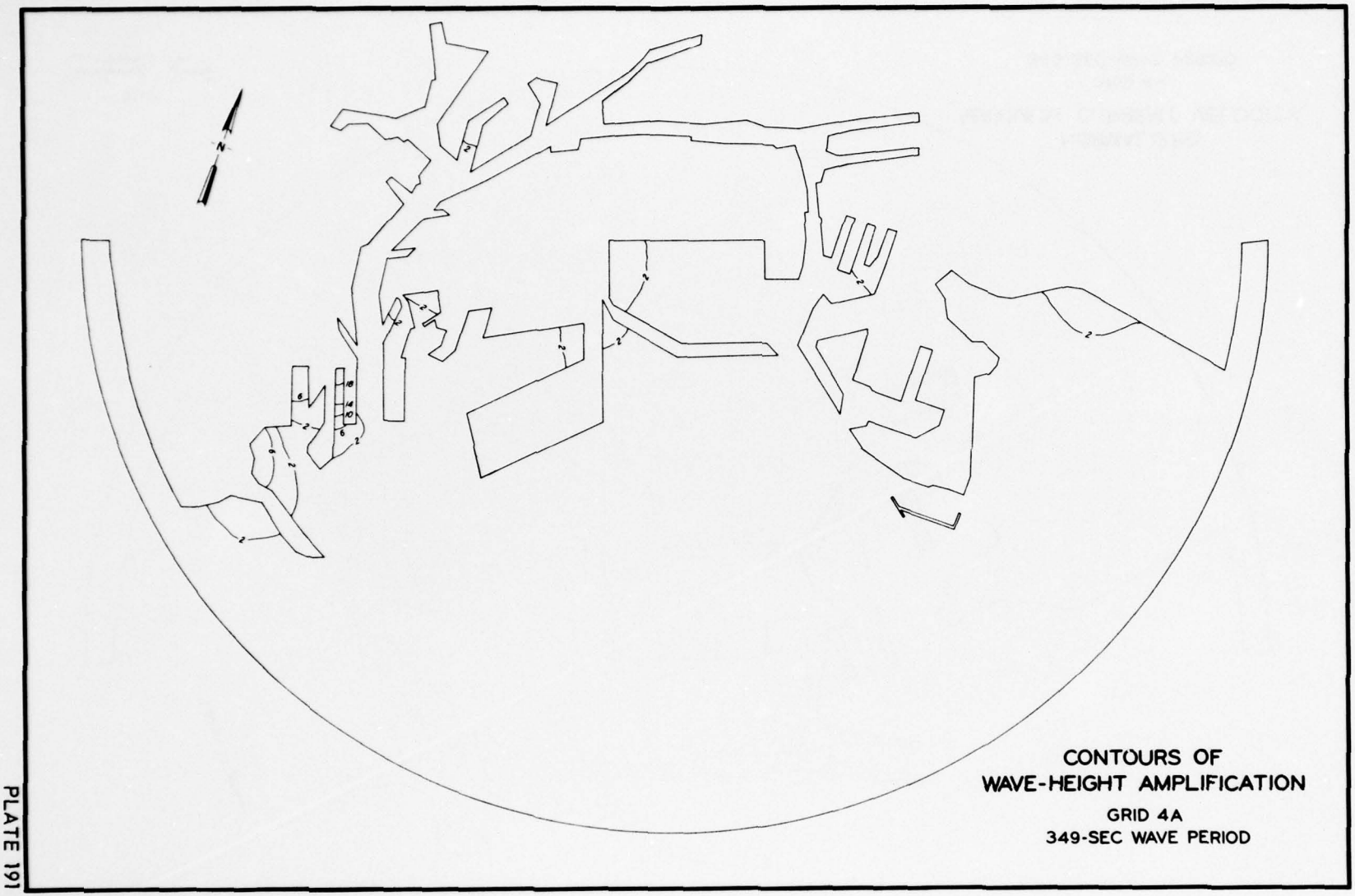
N
CONTOURS OF
WAVE-HEIGHT AMPLIFICATION
GRID 4A
349-SEC WAVE PERIOD

PLATE 191

PLATE 192

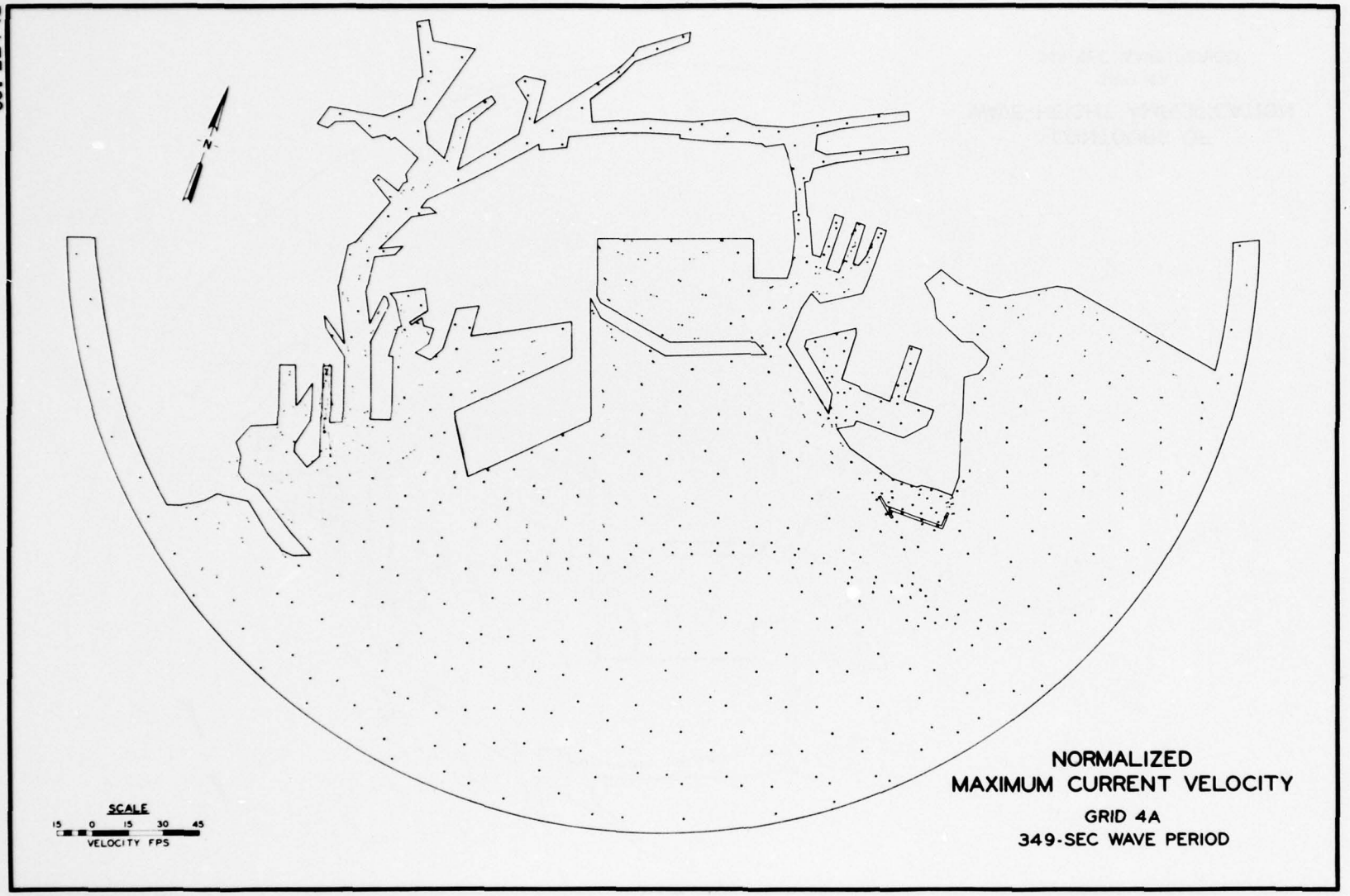

NORMALIZED
MAXIMUM CURRENT VELOCITY

GRID 4A
349-SEC WAVE PERIOD

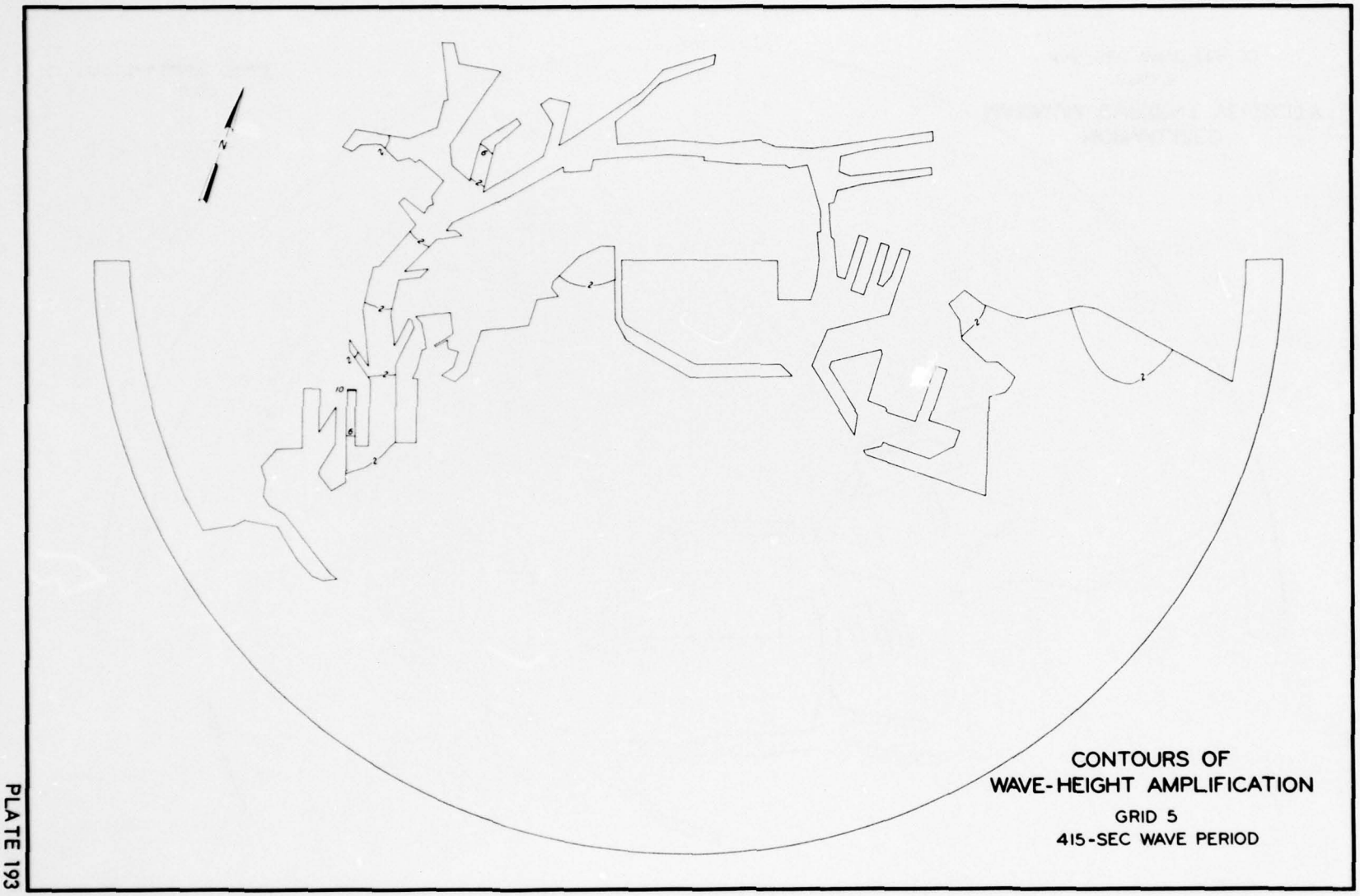

CONTOURS OF
WAVE-HEIGHT AMPLIFICATION

GRID 5
415-SEC WAVE PERIOD

PLATE 193

PLATE 194

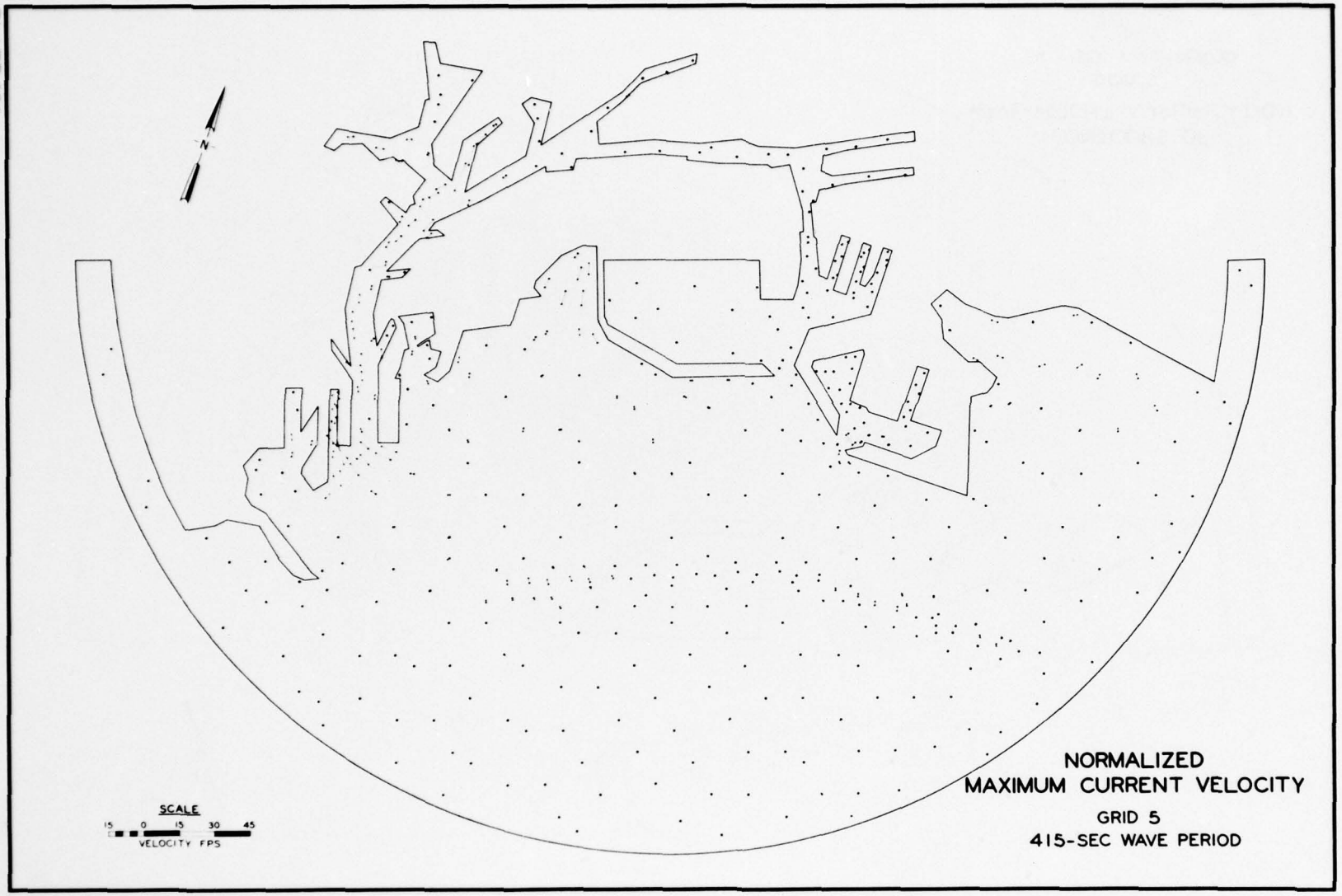

NORMALIZED
MAXIMUM CURRENT VELOCITY

GRID 5
415-SEC WAVE PERIOD

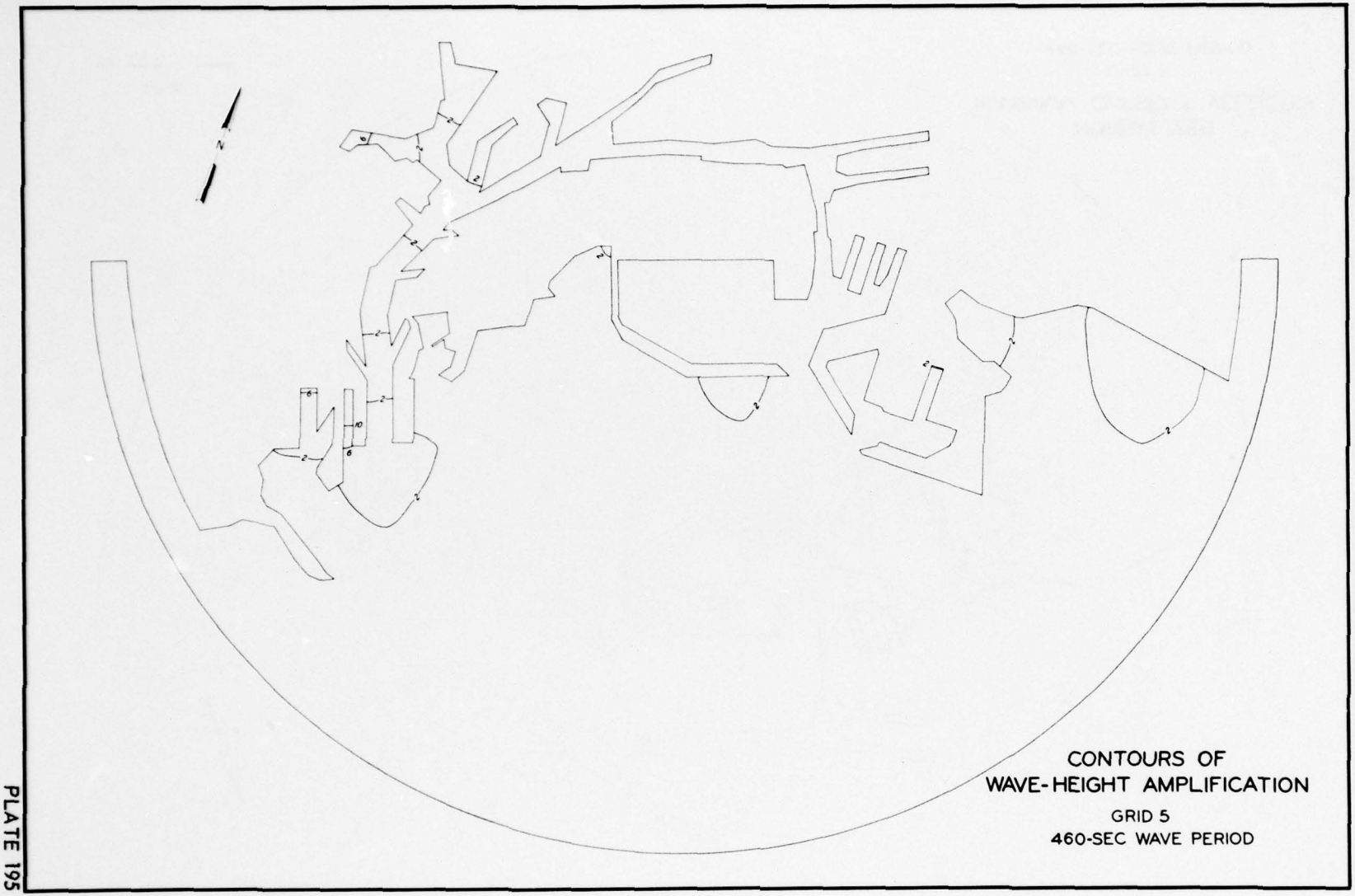

CONTOURS OF
WAVE-HEIGHT AMPLIFICATION

GRID 5
460-SEC WAVE PERIOD

PLATE 195

PLATE 196

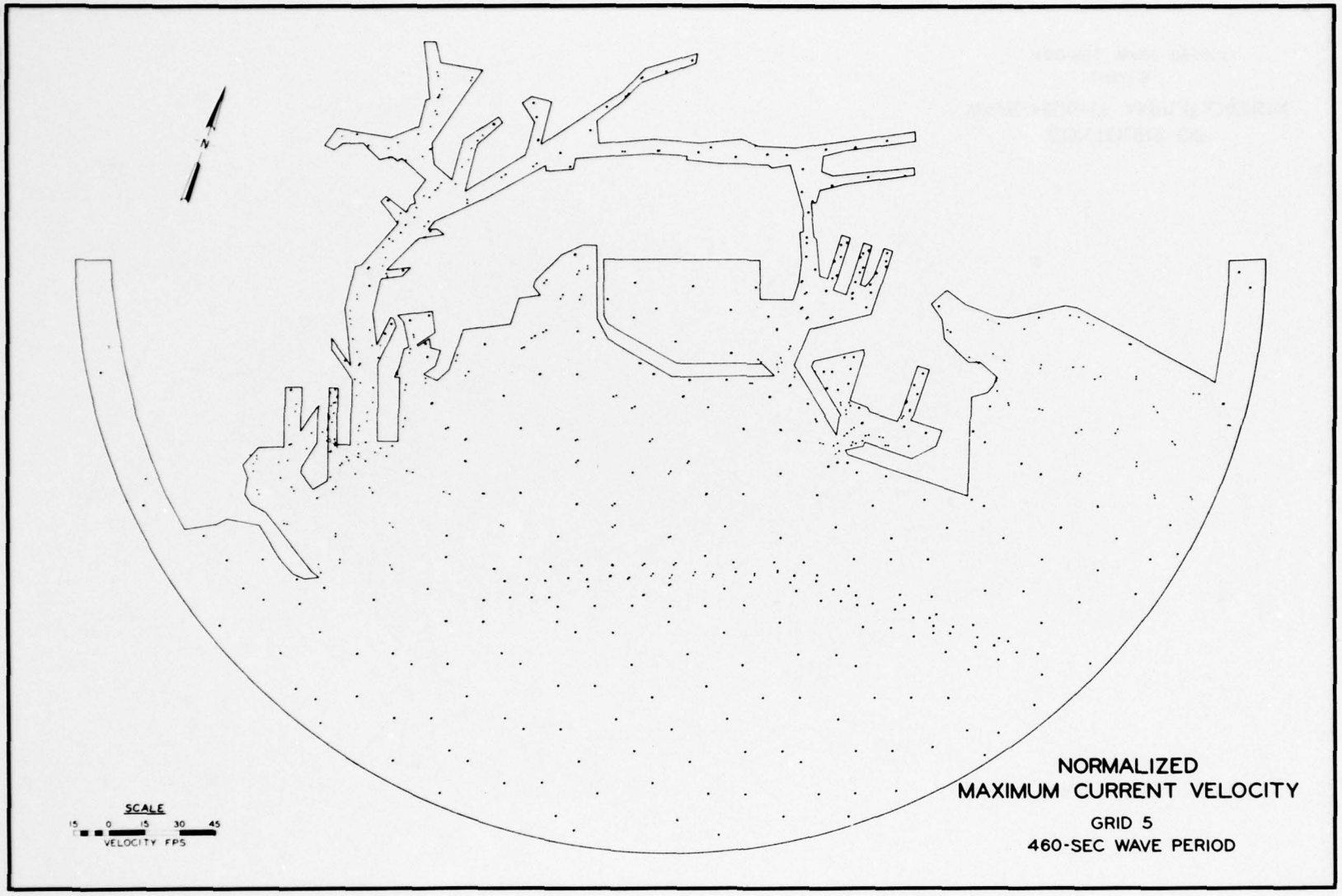

NORMALIZED
MAXIMUM CURRENT VELOCITY

GRID 5
460-SEC WAVE PERIOD

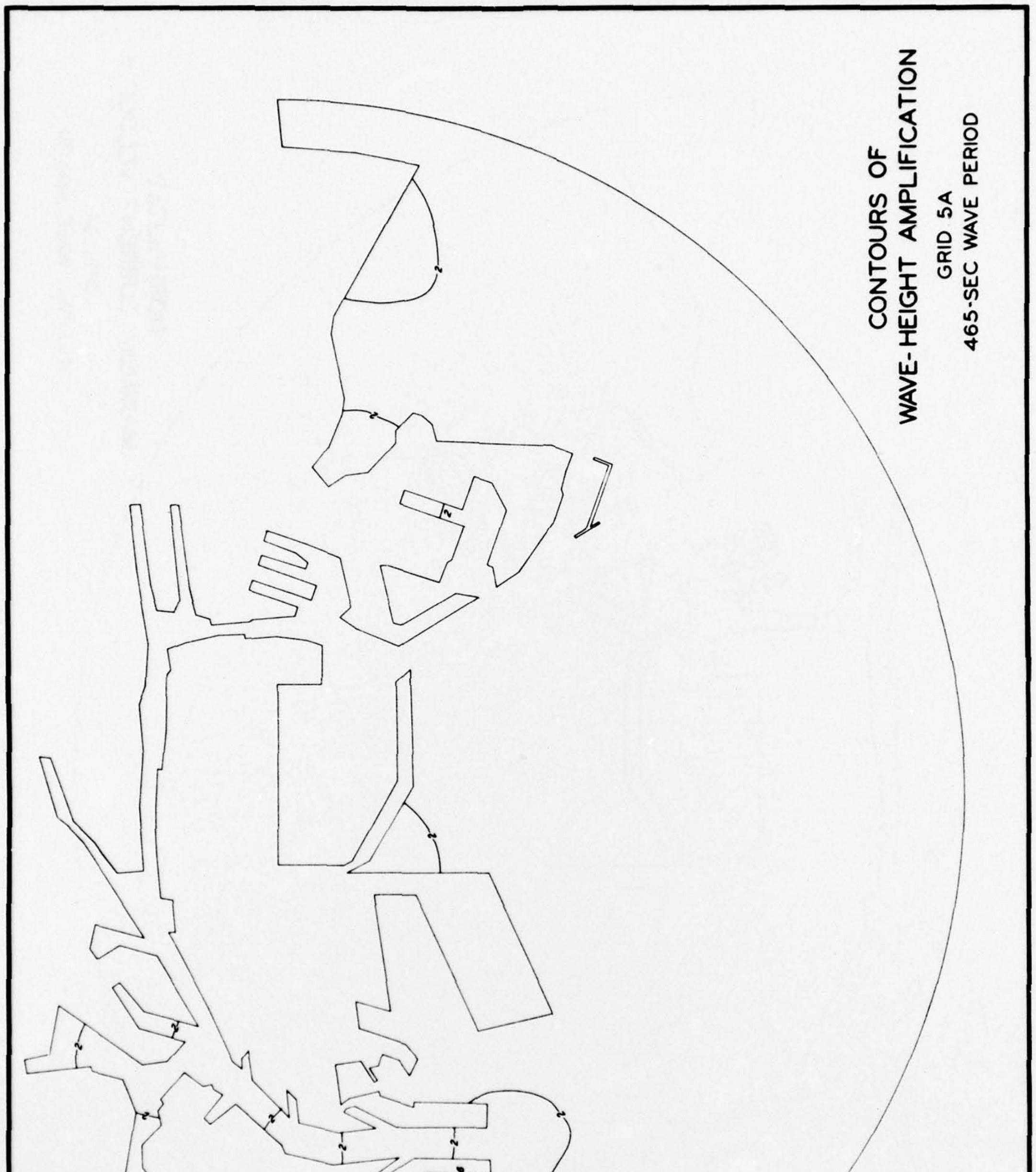
CONTOURS OF
WAVE-HEIGHT AMPLIFICATION
GRID 5A
465-SEC WAVE PERIOD
N

PLATE 198

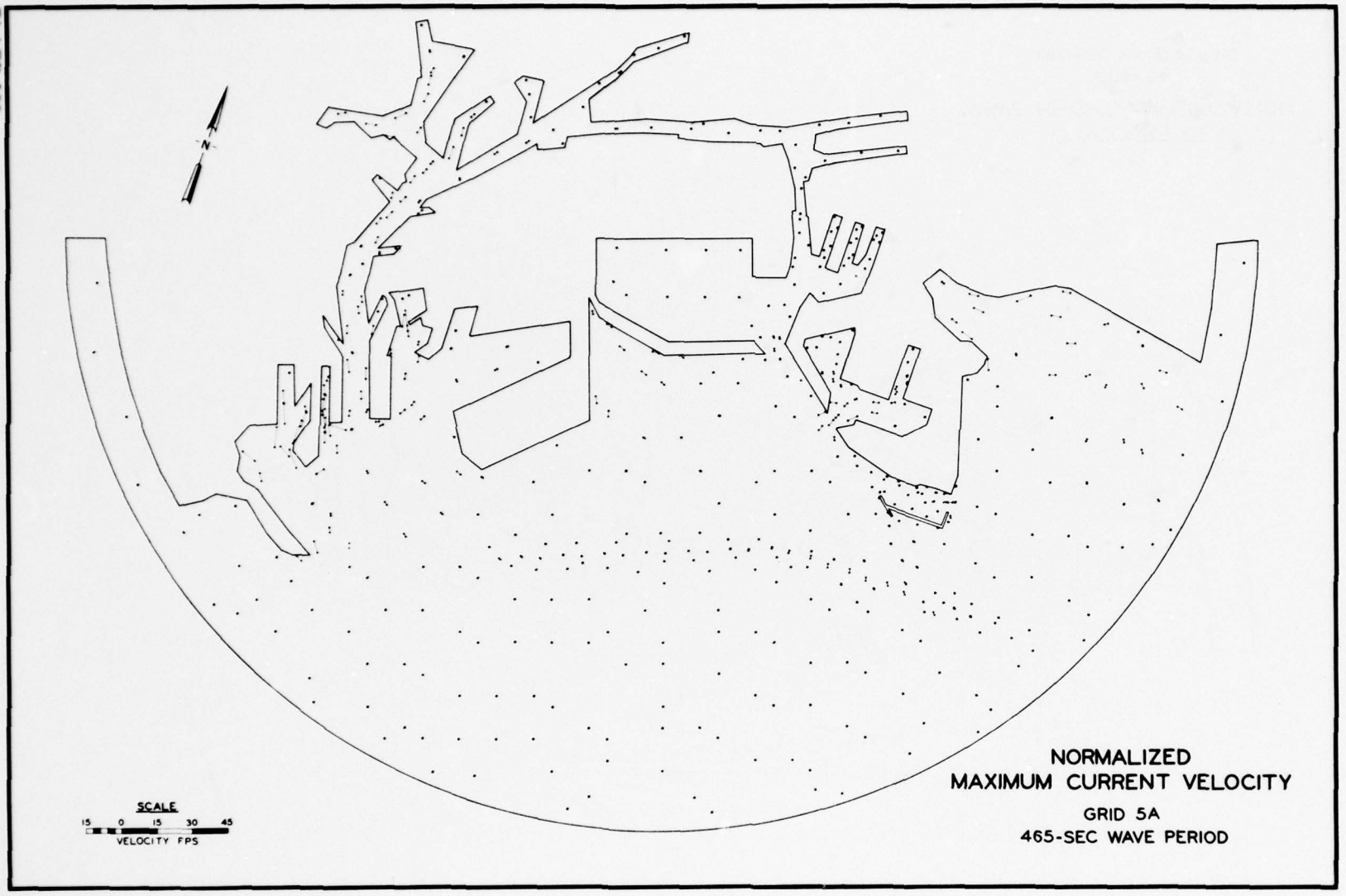

NORMALIZED
MAXIMUM CURRENT VELOCITY

GRID 5A
465-SEC WAVE PERIOD

APPENDIX A: NOTATION

a	Boundary of region
a_i	Amplitude of incident wave
a_t	Amplitude of transmitted wave
A	Region inside harbor
b_o	Incident wave amplitude
$b(w)$	Amplitude of frequency component w
d	Average rock diameter
g	Acceleration due to gravity, 32.2 ft/sec^2
G	Element slope matrix
h	Water depth, ft
H_n	Hankel function of the first kind of order n
i	Imaginary number
k	Wave number
n	Integer
n_a	Unit normal vector outward from region A
N	Interpolation function
r	Spherical coordinate, ft
R_e	Real number
t	Time, sec
T	Wave period
u	Velocity in x-direction, ft/sec
U	Total horizontal velocity, ft/sec
v	Velocity in y-direction, ft/sec
w	Angular frequency, radians/sec
x	Cartesian coordinate, ft
y	Cartesian coordinate, ft
α_n	Unknown coefficient
γ	Coefficient
Δ	Area of element
∇	Gradient operator, ft^{-1}
θ	Spherical coordinate, radians
λ	Wavelength of incident waves

ξ	Response of harbor
ϕ	Total velocity potential, ft^2/sec
ϕ_a	Total velocity potential evaluated on boundary a , ft^2/sec
ϕ_I	Velocity potential of incident wave, ft^2/sec
ϕ_R	Far field velocity potential, ft^2/sec
ϕ_s	Scattered wave velocity potential, ft^2/sec

In accordance with ER 70-2-3, paragraph 6c(1)(b), dated 15 February 1973, a facsimile catalog card in Library of Congress format is reproduced below.

Houston, James R

Los Angeles Harbor numerical analysis of harbor oscillations, by James R. Houston. Vicksburg, U. S. Army Engineer Waterways Experiment Station, 1977.

1 v. (various pagings) illus. 27 cm. (U. S. Waterways Experiment Station. Miscellaneous paper H-77-2)

Prepared for Port of Los Angeles, San Pedro, California.

Includes bibliography.

1. Harbor oscillations. 2. Los Angeles Harbor. 3. Numerical analysis. I. Port of Los Angeles. (Series: U. S. Waterways Experiment Station, Vicksburg, Miss. Miscellaneous paper H-77-2)
TA7.W34m no.H-77-2